

Molecular mechanism underlying pathogenesis of WNT signaling associated medulloblastoma

By

Satishkumar Vishram Singh

[LIFE09201004012]

**Tata Memorial Centre
Mumbai**

*A thesis submitted to the
Board of Studies in Life Sciences
In partial fulfillment of requirements*

For the Degree of

DOCTOR OF PHILOSOPHY

of

HOMI BHABHA NATIONAL INSTITUTE

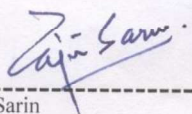


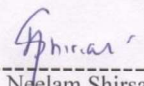
April 2018

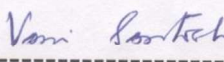
Homi Bhabha National Institute

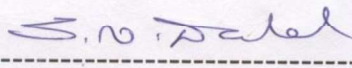
Recommendations of the Viva Voce Committee

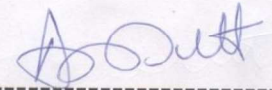
As members of the Viva Voce Committee, we certify that we have read the dissertation prepared by **Mr. Satishkumar Vishram Singh** entitled "Molecular mechanism underlying pathogenesis of WNT signaling associated medulloblastoma" and recommend that it may be accepted as fulfilling the thesis requirement for the award of Degree of Doctor of Philosophy.


Chairman – Dr. Rajiv Sarin Date: 26.04.18


Guide/Convener – Dr. Neelam Shirsat Date: 26.04.18


External Examiner – Prof. Vani Santosh Date: 26/04/2018

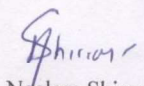

Member – Dr. Sorab Dalal Date: 26/4/18


Member - Dr. Amit Dutt Date: 26/04/18

Final approval and acceptance of this thesis is contingent upon the candidate's submission of the final copies of the thesis to HBNI.

I hereby certify that I have read this thesis prepared under my direction and recommend that it may be accepted as fulfilling the thesis requirement.

Date: 26.04.2018
Place: Navi Mumbai


Dr. Neelam Shirsat
Guide

STATEMENT BY AUTHOR

This dissertation has been submitted in partial fulfillment of requirements for an advanced degree at Homi Bhabha National Institute (HBNI) and is deposited in the Library to be made available to borrowers under rules of the HBNI.

Brief quotations from this dissertation are allowable without special permission, provided that accurate acknowledgement of source is made. Requests for permission for extended quotation from or reproduction of this manuscript in whole or in part may be granted by the Competent Authority of HBNI when in his or her judgment the proposed use of the material is in the interests of scholarship. In all other instances, however, permission must be obtained from the author.

Satishkumar Vishram Singh

DECLARATION

I, hereby declare that the investigation presented in the thesis has been carried out by me. The work is original and has not been submitted earlier as a whole or in part for a degree /diploma at this or any other Institution / University.

Satishkumar Vishram Singh

List of Publications Arising From the Thesis

Journal

1. **Singh SV**, Dakhole AN, Deogharkar A, Kazi S, Kshirsagar R, Goel A, Moiyadi A, Jalali R, Sridhar E, Gupta T, Shetty P, Gadewal N, Shirsat NV, 2017; Restoration of miR-30a expression inhibits growth, tumorigenicity of medulloblastoma cells accompanied by autophagy inhibition. Biochem Biophys Res Commun. 2017 Jul 27. pii: S0006-291X(17)31499-7. doi: 10.1016/j.bbrc.2017.07.140
2. **Satishkumar Vishram Singh**, Neelam Shirsat; DDX3X, a frequently mutated gene in medulloblastoma, encoding a DEAD box family RNA helicase can be expressed successfully as a recombinant protein in bacteria as a MBP-fusion protein. J.Biosci Tech, Vol 8(2),2017,813-820

Chapters in books and lectures notes: NIL

Conferences:

1. Poster presented titled “Chromatin modifying enzymes: Key players in medulloblastoma pathogenesis” in INDO-US conference “Advances in Enzymology: Implications in Health, Disease and Therapeutics” organized at ACTREC from 17th to 19th Jan, 2017.
2. Poster presented titled “MiR-30a-3p, a microRNA downregulated in medulloblastomas across all molecular subgroups appears to act as a tumor suppressor in medulloblastoma pathogenesis” in ISNOCON 2017 - 9th Annual conference Indian Society of Neuro-Oncology.

Others: NIL

Satishkumar Vishram Singh

**Dedicated
To
My Late. Mother**

ACKNOWLEDGEMENT

I take this opportunity to offer my sincere thanks to my mentor Dr. Neelam Shirsat for her guidance, incessant encouragement and prudent suggestions. Without her it would have been impossible to make this journey successful.

I am grateful to Prof. S.V. Chiplunkar (Director- ACTREC), Dr. R. Sarin (Former Director ACTREC), Dr. S. Zingde (Former Deputy Director ACTREC) for providing research facility and excellent infrastructure. I am fortunate to have Dr. Rajiv Sarin, Dr. Sorab Dalal and Dr. Amit Dutt as my doctoral committee members. Their critical analysis and helpful suggestions have contributed significantly to the work.

I am thankful to all lab my seniors Dr. Shailendra Upraity, Dr. Ratika Kunder, Dr. Kedar Yogi, Dr. Pooja Panwalkar and all my present lab members. The life in lab would have not been enjoyable without the presence of Umesh, Anant and sadaf. I owe special thanks to Dr. Ram Kumar Singh, Dr. Rajan Choidhary,, Akash Dubey and Manish Pandey for making my life in ACTREC happening. I would like to thank Dr. Aditi for her constant support, help and encouragement during my tough time in lab. This Ph.D work would have not been possible without the presence of common facilities like common instrument room, Sequencing facility and microscopy facility so, a special thanks to Mr. Uday dandekar, Mr. Naresh, Mrs. Sharada, vaishali and tanuja. Thanks to maya for frequent reminders of deadline. I am also thankful to student's community of ACTREC and my 2010 batch, who helped me in innumerable ways during the entire period.

I owe a lot more than I can express in words to my father, sisters and other family members for all their sacrifices and affectionate blessings. Last but not least, I would like to thank my mother who has provided me love, strength, motivation and guiding lessons of life. I don't know where

life will take me as I grow older, but one thing I know is that I will never be able to be a person better than you. I cherish precious memories of you and find strength in knowing that even though you are gone you still live on in my heart forever. Though, all cannot be mentioned, but none is forgotten.

CONTENTS

SYNOPSIS.....	1
List of Figures.....	13
List of Tables.....	16
List of Abbreviations.....	17
Chapter 1: INTRODUCTION.....	20
Chapter 2: REVIEW OF LITERATURE.....	26
2.1 Medulloblastoma: Epidemiology.....	27
2.2 Medulloblastoma Diagnosis, Risk Stratification and Treatment.....	27
2.3 Medulloblastoma: Historical view.....	29
2.4 Medulloblastoma: Result of developmental mechanism out of control.....	31
2.4.1 WNT signaling pathway.....	32
2.4.2 SHH signaling pathway.....	34
2.5 Medulloblastoma: Expression profiling leading to current consensus of subgrouping.....	36
2.5.1 WNT subgroup.....	37
2.5.2 SHH subgroup.....	38
2.5.3 Group 3.....	41
2.5.4 Group 4.....	41
2.6 World Health Organisation (WHO) classification of medulloblastoma 2016.....	42
2.7 Understanding the pathogenesis of WNT subgroup medulloblastoma.....	43
2.8 DDX3X: A member of the DEAD Box Family Helicase.....	45
2.9 Structure of DDX3X core domain and their functions.....	46
2.10 Functions of DDX3X in RNA metabolism.....	48
2.10.1 Role as a regulator of transcription.....	48
2.10.2 Role of DDX3X in mRNA export.....	49
2.10.3 DDX3X as a regulator of translation.....	49
2.11 Role of DDX3X in apoptosis.....	50
2.12 The debatable role of DDX3X as oncogenic or tumor suppressor in cancer.....	50

2.13	MircoRNAs: Small RNAs with a big role.....	52
2.14	Brief history of microRNAs.....	52
2.15	MicroRNA biogenesis and mode of action.....	53
2.16	MicroRNAs in cancer.....	55
2.17	MicroRNA deregulation in medulloblastoma and their functional significance.....	56
Chapter 3: MATERIALS and METHODS.....		59
MATERIALS.....		60
METHODS.....		63
3.1	Collection of sporadic medulloblastoma tumour tissues and normal cerebellar tissues.....	63
3.2	Exome sequencing of Tumor DNA and paired blood DNA sample.....	64
3.2.1	Genomic DNA extraction from Tumor and blood DNA.....	64
3.2.2	Exome sequencing of medulloblastoma tumor and paired blood DNA samples using Agilent SureSelect Human All Exon v2.0 (44M) kit.....	64
3.3	Sequencing of PCR products.....	65
3.3.1	PCR Amplification.....	65
3.3.2	Removal of unused primers and dNTPs from PCR products by Exonuclease I and Shrimp Alkaline Phosphatase.....	66
3.3.3	Clean up of PCR templates for removal of excess salt.....	67
3.3.4	Sequencing of the PCR products or plasmid vectors.....	68
3.4	Cloning of PCR products into target vector.....	68
3.4.1	PCR amplification and Phenol-Choroform method of DNA purification.....	69
3.4.2	Agarose Gel Electrophoresis.....	71
3.4.3	T4 Polynucleotide kinase reaction (Only for blunt end cloning).....	73
3.4.4	Restriction digestion.....	73
3.4.5	Dephosphorylation of Vector using Shrimp Alkaline Phosphatase (SAP).....	74
3.4.6	Ligation.....	75
3.4.7	Preparation of competent cells.....	75

3.4.8	Transformation of competent cells.....	77
3.4.9	Plasmid extraction by alkaline lysis method.....	78
3.5	Protein expression and purification from bacterial expression system.....	80
3.5.1	Protein expression in Bactreial expression system and detection by SDS-PAGE analysis.....	81
3.5.2	Purification of MBP tagged DDX3X from <i>E. coli rosetta (DE3)</i> strain.....	83
3.6	RNA Helicase assay.....	85
3.7	Luciferase Reporter Assay.....	89
3.7.1	Generation of Vector constructs for promoter luciferase reporter assay and for mRNAs containing complex 5'-UTR reporter assay.....	90
3.7.2	Luciferase assay.....	94
3.8	Extraction of nucleic acids.....	97
3.8.1	Genomic DNA Extraction from tissue culture cells.....	98
3.8.2	Total RNA extraction from fresh frozen tumour tissues and/or tissue culture cells by acid guanidinium Isothiocyanate-phenol chloroform extraction.....	99
3.8.3	Preparation of denaturing gels for RNA separation and quality assessment.....	102
3.9	Gene expression analysis by real time RT-PCR.....	104
3.9.1	Primer Designing.....	104
3.9.2	Reverse transcriptase PCR reaction for conversion of RNA to cDNA.....	104
3.9.3	Real Time PCR.....	106
3.10	Quantification of miRNA expression by Real time PCR.....	108
3.10.1	Stem- loop Reverse Transcription for miRNA.....	109
3.10.2	Real time PCR.....	110
3.11	Tissue culture media and reagents.....	111
3.12	Routine maintenance of cell Lines.....	112
3.13	Freezing and revival of cell cultures.....	113

3.14	Transient transfection of 293FT cells using BES buffer for Lentivirus production.....	114
3.15	Transduction with lentiviral particles and stable over-expression of miRNA in Daoy, D425 and D283 cell lines.....	115
3.16	MTT Cytotoxicity Assay.....	117
3.17	Clonogenic assay.....	118
3.18	Soft Agar Colony Formation Assay.....	118
3.19	Generation of orthotopic medulloblastoma xenograft in immunocompromised mice using stereotactic method of injection and assessment of in vivo tumorigenic potential of miR-30a expressing polyclonal populations of D283 cells.....	119
3.20	Bioluminescence imaging.....	124
3.21	Protein extraction of cultured cells.....	126
3.22	Estimation of Protein Concentration.....	127
3.23	SDS-Polyacrylamide Gel Electrophoresis (SDS-PAGE).....	129
3.24	Western Blot Analysis and Immuno-detection.....	131
3.25	Bioinformatic methods.....	135
3.25.1	Quality analysis of fastq reads.....	135
3.25.2	Alignment of fastq Reads to hg19 by BWA.....	135
3.25.3	Removal of duplicate reads.....	136
3.25.4	Refinement of Alignment by Genome Analysis Toolkit.....	136
3.25.5	Creating Pileup of aligned reads.....	137
3.25.6	Identification of Somatic Variants.....	138
3.25.7	Annotation of Somatic Variants.....	140
3.26	Copy number variation analysis using CopywriteR.....	141
Chapter 4: RESULTS.....		145
4.1	Identification of somatic mutations in WNT subgroup medulloblastoma by exome sequencing of tumour and paired blood DNAs.....	146
4.1.1	Exome sequence data Quality.....	147
4.1.2	Identification of single nucleotide variants in the WNT medulloblastoma tumour tissues.....	148
4.1.3	Copy number variations in the WNT subgroup Medulloblastoma.....	156

4.2	Understanding the functional relevance of the identified genetic alterations in <i>DDX3X</i> , a DEAD box family RNA helicase.....	158
4.2.1	Cloning of <i>DDX3X</i> in a bacterial expression vector pET-28a.....	159
4.2.2	Expression of <i>DDX3X</i> cloned in a bacterial expression vector pET-28a as 6X-His fusion protein in <i>E. coli BL21</i> cells.....	160
4.2.3	Solubilisation of recombinant 6X-His tagged <i>DDX3X</i> expressed in <i>E. coli BL21</i> cells using different non-ionic, ionic detergents and other additives.....	161
4.2.4	Expression of <i>DDX3X</i> cloned in a bacterial expression vector pET-28a as 6X-His fusion protein in <i>E. coli Rosetta-gami 2 (DE3) pLysS</i> cells.....	162
4.2.5	Cloning and expression of <i>DDX3X</i> in a bacterial expression vector pMAL-c5E as MBP fusion protein.....	165
4.2.6	RNA helicase assay with MBP- <i>DDX3X</i> fusion protein.....	167
4.2.7	Effect of <i>DDX3X</i> mutations on transcriptional regulatory activity of <i>DDX3X</i>	169
4.2.7.1	Effect of <i>DDX3X</i> expression on transcriptional activity of beta catenin.....	169
4.2.7.2	Effect of <i>DDX3X</i> expression on IFN beta promoter activity.....	171
4.2.8	Downregulation of <i>DDX3X</i> expression in Daoy and HEK 293FT cells using shRNA cloned in pLKO-tet vector.....	172
4.2.9	Effect of identified genetic alterations in <i>DDX3X</i> on its translational control.....	173
4.2.10	Effect of <i>DDX3X</i> downregulation on proliferation of Daoy cell.....	174
4.2.11	Effect of <i>DDX3X</i> downregulation on clonogenic potential of Daoy cells.....	176
4.3	Delineate the role of has-miR-30a in medulloblastoma cell behavior.....	178
4.3.1	MiR-30a expression levels in medulloblastoma subgroups and normal brain tissues.....	178

4.3.2	Evaluation of miR-30a-3p expression in mouse medulloblastoma tumor tissues from the <i>Smo</i> ^{+/+} transgenic mice and the <i>Ptch1</i> ^{+/-} knock-out mice and normal cerebellum by SYBR green real time RT-PCR.....	179
4.3.3	Construction of an inducible lentiviral vector for the expression of miR-30a.....	181
4.3.4	Effect of miR-30a Expression on growth characteristics of established medulloblastoma cell lines.....	182
4.3.4.1	Generation of stable polyclonal populations expressing miR-30a on doxycycline induction.....	182
4.3.4.2	Effect of miR-30a expression on the proliferation of the medulloblastoma cell lines.....	184
4.3.4.3	Effect of miR-30a expression on the clonogenic potential of Daoy medulloblastoma cells.....	185
4.3.4.4	Effect of miR-30a expression on the anchorage independent growth of medulloblastoma cells.....	186
4.3.5	Effect of miR-30a expression on <i>in-vivo</i> tumorigenicity of D283 cell lines.....	188
4.3.6	Molecular mechanism underlying growth inhibitory effect of miR-30a expression on medulloblastoma cells.....	189
Chapter 5:	DISCUSSION.....	192
5.1	The WNT subgroup medulloblastomas possess low number of genetic alterations.....	193
5.2	Mutations in the genes involved in the chromatin remodeling SWI/SNF complex and histone modifying ASCOM complex appear to play role in pathogenesis of the WNT subgroup medulloblastomas.....	194
5.3	DEAD-box helicase (<i>DDX3X</i>) is the second most frequently mutated gene in medulloblastoma after <i>CTNNB1</i> gene.....	198
5.4	Mutations result in loss of enzymatic activity of DDX3X.....	199
5.5	DDX3X: Tumor Suppressor or Oncogene?.....	201
5.6	Expression of miR-30 family miRNAs is downregulated in medulloblastoma.....	202

5.7 MiR-30a inhibits proliferation, anchorage independent growth and <i>in vivo</i> tumorigenicity of medulloblastoma cells by inhibiting autophagy.....	203
Chapter 6: SUMMARY & CONCLUSIONS.....	207
Chapter 7: Future Directions.....	213
BIBLIOGRAPHY.....	215
Appendix-I.....	225
Appendix-II.....	227
Appendix-III.....	235
PUBLICATIONS.....	238

SYNOPSIS



Homi Bhabha National Institute

SYNOPSIS OF Ph. D. THESIS

- 1. Name of the Student:** Satishkumar Vishram Singh
- 2. Name of the Constituent Institution:** Tata Memorial Centre, ACTREC
- 3. Enrolment No. :** LIFE09201004012
- 4. Title of the Thesis:** Molecular mechanism underlying pathogenesis of WNT signaling associated medulloblastoma.
- 5. Board of Studies:** Life Sciences

SYNOPSIS

1. Introduction:

Brain tumors are the most common solid tumors in children. Medulloblastomas account for about 20% of these tumors.¹ Medulloblastomas are highly malignant brain tumors, which are located classically in the posterior fossa of young children. All medulloblastomas are classified pathologically as grade IV, the highest grade of malignancy due to their aggressive nature. . Expression profiling studies including our own study have identified four molecular subgroups of medulloblastomas *viz.* WNT, SHH, Group 3 and Group 4. The WNT subgroup medulloblastomas show over-expression of genes belonging to the WNT signalling pathway. Almost 90% WNT subgroup tumors carry activating mutation in the gene encoding beta-catenin.^{2, 3} Mutant beta catenin alone is known to bring about aberrant proliferation but does not result in malignant transformation.⁴ The present study was undertaken to identify genetic alterations in the

WNT subgroup medulloblastomas that along with mutant beta-catenin bring about malignant transformation.

2. **Objective:**

To identify genetic alteration/s other than mutant beta catenin which lead to the development of WNT subgroup medulloblastoma.

3. **Work Plan:**

- I. Exome sequencing of WNT subgroup medulloblastoma tumor DNA and paired blood samples to identify the genetic alterations.
- II. Understand the functional relevance of identified genetic alteration/s in pathogenesis of medulloblastoma.
- III. Delineate the role of *hsa- miR-30a-3p* (located on chromosome 6) in medulloblastoma tumor cell behavior.

4. **Work done and Results**

4.1 **Exome sequencing of the WNT subgroup medulloblastoma tumor DNA and analysis of data**

Exome capture of 11 WNT subgroup tumor tissues and 6 paired blood sample DNA was done using Agilent SureSelect Human all exon 44 Mb kit and exome sequencing was done using Illumina HiSeq with average coverage of 50X. Quality of the sequence data was analysed by FASTQC. Clean reads were aligned to *hg 19 (GRCh37)* human reference genome build. Variants (SNP and InDel) were called using bio-informatics programmes viz. SAMtools, GATK and VarScan and then manually verified using Integrated Genomics Viewer and in some cases by Sanger Sequencing. Total coverage of the exome was more than 97% in each case with more than 70% exome covered with at least 20X coverage. The variants having at least 4 reads in tumor and paired blood with mapping quality of more than 60 and base quality more than 30 were further manually verified using Integrated Genome viewer. In the case of 6 tumor tissues having paired blood sample, the number of novel somatic variants were found to be 10-30. In the case of 5 tumors not having paired blood sample, the variants were shortlisted based on their absence in

the 60000 exome sequence database (ExAC Broad Institute).⁶ 30-50 novel non-synonymous SNPs/Indels were identified in the unpaired medulloblastoma tissues. Of the 11 tumor tissues studied, 8 tumors showed monosomy of chromosome 6 as analysed by CopywriteR programme. A total of 104 novel somatic variants (Non-synonymous - 78, synonymous – 11, splice site – 2, frame shift InDels – 4 and non-frameshift InDels – 9) have been identified and 63 of these non-synonymous somatic variants were further confirmed by Sanger sequencing. Novel somatic mutations were identified in the genes playing role in chromatin remodelling, histone modification, growth factor signalling and DNA repair.

4.2 Understanding the functional relevance of identified genetic alterations in *DDX3X*, a DEAD box family RNA helicase

Mutations in *DDX3X* gene (2 missense and 1 frameshift deletion) were found in 3/11 WNT medulloblastomas analysed. *DDX3X* is an ATP-dependent RNA helicase that has been reported to be mutated/altered in some other cancers including chronic lymphocytic leukemia.⁶ Based on the presence of the recurrent mutations in the *DDX3X* gene in various cancers, *DDX3X* is now recognized as a gene having pathogenic role in cancer. However, the precise role of *DDX3X* in pathogenesis of these cancers is not understood.

DDX3X is a 661 amino acid long protein and member of DEAD-box family of RNA helicases. It is located on X-chromosome and ubiquitously expressed in all tissues. Its structure can be divided into two structural domains: a helicase ATP binding domain (residues 211-403) and a helicase C-terminal domain (residues 414-575).⁷ *DDX3X* is a multifunctional protein having diverse roles in RNA metabolism.⁸ *DDX3X* acts as a transcriptional and translational regulator in multiprotein complexes that are likely to differ in the context of different cell types and in the presence of activation of different signaling pathways. Therefore, identification of *DDX3X*'s transcriptional and translational target genes in the medulloblastoma cells and in the presence of SHH or WNT signaling pathway activation would lead to understanding of *DDX3X*'s role in the pathogenesis of the WNT and SHH subgroup medulloblastomas.

In order to understand the functional impact of the *DDX3X* mutations, experiments were designed as described below.

4.2.1 To study effect of mutations in the DDX3X gene on helicase activity of the protein:

DDX3X cDNA was cloned in pET28a vector, an inducible vector which contains N-terminal 6X-His tag. His-tagged DDX3X protein was found to be expressed in insoluble fraction of *E. coli BL21* at both the induction temperature (18⁰C and 37⁰C) even with lowest amount (0.1mM) of IPTG and even after induction for different time points (3h, 6h and 9h) . DDX3X-pET28a vector expression in various *E.coli* strains like *pLysS*, *Rosetta-Gami* strains was also carried out to control inducible expression levels as well as to provide chaperones for proper folding. However, DDX3X was found to be expressed in insoluble fraction in all these cases. Buffers containing different detergents and additives also showed the DDX3X in insoluble fraction except in buffers that contained (0.3% and 1%) sarkosyl. Since all attempts to obtain expression of recombinant His-tagged DDX3X protein in soluble fraction failed, human DDX3X cDNA was then cloned in pMAL-c5E vector that expresses the gene of interest as a fusion downstream *malE* gene encoding Maltose binding protein (MBP). MBP tag is believed to act as a chaperone helping proper folding and thereby solubilisation of recombinant protein. MBP-DDX3X fusion protein (~120kD) was found to be expressed in soluble fraction at all three (18⁰C, 24⁰C and 37⁰C) temperatures with induction using 0.3 mM IPTG. This fusion protein was purified with amylose resin and eluted fraction with 10 mM maltose showed the presence of a single band at around 120 kD corresponding to MBP-DDX3X fusion protein but after digestion with TEV for 3 hrs at 4⁰C precipitation of DDX3X was seen indicating that DDX3X is insoluble when cleaved from MBP tag. Maltose was removed from purified protein by dialysis using Amicon Ultra centrifugal filter (Millipore). Freshly dialysed protein along with amylose resin bound protein was used for doing RNA helicase assay.

Helicase activity of MBP-DDX3X fusion protein was assessed by incubating it with a 6-FAM labelled 18 mer RNA oligonucleotide annealed to a 36 mer RNA oligonucleotide having 18 nucleotide long complementary sequence in a hybridization buffer supplemented with RNase inhibitor at 37⁰ C for 40 min and then analysing it on native acrylamide gel by electrophoresis in the presence of 0.1% SDS to inhibit secondary structure formation. Incubation of the hybrid with the bead bound MBP-DDX3X protein but not with eluted MBP-DDX3X protein shows migration of the hybrid at intermediate position between that

of hybrid and free 18 mer oligonucleotide indicating partial helicase activity of the fusion DDX3X protein. Since only partial helicase activity could be demonstrated for the recombinant DDX3X protein expressed in bacteria further experiments were performed to check the effect of DDX3X mutations by transfecting wild type and mutant DDX3X protein in mammalian cells.

4.2.2 Effect of identified genetic alterations in DDX3X on its translational regulation

Helicase activity of DDX3X is known to be essential for its translation regulatory function. DDX3X has been reported to facilitate translation initiation of mRNAs with long and complex 5'UTRs like Cyclin E1 through its helicase activity⁹. Therefore, to identify the effect of identified mutations on translation control activity of DDX3X luciferase reporter construct was generated by cloning Cyclin E1 5'UTR (183 nt) in pGL3 control vector upstream of luciferase gene and luciferase reporter assay was performed in a DDX3X knock-out 293FT clone. The relative luciferase activity was found to be increased by approximately 3 fold in case of the cells transfected with CRISPR resistant pcDNA3-DDX3X as compared to the control cells transfected with pcDNA3 indicating that DDX3X enhances the expression of genes having complex 5'UTR, whereas all the mutant of DDX3X failed to increase luciferase activity indicating loss of function nature of mutation. Further, cyclin E1 expression was found to be downregulated in DDX3X knock-down clones of HEK293FT cell line as well that of Daoy, a medulloblastoma cell line.

4.2.3 Downregulating DDX3X in Daoy and HEK 293FT cells using shRNA cloned in pLKO-Tet vector

Two shRNAs (one targeting 3'UTR region and other targeting ORF region nucleotide 301-320) were designed and cloned in a doxycycline inducible pLKO-Tet vector. Daoy and 293FT cells were transduced with lentiviral particles of these shRNAs and polyclonal population was selected using puromycin selection. Almost 90% downregulation of DDX3X was observed in Daoy cells using shRNAs against UTR (Daoy-UTR) and ORF (Daoy-301-ORF) induced with 8 µg and 4 µg doxycycline respectively. In the case of 293FT cells negligible downregulation of DDX3X was observed with UTR shRNA whereas shRNA against ORF region showed approximately 50% downregulation.

4.2.4 Effect of DDX3X downregulation on Daoy cells proliferation and their clonogenic potential:

The effect of DDX3X downregulation on proliferation and clonogenic potential of Daoy cells was studied by MTT and clonogenic assay. Daoy-301-ORF cells showed approximately 70% and 80% decrease in cell proliferation with 4 μ g and 8 μ g doxycycline respectively compared to their uninduced counterparts. Whereas in the case of Daoy-UTR cells the reduction in proliferation was 50% and 60% respectively upon induction with 4 μ g and 8 μ g doxycycline compared to their uninduced counterparts. In clonogenic assay Daoy-301-ORF cells showed approximately 90% reduction in the colony formation ability upon induction with 4 μ g doxycycline, whereas in the case of Daoy-UTR cells it was approximately 50% with 8 μ g doxycycline compared to their un-induced counterparts. Thus, DDX3X appears to have pro-proliferative role in Daoy medulloblastoma cell line.

4.3 Delineate the role of *hsa-miR-30a* in medulloblastoma tumor cell behavior

Genome of the WNT subgroup medulloblastomas is known to be relatively stable with only one known recurrent copy number alteration i. e. loss of one copy of chromosome 6. Expression of two microRNAs located on chromosome 6 viz. miR-206 and miR-30a was found to be downregulated in all medulloblastomas and in particularly WNT subgroup tumors.²

4.3.1 Evaluation of miR-30a levels in medulloblastoma tumor tissues and normal cerebellum

MiR-30a expression was evaluated in human sporadic medulloblastoma tumor tissues (n=15) and in normal cerebellum (n=4) tissues by real time RT-PCR. MiR-30a expression was found to be downregulated in medulloblastomas belonging to all the four subgroups by 30-600 folds and by 10-100 folds in three established medulloblastoma cell lines viz. Daoy, D425 and D283. The expression of murine homolog of human miR-30a was evaluated in medulloblastomas from the SHH subgroup mouse models viz. *Smo*^{+/+} transgenic mice and *Ptch1*^{+/-} knock-out mice. MiR-30a expression was found to be downregulated by ~10 fold in *Smo*^{+/+} transgenic mice tumors and by 20 fold in *Ptch1*^{+/-} knock-out mice tumors as compared to their normal cerebellar counterparts.

4.3.2 Effect of miR-30a Expression on growth characteristics of medulloblastoma cell lines

The effect of expression of miR-30a was studied in Daoy, D425 and D283 medulloblastoma cell lines. These cell lines were transduced with lentiviral particles of pTRIPZ-miR-30a construct that expressed miR-30a in doxycycline inducible manner. Stable polyclonal population of each of these 3 cell lines was selected in presence of puromycin. The effect of miR-30a expression on proliferation and clonogenic potential was studied by MTT, clonogenic assays respectively. Daoy cells stably expressing miR-30a showed ~50% reduction in both proliferation and clonogenic potential compared to their uninduced counterparts. D283 and D425 cells stably expressing miR-30a showed ~80% reduction in proliferation and ~60% reduction in clonogenic potential compared to their uninduced counterparts.

4.3.3 Effect of miR-30a expression on in-vivo tumorigenicity of D283 cell lines in immunodeficient mice

D283 cell line as well as its polyclonal population stably transduced with pTRIPZ-miR-30a construct was engineered to express firefly luciferase and then the cells were injected stereotactically in cerebellum of nude mice after doxycycline treatment. Bioluminescence imaging showed almost 400 fold increase in average radiance of the tumors formed within 3 weeks in mice injected with the parental D283 cells. On the other hand, average luminescence of the tumors formed in D283 cells expressing miR-30a increases only about 10 fold within the same time period. Thus, upon miR-30a expression tumor growth was found to be reduced by more than 100 fold ($p < 0.0001$). Therefore, miR-30a expression was found to bring about substantial decrease in tumorigenicity of the medulloblastoma cells.

4.3.4 Molecular mechanism underlying growth inhibitory effect of miR-30a expression on medulloblastoma cells

MiR-30a has been reported to inhibit autophagy by downregulating expression of Beclin1 and ATG5. In order to identify molecular mechanism by which miR-30a expression affects growth and clonogenic potential of the medulloblastoma cells, levels of Beclin1 and ATG5 were studied by western blotting in miR-30a expressing medulloblastoma cells. Significant reduction in Beclin1 as well as in ATG5 expression was observed upon miR-30a expression in D283 medulloblastoma cells. In order to check if

miR-30a expression inhibited autophagy in medulloblastoma cells, change in the levels of LC3B, upon miR-30a expression was investigated by western blotting. Doxycycline induction of miR-30a expression resulted in downregulation of total LC3B levels (LC3BI and LC3BII) both in the presence and absence of lysosomal inhibitor indicating autophagy inhibition. Accumulation of autophagic substrate SQSTM1/p62 is also used as a surrogate marker for autophagic flux. All the three medulloblastoma cell lines showed increased expression of SQST/p62 upon miR-30a expression indicating autophagy inhibition. Thus, miR-30a expression was found to inhibit autophagy in all the three medulloblastoma cell lines studied.

5. Summary and Conclusions

In the present study novel somatic mutations were identified in the genes playing role in chromatin remodelling, histone modification, growth factor signalling and DNA repair pathway in the WNT subgroup medulloblastomas. Recurrent mutations were identified in the gene encoding DDX3X, a multifunctional RNA helicase. Mutations in DDX3X were found to affect its translation regulatory role that is known to be dependent upon its helicase activity. Thus, mutation in DDX3X, identified in medulloblastoma tissues, appear to result in loss of its helicase activity. DDX3X downregulation in Daoy, medulloblastoma cell line resulted in substantial reduction in proliferation and clonogenic potential indicating essential role for DDX3X in growth of Daoy cells. Loss of one copy of chromosome 6 was found in 7 out of 11 WNT subgroup tumors. The expression of miR-30a located on chromosome 6 was found to be downregulated in the WNT subgroup tumors as well as other medulloblastoma subgroups and cell lines. Expression of miR-30a brought about 50% reduction in proliferation and clonogenic potential of all the three medulloblastoma cell lines studied. MiR-30a expression was found to bring about substantial decrease in tumorigenicity of the medulloblastoma cells. MiR-30a expression in medulloblastoma cells brought about reduction in both Beclin1 and ATG5 protein levels resulting in autophagy inhibition as judged by decrease in total LC3B levels and increase in SQSTM1/p62 levels indicating tumor suppressive role of miR-30a in medulloblastoma pathogenesis at least partly mediated by autophagy inhibition.

6. References

1. CBTRUS statistical report: Primary brain and central nervous system tumors diagnosed in the United States in 2006-2010. Q.T. Ostrom, H. Gittleman, P. Farah, A. Ondracek, Y. Chen, Y. Wolinsky, N.E. Stroup, C. Kruchko, J.S. Barnholtz-Sloan (2013) *Neuro Oncol* 15 Suppl 2 ii1-56.
2. Distinctive microRNA signature of medulloblastomas associated with the WNT signaling pathway Gokhale A. *et.al.*(2010) *J Can Res Ther*, 6:521-9
3. Molecular subgroups of Medulloblastoma: the current consensus. Taylor M. *et.al.* (2012) *Acta Neuropathol* 123:465–472
4. Regulation of Cerebral Cortical Size by Control of Cell Cycle Exit in Neural Precursors. Anjen Chenn and Christopher A. Walsh (2002) *Science* 297(5580): 365-369
5. The ExAC browser: displaying reference data information from over 60 000 exomes. Karczewski KJ, Weisburd B, Thomas B, *et. al.* (2017) [*Nucleic Acids Res.*](#) Jan 4; 45(Database issue): D840–D845.
6. Identification of recurrent truncated DDX3X mutations in chronic lymphocytic leukaemia. J. Ojha, C.R. Secreto, K.G. Rabe, D.L. Van Dyke, K.M. Kortum, S.L. Slager, T.D. Shanafelt, R. Fonseca, N.E. Kay, E. Braggio, (2015) *Br J Haematol* 169 445-448.
7. Cancer-Associated Mutants of RNA Helicase DDX3X Are Defective in RNA-Stimulated ATP Hydrolysis. L.B. Epling, C.R. Grace, B.R. Lowe, J.F. Partridge, E.J. Enemark (2015) *J Mol Biol* 427 1779-1796.
8. The role of the DEAD-box RNA helicase DDX3 in mRNA metabolism. Soto-Rifo R, Ohlmann T. (2013) *Wiley Interdiscip. Rev. RNA* 4(4), 369–385.
9. DDX3 regulates cell growth through translational control of cyclin E1. M.C. Lai, W.C. Chang, S.Y. Shieh, W.Y. Tarn (2010) *Mol Cell Biol* 30 5444-5453.

10. MiRNA-30a-mediated autophagy inhibition sensitizes renal cell carcinoma cells to sorafenib. Zheng B, Zhu H, Gu D, Pan X, Qian L, Xue B, *et al.* (2015) *Biochem Biophys Res Commun.* 459(2):234–9.

Publications in Refereed Journal:

a. Published:

1. **Singh SV**, Dakhole AN, Deogharkar A, Kazi S, Kshirsagar R, Goel A, Moiyadi A, Jalali R, Sridhar E, Gupta T, Shetty P, Gadewal N, Shirsat NV, 2017; [Restoration of miR-30a expression inhibits growth, tumorigenicity of medulloblastoma cells accompanied by autophagy inhibition.](#) [Biochem Biophys Res Commun.](#) 2017 Jul 27. pii: S0006-291X(17)31499-7. doi: 10.1016/j.bbrc.2017.07.140
2. **Satishkumar Vishram Singh**, Neelam Shirsat; DDX3X, a frequently mutated gene in medulloblastoma, encoding a DEAD box family RNA helicase can be expressed successfully as a recombinant protein in bacteria as a MBP-fusion protein. *J.Biosci Tech*, Vol 8(2),2017,813-820

b. Accepted: NIL

c. Communicated: NIL

Other Publications:

a. Book/Book Chapter: NIL

b. Conference/Symposium (Oral/Poster presentation):

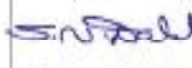
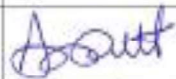
1. Poster presented titled “Chromatin modifying enzymes: Key players in medulloblastoma pathogenesis” in INDO-US conference “Advances in Enzymology: Implications in Health, Disease and Therapeutics” organised at ACTREC from 17th to 19th Jan, 2017.

2. Poster presented titled "MiR-30a-3p, a microRNA downregulated in medulloblastomas across all molecular subgroups appears to act as a tumor suppressor in medulloblastoma pathogenesis" in ISNOCON 2017 - 9th Annual conference Indian Society of Neuro-Oncology.

Signature of Student: 

Date: 16-8-17

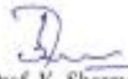
Doctoral Committee

Sr. No.	Name	Designation	Signature	Date
1.	Dr. Rajiv Sarin	Chairman		16-8-17
2.	Dr. Neelam Shirsat	Guide/Convener		16-8-17
3.	Dr. Sorab Dalal	Member		16/8/17
4.	Dr. Amit Dutt	Member		16/8/17

Forwarded Through:


 Dr. S.V. Chiplunkar
 Director, ACTREC
 Chairperson,
 Academic & training Program, ACTREC


 Dr. S. V. Chiplunkar
 Director
 Advanced Centre for Treatment, Research &
 Education in Cancer (ACTREC)
 Tata Memorial Centre
 Kharghar, Navi Mumbai-410210.


 Prof. K. Sharma
 Director, Academics
 TMC
PROF. K. S. SHARMA
 DIRECTOR (ACADEMICS)
 TATA MEMORIAL CENTRE,
 PAREL, MUMBAI

List of Figures

Figure 2.1: Sagittal MRI following gadolinium injections shows dense white medulloblastoma tumor marked in circle.....	29
Figure 2.2: The canonical WNT signaling pathway.....	34
Figure 2.3: SHH signaling.....	35
Figure 2.4: The structure of DEAD-box RNA helicase, DDX3X.....	47
Figure 2.5: Biogenesis of microRNAs.....	54
Figure 3.1: Stem- loop RT-PCR for miRNA.....	108
Figure 4.1: Mutations in the <i>DDX3X</i> gene identified in the WNT subgroup medulloblastomas.....	151
Figure 4.2: Mutations in SWI/SNF complex member ARID1B in the WNT subgroup medulloblastomas.....	152
Figure 4.3: Mutations in SWI/SNF complex member SMARCA4 and SMARCB1 in the WNT subgroup medulloblastomas.....	153
Figure 4.4: Mutations in the genes belonging to the ASCOM complex members MLL3 and KDM6A in the WNT subgroup medulloblastomas validated by Sanger sequencing.....	154
Figure 4.5: Recurrently altered genes and pathways in WNT subgroup medulloblastoma.....	155
Figure 4.6: Copy number variation in the WNT subgroup medulloblastomas as analyzed by CopywriteR software.....	157
Figure 4.7: Validation of <i>DDX3X</i> cDNA clone in pET-28a vector using Sanger sequencing.....	159

Figure 4.8: Expression of His-tagged DDX3X in <i>E. coli BL21</i> cells.....	160
Figure 4.9: Expression of 6X His- tagged DDX3X in <i>E. coli BL21</i> with lysis buffer containing different detergents.....	163
Figure 4.10: Expression of 6X His- tagged DDX3X in <i>E. coli BL21</i> with lysis buffer containing different sugar additives.....	163
Figure 4.11: Expression of 6X His- tagged DDX3X in <i>E. coli Rosetta-gami 2(DE3) pLysS</i> strain.....	164
Figure 4.12: Expression of MBP tagged DDX3X in <i>E. coli Rosetta- DE3</i> strain.....	166
Figure 4.13: Purification of MBP tagged DDX3X in <i>E. coli Rosetta DE3</i> cells.....	166
Figure 4.14: Helicase assay for recombinant MBP-DDX3X fusion protein.....	168
Figure 4.15: Luciferase reporter assay to check the effect of identified DDX3X mutants on trans-activation activity of mutant β -catenin.....	170
Figure 4.16: Luciferase reporter assay to check the effect of identified DDX3X mutants on IFN- β promoter activity.....	172
Figure 4.17: Western blot analysis of DDX3X expression in Daoy and 293 FT cells transduced with shRNAs against DDX3X and induced with doxycycline.....	173
Figure 4.18: Luciferase reporter assay to check translational regulation function of identified DDX3X mutants for mRNAs having complex 5' UTR in DDX3X knockdown 293FT clone 11.....	174
Figure 4.19: Effect of DDX3X downregulation on growth of Daoy medulloblastoma cell line.....	175
Figure 4.20: Effect of DDX3X downregulation on clonogenic potential of Daoy medulloblastoma cell line.....	177

Figure 4.21: Expression levels of 7 miR-30 family miRNA in human normal cerebellar tissues and human medulloblastoma tumor tissues analysed by Taqman Low Density array.....	180
Figure 4.22: Expression level of miR-30a in the normal cerebellum and in medulloblastoma tissues from <i>Smo</i> ^{+/+} and <i>Ptch1</i> ^{+/-} medulloblastoma mouse models.....	181
Figure 4.23: pTRIPZ-miR-30a vector construct.....	182
Figure 4.24: MiR-30a expression in the normal brain, medulloblastoma cell lines, and in the stable polyclonal populations expressing miR-30a.....	183
Figure 4.25: Effect of miR-30a expression on the growth of medulloblastoma cell lines.....	184
Figure 4.26: Effect of miR-30a expression on the clonogenic potential of Daoy medulloblastoma cell lines.....	186
Figure 4.27: Effect of miR-30a expression on the anchorage independent growth of medulloblastoma cell lines.....	187
Figure 4.28: Effect of miR-30a expression on tumorigenicity of medulloblastoma cell line.....	189
Figure 4.29: effect of miR-30a expression on autophagy in medulloblastoma cell lines.....	191

List of Tables

Table 2.1: Clinical characteristics of four molecular subgroups of medulloblastoma.....	40
Table 2.2: The molecular and genomic characteristics of molecular subgroups of medulloblastoma.....	40
Table 2.3: Summary of most common integrated medulloblastoma diagnoses with clinical correlates by WHO 2016 classification.....	43
Table 3.1: Primer sequences used for cloning of DDX3X, miR-30a and DDX3X-shRNAs.....	69
Table 3.2: Primers sequences for cloning 5'UTR, DDX3X and site directed mutagenesis.....	92
Table 3.3: Primers used for miR-30a real time PCR using SYBR green chemistry.....	104
Table 3.4: Antibodies used for Western blotting.....	134
Table 4.1: Point mutations and corresponding amino acid change in exon 3 of <i>CTNNB1</i> gene in the 11 WNT subgroup medulloblastomas as determined by Sanger sequencing.....	148
Table 4.2: Exome sequencing data statistics of the 11 WNT subgroup medulloblastoma tumors.....	149
Table 4.3: Total number of variants in the of 11 WNT subgroup medulloblastoma exomes.....	150

List of Abbreviations

APS - Ammonium persulfate

APC - Adenomatous Polyposis Coli

AR – Analytical Reagent

ATP – Adenosine triphosphate

BLAST - Basic local alignment search tool

Blbp – Brain Lipid Binding protein

CBTRUS - Central brain tumour registry of the United States

CGH – Comparative genomic hybridization

ChIP – Chromatin immunoprecipitation

CGNPs - Cerebellar Granule Neuron Progenitors

CNS - Central nervous system

CNV - Copy number variations

CSF - Cerebrospinal Fluid

CSI – Craniospinal irradiation

CTNNB1 - Beta-catenin

DDX3X - Dead box Helicase 3 X-linked

DEPC - Diethyl pyrocarbonate

DMEM - Dulbecco's Modified Eagle's Medium

DM's - Double Minute chromosomes

dNTP - Deoxynucleotide Triphosphate

EDTA - Ethylenediaminetetraacetic acid

FBS - Fetal Bovine Serum

FFPE - Formalin Fixed Paraffin Embedded

FISH - Fluorescent in situ hybridization

GAPDH - Glyceraldehyde 3-phosphate dehydrogenase

H & E - Hematoxylin and eosin

HRP - Horseradish Peroxidase

i17q - Isochromosome 17q

LC/A - Large Cell / Anaplastic

LC3B - Protein light chain 3B

LFS - Li-Fraumeni Syndrome

LMP - Low melting point

LOH - Loss of heterozygosity

LRLP - Lower Rhombic Lip Progenitor

MAPK - Mitogen-activated protein kinase

MBEN - Medulloblastoma with Extensive Nodularity

miRISC - MicroRNA induced silencing complex

miRNA - MicroRNA

MRI - Magnetic Resonance Imaging

MYC - V-Myc Avian Myelocytomatosis Viral Oncogene Homolog

OTX2 - Orthodenticle Homeobox 2

PAGE - Polyacrylamide gel electrophoresis

PBS - Phosphate Buffered Saline

PCR - Polymerase chain reaction

PNET - Primitive Neuroectodermal Tumor

PTCH1 - Patched 1

RT - Reverse Transcriptase / transcription

SCNA - Somatic Copy Number Aberrations

SDM - Site Directed Mutagenesis

SHH - Sonic Hedgehog

SMO - Smoothed

SNV's - Single Nucleotide Variations

SUFU Suppressor of Fused

TAE - Tris acetate EDTA buffer

TEMED - Tetramethylethylenediamine

UTR - Untranslated Region

WHO - World health organization

WNT - Wingless

Chapter 1

INTRODUCTION

Brain tumors are the most common solid tumors in children and among them the medulloblastoma is the most frequent. It accounts for ~ 20% of all childhood brain tumors. World health organization (WHO) classifies it as grade IV tumor, which is the highest grade of malignancy owing to its aggressive nature.[1] The risk stratification of medulloblastoma patients is carried out by taking into consideration clinical features, including the age at diagnosis, extent of surgical resection and metastatic status. Children ≤ 3 years of age or ≥ 1.5 cm² size of residual tumor post-surgery or those with leptomeningeal dissemination at the time of diagnosis are considered as high risk, and all other patients are considered as average risk. Current treatment regimen for medulloblastoma is trimodal and involves surgery followed by craniospinal irradiation (for children older than 3 years of age) and chemotherapy. Approximately 30% of the children show metastasis at the time of diagnosis. Five year event free survival of standard risk patients has been increased to more than 80%. However, patients at high risk have lower survival rates. In addition, most long-term survivors usually suffer from permanent neurocognitive impairment, endocrine dysfunction, and developmental deficit also in some cases secondary malignancies arising due to the intensive therapy administered to developing child brain [3].

Gene expression profiling studies have identified medulloblastoma to be a heterogeneous disease comprising of four core molecular subgroups. The four molecular subgroups are called WNT, SHH, Group 3 and Group 4. These four subgroups are not only distinct in their gene expression profile but also differ in terms of clinical features like overall survival rates. The WNT and SHH subgroups are associated with hyper activation of the WNT and SHH signaling pathways hence named as WNT and SHH respectively [4]. Hyper activation of WNT and SHH signaling pathways was first identified in medulloblastomas associated with two familial syndromes namely type 2 Turcot's syndrome and Gorlin's syndrome wherein germ line mutations in the

WNT pathway gene (*APC*) and SHH pathway gene (*PTCH1*) predispose patients to multiple malignancies [5, 6]. No specific signaling or developmental pathway has been yet identified to be associated with the Group 3 and Group 4 medulloblastoma. These two subgroup tumors have overlapping gene expression profile which involves a number of transcription factors involved in brain development. Expression of retina-specific genes in Group 3 and that of neuronal differentiation related genes in Group 4 distinguishes them from each other. Patients with the WNT subgroup tumors show best prognosis with ~ 95% overall survival and least incidence of metastasis. Group 3 tumors have worst survival rate of ~50% and highest incidence of metastasis at diagnosis.. SHH and Group 4 tumors have been known for the intermediate survival rates with the current treatment regimen [7].

Mutation in the *CTNNB1* gene encoding β -catenin is the predominant feature of the WNT subgroup medulloblastomas and is observed in ~90% of the WNT subgroup tumors. Apart from the activating mutation in β -catenin, loss of one copy of chromosome 6 is another alteration that is observed in ~75% cases of the WNT subgroup tumors [4]. Expression of mutant β -catenin in neural precursor cells in mouse brain has been shown to give proliferative advantage leading to increase in cerebral cortex size but does not lead to malignant tumor formation .[8]. Robinson *et al.* have also shown that expression of mutant β -catenin under *Blbp* promoter in transgenic mice disrupts the normal differentiation and migration of progenitor cells on dorsal brain stem leading to accumulation of aberrant cell collection on dorsal brain stem but this does not lead to the formation of malignant tumor. However, in the *TP53* homozygous deletion background this leads to tumor formation in approximately 15% mice after incubation of approximately 300 days [9]. Hence it is evident that mutation in β -catenin alone does not result in tumorigenesis and it requires second hit of *TP53* mutation for tumor formation. However, *TP53* mutations have been

reported in only 12.5% of the WNT subgroup tumors [10]. Therefore, it is necessary to identify additional genes responsible for pathogenesis of the WNT subgroup tumors which would also help in understanding pathogenesis of the WNT subgroup tumors and could lead to novel treatment strategies. With the advent of the next generation sequencing technology it is now possible to sequence genome more efficiently and economically. Technologies have recently been developed to capture entire coding portions / exons of all the protein coding genes from genomic DNA which can then be sequenced to get the genome-wide mutational spectrum of a tumor tissue. The present study therefore proposed to identify exome-wide mutational spectrum of the WNT subgroup tumors by sequencing exomes from the WNT subgroup tumors. Hence in the present study whole exome sequencing of 11 WNT subgroup medulloblastomas was done using the next generation sequencing (NGS) technology to identify genetic alterations other than in the β -catenin, which lead to development of the WNT subgroup medulloblastomas.

MicroRNAs (miRNAs) are small, ~ 22 nucleotide long, non-coding RNAs that function by regulating target gene expression post-transcriptionally. Single miRNA is believed to control expression of 10-100 genes [11, 12]. MicroRNA expression profiling of medulloblastoma tumor tissues carried out in our lab could distinguish the tumors, into the four molecular subgroups similar to the protein coding gene expression profiling. WNT subgroup tumors showed the most distinct miRNA profile with significant over-expression of miRNAs like miR-193a, miR-148a, miR-23b, miR-224-452 cluster and miR-365 in comparison to other subgroup tumor and normal cerebellar tissues. The miRNAs overexpressed in the WNT subgroup, including miR-193a-3p, miR-148a and miR-224 have been found to inhibit growth, invasion potential and tumorigenicity and increase radiation sensitivity when expressed in medulloblastoma cell lines indicating their functional significance in medulloblastoma biology. Expression of two microRNAs *viz.* miR-206

and miR-30a located on chromosome 6 was found to be down regulated not only in the WNT subgroup but all medulloblastoma subgroups. Earlier study from the lab has shown MiR-206 to act as a tumor suppressor gene by targeting OTX2, a known oncogene in medulloblastoma. MiR-30 family members were found to be downregulated in all the four subgroups of medulloblastoma compared to normal cerebellar tissues [13]. Downregulation of miR-30 family members has been reported in multiple cancers including breast cancer, lung cancers and colorectal cancers [14-16]. Among miR-30 family miRNAs, miR-30a is located on chromosome 6, a copy of which is deleted in more than 75% of the WNT subgroup medulloblastomas. Therefore, in the present study, role of miR-30a in the biology of medulloblastoma was investigated.

Briefly the study presented in this thesis includes

1. Exome sequencing of 11 WNT subgroup medulloblastoma tumors, identification of novel somatic alterations
2. Delineation of functional role of the *DDX3X* gene, second most commonly altered gene in the WNT subgroup medulloblastoma
3. Delineation of the role of *hsa-miR-30a* in medulloblastoma tumor cell behavior both *in vitro* and *in vivo*.

Chapter 2

REVIEW OF LITERATURE

2.1 Medulloblastoma: Epidemiology

Medulloblastoma is the most common malignant brain tumor of childhood, accounting for ~20% of all paediatric brain malignancies [1]. Approximately 70% cases occur in childhood (3 to 15 years of age), with 10-15% cases in infants (< 3 years of age). There is bi-modal distribution in age incidence, with peaks at 3 - 4 years and 8 - 9 years of age, but children of all ages can be affected. About 10% medulloblastomas also occur in adults. The disease occurs predominantly in males with a gender ratio of 1.5-2: 1 (male: female) [1]. Medulloblastoma is currently classified by WHO criteria as a grade IV tumor because of its invasive nature, metastatic capability and primitive cellular appearance [3].

2.2 Medulloblastoma Diagnosis, Risk Stratification and Treatment

Medulloblastoma patients present with symptoms of headaches, vomiting, lethargy and drowsiness. Most of these are caused by an increased intracranial pressure resulting in hydrocephalus (an excessive accumulation of fluid in the brain). The hydrocephalus in turn is a result of the blockage of the flow of Cerebrospinal fluid (CSF) in the fourth ventricle. Ataxia and behavioural changes may also be seen especially in the older children which are a result of disruption in the cerebellar function due to the tumor mass. Diagnosis is carried out primarily by using Computed tomography (CT) scan and Magnetic Resonance imaging (MRI). Imaging of the entire cerebrospinal axis as well as CSF cytology is frequently carried out to check for the presence of metastatic disease. The final diagnosis is based on histopathological analysis of the tissue resected by surgery [17].

The current risk stratification for the selection of patients for the differential treatment regimens stratifies patients in two categories *i.e.* (1) Standard risk and (2) High risk based on three factors

(a) age at diagnosis, (b) extent of tumor resection and (c) Chang metastasis staging [3]. Children ≤ 3 years of age or with a ≥ 1.5 cm² size of residual tumor post-surgery or those exhibiting leptomeningeal dissemination at the time of diagnosis are all considered to be high risk, and all other patients are treated as average risk. The age of the patient is an important criterion in the risk stratification since the therapeutic approach for infants includes avoidance of cranio-spinal radiation to minimize the adverse effects on the developing brain. WHO classifies medulloblastoma into four histological subtypes- classic, desmoplastic, large cell / anaplastic (LC/A) and medulloblastoma with extensive nodularity (MBEN) [3]. The LC/A histology is often associated with a poor prognosis. With the advent of the molecular subgrouping of medulloblastoma, changes in the risk stratification protocol are currently being considered .[18].

The treatment of medulloblastoma is trimodal with surgery being a primary mode of treatment followed by cranio-spinal irradiation (CSI) and chemotherapy. The standard risk patients receive reduced dose CSI of 23.4 Gy with a localized boost to posterior fossa to a total of 55.8 Gy, combined with a concurrent single drug chemotherapy followed by a multi-drug chemotherapy (Ref). The addition of adjuvant chemotherapy allowed the dose of CSI to be reduced from 36 Gy to 23.4 Gy without a significant decrease in survival, as demonstrated by an event free survival of 61-81% at 5 years, while better preserving neurocognitive function [19]. Protocols for high-risk patients generally include full-dose CSI of 36 Gy with a similar localized boost to posterior fossa with concurrent single drug chemotherapy and a more aggressive adjuvant regimen. With this treatment regimen, survival rates in high risk category are found to range from 43% -70% of five year event free survival, with a degree of compromise in neurocognitive function [19]. However, this current strategy of clinical risk stratification has been found to have several shortcomings (1). The disease recurs in 20-40% of standard risk patients indicating incorrect

classification, resulting into delay in giving more aggressive therapy. (2). Current risk stratification fails to identify many patients who meet high risk criteria, but could have been cured with low risk treatment regimens, and thus avoiding unnecessary neuro-cognitive decline and other side effects (3). By categorizing patients into only two categories, current clinical risk stratification inappropriately simplifies the true heterogeneity of tumor behaviour, consequently diluting efforts to titrate treatment more accurately.

2.3 Medulloblastoma: Historical view



Figure 2.1: Sagittal MRI following gadolinium injections shows dense white medulloblastoma tumor marked in circle [20].

Originally identified in 1925 by Cushing and Bailey as a “spongioblastoma cerebelli”, medulloblastoma was described as an undifferentiated neuro-epithelial neoplasm of the cerebellar vermis (midline) or,

infrequently the cerebellar hemispheres (lateral) (Fig. 2.1) [20]. However, they soon conceded that ‘spongioblast’ was not a well characterized individual cell type of central nervous system (CNS) and in 1925 they abandoned the spongioblast origin in favor of derivation from a hypothetical multipotent cell, the ‘medulloblast’ [21]. The medulloblast was thought to be one of the five stem cells populating the primitive neural tube. Although the existence of such a cell has never been proved, the name of medulloblastoma has stuck with sub-class of a broad category of tumors known as embryonal tumors. In 1973, Hart and Earle proposed that medulloblastoma like tumors occasionally observed in cerebral hemispheres should be named as primitive neuroectodermal tumors (PNETs) (ref). In 1983 L. Rorke proposed that this term be applied to large variety of embryonal CNS tumors, including medulloblastoma, ependymoblastoma, neuroblastoma and the pineoblastoma. The basis for this nomenclature was the assumption that PNETs share a common progenitor cell population, believed to be subependymal matrix layer and that their neoplastic transformation at various levels of the CNS leads to the tumor with similar morphology and biology [21]. However, after following this nomenclature for more than a decade, controversies for this classification started with the increasing evidences supporting that at least a subset medulloblastomas originates from external granular layer (EGL) of the cerebellum. This hypothesis was strongly supported by occasional presence of *PTCH1* mutations in medulloblastomas since the sonic hedgehog pathway controls cell proliferation in EGL during embryonal development [22]. Other alterations typically involved in the evolution of medulloblastomas, e.g. β -catenin and APC mutations were absent in pineoblastomas and extracerebellar PNETs further supported these controversies. The response to radiation therapy and chemotherapy also differed in that patients with supratentorial PNETs (SPNETs), particularly pineoblastomas, have a less favorable prognosis compared to medulloblastoma [23].

These differences in clinical and experimental findings led to the new WHO classification 2000, which kept the cerebellar medulloblastoma and its variants separate from supratentorial PNETs. Microarray based expression profiling analysis by Pomeroy *et al* was the first to clearly show that medulloblastoma constitutes a distinct tumor type with a distinguishable molecular profile, and is distinct from PNETs as well as Atypical teratoid and rhabdoid tumors (AT/RT) [24].

2.4 Medulloblastoma: Result of developmental mechanism out of control

The studies on the cytogenetic aberrations in medulloblastoma identified the isochromosome 17q (i17q), in which loss of the p arm of chromosome 17 occurs in the context of a 17q gain, as the most frequent chromosomal abnormality in this disease. Isochromosome 17q occurs in 40-50% of tumors and has been found to be associated with unfavorable prognosis [25]. Amplification of the *MYC* locus on 8q24, often in the form of Double Minute chromosomes (DM's), was reported in multiple medulloblastoma cell lines and confirmed in primary tumors. The *MYC* family of protooncogenes remain among the most prevalent targets of gene amplification in medulloblastoma [26, 27]. Medulloblastoma was thought to be a cancer originated from deregulation of developmental pathways because of its prevalence in children and occurrence in the part of brain i.e. cerebellum that develops postnatally. It was also postulated that the presence of both glial and neuronal differentiation markers in these tumors could be because of their cell of origin being a neural stem cells, suggesting cause of tumorigenesis lying in deregulated cerebellar development [28]. Initial evidence regarding involvement of developmental pathways in medulloblastoma came from the identification of germ line mutations in the *PTCH1* gene that encodes for a membrane bound receptor in sonic hedgehog (SHH) signaling pathway, in patients with Gorlin's syndrome. Patients suffering from this familial syndrome were known to be

susceptible to medulloblastoma and basal cell carcinoma [29]. The *PTCH1* gene was known to be a part of the SHH signaling pathway, indicating to the role of this signaling pathway in the pathogenesis of medulloblastoma. Subsequently mutations in *PTCH1*, *SMO* and *SUFU* genes involved in the SHH signaling pathway were identified in sporadic medulloblastomas as well [30-32]. Evidence for involvement of the WNT signaling pathway in medulloblastoma came from the identification of germ line mutations in the adenomatous polyposis coli (*APC*) gene in patients with Turcot's type II syndrome. These patients showed predisposition towards developing colorectal cancers and medulloblastoma. *APC* gene is a tumor suppressor gene that negatively regulates cytoplasmic β -catenin expression, which is the key effector of WNT signaling pathway [33]. While *APC* mutations predominantly occur in familial medulloblastomas they were also found in some sporadic medulloblastomas [34]. Sporadic medulloblastomas were found to carry mutations in additional WNT signaling pathway genes including activating mutations in *CTNNB1* and *AXINI* [35, 36].

2.4.1 WNT signaling pathway

The WNT signaling pathway has been implicated to play role in wide array of biological processes ranging from embryogenesis to stem cell pluripotency and cell fate decision during development [40]. The *WNT1* gene, originally named Int-1, was identified in 1982 as a gene activated by integration of proviral DNA of mouse mammary tumor virus in an attempt to identify genes that could cause breast cancer. The fly Wingless (*wg*) gene, which controls the segment polarity during larval development, was later shown to be homolog of Wnt1. The name WNT hence was derived from the fusion of Wingless and Int-1. Wnt ligands, a family of secreted cysteine rich glycosylated proteins, signal by two pathways: canonical (Wnt-1, Wnt-3a

and Wnt-8) and non-canonical (Wnt-4, Wnt-5a) [37]. A key component of the canonical WNT signaling pathway is β -catenin. In the absence of Wnt ligands, cytoplasmic β -catenin is recruited into the destruction complex where it is N-terminal phosphorylated by Casein kinase-1 (CK-1) and Glycogen synthase kinase-3 beta (GSK-3 β). Upon phosphorylation, β -catenin is recognized by E3 ubiquitin ligase beta transducing repeat containing protein (β -TrCP) which targets it for proteasomal degradation, ensuring that cytoplasmic levels of β -catenin remain low. Activation of canonical WNT signaling pathway is initiated by binding of ligand Wnt to a receptor complex composed of a seven-pass transmembrane receptor Frizzled (FZD) and its co-receptor low density lipoprotein receptor-related protein 5 (LRP5) or LRP6 in the plasma membrane. This interaction can be inhibited by secreted frizzled-related proteins (SFRPs), Dickkopf (DKK) family proteins and WNT-inhibitory factor 1 (WIF1) that act as negative regulators of this pathway. Next, Dishevelled (DSH) is recruited to the plasma membrane where it interacts with frizzled to mediate translocation of AXIN to the membrane and destabilization of the multi-protein complex, APC/AXIN/GSK-3 β . This inactivation enables the stabilization and further translocation of β -catenin to the nucleus where it forms a complex with TCF/LEF transcription factors. In absence of β -catenin, these proteins bind to Groucho family of proteins and repress target gene expression, while in complex with β -catenin, TCF/LEFs activate transcription of target genes like MYC, CCND1 (Fig. 2.2) [38]. Mutations in the WNT pathway genes *CTNNB1*, *APC* and *AXIN1* have been identified in approximately 10% of sporadic medulloblastomas in mutually exclusive manner [39].

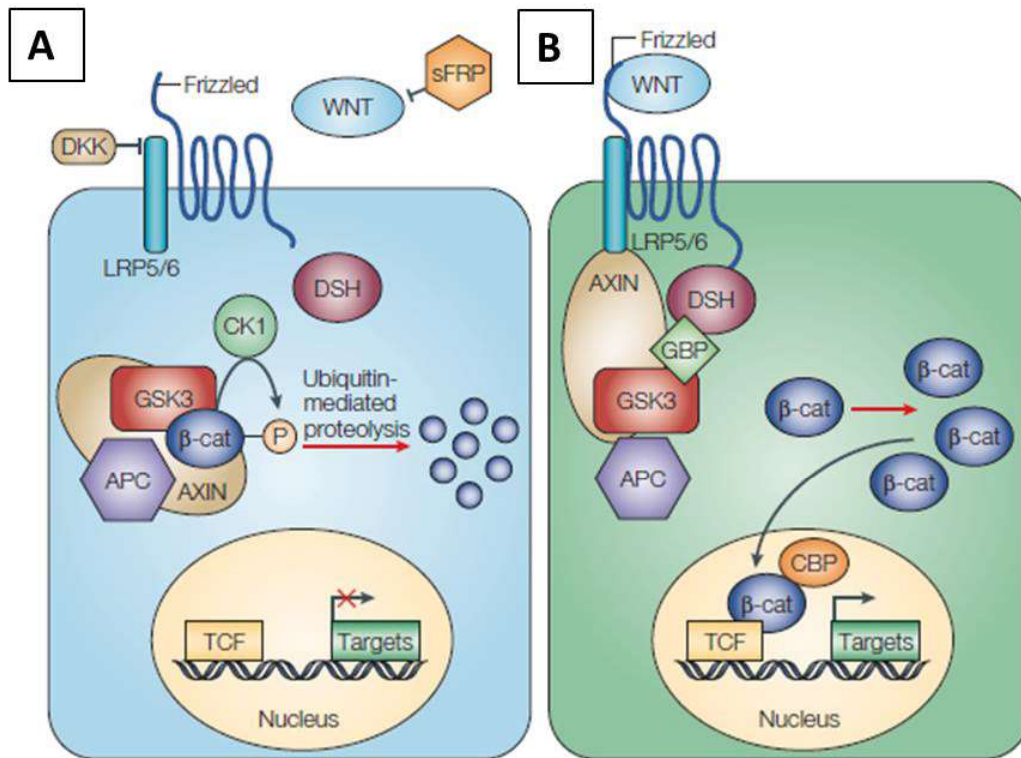


Figure 2.2: The canonical WNT signaling pathway. A) In the absence of WNT ligand (Inactive). B) In the presence of WNT ligand (Active).[40]

2.4.2 Sonic Hedgehog (SHH) signaling pathway

The SHH signaling pathway plays an important role in embryonic development with involvement in stem cell maintenance, proliferation and differentiation [41]. Early studies in *Drosophila* and mouse cell culture models established the mechanism of hedgehog signal transduction pathway. During hedgehog pathway signaling binding of SHH ligand to its receptor patched 1 (PTCH1), a 12-pass transmembrane protein relieves repression mediated by smoothed (SMO), a 7-pass transmembrane protein and activates signaling cascade that ultimately drives activation of GLI family of transcription factors. These transcription factors

activate target genes like *CCND1*, *N-Myc*. While in absence of the ligand SHH, PTCH1 inhibits the activity of SMO and suppressor of fused (SUFU) inactivates the GLI transcription factors to

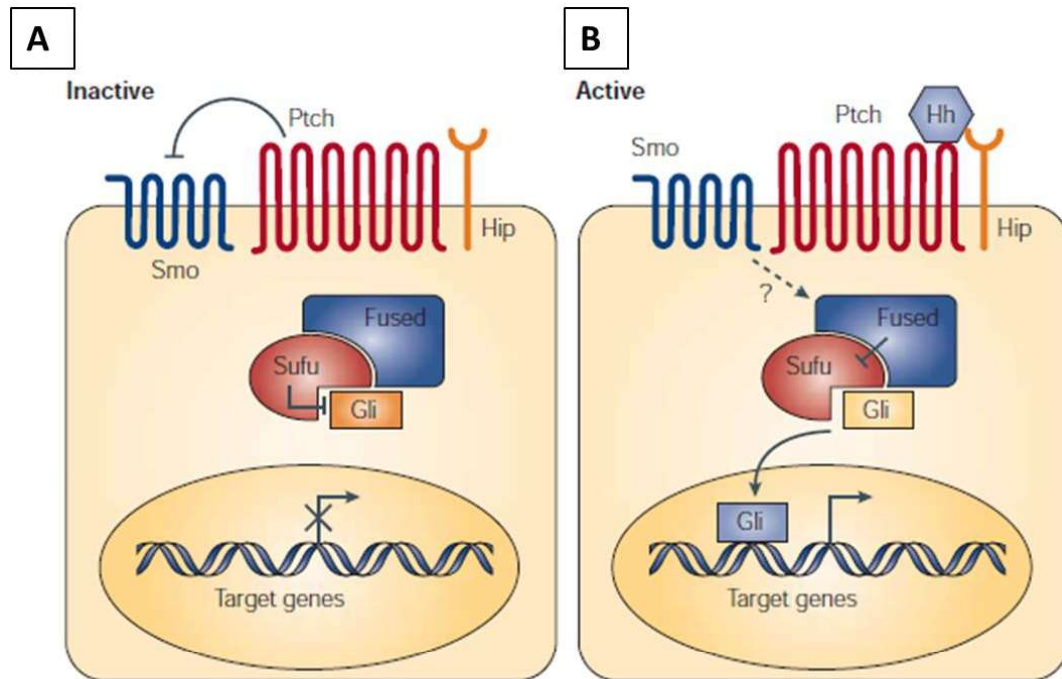


Figure 2.3: SHH signaling. A) In the absence of hedgehog ligand (Inactive). B). In the presence of hedgehog ligand (Active).[39]

prevent the SHH target genes from being transcribed (Fig. 2.3). The SHH pathway controls the normal development of the external granular layer (EGL) of developing cerebellum. SHH produced by purkinje cells results in induction of GLI family of transcription factors in cerebellar granule neuron precursor cells through activation of target genes like *Cyclin D1* (*CCND1*), *N-MYC* (*MYCN*) as a result of which these cells proliferate to form external granule layer during cerebellar development [41]. Mutations in SHH pathway genes (*PTCH1*, *SMO* and *SUFU*) have been identified in 25% of medulloblastoma in mutually exclusive manner.[39]

2.5 Medulloblastoma: Expression profiling leading to current consensus of subgrouping

Array Comparative Genomic Hybridization (CGH), Single Nucleotide Polymorphism (SNP) profiling and microarray based gene expression profiling studies of medulloblastomas performed by various groups have revolutionised the understanding of medulloblastoma biology.. A series of gene expression studies have led to identification of molecular subgroups of medulloblastoma. Thompson *et al.* in 2006, for the first time showed the existence of 5 molecular subgroups in a study of 46 medulloblastomas [42]. Even though monosomy of chromosome 6 was previously reported in medulloblastoma but this was the first study reporting the association of monosomy of chromosome 6 with mutations in *CTNNB1* gene. In this study Monosomy 6 and *CTNNB1* mutations were found to be mutually exclusive to *PTCH1* and *SUFU* mutations in medulloblastoma tumor tissues [42]. The study by Kool *et.al.*, in 2008 recapitulated earlier findings in a separate cohort of 62 medulloblastomas and showed the existence of 5 unique molecular subgroups of medulloblastomas having WNT or SHH signaling pathway activation as distinct subgroups and additional three subgroups of non-WNT non-SHH medulloblastomas [43]. The WNT and SHH tumors were shown to be very distinct in their expression profiles unlike as in study by Thompson *et al.* However, the non-WNT, non –SHH tumors were found to have an overlapping gene expression signature. This study also showed for the first time the association of increased metastasis rate in the non- WNT, non-SHH tumors. A strong correlation between patient age, gender, histology and molecular subgroups was shown by this study [43]. Gene expression profiling study by Northcott *et.al* on 103 tumors showed that medulloblastomas can be subgrouped with the highest confidence into four core molecular subgroups. Northcott *et al.* also showed the existence of subgroup association with the age, histology, chromosomal alterations and survival [44]. The study by Cho and colleagues on 194 medulloblastomas

identified six subgroups [45]. This included one WNT, one SHH and four non-WNT, non-SHH subgroups. Notably, the tumors carrying *MYC* amplification were found to have the worse prognosis within the tumors with the retinal gene expression signature commonly considered as group 3 tumors. This subgrouping of tumors was found to be of significance in the risk stratification of tumors based on their molecular subgroup [45]. Concurrent with the study by Northcott *et al.* in 2010, our group also identified 4 molecular subgroups of medulloblastomas by performing gene expression profiling of 19 medulloblastomas using Affymetrix Gene 1.0 ST array. These four molecular subgroups closely matched those reported by Northcott *et al* study [13].

In 2012, a meeting in Boston was held to resolve the differences in number of subgroups and their nomenclature reported by various groups and a consensus regarding the molecular subgroups was reached [4]. This supported the existence of four core molecular subgroups namely the WNT subgroup, SHH subgroup, Group 3 and Group 4 based on their gene expression profiles. This reaffirmed the fact that medulloblastoma is not a single disease entity but is composed of four core molecular subgroups that differ in their underlying biology, clinical presentation and demographics [4].

2.5.1 WNT subgroup

The WNT subgroup accounts for approximately 10-15% of all medulloblastoma tumors. WNT subgroup tumors occur often in older children and adults with median age of diagnosis of approximately 10 years. The male to female ratio in WNT subgroup patients is 1:1 [46]. However its incidence is almost double in the Indian cohort studied in our lab [47, 48]. These tumors frequently show classic histology. WNT subgroup is the best prognosis subgroup. These

patients are treated with standard risk treatment regimen and show overall survival rate of more than 90%. The tumors rarely show leptomeningeal dissemination. The WNT subgroup tumors show aberrant activation of WNT signaling pathway as a result of somatic mutation in the *CTNNB1* gene encoding β -catenin that occurs in > 90% of these tumors. This leads to activation of WNT signaling pathway genes including *WIFI*, *DKK1*, *LEF1*, *CCND1* and *MYC* in these tumors. A small proportion of WNT subgroup tumors show inactivating mutation in the WNT signaling inhibitor genes *APC* and *AXINI*. Presence of monosomy 6 is the most frequent chromosomal alteration in these tumors and is seen in > 75% of tumors [4, 39]. The lower rhombic lip progenitor (LRLP) cells have been indicated as the cells of origin for this subgroup giving rise to tumors closer to the brain stem rather than in the cerebellar hemispheres, in a mouse model of this subgroup [49].

2.5.2 SHH subgroup

The SHH subgroup accounts for approximately 25-30% of all sporadic medulloblastomas. Desmoplastic histology is most commonly associated with the SHH subgroup although the tumors of this subgroup may show classic or less often LC / A histology as well. It also has a 1.5:1 male to female ratio. The age distribution for this subgroup is bimodal with frequent incidence in both infants (0–3 years) and adults (> 16 years). These tumors are located often in the cerebellar hemispheres and rarely at midline. SHH patients are heterogeneous in survival rates with some having excellent survival while others in particular those with large cell anaplastic histology and/or presence of metastasis at diagnosis or *MYCN* amplification having poor prognosis. Overall SHH patients show intermediate survival rates of 60-80%, with metastasis at diagnosis in 20% of patients [46]. Approximately 25% of SHH tumors show

somatic mutations in one of the SHH pathway genes (*PTCH1*, *SUFU* and *SMO*) leading to activation of SHH signaling pathway and high expression of the SHH pathway genes including *HHIP1*, *EYA1* and *PDLIM3*. Common cytogenetic and mutational events include loss of chromosome 9q in 30-40% (harbouring the *PTCH1* gene), and 10q in addition to focal amplification of *GLI2*, *MYCN* and focal deletion of *PTCH1* [4]. The cerebellar granule neuron progenitors (CGNPs) that proliferate in response to SHH secreted by purkinje cells during the development of cerebellum have been identified as the cell of origin of these tumors [50]. This is the most well studied subgroup due to its initial characterization based on germline mutations in the *PTCH1* gene in Gorlin's syndrome patients and availability of mouse models of the disease. Two mouse models of this subgroup were the first of medulloblastoma mouse models to be established and have been extensively studied. The *Ptch1*^{+/-} mice with a tumor incidence of 15-20 % by six months of age and the *Smo*^{+/+} mice with an incidence of up to 90 % by 2-3 months of age are mouse models of medulloblastoma resulting from SHH pathway activation [51, 52]. Pharmacological small molecule inhibitors of *SMO* activity have been tested in phase 1 clinical trials, however the tumors were found to acquire additional mutations leading to rapid disease progression [53]. Nonetheless a combination therapy with the *SMO* inhibitor and PI3K inhibitors, has shown promise in pre-clinical studies of medulloblastoma [54].

Table 2.1: Clinical characteristics of four molecular subgroups of medulloblastoma. Percentages in parenthesis indicate percentage contribution of indicated subgroup tumors in all medulloblastomas.

Subgroup	WNT (10%)	SHH (30%)	Group 3 (25%)	Group 4 (35%)
Characteristics				
Survival	95%	75%	50%	75%
Metastasis	5-10%	15-20%	40-45%	35-40%
Age distribution	Older children and adults	Infants, Children and adults	Infants and young children	Older children and young adults
Histology	Classic, very rarely LCA	Classic > desmoplastic > LCA	Classic > LCA	Classic, rarely LCA
Gender Ratio	1:01	1.5:1	2:01	3:01

Table 2.2. Molecular characteristics of the four molecular subgroups of Medulloblastomas
Percentages in parenthesis indicate percentage contribution of indicated alteration in the subgroup

Subgroup	WNT (10%)	SHH (30%)	Group 3 (25%)	Group 4 (35%)
Characteristics				
Gene Expression	WNT signaling	SHH signaling	Common gene expression signature (LEMD1, FOXG1, EOMES)	
			Photoreceptor genes	Neuronal differentiation related genes
Chromosomal Alterations		3q gain (27%)	i17q (26%) 1p gain (35%) 7 gain (55%)	i17q (66%) 7 gain (47%)
	Monosomy 6 (75%)	9q loss (47%)	8p loss (33%) 16q loss (50%)	8p loss (41%)
Mutations	CTNNB1 (90%) TP53 (12.5%)	PTCH1 (28%) TP53 (13.8%)	-	-
Focal Amplification	-	MYCN (8%) GLI2 (5%)	MYC (17%) PVT1 (12%) OTX2 (8%)	SNCAIP (10%) MYCN (6%) CDK6 (8%)

2.5.3 Group 3

Group 3 tumors account for approximately 25% of all sporadic medulloblastomas. These tumors are more common in males, showing 2:1 male to female ratio. They occur almost exclusively in infants (< 3 y) and young children (3-16 y). This molecular subgroup is associated with multiple markers associated with poor outcome, including large cell / anaplastic histology, focal *MYC* amplifications and metastatic dissemination. Group 3 medulloblastomas are highly metastatic with approximately 45% patients showing metastasis at the time of diagnosis. These patients show 5-year survival of less than 50%. Thus group 3 patients have the lowest survival rates among four subgroups [46]. The drivers of Group 3 pathogenesis remain to be fully elucidated. Genomic amplification and overexpression of *MYC* (17%) and *OTX2* (11%) are seen in a mutually exclusive pattern [46]. Group 3 tumors have an overlapping gene expression signature with group 4 tumors that includes transcription factors involved in brain development, like *EOMES*, *FOXP1*, a testes specific gene *LEMD1*. The photoreceptor gene expression is specific to the Group 3 tumors which distinguishes it from the Group 4 tumors [13]. Cytogenetically, Group 3 medulloblastomas have the largest number of both broad and focal copy number alterations, including loss of chromosome 8p, 16q as well as gains of 1q and 7 among others. The most commonly observed chromosomal aberration is the isochromosome 17q, seen in approximately 26 % of group 3 tumors [4, 39].

2.5.4 Group 4

This subgroup constitutes approximately 35% of all medulloblastomas. It occurs at all ages, however rare in infants. Similar to group 3 tumors, classic and LCA histology is seen in group 4 tumors. There is a substantial gender bias observed in the Group 4 tumors, with the tumors occurring three times more frequently in males than in females. Approximately 35-40% patients

show metastasis at the time of diagnosis. Five year survival rate is ~75% for group 4 tumors. Therefore this group is considered to have intermediate prognosis with patients responding better to treatment than group 3 [46]. The mechanism of pathogenesis of this subgroup is least understood. No specific deregulated signaling pathways that predispose to group 4 tumors have been yet identified. Group 4 medulloblastomas demonstrate an overlapping gene expression signature with that of the group 3 tumors as described above. In addition these tumors show a neuronal signature including many genes associated with neuronal differentiation like *GRM8*, *KCNAI* and *UNC5D* and glutamate/GABA signaling which is distinct from the group 3 tumors [13]. Although isochromosome 17q is observed in both group 3 and group 4 tumors, it is more defining feature of Group 4 tumors as it occurs in approximately 66% of these tumors and remain associated with poor prognosis. Other cytogenetic alterations in Group 4 include loss of Chromosome.11p, Chromosome 8 and the X-chromosome, along with gains of Chromosome 7 and 18q. Additionally, focal amplifications of *CDK6* and *MYCN* are also observed. Recently, Northcott *et al.*, identified a tandem duplication of *SNCAIP*, a gene associated with Parkinson's disease and neurodegeneration in 10% of these tumors [55]. Although, the functional significance of this alteration is not yet known, mutual exclusivity of *SNCAIP* duplications to the other most common alterations in group 4 namely *MYCN* and *CDK6* amplification and their occurrence along with i17q indicates their possible role as one of the driver alterations underlying group 4 tumorigenesis [10, 55].

2.6 World Health Organisation (WHO) classification of medulloblastoma 2016

For the first time in 2016, in classification of tumors of the Central Nervous System, WHO used molecular parameters in addition to histology to define tumor entities, thus formulating a concept

that how CNS tumors to be diagnosed in molecular era. it is now widely accepted that there are four core molecular subgroups viz. WNT, SHH, Group 3 and Group 4 of medulloblastomas that have distinct clinical features. To generate more integrated diagnosis in case of medulloblastoma, the new WHO classification lists ‘histologically defined’ and ‘genetically defined’ medulloblastoma variants (Table 2.3) [56].

Table 2.3: Summary of most common integrated medulloblastoma diagnoses with clinical correlates by WHO 2016 classification [56].

Genetic profile	Histology	Prognosis
Medulloblastoma, WNT-activated	Classic	Low-risk tumour; classic morphology found in almost all WNT-activated tumours
	Large cell / anaplastic (very rare)	Tumour of uncertain clinicopathological significance
Medulloblastoma, SHH-activated, TP53-mutant	Classic	Uncommon high-risk tumour
	Large cell / anaplastic	High-risk tumour; prevalent in children aged 7–17 years
Medulloblastoma, SHH-activated, TP53-wildtype	Desmoplastic / nodular (very rare)	Tumour of uncertain clinicopathological significance
	Classic	Standard-risk tumour
	Large cell / anaplastic	Tumour of uncertain clinicopathological significance
Medulloblastoma, non-WNT/non-SHH, group 3	Desmoplastic / nodular	Low-risk tumour in infants; prevalent in infants and adults
	Extensive nodularity	Low-risk tumour of infancy
	Classic	Standard-risk tumour
Medulloblastoma, non-WNT/non-SHH, group 4	Large cell / anaplastic	High-risk tumour
	Classic	Standard-risk tumour; classic morphology found in almost all group 4 tumours
	Large cell / anaplastic (rare)	Tumour of uncertain clinicopathological significance

2.7 Understanding pathogenesis of the WNT subgroup medulloblastoma

As described earlier, approximately 90% of the WNT subgroup tumors show mutation in *CTNNB1* gene that encodes β -catenin leading to aberrant activation of WNT signaling pathway. Mutation in other WNT signaling pathway genes like *APC* and *AXINI* has been reported in very few cases. Apart from β -catenin mutation, monosomy of chromosome 6 is the only known

predominant alteration in WNT subgroup of medulloblastoma. Common tumor suppressor gene like *TP53* mutation is also very low (12.5%) in WNT subgroup medulloblastoma [4, 10]. WNT signaling is known to play important role in biological process from embryogenesis to maintenance of pluripotency of stem cell and stem cell fate determination but it is also well established by various studies that mutation in β -catenin alone cannot result in tumor formation [37, 40]. Chenn *et al.* in 2002, reported that expression of truncated β -catenin in subventricular zone precursor cells *in utero* under control of the nestin promoter lead to transgenic embryos with enlarged brain size with increased cortical surface area, but there was no tumor formation. They showed that truncated β -catenin can regulate the size of the neural precursor pool by influencing the decision to divide or differentiate, without increasing cell cycle rate, decreasing cell death or grossly altering neuronal differentiation and hence leading to enlarged brain and increased cerebral cortex size [8]. Chenn *et al.* in their another study showed that brain of adult transgenic animals over expressing stabilized β -catenin had remarkable change in brain size with enlarged forebrain but not the tumor formation [57]. Another study by Kratz *et al.* in adult murine transgenic animals has shown that upon postnatal expression of mutant β -catenin in differentiated neurons or glial cells no tumors, no pre-neoplastic changes or other CNS morphological alterations were detected [58].

Study by Gibson *et al.* gave more insight in understanding of WNT subgroup medulloblastoma tumorigenesis [49]. They showed that the genes specifically expressed in the human WNT subgroup medulloblastoma are more frequently expressed in lower rhombic lip (LRL) and embryonic dorsal brain stem than upper rhombic lip (URL) and developing cerebellum suggesting that SHH and WNT subgroup of medulloblastomas arise from distinct regions of hindbrain. They showed that ventricular zone cells expressing mutant β -catenin under *Blbp*

promoter (hind brain progenitor specific promoter) did not show any defect in proliferation, apoptosis or differentiation. Whereas at E16.5 mutant β -catenin expressing mice showed aberrant cell mass collection (expressing Olig3 and Pax6 LRL progenitor specific markers) in dorsal brain stem indicating that mutant β -catenin disrupts the normal differentiation and migration of progenitor cells in dorsal brain stem. This collection of cell mass persisted into adulthood but did not lead to tumor formation in wild type *TP53* background, but in homozygous *TP53* deletion background tumor formation was observed in 15% of mice. Even though these tumors exhibited expression and anatomical profile similar to human WNT subgroup medulloblastoma, they arose at a relatively longer latency (after more than 300 days of incubation) and with lower penetrance of 15% [49]. This indicated that second hit in terms of *TP53* mutation is required for transformation of LRL progenitor cells harbouring mutant β -catenin. However, *TP53* mutations are reported in only ~12.5% cases of WNT subgroup medulloblastoma [10]. Therefore, there must be some other genetic alteration/s as additional hits to *CTNNB1* mutation in WNT subgroup medulloblastoma, which may be present on either chromosome 6 or on other chromosomes that brings about tumorigenesis of the WNT subgroup medulloblastoma. Hence in the present study, exome sequencing of the WNT subgroup tumors was done to identify other genetic alteration apart from mutant β -catenin followed by investigating their functional role in WNT subgroup tumor pathogenesis.

2.8 DDX3X: A member of the DEAD Box Family Helicase

DDX3X (present on the X-chromosome) belongs to a highly conserved subfamily of the DEAD (Asp-Glu-Ala-Asp) box containing RNA helicases. In females, this gene escapes the X-chromosome inactivation. In the budding yeast, there are 25 members of the DEAD box family

and most of these are essential for viability and are not interchangeable indicating unique role for each of the DEAD box family members. *DDX3X* has orthologous genes in all eukaryotes ranging from yeast, plants and animals. Its paralogue *DDX3Y* present on the human Y chromosome is expressed at protein level, only in the testes and is necessary for normal spermatogenesis [59].

2.9 Structure of DDX3X core domain and their functions

RNA and DNA helicases are enzymes that catalyze unwinding of DNA/RNA duplexes in an energy dependent manner. They utilize free energy change of binding and hydrolyzing a nucleotide triphosphate. The family of RNA and DNA helicases are further classified in superfamilies based on the presence of conserved motifs. DDX3X belongs to SF2 superfamily, members of this superfamily are active as monomers or dimers. DEAD family and closely related DExD and DExH family helicases share conserved motifs clustered in the central region consisting of 350-400 amino acids. The N-terminal and C-terminal extension on the other hand differ among the family members but are often conserved among orthologs, indicating role of these domains in specific function of each of the helicase [60]. Like other members of DEAD box helicase family, DDX3X consists of central core structure containing two globular RecA like domains called domain I and domain II. Both domain I and II have a fold belonging to RecA superfamily that contains 5 beta-strands surrounded by 5 alpha-helices. The full length DDX3X protein consists of 662 amino acids and has ATPase and RNA unwinding activity. A truncated form (V168-G582) of DDX3X has been co-crystallized with AMP and its structure is studied, which showed that DDX3X central helicase core consists of 12 conserved motifs. These motifs are involved in ATP binding, RNA binding and linking the two processes [61]. The specific motifs involved in each of these processes are shown in Fig.2.4. A recent study has shown that the N-terminal amino acids (135-168), known as ATP-binding loop, interacts with ATP in an

RNA-stimulated manner [62]. DDX3X and DDX3Y share an additional conserved motif (AA 250-259) inserted in between motifs I and Ia. This insertion is a part of a 43 amino acid long region present between nucleotide binding motif I and RNA binding motif Ia that was found to form an alpha helix positioning a positive loop in close proximity to a putative RNA ligand. This DDX3X/Y specific insertion motif was shown to be important for ATP hydrolysis and RNA/DNA unwinding [61].

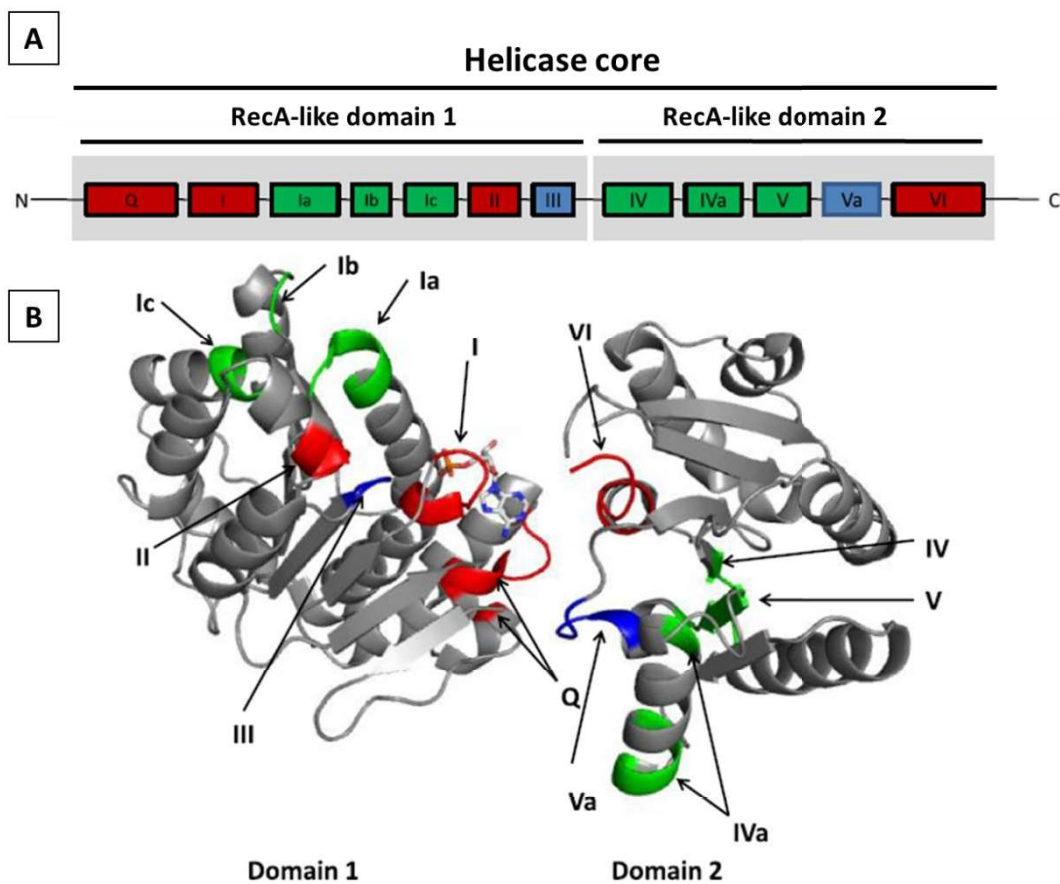


Figure 2.4: The structure of DEAD-box RNA helicase, DDX3X [63].

A. The Core Domain structure of the DDX3X. The motifs in red color are involved in ATP binding, motifs in green color are involved in RNA binding and motifs in blue are involved in linking the two processes. B. Crystal Structure of DDX3X bound with AMP, showing the two helicase core globular subdomains. The color pattern is same as in A.

2.10 Functions of DDX3X in RNA metabolism

The secondary structure of RNA and its interaction with other proteins are important for the function of RNA and the cell as a whole. This process is regulated by chaperons like RNA helicases, which are able to unwind or displace the bound protein in an energy dependent manner. DDX3X is a RNA helicase and has ATPase and helicase activity. It is abundantly expressed in all tissues. So, it has been found to play multiple roles in RNA metabolism including transcription, splicing, translation and mRNA transport [64].

2.10.1 DDX3X as a regulator of transcription

DDX3X has been shown to be a critical component of the TBK1/IKK ϵ mediated induction of the anti-viral Interferon I signaling pathway. DDX3X acts as a scaffold facilitating interaction between TBK1/IKK ϵ that results in phosphorylation mediated activation of IRF3 transcription factor and subsequent induction of the IFN- β promoter. N-terminal domain (1-408 AA) of DDX3X was found to be sufficient for the induction of the IFN- β promoter [65]. Upregulation of the CDK inhibitor p21 by DDX3X was found to be dependent on the ATPase activity but independent of helicase activity of DDX3X. Binding sites for the transcription factor SP1 in the p21 promoter region were found to be essential for DDX3X mediated transactivation of p21 promoter, although it is not known if DDX3X binds directly or indirectly to the p21 promoter region [66]. DDX3X has been shown to downregulate E-cadherin expression by association with the E-cadherin promoter region as demonstrated by chromatin immunoprecipitation assay [67, 68]. DDX3X has been found to be a subunit of the mammalian mediator complex further supporting its role in transcription activation [69]. DDX3X has also been suggested to play role

in mRNA splicing as it has been reported to be associated with functional spliceosome but nothing more is known about role of DDX3X in splicing [63, 70].

2.10.2 Role of DDX3X in mRNA export

DDX3X interacts with two nuclear export shuttle proteins TAP and CRM1. TAP is the main mRNA exporter and C-terminal of DDX3X (residues 536-661) interacts with TAP. Studies have shown that DDX3X is not required for general mRNA export but it is possible that it is required for nuclear exports of a particular subset of mRNA via TAP. CRM1 is the receptor that exports proteins containing leucine rich Nuclear Export Signal (NES). This CRM1-DDX3X interaction is exploited by HIV to export its incompletely spliced RNA from nucleus into cytoplasm. The CRM1 interaction is mediated by residues 260 to 517 of DDX3X [71, 72].

2.10.3 DDX3X as a regulator of translation

Localization of DDX3X in stress granules under stress conditions suggested role for DDX3X in translational control. A number of studies have reported DDX3X interaction with multiple components (eIF3, eIF4A, eIF2 α , PABP1) of the translation initiation machinery [73-75]. Translation of HIV-1 RNA has been found to be repressed in DDX3X depleted cells while the global translation was not significantly affected [64]. DDX3X has been found to promote translation of viral and cellular RNAs having complex 5'UTRs. DDX3X S382L mutant that lacks helicase activity fails to promote translation of RNAs with complex UTRs indicating regulation of translation requires the helicase activity [76]. On the other hand, overexpression of DDX3X has been shown to result in translocation of DDX3X protein to stress granules along with components of the translation initiation machinery, thus inhibiting translation. DDX3X

overexpression has also been shown to inhibit cap-dependent translation by interacting with eIF4E that results in disruption of cap binding complex [75, 77].

2.11 Role of DDX3X in apoptosis

Initial study by Jope *et al.* have shown anti-apoptotic role for DDX3X. They have shown that DDX3X forms an anti-apoptotic complex with GSK-3 β and cellular inhibitor of apoptosis protein-1 (cIAP-1). This anti-apoptotic complex binds to death receptor and inhibits the apoptosis [78]. However another study by Sun *et al.* has shown that, following DNA damage, DDX3X regulates apoptosis in a p53-dependent manner [79]. In cells expressing wild type p53, DDX3X associates with p53, increases p53 accumulation, and positively regulates camptothecin induced apoptotic signaling via activation of caspase 7. Paradoxically, in cells expressing mutant or non-functional p53, DDX3X inhibits apoptosis by reducing caspase 3 activation [79].

2.12 The debatable role of DDX3X as an oncogenic or a tumor suppressor in cancer

Recurrent truncating mutations in the *DDX3X* gene have been reported in Chronic Lymphocytic Leukemia while homozygous deletions reported in the gingivo-buccal oral squamous cell carcinomas from the Indian tobacco chewers and in HPV positive head & Neck carcinomas [80-82]. Downregulation of DDX3X expression has been reported in the HBV positive hepatocellular carcinoma [83]. The presence of truncating mutations, homozygous deletions and down-regulation of expression of the *DDX3X* gene suggest *DDX3X* to function as a tumor suppressor gene. Downregulation of *DDX3* gene expression has been shown to bring about premature entry into S phase and increase in proliferation of NIH3T3 fibroblasts accompanied by upregulation of Cyclin D1 expression and downregulation of CDK inhibitor p21 [66]. Ectopic

expression of DDX3X in HCT116 and HeLa cell lines has been shown to inhibit proliferation of these cell lines. DDX3X downregulation has also been shown to enhance RAS-induced anchorage-independent growth and to resist serum-deprivation induced apoptosis of NIH3T3 cells [66].

On the other hand, *DDX3X* has also been shown to act as an oncogene by upregulating Snail transcription factor and repressing E-cadherin expression to bring about epithelial mesenchymal transition of MCF7 breast cancer cells. DDX3X protein and mRNA levels positively correlate with tumorigenicity of breast cancer cell lines *i.e.* aggressive breast cancer cell line has higher levels of DDX3X protein. It has been shown that MCF10A cells stably over-expressing DDX3X increase in anchorage independent growth, motility and invasion [67, 84]. DDX3X has also been reported act as an anti-apoptotic factor by repressing caspase activation as a part of a protein complex associated with the death receptors [78]. DDX3X has been reported to be essential for *MEIS1* and *TLOC* oncogene induced tumorigenesis of mouse embryonic fibroblasts and mammary epithelial cells respectively [85, 86].

We have done the exome sequencing of the WNT subgroup tumors and identified mutations in the *DDX3X* in 3 tumors (shown in results). Two of the identified mutations are missense located in the D1 domain of the DDX3X whereas the mutation in third tumor is truncating which leads to the truncation of the DDX3X after 242 amino acids leading to loss of its helicase core domain. DDX3X is a multifunctional protein having diverse roles in RNA metabolism with Its N-terminal domain required and sufficient for some of its transcriptional regulator activity that is independent of its ATPase and helicase activity. On the other hand, its ATP-dependent helicase activity has been reported be necessary for its role as a regulator of translation. DEAD box helicases are known to lack substrate specificity *in vitro*. The substrate specificity and regulation

of enzyme activity of the DEAD box proteins is known to be influenced by protein cofactors *in vivo* hence its transcriptional and translational regulatory activity in multi-protein complexes are likely to differ in the context of different cell types and in the presence of activation of different signaling pathways. Therefore, DDX3X's role in cancer needs to be investigated in the appropriate context. Hence the present study was done to identify DDX3X's transcriptional and translational target genes in medulloblastoma cells, which would lead to understanding of DDX3X's role in pathogenesis of medulloblastoma.

2.13 MicroRNAs: Small RNAs with a big role

The central dogma of molecular biology states that genetic information is transferred from DNA to RNA and then from RNA to protein, the functional unit of cell. Several exceptions to the central dogma were subsequently noted including the process of reverse transcription and identification of non-coding RNAs including microRNAs. MicroRNAs (miRNAs) are small, evolutionarily conserved, single stranded, non-coding RNA molecules that regulate target gene expression post-transcriptionally by binding to target mRNA.

2.14 Brief history of microRNAs

MicroRNAs are a class of endogenous, small, non-coding, single-stranded RNA molecules, ~22 nucleotides in length. The first miRNA, lin-4 in *Caenorhabditis elegans*, was discovered in 1993 by the joint efforts of Ambrose and Ruvkun's laboratories. This miRNA lin-4 was found to encode a 22 nucleotide long non-coding RNA that contained sequences partially complementary to 7 conserved sites located in 3'-UTR region of lin-14 mRNA [87, 88]. Almost 7 years after discovery of first miRNA, let-7, also required for *C. elegans* larval development, was identified in 2000. The finding that let-7 was conserved across species from flies to humans and targets the

RAS oncogene homolog in *C. elegans*, triggered a revolution in the research of miRNAs [89-91]. Multiple studies have focused on searching for new microRNAs and elucidating their function in normal cellular functioning as well as in disease, especially cancer. There are currently 2588 annotated miRNAs in human genome [92]. A single miRNA can potentially regulate several genes while a single gene may be regulated by multiple miRNAs thus creating a complex interaction network [93].

2.15 MicroRNA biogenesis and mode of action

MicroRNA encoding genes are located throughout the genome, with some encoded within introns of protein coding genes (intragenic), while some in noncoding RNA (ncRNA) transcription units (intergenic). Majority of the miRNAs are transcribed by RNA polymerase II. Many miRNA precursors which are found in cluster are transcribed in form of polycistronic transcripts from a single promoter, while intergenic miRNA clusters are processed from parent gene transcript via alternate splicing mechanism [93, 94].

The biogenesis and maturation of miRNAs involve several processing steps, namely cropping, nuclear export and dicing, which are compartmentalized in nucleus and cytoplasm (Ref). MiRNA genes are generally transcribed by RNA polymerase II into long (> 1 Kb) primary transcripts (pri-miRNAs), which contain a 5' 7-methyl guanosine cap, a 3' poly (A) tail and a local hairpin structure. The stem-loop structure is cropped by the nuclear enzyme Droscha and cofactor DGCR8/Pasha into a ~70-nucleotide precursor miRNA (pre-miRNA). The pre-miRNA is then translocated by exportin-5 and RanGTP to the cytoplasm, where it is further processed into a ~22-nucleotide miRNA duplex by the enzyme Dicer. The miRNA duplex is unwound and one strand (the mature miRNA) is assembled with argonaute protein into the effector complex

termed miRNA containing ribonucleoprotein (miRNP) complex to mediate translational repression and/or mRNA degradation of target mRNA. The first 2–8 nucleotides (the “seed” sequence) at the 5’ region of miRNA are essential for interaction with the miRNA binding site in the 3’-UTR of target mRNA. The mechanism of inhibition depends on the degree of miRNA-mRNA complementarity (imperfect or perfect) that results in either inhibition of protein synthesis or mRNA degradation (Fig. 2.5) [93, 95].

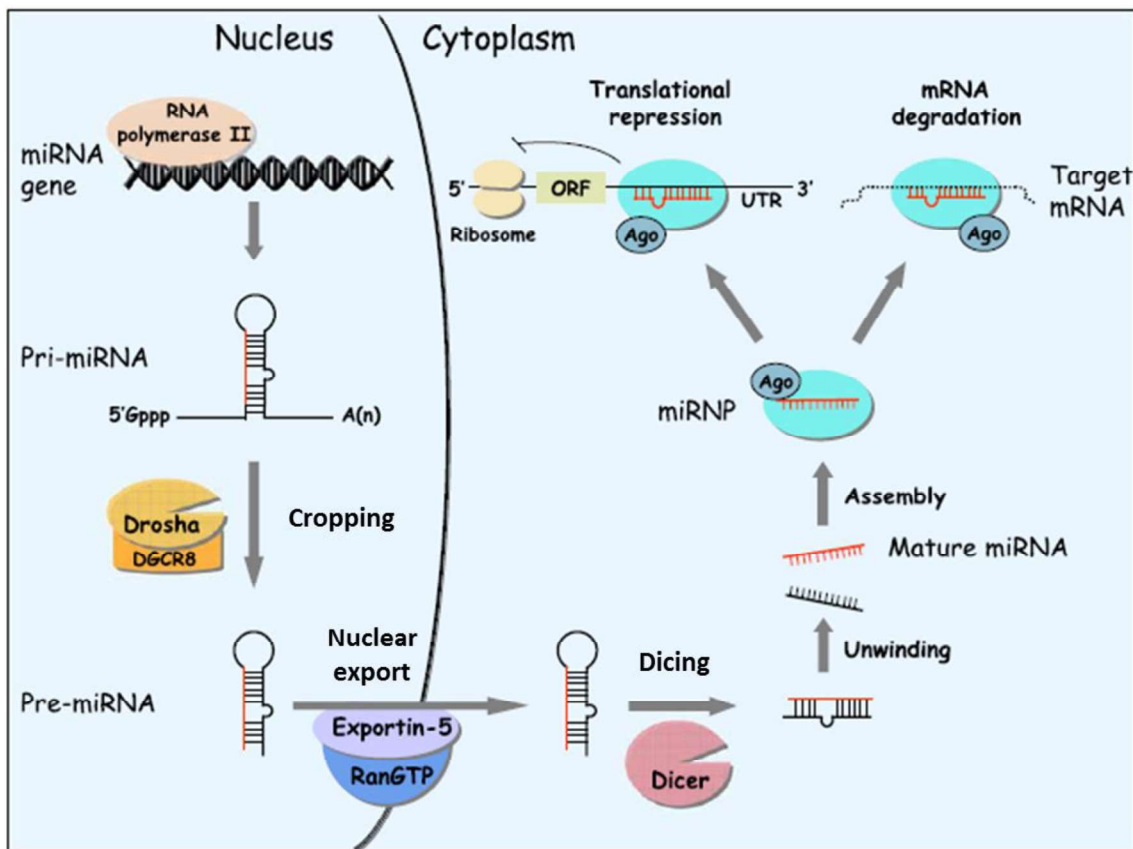


Figure 2.5: Biogenesis of microRNAs [95].

The figure shows the multi-step process of miRNA biogenesis comprising of three main events: cropping, nuclear export and dicing.

2.16 MicroRNAs in cancer

The early evidence that miRNAs have potential to play role in cancer came from the first miRNAs discovered in *C. elegans* and *Drosophila* *i.e.* lin-4 and let-7 respectively that were found to control proliferation and apoptosis of cells. Thus their deregulation could contribute to disease like cancer. The first study indicating role of miRNA in human cancer was in 2002 [96]. This study found miR-15a and miR-16-1 to be located in chromosome 13q14, a region frequently deleted in chronic lymphocytic leukemia (CLL). Subsequently, frequent deletion or downregulation of these miRNAs was detected in more than 60% of CLL cases [96, 97]. Cimmino *et al.* reported that putting back these miRNAs in CLL cell lines resulted in induction of apoptosis and found that their expression inversely correlated with anti-apoptotic *BCL2* expression [98]. Let-7 family of miRNAs was the first group of miRNAs that was shown to possess tumor suppressive activity. Loss or downregulation of let-7 expression in lung cancer was shown to increase expression of RAS proto-oncogene thus promoting cell growth and in turn tumorigenesis [91]. Subsequent studies showed that miRNAs can play both kinds of roles *i.e.* they can be tumor suppressive or oncogenic. MiR-155, one of the first oncogenic miRNA described, is over expressed in many cancers like breast cancer, colon cancer, lung cancer, CLL and acute myeloid leukemia (AML) [99]. Costinean *et al.* were first to develop transgenic mouse that specifically overexpressed miR-155 in early B-cell. In these mice pre-leukemic expansion of the pre-B cell population ultimately leading to B cell tumor was observed [100]. Another miRNA miR-21 was coined to be onco-miR due to its overexpression in several cancers including AML, CLL, breast cancer, glioblastoma and medulloblastoma, with PTEN identified as one of its target [101, 102]. Studies by O'donnell *et al.* revealed that miR-17-92 inhibits E2F1, so inhibits MYC mediated cellular transformation [103]. Further miR-372 and miR-373 have

been shown to have oncogenic function in testicular germ cell tumors [104]. A single miRNA is known to target more than 100 mRNAs. Moreover, 60% of human protein coding genes have been predicted to contain miRNA binding sites within their 3'-UTRs. Given their wide impact on gene expression, it is not surprising that they play an important role in disease phenotypes such as cancer.

2.17 MicroRNA deregulation in medulloblastoma and their functional significance

Ferretti *et al.* in 2002 reported the first global expression profiling miRNA in medulloblastoma [105]. They performed expression profiling of 248 miRNAs in 14 primary medulloblastoma tumors and reported consistent downregulation of a number of miRNAs compared to normal cerebellum. Functional validation of two of the downregulated miRNAs *viz.* miR-9 and miR-125a showed inhibition of proliferation and decreased anchorage independent growth upon expression of these miRNAs in Daoy and D283 medulloblastoma cell line by targeting pro-proliferative truncated form of neurotrophin receptor Trkc [105]. Northcott *et al.* in their study on profiling of 427 miRNAs in 90 primary medulloblastoma reported miR-17/92 cluster to be upregulated in medulloblastomas with activated SHH signaling compared to other subgroups and to act as positive effector of SHH mediated proliferation, suggesting growth advantage to those tumors having miR-17/92 overexpression or amplification. They also showed that medulloblastomas in which miR-17/92 was upregulated also had elevated levels of MYC/MYCN expression [106]. Cho *et al.* reported the increased expression of miR-183-96-182 cluster in clinically most aggressive medulloblastoma subgroups associated with genetic amplification of *MYC*. Knockdown of entire cluster resulted in enrichment of gene associated with apoptosis and dysregulation of the PI3K/AKT/mTOR signaling axis [107]. MiR-182 was specially found to

promote cell motility/invasion and leptomeningeal spread and tumorigenesis *in vivo*, in SHH subgroup mouse models [108]. A brain enriched miRNA, miR-124a was found to be downregulated in medulloblastoma and reported to be targeting CDK6, one of the marker for adverse prognosis in medulloblastomas [109]. MiR-134a, another miRNA downregulated in medulloblastoma, upon re-expression in medulloblastoma cell lines showed to induce apoptosis, G2 arrest and senescence and render these cells more susceptible to chemotherapeutic agents. This effect of miR-134a is mediated by targeting *MAGE-A* gene family [110, 111].

MiRNA expression profiling carried out in our lab on a set of 4 normal cerebellum tissues and 19 medulloblastoma tumor tissues could successfully classify the normal cerebellum from the tumors [47]. Interestingly, the miRNA expression profile could also independently classify the tumors into the four core molecular subgroups. The WNT subgroup showed a distinct set of highly expressed miRNAs including miR-193a, miR-224, miR-148a, miR-204, miR-365. The SHH subgroup showed downregulation of miR-153, miR-204 and miR-135b. MiR-135b was found to be upregulated in the non-WNT, non-SHH tumors. Furthermore, miR-182 and miR-183 were found to be upregulated and miR-204 downregulated in most group 3 tumors. The miR-379/miR-656 and miR-127/miR-432/miR-433 cluster present in an imprinted region on chromosome 14 was found to be highly expressed in the normal cerebellum and group 4 tumors [47]. This differential expression was validated on 101 medulloblastoma tissues. A set of 12 protein coding and 9 miRNA coding genes was used to develop an assay to classify medulloblastoma tumor tissues into the molecular subgroups that was validated on an independent cohort of 34 primary medulloblastomas from DKFZ, Germany [48]. The miRNAs overexpressed in the WNT subgroup medulloblastomas including miR-193a, miR-224 and miR-148a have been shown to inhibit growth of the medulloblastoma cell lines [13, 112]. This

indicates that the upregulation of these miRNAs in the WNT subgroup medulloblastomas may contribute to the excellent survival of this subgroup. These data indicate to the important role for miRNAs in the biology of medulloblastoma.

In the miRNA profiling study done by our group, seven miRNAs (miR-30a-3p, miR-30a-5p, miR-30b, miR-30c, miR30d, miR-30e-3p and miR-30e-5p) of miR-30 family were found to be downregulated in medulloblastoma tissues irrespective of their subgroup affiliations compared to human normal cerebellum [13]. MiR-30 family of miRNAs has been reported to be downregulated in several other cancers like breast cancer, lung cancer and colorectal cancers [14, 113, 114]. These miRNAs share the same seed sequence at the 5' end but different sequences at the 3' end [92]. Among these miRNAs miR-30a is the most studied miRNA. MiR-30a is located on chromosome 6 and in WNT subgroup of medulloblastoma approximately 75% of tumors show loss of one copy of chromosome 6. Hence in the present study role of miR-30a in medulloblastoma tumorigenesis was investigated both *in vitro* and *in vivo*.

Chapter 3

MATERIALS & METHODS

MATERIALS:

The following chemicals were obtained from **Applied Biosystems, Life technologies**, Carlsbad, CA, USA:

2X TaqMan Universal PCR Master Mix (Part No. 4304437); 2X Power SYBR

Green PCR Master Mix (Part No. 4367659), 2X TaqMan PreAmp Master Mix (Part No.4384266), TaqMan MicroRNA Assays (Part No. 4427975) - Assay IDs for each miRNA assays are: hsa-miR-30a-3p (000416), RNU48 (001006); MicroAmp optical 384-well Reaction Plate with Barcode (Part No. 4309849) and MicroAmp Optical Adhesive Film Kit (Part No.4313663).

The following chemicals were obtained from **Invitrogen, Life technologies**, Carlsbad, CA, USA:

MMLV-RT 200 U/ul (Cat No. 28025-013), Dulbecco's modified Eagle medium (Cat. No.12800-058), DNase I, amplification grade (Cat No. 18068-015), Fetal bovine serum (CatNo. 16140-071), LMP (low melting point) agarose, Trypsin, L-Glutamine, Formamide (Cat. No.15515)

The following chemicals were obtained from **Sigma-Aldrich**, St Louis, MO, USA:

Agarose, Proteinase K, Guanidium Isothiocyanate (GITC), Diethyl pyrocarbonate (DEPC), DMSO, EDTA, Ethidium bromide, BES (B4554-25G), Puromycin (Cat No.P8833-25MG), Ammonium persulphate.

The following chemicals were obtained from **Amersham Lifesciences, GE Healthcare Life Sciences**, Pittsburgh PA, USA:

dATP, dGTP, dTTP, dCTP (100 mM each) (Cat. No.27-2035-01), Random hexamers pd(N)₆ Sodium salt.

The following chemicals were obtained from **Thermo Scientific, Life technologies**, Carlsbad, CA, USA:

10X PCR Buffer, Exonuclease I, Gene Ruler 1 Kb DNA ladder, Shrimp Alkaline Phosphatase (SAP) (Cat. No. EF0511), 25 mM MgCl₂, Taq DNA polymerase (1U/ μl) (Cat. No. EP0404), T4-DNA ligase (Cat No.E0011), DpnI (Cat No- ER1701) SuperSignal® West Pico chemiluminescent substrate (Pierce-Thermo scientific, Cat. No.34077)

The following chemicals were obtained from **Merck, Qualigens**, dermstadt, Germany; **Qualigens**, Thermo Fisher Scientific India Pvt Ltd, Mumbai or **S D fine-chem limited**, Mumbai, India:

Xylene, Methanol, Glacial Acetic Acid, Potassium Acetate, Sodium Acetate, N-laurylsarcosine. Sulfuric Acid (LR), Potassium dichromate (LR), Tri-Sodium citrate (LR), Citric Acid (LR), Hydrogen peroxide, Methanol.

The following reagents were obtained from **New England Biosciences (NEB)**, Ipswich, MA, USA: Standard Taq DNA polymerase (Cat No.M0273L), T4PNK (M0201)

The following reagents were obtained from **S.D Fine-chem limited**, Mumbai, India:

NaCl (Cat No.20241 AR), Na₂HPO₄.2H₂O (Product no. 20383 AR), CaCl₂.2H₂O (Sigma C-3306)

The following **kits** were obtained from the companies specified in brackets:

Recover All RNA extraction kit (Ambion, Life technologies, Carlsbad, CA, USA; Cat No. AM1975)

QiaAmp DNA mini kit (Qiagen, Limburg, Netherlands; Cat No. 51304)

Qiagen Plasmid Midi kit (Qiagen, , Limburg, Netherlands; Cat No – 12143)

QIAquick Gel Extraction Kit (Qiagen, , Limburg, Netherlands; Cat No-28704)

The water used for the preparation of all solutions and reagents was Ultrapure water (Resistivity = 18 MΩ cm) obtained from a Milli-Q water plant (**Millipore**, Billerica, MA,USA).

Disposable plastic ware (certified DNase, RNase, and protease-free) was obtained from **Axygen**, California, USA.

Disposable sterile plastic ware for tissue culture was obtained from **Nunc**, Rochester, NY, USA.

Primers:

All PCR primers were synthesized and obtained from **Sigma Genosys, Bengaluru, India** in the lyophilized form.

3.1 Collection of sporadic medulloblastoma tumour tissues and normal cerebellar tissues

Approval for the project was obtained from the Institutional Review Board and Ethics Committee of Tata Memorial Hospital (T.M.H) and King Edward Memorial (K.E.M.) Hospital, Mumbai. Medulloblastoma tumor tissues were obtained with written informed consent of the patient or the parent in case of patients less than 18 y of age. In case of patients in the age group 7 to 18 yr, an assent was also obtained from the minor patient, in addition to the parent's consent. The consent form, assent form and the information sheet were approved by the Institutional Ethics committee. Immediately following surgery, the tumour tissues were snap-frozen in liquid nitrogen and stored at -80°C until use. Normal cerebellar tissues were obtained from Brain Tissue Repository, NIMHANS, Bengaluru that included two normal developing cerebellar tissues from children less than 1 yr of age and six normal adult cerebellar tissues.

This part of the study was approved by the institutional animal ethics committee. The normal cerebellar tissues at various stages of development (Day 7, 14 and 21) were obtained from C57 / BL6 mice after administration of euthanasia with overexposure to CO_2 . *Ptch1*^{+/-} mice and *Smo*^{+/+} mice were obtained from Dr. Matthew Scott (Stanford School of Medicine, Stanford, CA, USA) and Dr. James Olson (Fred Hutchinson Cancer Research Centre, Seattle, WA, USA) respectively. The tumors formed in these SHH subgroup medulloblastoma mouse models were obtained in a similar manner. The tissues were flash frozen in liquid nitrogen and then stored at -80°C until use.

3.2 Exome sequencing of Tumor DNA and paired blood DNA sample

3.2.1 Genomic DNA extraction from Tumor and blood DNA

Method

A. For Tumor tissue

1. Medulloblastoma tumor tissues obtained from surgical resection were snap frozen and stored at -70°C. Before extraction of genomic DNA, frozen sections of the tumor tissue were examined by light microscopy to ensure presence of at least 90% tumor cells.
2. Genomic DNA was extracted from the tumor sections using QIAamp DNA Mini Kit (QIAGEN, Cat. No. 51304) as per the manufacturers instruction.

B. For paired blood sample

1. 200 µl of the blood sample was used for the extraction of DNA. Peripheral blood lymphocyte DNA was extracted using QIAamp DNA Mini Kit (QIAGEN, Cat. No. 51304) as per the manufacturers instruction.

3.2.2 Exome sequencing of medulloblastoma tumor and paired blood DNA samples using Agilent SureSelect Human All Exon v2.0 (44M) kit

Method

1. Whole exome library preparation for the 11 medulloblastoma tumor and 6 paired blood DNA was done using Agilent SureSelect Human All Exon v2.0 (44M) kit as per the manufacturers protocol.

2. Briefly, genomic DNA sample (1.5 μg for each sample) was randomly fragmented into fragments with a base pair peak of 150 to 200bp, and then adapters were ligated to both ends of the resulting fragments. The adapter-ligated templates were purified by the Agencourt AMPure SPRI beads and fragments with insert size about 200bp were excised. Extracted DNA was amplified by ligation-mediated polymerase chain reaction (LM-PCR), purified, and hybridized to the SureSelect Biotinylated RNA Library (BAITS) for enrichment. Hybridized fragments were bound to the strepavidin beads whereas non-hybridized fragments were washed out after 24h. Captured LM-PCR products were subjected to Agilent 2100 Bioanalyzer to estimate the magnitude of enrichment. Each captured library was then loaded on Hiseq2000 platform, and high-throughput sequencing for each captured library was performed to get an average coverage of approximately 50X.
3. The data obtained was analysed as described in bio-informatics section 3.25 and section 3.26.

3.3 Sequencing of PCR products for identifying mutations in exon 3 of β -catenin and validating the identified somatic mutations.

3.3.2 PCR Amplification

The reaction was made as follows

Components	Volume	Final Concentration
10X standard Taq buffer	1 μl	1X
10mM dNTP mix	0.2 μl	0.2mM
Forward primer (10pmol/ μl)	0.3 μl	3pmol
Reverse primer (10pmol/ μl)	0.3 μl	3pmol

Taq Polymerase (1 U/ μ l)	0.25 μ l	0.25 U
Genomic DNA		25ng
Autoclaved Milli-Q water		Make up volume to 10 μ l

PCR Conditions were as follows

Temperature	Time	Cycles
98°C	3 min	1
98°C	30 sec	30
Annealing temperature	45 sec	
72°C	30 sec	
72°C	5min	1

3.3.3 Removal of unused primers and dNTPs from PCR products by Exonuclease I and Shrimp Alkaline Phosphatase

PCR amplified products contain unused primers and dNTPs. If not removed these primers and dNTPs interfere with subsequent reactions. Exonuclease I (Exo) has an exonuclease activity and degrades any single stranded DNA. Shrimp Alkaline Phosphatase (SAP) removes the phosphate groups from dNTPs.

Method:

1. To remove unused primers and dNTPs, 1 μ l of master mix of Exonuclease I and Shrimp

Alkaline Phosphatase was added for every 10 μ l of PCR product as per table below:

Constituents	Volume	Final Concentration
10X PCR buffer	0.1 μ l	1X
Exo I (10U/ μ l)	0.05 μ l	0.5U
SAP (1U/ μ l)	0.5 μ l	0.5U
Autoclaved MQ water	0.350 μ l	

Total Volume	1 μ l	
--------------	-----------	--

2. 5 μ l of the master mix was added to 50 μ l of the PCR product. The reaction mixture was mixed by tapping and spun briefly. The reaction was incubated at 37 °C for 2 hr and the enzymes heat inactivated by incubating at 85 °C for 20 min.
3. The reactions were then processed further to remove inactivated enzymes and excess salt.

3.3.4 Clean up of PCR templates for removal of excess salt

1. Autoclaved MQ water was added to Exo-SAP treated PCR products so as to make up the volume to 100 μ l. To this, 10 μ l of 3M sodium acetate pH 5.2 and 250 μ l of chilled absolute ethanol were added.
2. The sample was mixed thoroughly by vortexing and incubated on ice for 25 min. Incubation at lower temperature or longer periods may cause precipitation of salts and hence is not recommended.
3. The tube was spun at 14000 rpm for 20 min at 4 °C and the supernatant was discarded carefully. (Note: The pellet may be very small or may not be visible at all. Still proceed with next step.)
4. The pellet was washed with 500 μ l of freshly prepared 70 % ethanol and centrifuged at 14,000 rpm for 10 min at room temperature.
5. The supernatant was discarded and step 4 was repeated.
6. The supernatant was aspirated and pellet was air dried. Pellet was re-suspended in 8-10 μ l of 1 M TE Buffer, pH 8.0.
7. To check the quality and quantity of PCR product, 2 μ l of the PCR product was loaded on a 1 % agarose gel and visualized. 50ng of good quality PCR product was used for sequencing.

3.3.5 Sequencing of the PCR products or plasmid vectors

In a 0.2 ml PCR tube, 1.5pmol of either forward or reverse primer and 5-10ng of Exo-SAP treated PCR amplified product were added. In case sequencing of Vectors, 100ng DNA was used. The sequencing reactions were carried out in Eppendorf Master Cycler using Big Dye Terminator Kit V 3.1, which has different fluorescent dye for each terminator ddNTP as per manufacturer's instructions. The reactions were cleaned up to remove excess salt. The reactions were run in either a 50 cm or 80 cm capillary filled with POP4 or POP6 polymer (Applied Biosystems, U.S.A) in 3100 Avant Genetic Analyzer (Applied Biosystems, U.S.A). The size of capillary used depended on the PCR product size.

3.4 Cloning of PCR products into target vector

The cDNA of DDX3X and genomic region of miR-30a were PCR amplified from pCMV-myc-DDX3X vector (a kind gift from Dr. Laura Madrigal-Estebas, Trinity College, Dublin) and genomic DNA of normal human peripheral blood lymphocyte by using high fidelity phusion polymerase respectively. DDX3X cDNA was cloned in pET-28a and pMAL-c5E vector using BamHI and EcoRI restriction enzymes. The forward primer for cloning of DDX3X was designed such that it contains TEV protease cleavage sequence before ATG start codon, so that after expression recombinant tagged DDX3X protein, 6X-His or MBP tag can be cleaved from DDX3X protein. PCR amplified genomic region encoding miR-30a was cloned into HpaI and EcoRI site in the pTRIPZ doxycycline inducible lentiviral vector. DDX3X shRNAs (targeting open reading frame and UTR regions) were annealed and then ligated after T4 PNK treatment. Primers used for cloning are shown in table 3.1

Gene name	Primer	Sequence
DDX3X (cloning in bacterial expression vectors)	Forward primer with TEV site	GATGGATCCGAGAACCTGTACTTTCAG GGTATGAGTCATGTGGCAGTGGAA
DDX3X (cloning in bacterial expression vectors)	Reverse	GTCGAATTCCTATCAGTTACCCCACCAG TCAAC
MiR-30a	Forward	GCTGTTAACGCCACTTGCCTATTTACTT CTTG
MiR-30a	Reverse	ACGGAATTCACCTCCTCAATGCCCTGCT
DDX3X-shRNA-301	Forward	CCGGCGGAGTGATTACGATGGCATTCTC GAGAATGCCATCGTAATCACTCCGTTTT T
DDX3X-shRNA-301	Reverse	AATTA AAAACGGAGTGATTACGATGGC ATTCTCGAGAATGCCATCGTAATCACTC CG
DDX3X-shRNA-UTR	Forward	CCGGCCCTGCCAAACAAGCTAATATCTC GAGATATTAGCTTGTTTGGCAGGGTTTT T
DDX3X-shRNA-UTR	Reverse	AATTA AAAACCCTGCCAAACAAGCTAA TATCTCGAGATATTAGCTTGTTTGGCAG GG

Table 3.1 Primer sequences used for cloning of DDX3X, miR-30a and DDX3X-shRNAs

3.4.2 PCR amplification and Phenol-Choroform method of DNA purification

Reagents: 5X phusion HF buffer, 10mM dNTP mix, Phusion polymerase, Tris saturated phenol

Tris Saturated Phenol: Distilled phenol kept at -20°C was carefully thawed to RT by keeping it at 60°C preferably in waterbath. The cap of the bottle was loosened to release any pressure built on thawing the phenol. As phenol is acidic, it needs to be neutralised to avoid degradation of

DNA. 25ml of phenol was taken and equal volume of autoclaved Milli-Q in sterile Nunc tube. It was mixed thoroughly by shaking the tube and allowed to rest until two phases separate. Upper phase was removed. This was repeated once to saturate phenol with water. To the water saturated phenol, equal volume of 1 M Tris, pH 8.0 is added and mixed thoroughly by shaking the tube and allowed two phases to separate. Upper phase was removed and same set of steps were repeated with 0.1M Tris, pH 8.0. pH of the phenol phase was subsequently achieved to be 7.0 or above. 10-15ml of 10 mM Tris, pH 8.0 was added on top of the phenol phase for long-term storage in refrigerator and exposure to light was avoided by covering tube with Aluminium foil.

Method

1. All reagents required for the reaction except for the enzyme were thawed and kept on ice.
2. For each PCR reaction 25ng of human lymphocytic genomic DNA was added in the end to the 0.2 ml tube containing the PCR components.
3. The PCR Reaction mix was prepared as follows for High Fidelity Phusion polymerase:

Components	Volume	Final Concentration
5X Phusion buffer (HF)	2 μ l	1X
10mM dNTP mix	0.2 μ l	0.2mM
Forward primer (10pmol/ μ l)	0.2 μ l	2pmol
Reverse primer (10pmol/ μ l)	0.2 μ l	2pmol
Phusion Polymerase (2 U/ μ l - NEB)	0.1 μ l	0.2 U
Genomic DNA/plasmid DNA		25ng/5ng
Autoclaved Milli-Q water	Make up volume to 10 μ l	

4. Reactions were carried out in Eppendorf MasterCycler 5333 (Eppendorf, Germany). All precautions were taken to avoid PCR related contamination. All reagents and PCR products were handled using filter tips.
5. The PCR cycling parameters were as follows:

Temperature	Time	Cycles
98°C	5 min	1
98°C	30 sec	30
Annealing temperature	45 sec	
72°C	30 sec	
72°C	10 min	1

6. 5µl of the PCR product was run on 1% agarose gel and visualized using UV transilluminator. The PCR product was further purified using phenol:chloroform, before using it for cloning.
7. Equal volume of Tris Saturated phenol was added to the PCR, mixed and centrifuged at 12,000 rpm, for 15 min, at 20°C.
8. To the supernatant equal volume of phenol:chloroform (1:1) was added, mixed and centrifuged at 12,000 rpm, for 15 min, at 20°C.
9. To the supernatant equal volume of chloroform was added, mixed and centrifuged at 12,000 rpm, for 15 min, at 20°C.
10. Then 1/10th volume of 3M sodium acetate pH 5.2 was added and mixed.
11. Then 2.5X volume chilled absolute alcohol (kept at -20°C to chill) was added, mixed well and kept for precipitation overnight at -20°C.
12. Next day, the mixture was centrifuged at high speed (16,000 rpm) for 20 min at 4°C.

13. The pellet was washed with 70% alcohol (500 μ l) and centrifuged at 12,000 rpm for 10min at 4°C; twice.

14. The pellet was air-dried and dissolved in minimum of 10 μ l T.E buffer.

3.4.2 Agarose Gel Electrophoresis

Reagents:

1. 50 X Tris-acetate-EDTA (TAE) buffer: 121g Tris and 18.6g EDTA was dissolved in 300ml of Milli-Q water followed by addition of 28.55ml glacial acetic acid. Volume was made up to 500ml and was autoclaved.
2. Ethidium Bromide stock (10 mg/ml): Dissolve 10mg Ethidium Bromide in 1ml of autoclaved Milli-Q water.
3. 6 X DNA loading dye: Dissolve 0.25% bromophenol blue, 40% (w/v) sucrose in Milli-Q water.

Method-

1. The appropriate amount of agarose was weighed into a measured volume of 1X TAE buffer to make a 1% gel. The slurry was heated in a microwave oven until the agarose was dissolved completely and ethidium bromide to a final concentration of 0.5 μ g/ml (from a 10 mg/ml stock) was added when the gel solution had cooled to about 40°C.
2. A gel tray was cleaned, the gel was poured into the gel tray and a clean comb was inserted in the slot provided in the tray. The gel was allowed to set at room temperature for 30-45 minutes.

3. After the gel had completely set, the gel was placed in the electrophoresis tank filled with 1X TAE buffer. The buffer should be just enough to cover the gel to a depth of about 3 mm and the comb was carefully removed.
4. The DNA samples were mixed with 6X loading buffer at 1X final concentration and loaded into the wells of the gel. The gel was run in electrophoresis chamber at 40mA constant current, till the dye had migrated about three-fourths of the gel.
5. The DNA was visualized by observing the gel on a UV transilluminator.

3.4.3 T4 Polynucleotide kinase reaction (Only for blunt end cloning)

For blunt-end cloning, Phusion DNA polymerase used for PCR amplification of insert produces blunt ends on the amplified fragment, which lack terminal 5' phosphate groups. T4 Polynucleotide kinase was used to add a phosphate group to the 5' end of the amplicon to facilitate cloning with the vector.

Reagents: 10X T4 Polynucleotide Kinase Reaction buffer, T4 Polynucleotide Kinase (10U/ μ l).

Method:

1. All reagents required for the reaction except for the enzyme were thawed and kept on ice.
2. The reaction was set up as follows:

Components	Volume
10X T4 Polynucleotide Kinase Reaction buffer	2 μ l
DNA	5-10 μ l (1- 300pmol termini)
T4 Kinase (10U/ μ l)	1 μ l (1U)
Auotclaved Milli-Q water	Make up the volume to 20 μ l

3. The reaction was incubated at 37°C for 30min and then heat inactivated at 65°C for 20 min.

3.4.4 Restriction digestion

Reagents: 10X buffer, Restriction Enzyme (R.E)

Method:

1. All reagents required for the reaction except for the enzyme were thawed and kept on ice.
2. For a typical restriction enzyme reaction, 2-3 U of enzyme was used to digest ~1µg DNA in a reaction volume of 20 µl; at the recommended temperature for at least 4 h. (If more than one reaction was performed a master mix was prepared containing the buffer, enzyme and Milli-Q water).
3. The reaction was heat inactivated at the recommended temperature for 15-20 min (most enzymes are inactivated at 65°C for 15 min).
4. For cloning the digested product, the volume of the reaction was made to 200 - 300 µl with TE. The mixture was purified by phenol-chloroform method and precipitated with ethanol as described for PCR products.

3.4.5 Dephosphorylation of Vector using Shrimp Alkaline Phosphatase (SAP)

The digested vector was treated with Shrimp Alkaline Phosphatase to remove the 5'-phosphate from the last base to avoid a bond formation between the ends of the vector during the ligation process.

Reagents: 10X R.E digestion buffer, Shrimp Alkaline Phosphatase (1U/ µl)

Method:

1. All reagents required for the reaction except for the enzyme were thawed and kept on ice.

2. The reaction was set up as follows:

Components	Volume
10X R.E digestion buffer	3 μ l
Shrimp Alkaline Phosphatase (1U/ μ l)	1 μ l (1 U)
R.E digested DNA mixture	10-20 μ l (1-10pmol termini)
Autoclaved Milli-Q water	Make up volume to 30 μ l

3. This reaction was incubated at 37°C for 60 min.

4. The reaction was terminated by heat inactivation at 65°C for 15 minutes.

3.4.6 Ligation

Reagents: 10X Ligation buffer, T4 DNA Ligase (5U/ μ l), 50% PEG 4000 solution.

Method:

1. All reagents required for the reaction except for the enzyme were thawed and kept on ice.

Components	Blunt-end Ligation	Sticky-end Ligation
	Volume/ amount	Volume/amount
Linear vector DNA	60 fmol vector ends	30 fmol vector ends
Insert DNA (PCR product)	180 fmol insert ends	90 fmol insert ends
10X Ligation buffer	2 μ l	2 μ l
50% PEG 4000 solution	2 μ l	-
T4 DNA Ligase (5U/ μ l)	1 μ l (5 U)	0.4 μ l (2U)
Autoclaved Milli-Q water	Make up volume to 20 μ l	Make up volume to 20 μ l

2. The mixture was incubated for 16 hour at 22°C (cold bath) and inactivated by incubating at 65 °C for 10 min.

3.4.7 Preparation of competent cells

Reagents:

Transformation buffer (TB): 0.3g PIPES, 0.22g of CaCl₂-2H₂O, 1.86g of KCl were dissolved in 95ml Milli-Q and pH was adjusted to 6.7-6.8 with 5M KOH. The initial white precipitate may form at low pH, however once the right pH is adjusted, solution should become clear. 1.09g of MnCl₂ was added in this solution and final volume was made up to 100ml and filter-sterilised using 0.22µm filter.

Super Optimal Broth (SOB): 20g of tryptone, 5g of yeast extract was dissolved in 995 ml of Milli-Q water. 2ml of 5M NaCl and 1.25ml of 2M KCl was added to achieve final concentrations of 10mM and 2.5mM respectively. Solution was autoclaved and 5ml of 2M MgCl₂ solution prepared and sterilised separately was added just before use.

Luria Broth (LB): 1g of tryptone, 0.5g of yeast extract and 0.5g of NaCl was dissolved in 100ml of milli-Q water and autoclaved

SOB agar plates: 1.5-2g Agar agar was dissolved in 100ml of SOB (or LB), autoclaved and poured in pre-sterilised plastic plates.

Method-

1. *E.coli* strains DH5α or stb13 cells were freshly streaked from the glycerol stocks on the SOB agar plates one day prior to inoculation into SOB for competent cells preparation.
2. 200ml of SOB medium (10% of flask volume) was prepared and autoclaved in wider neck 2L flask. All the steps here onwards are performed in aseptic conditions created by laminar hood.
3. A single colony from freshly streaked SOB plate was inoculated into the 200ml SOB and flask was incubated at 18⁰C at 150-200 rpm till O.D at 600 nm reaches to 0.4. O.D at

600nm was checked at regular intervals by taking out 1ml of growing culture in aseptic conditions by using spectrophotometer.

4. Culture was centrifuged at 3000 rpm for 15 min at 4⁰C when O.D reaches 0.4 or in when it's in between 0.4 to 0.7.
5. Supernatant was discarded and one third volume of ice cold transformation buffer (134ml for 200ml culture) was added slowly onto the pellet so as to disturb the pellet.
6. Cell pellet was resuspended in TB with **gentle pipetting** for 5-10 min and was incubated on ice for additional 10 min. Care was taken to avoid any bubbling during res-suspension of cell pellet.
7. After incubation this was centrifuged at 3000 rpm for 15 min at 4⁰C and cell pellet was resuspended in 16ml of TB(1/12.5 volume of initial culture volume i.e. for 200ml) as described in earlier step.
8. 1.12ml of DMSO (final concentration of 7%) was added on walls of suspension tubes slowly and was mixed by shaking or by gentle pipetting once or twice.
9. This solution was then aliquoted in volumes of 100µl in 1.75ml prechilled sterilised eppenderoff tubes and snap-frozen in liquid nitrogen as quickly as possible.
10. The competent cell vials were kept at -70⁰C and were taken out on ice just before use.

3.4.8 Transformation of competent cells

Reagents: *Stbl3* or DH5α ultra-competent cells, SOC broth, LB broth

Method:

1. *Stbl3* or DH5α ultra-competent cells, stored at 80⁰C was thawed on ice by tap-mixing intermittently and kept on ice.

2. 2-20 μ l of the ligation mixture DNA was added to the cells and incubated on ice for 30 min, followed by heat shock for 45s at 42°C.
3. Then the transformation mixture was subjected to cold shock by immediately transferring on ice for 5 min.
4. 900 μ l SOC broth was added and incubated on shaker incubator for 1hr at 37°C.
5. The mixture was spread on LB agar plate containing ampicillin (100 μ g/ml) and incubated at 37°C for 16-18h.
6. The colonies obtained were then inoculated in LB broth containing ampicillin (100 μ g/ml) and plasmid DNA was extracted from the cultures using alkaline lysis method.

3.4.9 Plasmid extraction by alkaline lysis method

Reagents

Solution I: Glucose Tris EDTA solution:

Components	Volume	Final concentration
2M Glucose	1.25 ml	50 mM
0.5 M EDTA	1.0 ml	10 mM
2 M Tris, pH 8.0	0.625 ml	25 mM
Final volume	Make up to 50ml with autoclaved Milli-Q water	

Solution II: (Prepared just before use)

Components	Volume	Final concentration
5M NaOH	0.2 ml	0.2 N
20% SDS	0.25 ml	1%

Final Volume	Make up to 5ml with autoclaved Milli-Q water
--------------	--

Solution III/ (3 M Potassium 5 M acetate, pH 4.8):

Weigh 14.7 g of Potassium acetate. Dissolve in 20 ml Milli Q water. Make up the volume to 30 ml. To 30 ml of 5 M Potassium acetate, add 5.5 ml of glacial acetic acid and 10 ml of Milli-Q water. Check the pH, if it's not approx 4.8 add more acetic acid. Make up the volume to 50 ml with MilliQ water. Sterilise by Autoclaving.

Method:

1. 1.5 ml of bacterial cultures was centrifuged at 3000 rpm for 5 min at room temperature in 1.5ml eppenderoff tube. The cell pellet was resuspended in ice cold 100µl solution I by vortexing and incubated for 5 min at room temperature.
2. 200µl freshly made solution II was added and mixed by gentle inversion followed by incubation for 5 min on ice.
3. 150µl solution III was added and immediately mixed by vortexing for 10 sec, followed by incubation for 5 min on ice.
4. The tube was centrifuged at 13000 rpm for 5 min, clear supernatant was removed in a fresh tube without disturbing the pellet.
5. To this supernatant, equal volume of phenol-chloroform (1:1) (for example, 250µl of Tris-saturated phenol and 250µl of chloroform was added for 500µl of supernatant.
6. The tube was vortexed and centrifuged at 12000 rpm for 5 min, aqueous layer was removed carefully to fresh tube.

7. Equal volume of chloroform was added to the aqueous layer and tube was vortexed to thoroughly mix the contents.
8. Step 6 was repeated.
9. 1ml (or 2X volume) of absolute ethanol was added to the supernatant, mixed by inversion and allowed to precipitate at room temperature for 5 min.
10. The tube was centrifuged at 13000 rpm at room temperature for 5 min, the supernatant decanted carefully; 1 ml of 70% ethanol was added to the DNA pellet and re-spun at 13000 rpm for 5 min. The ethanol was aspirated and the DNA pellet air dried.
11. The plasmid pellet was dissolved in 30-50 μ l TE containing RNase (1 μ g/ml) and further screened for insert and orientation by Restriction digestion analysis.
12. The positive constructs were further prepared on a large scale and purified using, Qiagen DNA Midi kit according to manufacturer's protocol.

3.5 Protein expression and purification from bacterial expression system

3.5.1 Protein expression in Bacterial expression system and detection by SDS-PAGE analysis

Reagents:

Competent cells: *E. coli BL21 (DE3)*, *E. coli rosetta (DE3)* and *E. coli rosettagami 2 (DE3)pLysS*

Cell lysis buffer: 20 mM Tris-HCl pH 8.0, 100 mM NaCl, 0.1% Triton X-100, 2 mM BME, 5% glycerol

Wash buffer: 20 mM Tris-HCl pH 8.0, 100 mM NaCl, 5% Glycerol 0.1% Triton X-100, 2 mM BME and 1 mM Maltose

Elution buffer: 20 mM Tris-HCl pH 8.0, 100 mM NaCl, 2 mM dTT, 10% Glycerol and 10 mM Maltose

Dialysis buffer: 20 mM Tris-HCl, 50 mM NaCl, 2 mM dTT and 10% Glycerol

Antibiotics: Kanamycin (50 mg/ml), Ampicillin (100 mg/ml)

Laemmli buffer: 60 mM Tris-HCl, 2% SDS, 10% Glycerol

EDTA-free protease inhibitor cocktail from Roche, Basel, Switzerland

Amicon Ultra centrifugal filter (Millipore), (10-50 kDa cut-off), Amylose resin, Sterile LB broth, IPTG (Hi-media), Glycerol

30 % acrylamide solution: 29.2 g acrylamide, 0.8 g bis-acrylamide were dissolved in approximately 50-60 ml autoclaved Milli-Q water and the final volume was made up to 100 ml. Solution was filtered through ordinary filter paper and stored in an amber colored bottle at 4 °C.

20% SDS: 20 g SDS was dissolved in 80 ml of Milli-Q water, heated at 60°C to assist the dissolution. The final volume was made up to 100 ml, and stored at room temperature.

1M Tris pH 8.8 and pH 6.8: 60.55 g Tris was dissolved in 400 ml Milli-Q water. pH was adjusted to 8.8 and 6.8 with concentrated HCl, the final volume was made up to 500 ml with Milli-Q water and autoclaved. Solutions were stored at 4°C.

10X electrode buffer: 30 g Tris, 143 g glycine, 20 g SDS were dissolved in approx. 700 ml Milli-Q water and the final volume was made up to 1 L. Stock solution was diluted to 1X with Milli-Q water before use (1X buffer is 25 mM Tris, 190 mM Glycine, 0.2% SDS).

0.5 % Coomassie Blue staining solution: 0.5 g of Coomassie Blue staining dye was dissolved in 50 ml of methanol (LR grade) by constant stirring. The final volume was adjusted to 100 ml by adding 40 ml of Milli-Q water and 10 ml of glacial acetic acid. The staining solution was filtered through filter paper and stored at room temperature for 1 month.

Destainer: Methanol (LR), glacial acetic acid (AR) and Milli-Q water mixed in the proportion 5:1:4 and stored at room temperature.

Loading Dye: 0.025% Bromophenol Blue was dissolved in 1X Sample Buffer.

Method:

1. Bacterial expression construct (pET28a or pMAL-c5E) containing DDX3X cDNA was transformed in the bacterial expression host strain [pET28a in *E. coli BL21 (DE3)* or *E. coli rosettagami 2 (DE3)pLysS* and pMAL-c5E in *E. coli rosetta (DE3)*].
2. **Inoculation:** A single colony was selected from freshly transformed agar plate and inoculated it in 100 ml LB broth containing required concentration of desired antibiotic (50 μ M/ml of kanamycin and 100 μ M/ml of ampicillin final concentration). Incubated the pre-inoculum on shaker incubator at 18°C/37°C overnight (12-16 hrs).
3. **Dilution:** Diluted the 1000 ml culture with 10 ml of pre-inoculum (1:100 ratios) of autoclaved LB broth containing appropriate concentration of antibiotic. Grown the diluted culture on shaker incubator at 18°C/37°C until all the cells reached mid-log phase i.e. A_{600} between 0.4 – 0.6.
4. **Induction:** The cell growth was arrested by cooling the grown culture and optimized concentration of IPTG was added to induce the expression of desired protein followed by

further incubation of the culture on shaker incubator at optimal temperature for optimal time point.

5. **Harvesting:** The culture was transferred to centrifuge bottles after the induction of desired time and centrifuged for 10 minutes at 6000 rpm at 4°C. The pellet was re-suspended in small amount of supernatant and centrifuged for 15 minutes at 5000 rpm, 4°C.
6. **Storage:** The pellet obtained was either processed for detection of desired protein and its purification or stored at -80°C until further used.
7. **Re-suspension:** Bacterial pellet was re-suspended in desired volume of lysis buffer supplemented with protease inhibitor (1 mM PMSF and 1X protease inhibitor cocktail).
8. **Cell lysis:** Transferred the suspension devoid of any clump into centrifuge tubes and sonicated the cell suspension at 70-pulse rate and 70 power with 1 minutes of duty cycle in ice bucket. This process disrupts the cell wall using high frequency sound waves. Sonication process involves application of sound energy using an ultrasonic bath or probe to disrupt the cell wall and cellular contents oozes out.
9. **Centrifugation:** The cell lysate was centrifuged at 18000 rpm for 45 minutes at 4°C to remove cell debris. Supernatant was collected (as soluble fraction) and pellet was re-suspended in 1X laemmli buffer (as insoluble fraction).

Analysis by SDS-PAGE: soluble and insoluble fractions were loaded on SDS-PAGE with molecular weight marker and run for separation of proteins. After the run was completed gel was stained with coomassie followed by destaining to visualise the bands.

3.5.2 Purification of MBP tagged DDX3X from *E. coli rosetta (DE3)* strain

Method:

1. All the purification steps starting from re-suspension to elution and TEV cleavage were done at 4⁰C.
2. Steps 1 to 9 were followed.
3. **Equilibration of amylose resin beads:** Amylose resin was given five column volume washes with autoclaved milli-Q to remove traces of ethanol, as the beads are stored in 20% ethanol. Further, five column volume washes was given with lysis buffer to calibrate the resin.
4. **Binding:** The soluble protein was carefully transferred into the column containing the affinity resin, and protein was allowed to bind for 1 h at 4⁰C with gentle shaking. After binding flow through was collected by gravity flow and rechecked the unbound fraction by SDS-PAGE analysis.
5. **Washing:** Non-specifically bound proteins were removed from the affinity matrix by washing it three times with wash buffer. A small aliquots of each wash was taken for SDS-PAGE analysis. Small aliquot of protein bound resin was also taken for SDS-PAGE analysis.
6. **Elution:** The protein bound to amylose resin was eluted by passing the elution buffer containing 10 mM maltose through affinity matrix by gravity flow. Different aliquots of eluted protein were collected and 10 µl of each aliquot was analysed by SDS-PAGE.
7. **TEV Protease Cleavage:** MBP tag of the fusion protein was removed by incubating the eluted protein with 20 units of 6XHis-TEV protease in elution for 3 h at 4⁰C.

8. **Equilibration of centricon (for Dialysis of eluted protein to remove maltose and change the buffer):** Centricon (10-50 KDa molecular weight cut off) was washed with water to eliminate traces of alcohol and equilibrated with dialysis buffer by centrifuging it with dialysis buffer at 4000 rpm for 15 minutes at 4°C.
9. **Dialysis of eluted protein:** Eluted protein was diluted with dialysis buffer and then put in the equilibrated centricon. Centricon was then centrifuged at 4000 rpm at 4°C. The flow through in lower tube of the centricon was discarded and step 9 is repeated two more times. The dialysed protein was collected from the upper chamber of centricon once the desired volume of dialysed protein was achieved.

3.6 RNA Helicase assay

Reagents: All the reagents are made in DEPC-treated autoclaved Milli-Q water.

1. 18 mer RNA oligonucleotide labeled with 6-Carboxyfluorescein (6-FAM) fluorescent dye (Sigma)
Sequence: 5'-CCCAAGAACCCAAGGAAC-3'
2. 36 RNA oligonucleotide having complementary sequence of 18 mer oligo in middle portion (Sigma)
5'-ACCAGCUUUGUCCUUGGGUUCUUGGGAGCAGCAGG-3'
3. Ultra-pure Glycerol (Invitrogen)
4. 30 % acrylamide solution: 29.2 g acrylamide, 0.8 g bis-acrylamide were dissolved in approximately 50-60 ml autoclaved Milli-Q water and the final volume was made up to 100 ml. Solution was filtered through ordinary filter paper and stored in an amber colored bottle at 4 °C.

5. 20% SDS: 20 g SDS was dissolved in 80 ml of Milli-Q water, heated at 60°C to assist the dissolution. The final volume was made up to 100 ml, and stored at room temperature.
6. 5X Tris Borate EDTA buffer: Weigh 54 g of Tris base (FW = 121.14 Sigma) and add 27.4 g of Boric acid (FW = 61.83 Sigma) and dissolve in approximately 900 ml autoclaved Milli-Q water. Then add 20 ml of 0.5 M EDTA (pH=8.0) and then adjust the final volume to 1 Litre. The pH of concentrated buffer should be approximately 8.3.
7. Tris-HCl (pH=7.5): 6.055 g Tris was dissolved in 40 ml of Autoclaved DEPC Milli-Q water. pH was adjusted to 7.5 with concentrated HCl, the final volume was made up to 500 ml with Milli-Q water and autoclaved. Solutions were stored at 4°C.
8. 5 M NaCl in autoclaved DEPC Milli-Q water
9. 0.5 M EDTA in Autoclaved DEPC milli-Q water
10. 0.1M DTT Sigma
11. BSA 10 mg/ml
12. 100 mM ATP Thermo Fisher Scientific
13. 50 mM MgCl₂, Thermo Fisher Scientific
14. Bromophenol Blue

Buffers to be made before starting Assay:

1. 5X RNA annealing buffer:

Reagents	Stock	Required for 1X	Volume required for 5X (1 ml)
TrisHCl (pH=7.5)	1 M	10 mM	50 µl
NaCl	5 M	50 mM	50 µl

EDTA	500 mM	1 mM	2 μ l
DEPC milli-Q			898 μ l
Total			1 ml

2. Make the 5X helicase assay buffer as mentioned below:

Reagents	Stock	Concentration for 1X	Volume to be taken from stock (for 100ul of 5X)
TrisHCl (pH=7.5)	1 M	50 mM	25 μ l
DTT	100 mM	1 mM	5 μ l
BSA	10 mg/ml	0.2 mg/ml	10 μ l
glycerol	50 %	5 %	50 μ l
ATP	100 mM	1 mM	5 μ l
MgCl ₂	50 mM	10 mM	*
DEPC Milli-Q	-	-	5 μ l
Total	-	-	100 μ l

(*MgCl₂ to be added separately to the helicase reaction)

3. 5X RNA loading Dye

Reagents	Stock	Required concentration (for 5X)	Dilution from stock (for 5X)
TrisHCl (pH=7.5)	1 M	100 mM	100 μ l
SDS	20 %	0.5 %	25 μ l
glycerol	100 %	50 %	500 μ l
Bromophenol Blue	-	0.5 %	-
DEPC Milli-Q	-	-	375 μ l
Total	-	-	1000 μ l

Method:1. RNA oligo Annealing protocol

Add the component as mentioned below:

Component	Volume (μ l)
36mer RNA Oligo (200 μ M)	5
18mer 6FAM RNA oligo (200 μ M)	3
5X Annealing Buffer	6
DEPC MQ	16
Total	30

- Mix well and keep at 95⁰C for 5 minutes.
- Gradually bring it to room temperature.
- Set the helicase assay as mentioned in following table:

Reagents	Volume
5X helicase assay buffer	5 μ l
MgCl ₂ (50mM)	5 μ l
Annealed RNA oligo (20 nM final concentration)	2.5 μ l
RNase Inhibitor (5 U/ μ l)	1 μ l
100X Protease inhibitor	0.3 μ l
Protein (0.2, 0.4 and 0.8 μ M final concentration)	-
Total	Adjudt final volume 25 μ l with DEPC milli-Q

5. Incubate at 37⁰C for 1 h and then stop the reaction by adding 50 mM EDTA and RNA loading dye then analyse them on 10% non-denaturing PAGE in 1X TBE with 0.1% SDS
6. 10% non-denaturing gel composition in 1X TBE

Reagents	Volume for 15 ml
30% Acrylamide	5 ml
10X TBE	1.5 ml
50% Glycerol	0.75 ml
20%SDS	75 μ l
TEMED	7.5 μ l
20% APS	50 μ l
Milli-Q	6.61 ml

7. Run gel in 1XTBE with 0.1% SDS at 12 mA constant current in cold room and then visualize.

3.7 Luciferase Reporter Assay

Promoter Luciferase assay: TOPflash construct containing three consecutive TCF4 binding sites and mutant β -catenin cloned in pcDNA3.0 were already available in lab. pCMV-myc vector containing DDX3X cDNA (a kind gift from Dr. Laura Madrigal-Estebas, Trinity College, Dublin) was cloned in pcDNA3.0 expression vector. Co-transfection of TOPflash constructs with or without mutant β -catenin and with wild type or mutants of DDX3X along with EGFP expression plasmid was done using Calcium phosphate BES buffer method in 293FT cells. For IFN β promoter luciferase reporter assay, co-transfection of EGFP expression plasmid, IFN β promoter construct alone or with TBK1 or IKK ϵ or IPS-1 and wild type DDX3X or its mutants

was done in 293FT cells. Luciferase activity normalised by EGFP fluorescence was reported as promoter activity.

Luciferase reporter assay for mRNAs containing complex 5'-UTR: Cyclin E1 contains a complex 5'-UTR. Cyclin E1 5'UTR was amplified from genomic DNA of normal human peripheral blood lymphocytes using Phusion Taq polymerase. Reporter construct containing complex 5'-UTR was generated by cloning cyclin E1 5'UTR downstream of SV40 promoter and upstream of luciferase sequence in pGL3 control vector. 293FT cells were transfected with the luciferase reporter plasmid, EGFP expression vector and wild type or mutant DDX3X using calcium phosphate BES buffer method. Luciferase activity was assessed from the total protein extracted from the transfected 293FT cells and was normalized against the EGFP fluorescence.

3.7.1 Generation of Vector constructs for promoter luciferase reporter assay and for mRNAs containing complex 5'-UTR reporter assay

Reagents

1. Plasmids: pcDNA3.0 (Invitrogen, Life Sciences, Carlsbad, CA, USA); pGL3 control ((Promega, Madison, WI, USA)
2. Enzymes: Phusion Taq Polymerase, Klenow Fragment, Restriction Enzymes, T4 DNA Ligase, standard Taq Polymerase, T4PNK.
3. QIAquick Gel Extraction Kit

1) Luciferase reporter construct containing complex 5'-UTR mRNA – Complex 5'-UTR of cyclin E1 mRNA was PCR amplified using phusion Taq polymerase from genomic DNA of normal human peripheral blood lymphocytes. Primers were designed such that they harbour HindIII restriction enzyme sites on their both ends. Amplified fragments were digested with

HindIII restriction enzyme and then blunt end cloning was done downstream of SV40 promoter of pGL3 control vector.

2) pcDNA3-DDX3X – pCMV-myc vector containing DDX3X cDNA was gifted by Dr. Laura Madrigal-Estebas, Trinity College, Dublin. DDX3X cDNA was amplified from this plasmid using Phusion Taq DNA polymerase and purified by precipitation. After precipitation it was restriction digested with BamHI and EcoRI followed by ligation with pcDNA3.0 expression vector digested with same enzyme.

3) Mutant DDX3X constructs – DDX3X mutations identified in this study (G242fs deletion, Q265H and A367T) were generated in pcDNA3-DDX3X by using site directed mutagenesis PCR reaction. Mutation was confirmed by Sanger Sequencing.

Primer sequences used in cloning and site directed mutagenesis are given in table 3.2

Name of the Gene	Forward/Reverse	Sequence
Cyclin E1 5'-UTR	Forward	GATAAGCTTTCTGAGCCGGGCG CAGGA
Cyclin E1 5'-UTR	Reverse	GATGGGGCTGCTCCGGCC
Cyclin E1 5'-UTR	Reverse nested	GACAAGCTTGATGGGGCTGCTC CGGCCTGAGGCCAGGGTCTTGTC CGCGGC
DDX3X (cloning in pcDNA3)	Forward	GGTGGATCCATGAGTCATGTGG CAGTGGAA
DDX3X (cloning in pcDNA3)	Reverse	GTCGAATTCCTATCAGTTACCCC ACCAGTCAAC
DDX3X_SDM_G242fs	Forward	GAAGGAAAATGGAGGTATGGGC GCCG
DDX3X_SDM_G242fs	Reverse	CGGCGCCCATACCTCCATTTTCC TTC
DDX3X_SDM_Q265H	Forward	GAGTTGGCAGTACACATCTACG

		AGGAAGC
DDX3X_SDM_Q265H	Reverse	GCTTCCTCGTAGATGTGTACTGC CAACTC
DDX3X_SDM_A367T	Forward	CACTATGATGTTTAGTACTACTT TTCCTAAGG
DDX3X_SDM_A367T	Reverse	CCTTAGGAAAAGTAGTACTAAA CATCATAGTG
DDX3X_SDM_R534H	Forward	GTATTGGTCGTACGGGACATGTA GGAAACCTTGGC
DDX3X_SDM_R534H	Reverse	GCCAAGGTTTCCTACATGTCCCG TACGACCAATAC
DDX3X_SDM_P568L	Forward	GAAGCTAAACAAGAAGTGCTGT CTTGGTTAGAAAACATGG
DDX3X_SDM_P568L	Reverse	CCATGTTTTCTAACCAAGACAGC ACTTCTTGTTTAGCTCT

Table 3.2 Primers sequences for cloning 5'UTR, DDX3X and site directed mutagenesis.

Method:

1. Primers were designed to have (a) T_m more than or equal to 78°C . T_m can be calculated by the formula $T_m = 81.5 + 0.41(\%GC) - 675/(\text{length in bases}) - \%mismatch$, (b) Forward primer length between 25 to 45 bases with desired mutation at the centre (c) reverse primer should be exactly complimentary to Forward primer, (d) GC content of more than 40% and terminating in G or C.

2. PCR reaction was set up as follows

Components	Volume per 10μl Reaction	Final Concentration
5XHF buffer	2 μ l	1X
10mM dNTPs	0.2 μ l	2mM

10pmol/ μ l Forward primer	0.2 μ l	2pmol
10pmol/ μ l Reverse Primer	0.2 μ l	2pmol
Template (vector DNA)	10ng	-
Phusion Taq Polymerase (2U/ μ l)	0.5 μ l	1 U
DMSO (optional)	0.3 μ l	3%
Autoclaved Milli-Q	Make up to 10 μ l	

PCR Reaction conditions were as follows

Temperature	Time	No. Of. Cycles
98 ⁰ C	3 min	1
98 ⁰ C	1 min	20
50-60 ⁰ C (variable)	45 sec	
72 ⁰ C	1 min per kb	
4 ⁰ C	∞	

3. PCR product was digested with DpnI enzyme. Reaction conditions were as follows

Components	Volume	Final Concentration
10X Tango buffer	2 μ l	1X
PCR product	15 μ l	100-200ng
DpnI (10U/ μ l)	1 μ l	
Autoclaved Milli-Q	Make up volume to 20 μ l	

4. Reaction mixture was incubated at 37⁰C for 12-16 hr and was inactivated at 80⁰C for 20 min.

5. 5 μ l of PCR product before and equivalent PCR product after DpnI digestion was loaded on 1% agarose gel to ensure persistence of full length PCR product post DpnI digestion.

6. 5 μ l of DpnI digested DNA was transformed in DH5 α competent cells.

7. Plasmid DNA was extracted from 10-20 DH5 α colonies formed by alkaline lysis method.

8. Plasmid DNA was given for sequencing with DDX3X G242 forward primer to confirm the mutation.

3.7.2 Luciferase assay

Reagents:

Cell lysis buffer:

Components	Volume	Final Concentration
1M Glycine-glycine pH 7.8	1.25 ml	25mM
1M MgSO ₄	0.75 ml	15mM
250mM EGTA	0.8 ml	4mM
Triton X-100	0.5 ml	1% (v/v)
100mM DTT	*	1mM
Autoclave Milli-Q	Make up to 50 ml	

Luciferase Assay Buffer

Components	Volume	Final Concentration
1M Potassium phosphate buffer pH7.8	0.75 ml	15mM
1M Glycine-glycine pH7.8	1.25 ml	25mM
1M MgSO ₄	0.75 ml	15mM
250mM EGTA	0.8 ml	4mM
100mM ATP	*	2mM
100mM DTT	*	1mM
Autoclave Milli-Q	Make up to 50 ml	

Luciferin Solution

Components	Volume	Final Concentration
1M Glycine-glycine pH7.8	1.25 ml	25mM
1M MgSO ₄	0.75 ml	15mM
250mM EGTA	0.8 ml	4 mM
20mM D-Luciferin	*	0.2mM

100mM DTT	*	2mM
Autoclave Milli-Q	Make up to 50 ml	

(*Note- Add DTT, ATP and D-Luciferin just before use)

Method:

1. 293FT cells were trypsinised, counted and seeded as 2×10^5 cells per 35mm dish, 5×10^4 cells per well of 24 well late or 1×10^4 cells per well of 96 well plate.
2. 16-24 hr post seeding, transfection of total of 6 μ g DNA for 35mm dish, 1.5 μ g DNA per well of 24 well dish and 0.3 μ g DNA per well of 96 well was done using BES buffer method.
3. DNA mixture was prepared in autoclaved Milli-Q as given below.

1) For IFN β Promoter Luciferase Reporter assay –

Components	Final Amount/ volume		
	35mm dish	24 well plate (for one well)	96 well plate (for one well)
IFN β promoter	500ng	125ng	25ng
TBK1/IKK ϵ /IPS-1	1 μ g	250ng	50ng
pcDNA3-GFP	500ng	125ng	25ng
pcDNA3/DDX3X WT/Mutants	4 μ g	1 μ g	200ng
Autoclaved Milli-Q	Make up volume to 50 μ l	Make up volume to 12.5 μ l	Make up volume to 2.5 μ l
0.5M CaCl ₂	50 μ l	12.5 μ l	2.5 μ l
2X BBS	100 μ l	25 μ l	4 μ l

2) For TOPflash Luciferase Reporter assay -

Components	Final Amount/ volume		
	35mm dish	24 well plate (for one well)	96 well plate (for one well)

TOPflash reporter	500ng	125ng	25ng
B-catenin	500ng	125ng	25ng
pcDNA3-GFP	500ng	125ng	25ng
pcDNA3/DDX3X WT/Mutants	4.5µg	1125ng	225ng
Autoclaved Milli-Q	Make up volume to 50µl	Make up volume to 12.5µl	Make up volume to 2.5 µl
0.5M CaCl ₂	50µl	12.5 µl	2.5 µl
2X BBS	100µl	25 µl	5 µl

3) Luciferase Reporter assay for mRNA containing complex 5'-UTR-

Components	Final Amount/ volume		
	35mM dish	24 well plate (for one well)	96 well plate (for one well)
5'UTR reporter Plasmid	500ng	125ng	25ng
pcDNA3-GFP	500ng	125ng	25ng
pcDNA3/DDX3X WT/Mutants	5µg	1.25µg	250ng
Autoclaved Milli-Q	Make up volume to 50µl	Make up volume to 12.5µl	Make up volume to 2.5 µl
0.5M CaCl ₂	50µl	12.5 µl	2.5 µl
2X BBS	100µl	25 µl	5 µl

4. Following addition of 0.5M CaCl₂ to the DNA mixture, appropriate volume of 2XBBS was added and then the mixture was mixed by pipetting gently two to three times to ensure thorough mixing of all components.

5. Tubes were incubated for 20 min at RT, following which mixture was added to respective wells or dish.

6. Medium was changed after 16 h from transfection. Lithium chloride was added at final concentration of 25mM whenever necessary.
7. 72 hr after transfection, medium was removed and cells were washed twice with ice cold 1X PBS.
8. Appropriate volume of cell lysis buffer (200 µl per 35mm dish, 50 µl per well of 24 well plate or 96 well plate was added to the cells. Cells were scraped from the plate and lysis of cells was ensured by pipetting the volume up and down several times.
9. Lysate was transferred to the microcentrifuge tube and centrifuged at 16000 rpm, 4⁰C for 5 min.
10. Supernatant was transferred in fresh microcentrifuge tubes and fluorescence and luminescence was measured using Mithras LB940 multimode reader as described below.
11. 10µl of sample was added per well of 384 well Optiplate (Cat No. 6007290, Perkin Elmer) and fluorescence was measured at excitation and emission wavelengths of 485nm and 515nm. Each sample was assayed in triplicates.
13. 20µl of assay buffer and 10ul of Luciferin solution were added to sample and mixed twice by pipetting.
14. Luminescence was read immediately at exposure time of 0.1 sec.

3.8 Extraction of nucleic acids

Prior to RNA and DNA extraction, cryosections of fresh frozen tumour tissues were stained for hematoxylin and eosin and examined by light microscopy to ensure at least 90 % tumour content.

3.8.1 Genomic DNA Extraction from tissue culture cells

Reagents

8 M Potassium acetate: Weigh 39.26 g Potassium acetate in 50 ml sterile NUNC tube. Dissolve in MQ water. Make up the volume to 50 ml. Autoclave.

Solution A: Add 2.5 ml (2 M Tris, pH 9.0), 10 ml (0.5 M EDTA), 2.5 ml (20 % SDS) in 35 ml sterile MQ water. Autoclave.

Method

1. The medium was poured off, cells were washed with 1 X PBS twice and cells were lysed by adding 1.0 ml of Solution A (0.1 M Tris pH 9.0, 0.1 M EDTA, 1% SDS) for 35 mm culture dish and immediately incubating the sample for 30 min at 70°C.
2. 140 µl of 8 M potassium acetate was added per 1.0 ml of the Solution A and tube was shaken vigorously to ensure proper mixing of reagents.
3. The tube was incubated on ice for 30 min and centrifuged at 10,000 rpm for 15 min at 4°C.
4. The supernatant was transferred carefully to a fresh tube using a cut 1 ml pipette tip. DNA was precipitated by adding 0.5 volumes of isopropanol. Sample was mixed by vigorous shaking and incubated at room temperature for 5-10 min.
5. The tube was centrifuged at 10,000 rpm for 10 min at room temperature and supernatant was poured off. DNA pellet was washed with 1 ml of 70% ethanol by incubating tube at room temperature for 5 min.
6. The tube was centrifuged at 10,000 rpm for 5 min at room temperature to recover the pellet. The 70% ethanol was poured off and the tube was kept inverted on tissue paper to drain off remaining droplets.

7. The pellet was air-dried, and 50 μ l of TE containing RNase (50 μ g/ml) was added. The tube was incubated at 37°C for 1-2 h with intermittent tapping to both dissolve the genomic DNA as well as to digest the RNA.
8. The quality of DNA was checked by electrophoresing 2 μ l on a 0.8% agarose gel. DNA was quantified by determining absorbance at 260/280 nm.

3.8.2 Total RNA extraction from fresh frozen tumour tissues and/or tissue culture cells by acid guanidinium Isothiocyanate-phenol chloroform extraction Reagents:

Preparation of DEPC-treated Milli-Q water: Water was collected from the Milli-Q plant directly in sterile 50ml NUNC tubes. 50 μ l DEPC was added to 50ml Milli-Q water, mixed vigorously and left overnight at 37°C, with the tubes loosely capped. The tubes were autoclaved on the following day. The DEPC-treated Milli-Q water was used for preparing all the reagents required for RNA extraction.

1 M Sodium citrate, pH 7.0: 14.7 g Sodium citrate-dihydrate was dissolved in about 35 ml autoclaved Milli-Q water. pH was adjusted to 7.0 with few drops of 1 M citric acid and the volume was made up to 50 ml. (1 M Citric acid was prepared by dissolving 10.5 g powder in 50 ml DEPC-treated water.) 50 μ l of DEPC was added to both 1 M citrate and citric acid solution, tubes were mixed vigorously and left at 37°C overnight. The solutions were autoclaved the next day, and stored at room temperature.

10% N-lauryl-sarcosine: 5g N-lauryl-sarcosine was dissolved in DEPC-treated water and the final volume was made up to 50 ml. Resulting solution was neither treated with DEPC, nor autoclaved. It was kept at 65°C for 1 h, and stored at room temperature.

4 M Guanidine Isothiocyanate (GITC): (Prepared in 25 mM Sodium citrate pH 7.0, 0.5% Sarcosyl). 23.6 g of guanidine isothiocyanate was dissolved in 40 ml DEPC-treated water. 1.25 ml of 1 M sodium citrate and 2.5 ml of 10 % sarcosine was added and the final volume was made up to 50 ml with DEPC-treated water. The final solution was neither treated with DEPC nor autoclaved. Solution D was prepared from GITC by adding β -mercaptoethanol at a final concentration of 0.1 M. This solution is stable at room temperature for one month.

Phenol (Saturated with DEPC-treated water): 25 ml DEPC-treated water was added to 25 ml distilled phenol at room temperature in a sterile NUNC tube. The tube was mixed vigorously by inverting several times. The phenol was kept at 4°C until the two phases separated (30-60 min). The upper water phase was replaced with fresh DEPC-treated water, mixed once again and stored at 4°C.

2 M Sodium acetate, pH 4.0: 13.6 g sodium acetate was dissolved in about 25 ml of Milli-Q water and pH was adjusted to 4.0 with glacial acetic acid. Final volume was made up to 50 ml with Milli-Q water. 50 μ l DEPC was added to the solution, mixed vigorously and left at 37°C overnight. The solution was autoclaved the following day and stored at room temperature.

Chloroform

Absolute alcohol

70 % alcohol

Only RNase free sterile plastic wares were used.

Method:

1a. For tissue samples: Approximately 30-50 mg of frozen tumour tissue was collected in a chilled homogenization collection tube. This was homogenized with approximately 2-3 ml of Solution D. The tissue lysate was collected in a microcentrifuge tube and immediately passed

through a 26-gauge needle at least ten times. The lysate was triturated until it lost its viscosity, resulting in complete shearing of genomic DNA.

- 1b. For tissue culture cells: The medium was poured off, cells were washed with 1 X PBS twice and 0.5ml of Solution D was added per well of 24 well plate. The cell lysate was collected by tilting the plate and was passed immediately through a sterile syringe fitted with a 26 gauge needle. This was done at least ten times until the lysate lost its viscosity, resulting in complete shearing of the genomic DNA. At this stage the lysate was either stored at -20°C or processed further immediately.
2. 50µl of 2 M Sodium acetate pH 4.0 was added per 0.5 ml lysate and mixed by inverting the tubes.
3. Next, 0.5ml DEPC-water-saturated phenol and 0.2 ml chloroform was added successively to the tube and the contents of the tube were mixed thoroughly by vortexing for 1 min. The cap of the tube was loosened to release the pressure and then vortexed again for 30 sec.
4. The tube was kept on ice for 15 min and then centrifuged for 15 min at 4°C at 10,000 rpm in a table-top centrifuge. The upper aqueous layer obtained was transferred to a fresh micro-centrifuge tube and centrifuged once again to settle any traces of phenol.
5. The aqueous phase was then transferred to a fresh tube and an equal volume of isopropanol (0.5 ml per tube) was added. This was mixed by brief vortexing and kept at -20°C overnight for precipitation of RNA.
6. Next day, the tube was centrifuged at 12,000 rpm at 4°C for 20 min to pellet down the precipitated RNA. The supernatant was decanted carefully so as to not disturb the RNA pellet.
7. The RNA pellet was washed with 0.5ml of 70 % ethanol, kept at room temperature for 2 min, and re-centrifuged at 12,000 rpm at 4°C for 10 min. The supernatant was decanted, and the left over alcohol was allowed to dry by keeping the tube open with a clean tissue paper to

cover it. The RNA pellet was air-dried, and dissolved in a minimum of 10µl DEPC-treated water. For dissolving the RNA, it was first kept on ice for about 60 min with intermittent vortexing and spinning, followed by heating at 65°C for 10 min. The dissolved RNA was subsequently stored at -80°C.

8. RNA was quantified spectrophotometrically (O.D. at 260/280 nm) using the NanoDrop UV-Vis spectrophotometer. The integrity of RNA was ascertained by denaturing agarose gel electrophoresis. The ratio of 28s rRNA to 18s rRNA is approximately 2:1 in a good quality RNA.

3.8.3 Preparation of denaturing gels for RNA separation and quality assessment

Formaldehyde containing agarose gel was used for checking the integrity of RNA from fresh frozen tumour tissues. Unlike DNA, RNA has a high degree of secondary structure, making it necessary to use a denaturing gel. Formaldehyde in the gel disrupts secondary RNA structure enabling the RNA molecules to be separated by charge migration.

Reagents:

Agarose

10X MOPS: 41.6 g MOPS, 16.7 ml of 3 M sodium acetate pH 5.0, 20 ml of 0.5 M EDTA pH 8.0. Adjust pH to 7.0 with 5 M NaOH and make up the volume to 1 litre with DEPC water.

Autoclave the solution and store in an amber colored bottle.

Formaldehyde

Formamide

10X RNA loading dye: 1mM EDTA pH 8.0, 50 % v/v glycerol, 0.4 % bromophenol blue.

Method:

1. For a 50 ml volume, 1 % agarose gel was prepared as follows: 0.5 g agarose was weighed into 35 ml of autoclaved Milli-Q water. The slurry was heated in a microwave oven until the agarose dissolved completely. 5 ml 10 X MOPS was added make the final concentration to 1 X and the slurry was mixed properly and placed at 60 °C for 10 min.
2. Next, 10 ml formaldehyde (37 % solution) – GR grade, was added and the formaldehyde-agarose slurry was kept at 60 °C for 15 min.
3. Ethidium bromide to a final concentration of 0.5 µg/ml (2.5 µl), was added to the agarose mix, and the mixture was poured in a gel tray and allowed to set at room temperature for 30-45 min.
4. After the gel had completely set, it was placed in the electrophoresis tank filled with 1 X MOPS buffer (30 ml MOPS + 30 ml formaldehyde-LR grade + 240 ml Milli-Q), just enough to cover the gel.
5. For sample preparation, RNA was mixed with 10 X MOPS (final concentration 1 X MOPS) and freshly prepared formamide: formaldehyde (3:1) mixture. For example; for 2 µl of 1 µg RNA, 1 µl of 10 X MOPS and 6 µl formamide: formaldehyde (3:1) was added. This mix was subsequently placed at 60 °C for 20 - 30 min.
6. 10 X RNA loading dye at 1 X final concentration was added to the above mix and loaded into the wells of the gel. The gel was electrophoresed at 60 mA constant current, till the dye had migrated almost to the other end of the gel.
7. The gel was then placed in Milli-Q water overnight to wash off excess of ethidium bromide. RNA was visualized by observing the gel under a UV transilluminator.

3.9 Gene expression analysis by real time RT-PCR

3.9.1 Primer Designing

The primers for real time RT-PCR analysis were designed such that they correspond to two adjacent exons, and are located at exon boundaries to avoid amplification of genomic DNA. The amplicon size was maintained around 100 bp. Primers were designed using the Oligo Explorer Software v 1.1.2. BLAST (www.ncbi.nlm.nih.gov/BLAST) and e-PCR feature of BiSearch software were performed to ensure primer specificity. The primers were reconstituted in TE Buffer, pH 8.0 to a concentration of 100 pmol/ μ l. For working stock of 10 pmol/ μ l, the primers were further diluted 1:10 using TE Buffer. All primers were stored at -20°C . Sequences of the primers used in the present study are listed below in table 3.3

Gene name	Forward/Reverse	Sequence
Hsa-miR-30a	Forward	GTCACGCTTTCAGTCGGATGTT
Hsa-miR-30a	Stem-loop primer	RT GTCGTATCCAGTGCAGGGTCCGAGGTATTTCGCAC TGGATACGACGCTGCA

Table 3.3 Primers used for miR-30a real time PCR using SYBR green chemistry

3.9.2 Reverse transcriptase PCR reaction for conversion of RNA to cDNA

Reagents:

5 X First Strand Buffer, M-MLV RT enzyme (200 U / μ l), 0.1 M DTT (all three from Invitrogen), 10 mM dNTP mix, RNase Inhibitor (20 U / μ l), p (dN) 6 primer(100 ng / μ l)

Method:

1. A 10 μ l reaction was set up for the cDNA synthesis from 1 μ g of DNase-treated total RNA
2. First, the following components were added to a nuclease-free microcentrifuge tube:

Components	Volume	Final Concentration
DNase-treated total RNA	-	500 ng
10mM dNTP mix	0.5 μ l	1 mM

100ng/ μ l random hexamers p(dN) ₆	0.5 μ l	0.5mM
DEPC treated Milli-Q water	Make up volume to 5 μ l	

3. RNA was heated at 65 °C for 5 min to denature RNA secondary structures and chilled on ice for 2 minutes.

4. Reaction mix was prepared on ice by adding the following components:

Components	Volume	Final Concentration
5X first strand buffer	2 μ l	1X
0.1M DTT	1 μ l	0.01M
RNase inhibitor (20U/ μ l)	0.25 μ l	5U
DEPC treated Milli-Q water	Make up volume to 3.5 μ l	

5. The reaction mix was added to the RNA, mixed by gentle pipetting, and incubated at 37 °C for 5 min to allow annealing of random primers to the RNA.

6. 0.5 μ l (100 U) of M-MLV RT was added to the reaction tube and mixed by gentle pipetting. The tubes were transferred to the thermal cycler (Eppendorf) and thereafter the following conditions were followed:

Temperature	Time
25 °C	10 min
37 °C	60 min
70 °C	15 min
4 °C	∞

7. The cDNA synthesized was then used for analyzing gene expression levels by real time PCR or stored at -20 °C.

3.9.3 Real Time PCR

Reagents:

2 X Power SYBR Green Master Mix, 10 pmol / μ l each gene specific Forward and Reverse primers, DEPC- treated Milli-Q water

Method:

1. The cDNA obtained from the reverse transcription reaction was diluted to 5ng/ μ l with DEPC- treated Milli-Q water for use in the PCR reaction. The PCR reaction was set up as follows:

Master Mix I:

Components	Volume	Final Concentration
2X SYBR Green Master Mix	2.5 μ l	1X
cDNA (5ng)	2 μ l	10ng
Total Volume	4.5 μ l	

Master Mix II:

Components	Volume	Final Concentration
10pmol/ μ l Forward primer	0.25 μ l	0.5pmol
10pmol/ μ l Reverse primer	0.25 μ l	0.5pmol
Total Volume	0.5 μ l	

2. The Master Mix I was then loaded into the wells of a 384-well microtitre optical plate followed by addition of master mix II to each well.
3. The plate was covered with an optical cover sheet and sealed with the help of an applicator. The applicator was pressed evenly over the optical cover sheet several times to ensure proper sealing of the wells.
4. The sealed plate was then centrifuged briefly at 2500 rpm for 2 min to spin down the reactions and remove air bubbles if any.

5. The plate was loaded in the Real Time PCR machine (ABI Prism 7900HT Sequence Detection System/ QuantStudio 12K Flex, Applied Biosystems, USA) and run on default cycling parameters.

PCR cycling parameters:

Temperature	Time	No. Of Cycles
50 °C	10min	Hold
95 °C	10min	Hold
95 °C	15 sec	40
60 °C	1min	

6. The 50 °C incubation is to activate UNG glycosylase enzyme that prevents carry over PCR contamination followed by an initial denaturation step for 10 min with activation of HotStart Taq polymerase and then 40 cycles of denaturation-annealing-extension. In case of SYBR Green Assays after completion of 40 cycles, the dissociation curve step of the amplified products was performed to determine the formation of primer dimers, if any.

7. Amplification data was collected in real time by the machine and stored in the SDS 2.1 or QuantStudio software. After completion of the runs, the data was analyzed using these same softwares.

8. *GAPDH* was used as the housekeeping gene control. The expression of the gene of interest, relative to *GAPDH* levels was quantified and expressed as Relative Quantity (RQ), calculated by the comparative Ct method.

9. The expression of the gene of interest, relative to *GAPDH* (or *RNU48* in case of miRNAs) levels were quantified and expressed as Relative Quantity (RQ), calculated as Ct (gene of

interest) – Ct (*GAPDH*) = Δ Ct. The Relative quantity was calculated as $[2^{-(\Delta Ct)} \times 100]$. Ct = Threshold cycle as automatically determined by the SDS 2.1 or QuantStudio software.

3.10 Quantification of miRNA expression by Real time PCR

MiRNA quantification involves a stem-loop reverse transcription followed by real time PCR. Mature miRNAs are only 20-23 nucleotides in length. The stem-loop RT primers hybridize to mature miRNA molecule at the 3' end and then get reverse transcribed with the help of a reverse transcriptase enzyme. The RT product is then quantified by conventional TaqMan PCR with miRNA specific forward primer, reverse primer corresponding to part of the stem-loop RT primer (excludes the loop region) and the TaqMan probe.

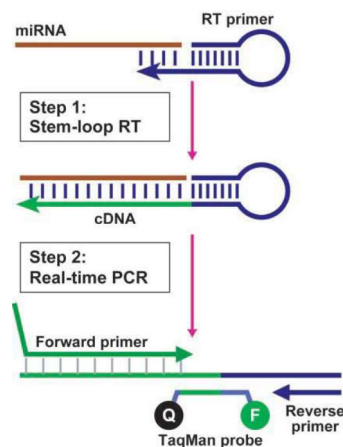


Figure 3.1: Stem- loop RT-PCR for miRNA. Schematic description of stem-loop RT- PCR for miRNA quantification using TaqMan miRNA Assays

Total RNA, 50ng, was reverse transcribed using stem-loop 5X RT primer and Multiscribe Reverse transcriptase as per the manufacturer's instructions. The reaction conditions were as follows:

3.10.1 Stem- loop Reverse Transcription for miRNA

Reagents:

10 X RT Buffer, 100mM dNTP mix, 5 X RT Primers for RNU48, miR-30a-3p, RNase Inhibitor (20 U/ μ l), Multiscribe M-MLV RT enzyme (50 U/ μ l), DEPC- treated Milli-Q water

Method:

1. All the reagents required were thawed and mixed well by tapping and pulse spinning.
miRNA reverse transcription primers were thawed on ice.
2. A 5 μ l reaction was set up from 50ng of RNA extracted from stable pTRIPZ or pTRIPZ-miR-30a expressing polyclonal populations of medulloblastoma cell lines.
3. The reaction contained the following components:

Components	Volume	Final Concentration
10 X RT Buffer	0.5 μ l	1 X
100mM dNTP mix	0.1 μ l	0.5mM
5 X RT primer	2.0 μ l	1 X
RNase inhibitor (20 U/ μ l)	0.1 μ l	2 U
Multiscribe MMLV-RT (50 U/ μ l)	1 μ l	50 U
Total RNA	50ng	
DEPC treated MQ water	Make up volume to 5 μ l	

4. A master mix was first prepared in a 0.5 ml tube excluding the RNA making up the total volume to 3 μ l.
5. Before adding MMLV-RT, the PCR machine was set and kept on hold at 16 °C and the lid temperature was set to 105 °C. The contents of the tube were gently mixed by tapping followed by a pulse spin.

6. 3µl of master mix was then dispensed into each 0.2 ml tube followed by addition of 2µl of the diluted RNA sample (5ng or 100ng/µl) to the respective tubes. The reaction mix was gently tapped and pulse spun and transferred to a thermal cycler. The reaction conditions were as follows:

Temperature	Time
16 °C	30 min
42 °C	30 min
85 °C	5 min
4 °C	∞

3.10.2 Real time PCR

Reagents:

2 X Taqman PCR Master Mix, 20 X Taqman miRNA Assays (miRNA Primer-Probe), DEPC-treated Milli-Q water

Method:

1. cDNA obtained from the stem- loop reverse transcription reaction was diluted to 5 ng/µl (Fresh frozen tissue) with DEPC-treated Milli-Q water for use in the PCR reaction. The PCR reaction was set up as follows:

Master Mix I:

Components	Volume	Final Concentration
2 X Taqman PCR Master mix	2.5µl	1 X
cDNA (5ng or 20ng /µl)	2.0µl	10ng
Total volume	4.5µl	

Master Mix II:

Components	Volume	Final Concentration
20 X Probe-Primer Mix	0.25µl	1 X
DEPC treated Milli-Q water	0.25µl	
Total volume	0.5µl	

The steps following this were same as that in real time PCR for gene expression analysis (refer section 3.9.3 steps 2-7). RNU48 was used as the housekeeping small RNA internal control for miRNAs. The expression of the miRNA of interest, relative to RNU48 levels was quantified by the comparative Ct method (Refer section 3.9.3 steps 8-9).

3.11 Tissue culture media and reagents

1. Tissue culture medium: Commercially available powdered medium, Dulbecco's Modified Eagle Medium (DMEM) containing high glucose, pyridoxine hydrochloride and sodium pyruvate or Dulbecco's Modified Eagle Medium:Nutrient mixture (DMEM/F12) was prepared as per the manufacturer's instructions.

The powdered medium was reconstituted by dissolving it in ~ 800 ml autoclaved Milli-Q water under sterile conditions. 3.5 g Sodium bicarbonate was added and the pH was adjusted to 7.5 using 1N HCl (about 11 ml). The volume was made up to 1 L in a sterile volumetric flask and the medium was filter sterilized through a 0.22 µm pore size filter membrane (Cat no. GSWP04700) fitted in a sterile filtration assembly. The filtered medium was stored as 500 ml aliquots at 4°C. The complete medium contained DMEM supplemented with 10 % fetal bovine serum (FBS), Invitrogen (Cat. No.16140-071). 1 ml of the 100 X antibiotic (Penicillin and streptomycin) stock solution was added per 100 ml of complete medium if required.

2. 100 X antibiotic mix: 10,000 units penicillin G (Alembic Ltd, Vadodara, India) and 10,000 μ g streptomycin sulphate, available as injection vials (Abbott Healthcare Pvt. Ltd, Ahmedabad, India) were dissolved per ml in Milli-Q water, filter sterilized and stored at 4 °C.
3. 10 X phosphate buffered saline (PBS): 80.8 g NaCl, 2 g KCl, 12.6 g Na₂HPO₄.2 H₂O, 2 g KH₂PO₄, and 10 g glucose was dissolved in autoclaved Milli-Q water and the volume made up to 1 L. The solution was filter sterilized and stored at 4 °C.
4. 10 X Trypsin (0.25 %): 2.75 g of trypsin was added to 110 ml of autoclaved Milli-Q water and allowed to dissolve overnight on a magnetic stirrer. The solution was sterilized by filtering through a 0.22 μ m pore size Millipore filter. The solution was stored as 10 ml aliquots at -20 °C. 10 X stocks were diluted to 1 X working solution with 1 X PBS. Working solution was stored at 4 °C.

3.12 Routine maintenance of cell Lines

All glassware and plastic-ware used for tissue culture work were sterile. For maintenance and experimental use, all adherent cells (like HEK 293FT, Daoy) were trypsinized and passaged. While semi adherent cells like D425 Med and D283 Med were directly collected in medium and did not need trypsinization. The detailed procedure is as follows:

1. Spent medium was aspirated out using a Pasteur pipette and the cells in the plate were rinsed twice with 1 X PBS.
2. 1 X trypsin was added to the tissue culture dish, and was removed after the cells started to round up but just before the cells started detaching. The cells were collected in 1 X PBS and the cell suspension was transferred to a centrifuge tube containing about 1 ml complete medium as serum inhibits trypsin activity and tightly corked.

* In case of D425 Med, D283 Med cells, cells were dislodged, resuspended in medium with the help of Pasteur pipette and cell suspension is transferred to a centrifuge tube.

3. The cell suspension was centrifuged for ~ 2 min at 1000 rpm in REMI bench top centrifuge. The supernatant was discarded and the cell pellet was loosened by tapping the tube gently.
4. The cells were suspended in an appropriate volume of complete medium (DMEM or DMEM-F12 supplemented with 10 % FBS), cell count was taken using a hemocytometer, and the required cell number was seeded in tissue culture dishes, and incubated at 37 °C in a humidified 5 % CO₂ incubator. The cultures were passaged twice a week (at around 70-75% confluency) or were frozen when required. The cells were not passaged for too long and fresh vial of frozen cells was revived at regular time intervals.

3.13 Freezing and revival of cell cultures

1. For freezing of cells, 80-90 % confluent cultures were trypsinized as described above. The cell pellet was loosened by tapping the tube gently, and the centrifuge tube was placed on ice for one-two minutes. Pre-chilled freezing medium (90 % FBS + 10 % DMSO) was added drop wise to the cell pellet (~ 1 x 10⁶ cells / ml of freezing mixture) on ice, with constant shaking to ensure an even cell suspension and transferred to pre-chilled vials. These vials were cooled gradually and then stored in liquid nitrogen.
2. To revive the frozen cells, a vial containing frozen cells was removed from liquid nitrogen and immediately thawed in a water-bath at 37 °C. As soon as the cell suspension thawed, it was transferred to a centrifuge tube containing 5 ml complete medium and centrifuged at 1000 rpm for 2 min. The supernatant was discarded; cell pellet was loosened by tapping the tube gently and re-suspended in 5 ml complete medium and centrifuged again. The supernatant was discarded and the cells were re-suspended in an appropriate volume of complete medium.

The medium was replaced after the cells had adhered to the tissue culture dish, preferably on the same day or next day of revival.

3.14 Transient transfection of 293FT cells using BES buffer for Lentivirus production

Calcium phosphate mediated transfection method was used to transiently transfect plasmid DNAs in 293FT cells (Kingston, 2001).

Reagents:

2X BBS (BES Buffered Saline) [50mM BES, 280mM NaCl, 1.5mM Na₂HPO₄·2H₂O]:

For 50 ml BBS solution, 0.533 g BES, 0.818 g NaCl and 0.0134 g Na₂HPO₄·2H₂O were dissolved in 45 ml autoclaved Milli-Q water and the pH was adjusted exactly to 6.95 using 5 M NaOH. Final volume was made up to 50ml and pH was checked again. Solution was filter sterilized through 0.22µm filter and stored as 0.5 ml aliquots at -20°C.

0.5 M CaCl₂: 3.675 g CaCl₂·2H₂O was dissolved in 45 ml of Milli-Q water. The volume was made up to 50 ml and filter sterilized using 0.22µm filter. The solution was stored as 0.5 or 1 ml aliquots at -20°C.

The reagents required for transfection were removed from -20°C and thawed at RT beforehand and all plasmid DNAs used were purified through Qiagen Plasmid Midi Kit.

Method:

1. One day prior to transfection, the cells were trypsinized (the plate should not be over confluent). $\sim 8 \times 10^5$ 293FT cells were seeded in a 55mm plate. The plate should be around 70-80% confluent at the time of transfection.
2. Next day, 4 h before transfection, medium was replaced with fresh complete medium. The cells were transfected with total 12µg plasmid DNA using BBS.

3. A total of 12µg of plasmid DNA (i.e. 6 µg pLKO-Tet-DDX3X-shRNA301/UTR/empty vector or 6 µg miR-30a expressing pTRIPZ plasmid/ empty pTRIPZ + 4.5 µg pPAX2 + 1.5 µg pMD2.g) was diluted to 100µl in autoclaved Milli-Q in a sterile tube.
4. 100µl of 0.5 M CaCl₂ was added drop wise to the DNA in a tube (The contents were not mixed).
5. Then, 200µl 2X BBS was added drop wise and mixed gently by pipetting 3 – 4 times. The DNA-CaCl₂ mix was incubated at RT for 20 min.
6. After 20 min, the DNA-CaCl₂ complexes were mixed gently by pipetting and added over the cells drop wise, mixed well by gentle swirling the medium in the plate and incubated at 37°C in CO₂ incubator for 16 h.
7. After 16 h, the transfection medium was replaced with fresh complete medium.
8. 48 h post transfection, the virus containing supernatants was harvested and filtered using 0.45µm filter. The viral supernatant at this point was either used as it is for transduction of medulloblastoma cell lines or after concentration performed by ultracentrifugation at 25000 rpm, 4 °C. If required, virus containing supernatants was stored at -80°C until use.

3.15 Transduction with lentiviral particles for generating DDX3X knockdown in Daoy cell or stable over-expression of miRNA in Daoy, D425 and D283 cell lines

Stable polyclonal populations of DDX3X knockdown Daoy clone by two shRNAs (301-targeting open reading frame and UTR-targeting in 3'-UTR region) and empty pLKO-Tet vector were generated by infecting the respective lentiviral particles. Stable inducible polyclonal populations of Daoy, D425 and D283 cells expressing miR-30a and empty pTRIPz vector were generated by infecting these cells with lentiviral particles of pTRIPz constructs. For checking the viral titer,

1ml of serially diluted viral supernatant was used to transduce 5×10^4 293FT cells in a 35mm dish.

All lentiviral procedures, were handled in appropriately certified bio-safety level 2 cabinets (Esco Technologies, Hatboro, PA, USA); infected cultures/spent fluids/contaminated disposables were treated with 10% sodium hypochlorite and autoclaved in biohazard bags prior to disposal, following recommended guidelines.

Method:

1. 5×10^4 cells of Daoy or 293FT and 1×10^6 cells of D425 and D283 cells were seeded in a 35 mm dish one day prior to transduction.
2. 1 ml of diluted, neat or concentrated viral supernatant supplemented with Polybrene ($4\mu\text{g}/\text{ml}$) was used for infecting cells seeded.
3. 16 h post infection the viral supernatant was replaced with fresh medium.
4. For checking of viral titre, 72 h post-transduction, the number of 293FT RFP-positive cells was estimated using Flow cytometry analysis (FACS Calibur, BD Biosciences, USA). The viral titer was calculated using the formula – $(F \times C/V) \times D$, (where, F-frequency of RFP expressing cells, C-Number of cells at the time of seeding, V- Volume of viral supernatant used for transduction and D- Dilution factor of the viral supernatant).
5. The Daoy cells transduced with the miRNA-expressing constructs were trypsinized and seeded in two 55 mm dishes 72 h post-transduction.
6. For stable transfection, the infected cells were selected in the presence of puromycin ($250\text{ng}/\text{ml}$ for Daoy, $200\text{ng}/\text{ml}$ for D425 and D283) at least for 6-9 days.
7. The cells were split before they reached 70-80% confluency and always maintained in the presence of puromycin.

8. MiR-30a expression/DDX3X downregulation before and 72 h after induction with doxycycline (4µg/ml) was checked in these stable polyclonal populations using Real time RT-PCR (for miR-30a expression) and western blotting (for DDX3X knockdown).
9. The cells induced in the presence of doxycycline for 72 h were seeded for various experiments.

3.16 MTT Cytotoxicity Assay

Reagents:

Acidified SDS: 10% SDS in 0.01N HCl. 10 g SDS was dissolved in 80 ml autoclaved Milli-Q water, heated at 60°C for 1 h to assist the dissolution. 88.4µl of concentrated HCl was added so that, HCl concentration was 0.01N and the final volume was adjusted to 100 ml. The solution was stored at room temperature.

MTT: 5 mg / ml in 1X PBS. (50 mg MTT powder was dissolved in 10 ml 1X PBS, mixed by vigorous shaking. The solution was stored in dark at 4°C).

The growth kinetics of the stable miR-30a expressing polyclonal populations of Daoy, D283 and D425 cells was analyzed by MTT assay over a period of 10 days.

Method:

1. 500 cells of Daoy or 1000 cells of D283 or D425 were seeded in triplicates in a 96 well micro-titre plate in 100µl complete medium and medium was replenished at three day intervals.

2. At the desired time points, after medium replenishment 20µl MTT solution was added to each well, after which the plate was incubated at 37°C in CO₂ incubator for a period of 4 h to let formazan crystals form.
3. The formazan crystals formed were dissolved by adding 100µl of acidified SDS to each well with overnight incubation at 37°C.
4. Next day, the optical density was read on an ELISA plate reader (SpectraMax- 190, Molecular Devices, USA) at 540 nm against a reference wavelength of 690 nm.

3.17 Clonogenic assay

Clonogenic assay was performed to study the clonogenic potential of stable miR-30a expressing polyclonal population of Daoy and DDX3X knockdown population of Daoy cells.

Method:

1. 72 h post doxycycline induction, cells were trypsinized and 1000 cells were seeded per 55 mm plate. Cells were maintained in presence of puromycin and/or doxycycline.
2. The cells were allowed to grow for 8-10 days with medium change at every three days until microscopically visible colonies formed.
3. The cells were fixed in chilled methanol: acetic acid (3:1), stained with 0.5% crystal violet dye and the colonies were counted using stereomicroscope. Average colony count from three plates each was represented as histograms.

3.18 Soft Agar Colony Formation Assay

Anchorage-independent growth of Daoy, D283 and D425 cells stably transduced with miR-30a expressing pTRIPz lentiviral vectors was studied by their potential to form colonies in soft agar medium.

Method:

1. For the soft agar medium, 2 X DMEM containing 20 % FBS was mixed with an equal volume of molten 2 % low melting point (LMP) agarose, and 1 ml of this mixture was poured into a sterile 35 mm dish to obtain a basal layer of 1 % agarose in complete medium (DMEM + 10 % FBS or DMEM/F12+20%FBS). The agarose was allowed to set for ~ 1 h at room temperature before seeding the cells.
2. 7500 Daoy cells were trypsinized and suspended in 1 X DMEM supplemented with 10 % FBS. Similarly, 1000 cells of D283 or D425 were suspended in 1X DMEM/F12+20% FBS.
3. 2 % LMP molten agarose and 2 X DMEM + 20 % FBS for Daoy or 2X DMEM/F12 +20% FBS for D283 or D425 were added to the cell suspension such that the final concentration of agarose in the suspension was 0.4 % and serum content was 10 %.
4. The contents were mixed properly using a micropipette and 1 ml of this mixture was added to a 35 mm dish pre-coated with the basal layer.
5. The agar was allowed to solidify for about 1 – 2 h at room temperature and then the plates were incubated at 37 °C, 5 % CO₂.
6. The cells were fed with 0.1 - 0.2 ml complete medium every 3 days throughout the duration of the experiment.
7. After 3~ 4 weeks of incubation, colonies (comprising of 10-15 cells per colony) were counted under microscope from the entire plate. Average colony count from plates per group was represented as histograms.

3.19 Generation of orthotopic medulloblastoma xenograft in immunocompromised mice using stereotactic method of injection and assessment of in vivo tumorigenic potential of miR-30a expressing polyclonal populations of D283 cells.

D283 cells transduced with pTRIPZ-miR-30a construct were transfected with a pcDNA3.1 vector expressing firefly luciferase under CAG (CMV early enhancer/chicken beta-actin promoter) promoter. Tumourigenic potential of these cells with or without doxycycline treatment was studied.

Reagents:

1. Anaesthetic agent (Ketamine and Xylazine)
2. Analgesic (Buprenorphine, Neon Laboratories, India)
3. Sterile ocular lubricant (Neosporin, Neon Laboratories, India)
4. Sterile phosphate-buffered saline
5. 70% ethanol
6. Bone wax (Cat. No. W810, Ethicon Inc, Johnson & Johnson Ltd)
7. Tissue adhesive- VetBond™ (n-butyl cyanoacrylate) Cat. No. 1469SB, 3M Animal care products, St Paul, MN, USA)

Equipments:

1. Syringe needle 30G
2. Glass Syringes, 5µl Hamilton Co, Model 75 RN Syringe, 700 Series; volume 5µl; Cat. No. 7634-01)
3. Needles, 26G, 2” compatible for 5µl syringes (26GA RN 70mm PT3 6PK, Cat. No. 7804-03, Hamilton)

4. Sterile cotton buds
5. Surgical instruments include Fine forceps, Iris Scissors, Blunt forceps, sterile scalpel blades (Local make).
6. Small animal stereotaxic frame (Harvard Apparatus, MA, USA)
7. Electric microdrill and bits (Cat. No.67-1000, Ideal Micro Drill Kit, Cell Point Scientific, Gaithersburg, MD, USA)
8. Heating pad/chamber (with thermometer)
9. Electric clippers

Animals Used: Immunocompromised mice: 6 to 8 week old BALB/c Nude mice (CAnN.Cg-Foxn1nu/Crl strain) received from Charles River, USA.

Method:

A) Preparation of cells:

1. D283 cells were collected in medium by triturating using glass pipette. A short spin at 1500 rpm for 1 min was given to remove any dead cells. Cell pellet is resuspended in fresh medium.
2. Cells were counted using haemocytometer and required volume of culture suspension to carry 2×10^5 cells was spun down at 2000 rpm for 3 min.
3. Cells were washed once with sterile 1X PBS and resuspended in PBS to make final volume of 5 μ l carrying 2×10^5 cells
4. Cell suspension was kept on ice till the time of injection.

B) Equipment and specimen setup:

1. Small animal stereotaxic frame was assembled as per manufacturer's instructions.
2. Heating chamber necessary for post-procedural care is turned on to maintain temperature of 37°C.

3. Animals were weighed to decide dosage of anaesthetic agent. Typically 6-8 weeks old animals with minimum of 20g body weight were used for the intracranial injections.
4. Ketamine and Xylazine were diluted 1:1 in sterile 1X PBS and were mixed to get final concentration of 90-120mg/kg body weight (ketamine) and 20mg/kg body weight (xylazine). Diluted stocks of ketamine and xylazine were preserved at 4⁰C for up to one week.

C) Surgical procedure:

Preoperative animal preparation:

1. Mouse was anesthetized by administering ketamine-xylazine mixture through intra-peritoneal route by using sterile 30G syringe needle.
2. Lubricating ophthalmic ointment (Neosporin) was applied on both the eyes of mouse to prevent drying of the cornea.
3. Hair from surgical site were removed with electric clipper or razor in case of NOD-SCID mice.
4. Surgical site was disinfected by wiping the area by cotton tipped buds soaked in 70% ethanol.
5. Anesthetized mouse was positioned appropriately in stereotactic apparatus with incisors locked in mouth fixture at front and ears in ear holders of stereotactic apparatus. Ear bars were adjusted in ears at occiput of head level gently and then were tightened firmly. **Height of mouth fixture and ear bars was adjusted so that head is maintained absolutely steady and flat.**

Preoperative cell preparation:

1. Hamilton syringes and needles (26G) was washed several times by rinsing it with sterile PBS before aspirating cell culture.

2. Cells in microcentrifuge tube were re-suspended by tapping gently or by pipetting prior to each injection to prevent cell clumping.
3. 5 μ l of cell suspension was drawn into Hamilton syringe with great care to avoid aspiration of bubbles.

Surgical opening of skull:

1. 1.0-1.5 cm midline sagittal incision was taken with a sterile disposable scalpel blade or iris scissors along the superior aspect of the cranium from intra-aural line towards the anterior aspect of head.
2. Bregma (intersection of coronal and sagittal sutures) anteriorly and lambda (conjunction of sagittal and lambdoidal sutures) posteriorly was identified as they are used to serve as landmarks for stereotactic localization prior to injection.
3. Fascia over area of skull was removed by using forceps and scalpel. This was done to make the injection site easily accessible to drill into skull.

Injection of cells:

1. A guiding needle was attached to the holder attached to dorso-ventral (DV) axis of stereotactic apparatus and was adjusted to 2.5 mm posterior to lambda at midline by using vernier scale on antero-posterior (AP) axis. (DV and AP coordinates to achieve injection precisely in the cerebellum were chosen by referring to book named Paxinos and Franklin's the Mouse Brain in Stereotaxic Coordinates: An Atlas of the stereotaxic coordinates of mouse brain)
2. Using microdrill with sterile drill bit, a small burr hole was made as per the coordinates set by guiding needle. Sufficient care was taken so as to keep drilling superficial in order to avoid traumatic injury to brain.

3. 5µl syringe was attached to stereotactic apparatus holder and put cautiously into drilled burr hole.
4. Needle was maintained perpendicular to skull and slowly inserted 3 mm deep into the brain. After waiting for 1 min, needle was taken aback by 0.5 mm and cell suspension was delivered slowly (5µl over 2-3 min).
5. Skull was kept dry during injection, with sterile swabs to remove any tissue fluid and/or cell suspension that may have refluxed out of the burr hole.
6. Syringe was kept in place for one to two minutes before slowly withdrawing upon completion of injection.
7. Site of burr hole was plugged with bone wax, and skin was closed with the help of tissue adhesive VetBond.
8. Ear holders were unscrewed from the ears of the animal and incisors were removed from mouth fixture.
9. Animal was transferred to heating pad/chamber maintained at 37⁰C till it regains consciousness.
10. Animals injected with doxycycline treated D283 pTRIPZ-miR-30a polyclonal population were fed with doxycycline (1mg/ml) through 5% sucrose-water, while animals injected with doxycycline treated D283 polyclonal population were fed with 5% sucrose water.
11. Animals were sacrificed at 4th week by using over-exposure to CO₂ as a method of euthanasia.

3.20Bioluminescence imaging

Instruments:

Xenogen IVIS spectrum imaging system (Caliper Life Sciences, Hopkinton, MA).

Reagents:

- 1) D-luciferin, potassium salt (Cat. No.L8220 Biosynth AG, Switzerland) (30mg/ml): 30mg of D-luciferin powder is dissolved in 1X PBS and can be stored in -20⁰C.
- 2) Isoflorane (Forane 250ml Inj, Abott laboratories, India)

Method:

1. Mice were anaesthetised with isoflurane.
2. In case of isoflurane system of gas anaesthesia, exhaust system of isoflurane was switched on, then animals were put in incubation chamber and exposed to 3% isoflurane till animals are anaesthetized and breathing rate is regularised.
3. 100µl of 30mg/ml of D-luciferin (prepared fresh in 1X PBS) at (150 mg/kg body weight) was administered to anesthetised mice via intra-peritoneal route using sterile 30G syringe needle and animal is shifted to imaging chamber of the IVIS system. In case of isoflurane based anaesthesia, 3% isoflurane was delivered through nose cones provided inside the imaging chamber.
4. Image was acquired ~5 min after injection on auto exposure setting so as to determine optimal exposure time using Living Image 4.0 software provided with the instrument. Images were always captured so that count of photons was detected in the recommended detectable range for the instrument i.e. 600 to 60000. Exposure time and Camera aperture (f/Stop) settings were adjusted in case required.
5. 8-10 serial images at interval of 2min were taken till the luminescence reaches its peak. Image showing peak luminescence indicates peak enzyme activity that can be achieved and hence is used as a representative of tumour growth at that time point in a particular animal.

6. Region of interest (ROI) was precisely drawn over site of luminescence (represents site of the tumour) in overlay images and the total luminescence was calculated in terms of radiance (photons/sec/cm²/steradian) or total flux (photons/sec) which represents normalised luminescence.
7. Tumour growth on different time points was represented as radiance of that time point. Fold change in radiance measured on 3rd week post implantation of cells to 1st week was calculated and compared between mice injected with either doxycycline treated D283 control and D283 pTRIPZ-miR-30a polyclonal population.

3.21 Protein extraction of cultured cells

Reagents:

10X phosphate-buffered saline (PBS): (1.5 M NaCl, 89.8 mM Na₂HPO₄·2H₂O, 28.8mM NaH₂PO₄·2H₂O). 90 g NaCl, 16 g Na₂HPO₄·2H₂O, 4.5 g NaH₂PO₄·2H₂O per litre; pH adjusted to 7.5 with 5N NaOH, autoclaved and stored at room temperature. 10X stock was dilute to 1X with autoclaved Milli-Q water and stored at room temperature.

Lamelli buffer or 1X sample buffer: 62.5 mM Tris-HCl pH 6.8, 2% SDS, 10% glycerol. Total protein was extracted in sample buffer from doxycycline un-induced and induced miR-30a expressing polyclonal populations of Daoy and D283, 72 post transfection as described below.

Method:

1. (Step only for Autophagy experiment) Starvation and chloroquine treatment of cells for Autophagy Experiments: Complete medium was poured off from the culture dishes and cells were washed with 1X PBS and then cells were incubated in 1X PBS for 1 h at 37⁰C in 5% CO₂ incubator for starvation. For chloroquine treatment, 50 μM final concentration

of chloroquine was added to the cells in the complete medium or in 1X PBS in case of starved cells. Then after 1h cells were taken for protein extraction as described below.

2. The medium was poured off from the culture dishes and the cells were rinsed twice with 1X PBS gently.
3. The PBS was drained off completely and cells were lysed in 1X sample buffer. About 0.5 – 0.6 ml sample buffer was used for protein extraction from 90 mm dishes with 80-90% confluency. The viscous lysate, due to release of genomic DNA along with proteins from the cells, was collected by swirling the plate several times and transferred into a 1.75 ml microfuge tube.
4. The tubes were immediately kept in a boiling water bath for 7 min, cooled to room temperature and centrifuged at 15,000 rpm for 1.5 h at 20°C to pellet down the genomic DNA. The DNA pellets were discarded.
5. The supernatant lysates containing protein were carefully transferred to fresh tubes and stored at -20°C until further use.

3.22 Estimation of Protein Concentration

The proteins extracted in sample buffer from various cells (described above) were estimated using this method.

Reagents-

1 mg/ml BSA: 10 mg BSA (sigma) was weighed and dissolved in 1 ml autoclaved Milli-Q water to obtain a stock of 10 mg / ml. This stock was further diluted 1:10 in water to obtain a working stock of 1 mg/ ml. BSA stocks were stored at -20°C.

Solution A: Cu-tartrate CO₃ (CTC)

a) 20% Na₂CO₃: 20 g was dissolved in 100 ml Milli-Q water.

b) 0.2 g CuSO₄ was dissolved in 40 ml Milli-Q water.

c) 0.4 g potassium tartarate was dissolved in 40 ml Milli-Q water.

CuSO₄ and potassium tartarate were mixed (b + c) and the volume was made up to 100 ml with Milli-Q water. Final concentration of CuSO₄ is 0.2% and potassium tartarate is 0.4%. To this, 100 ml of 20% Na₂CO₃ (a) was added slowly with constant stirring. This solution A was stored in dark at room temperature.

Solution B: 10% SDS. 10 g of SDS was dissolved in 80 ml Milli-Q water, heated at 60°C to assist dissolution. The final volume was adjusted to 100 ml and stored at room temperature.

Solution C: (0.8 N NaOH) 16 g of NaOH was dissolved in 100 ml of Milli-Q water, and the volume made up to 500 ml and was stored at room temperature (Note: Do not autoclave).

Reagent A: Prepared by mixing solutions A, B, C, and Milli-Q water in a proportion of 1:1:1:1 just before use. (Note: Mixing NaOH with 10% SDS results in a glue like insoluble precipitate. Therefore dilute the SDS first in the required volume of water and then add NaOH and CTC to it.)

Reagent B: Folin-Ciocalteu reagent was diluted 1+5 in Milli-Q water just before use.

Method:

1. 2 µl of protein sample to be estimated was diluted in 1 ml of Milli-Q water in duplicates.

2. BSA standards, ranging from 1 µg to 20 µg were prepared in duplicate by appropriately diluting from 1 mg/ml stock of BSA, in 1 ml of Milli-Q water. 2 µl of the sample buffer used for extraction of protein to be estimated was also added. "Blank" tubes were prepared by adding only 2 µl of the sample buffer.

3. 1 ml of freshly prepared reagent A was added to each tube, immediately mixed on a vortex mixer, and kept in dark at room temperature for 10 min. Then 0.5 ml of freshly diluted reagent B was added to each tube, immediately mixed on a vortex mixer and incubated in dark at room temperature for 30 min.

4. The absorbance of the blue colour developed was read at 750 nm against blank in a spectrophotometer (Shimadzu UV-160A, UV-visible recording spectrophotometer), and the concentration of the unknown protein samples was calculated by using the BSA standard plot.

3.23 SDS-Polyacrylamide Gel Electrophoresis (SDS-PAGE)

The proteins extracted in sample buffer were separated by SDS-PAGE for western blotting.

Reagents:

30 % acrylamide solution: 29.2 g acrylamide, 0.8 g bis-acrylamide were dissolved in approximately 50-60 ml autoclaved Milli-Q water and the final volume was made up to 100 ml. Solution was filtered through ordinary filter paper and stored in an amber colored bottle at 4 °C.

20% SDS: 20 g SDS was dissolved in 80 ml of Milli-Q water, heated at 60°C to assist the dissolution. The final volume was made up to 100 ml, and stored at room temperature.

1M Tris pH 8.8 and pH 6.8: 60.55 g Tris was dissolved in 400 ml Milli-Q water. pH was adjusted to 8.8 and 6.8 with concentrated HCl, the final volume was made up to 500 ml with Milli-Q water and autoclaved. Solutions were stored at 4°C.

10X electrode buffer: 30 g Tris, 143 g glycine, 20 g SDS were dissolved in approx. 700 ml Milli-Q water and the final volume was made up to 1 L. Stock solution was diluted to 1X with Milli-Q water before use (1X buffer is 25 mM Tris, 190 mM Glycine, 0.2% SDS).

0.5 % Coomassie Blue staining solution: 0.5 g of Coomassie Blue staining dye was dissolved in 50 ml of methanol (LR grade) by constant stirring. The final volume was adjusted to 100 ml by adding 40 ml of Milli-Q water and 10 ml of glacial acetic acid. The staining solution was filtered through filter paper and stored at room temperature for 1 month.

Destainer: Methanol (LR), glacial acetic acid (AR) and Milli-Q water mixed in the proportion 5:1:4 and stored at room temperature.

Loading Dye: 0.025% Bromophenol Blue was dissolved in 1X Sample Buffer.

Method:

1. Two clean glass plates (one of which was notched), separated by 1.5 mm thick spacers were clamped together. The sides and the bottom of the plates were sealed using 3% agar. The resolving gel of the required percentage (10%) was prepared by mixing the following

Components	Final Concentration of Acryl amide		
	10%	12%	20%
30% Acrylamide	10 ml	12 ml	20 ml
1M Tris-Cl pH8.8	11.2 ml	11.2 ml	11.2 ml
20%SDS	0.15 ml	0.15 ml	0.15 ml
Milli-Q water	8.65 ml	6.65 ml	-
TEMED	20 µl	20 µl	20 µl
20% Ammonium persulfate	50 µl	50 µl	50 µl

2. The gel solution was poured between the two glass plates taking care to avoid air bubbles. Water was carefully layered over the gel and it was allowed to polymerize (approximately 20 – 30 min).
3. Following polymerization, the water layer was removed and a 5% stacking gel was prepared and overlaid over the resolving gel.

5% stacking gel composition

Components	Volume to be added
30% acrylamide solution	1.67ml
1 M Tris-HCl pH 6.8	1.75ml
20% SDS	100 μ l
Milli-Q water	6.98ml
TEMED	10 μ l
20% ammonium persulphate	25 μ l

4. A comb of 1.5 mm thickness was inserted immediately into the stacking gel solution between the two plates to form wells. After polymerization of the stacking gel, the comb was gently removed and the wells were cleaned by flushing first with water and then with 1X electrode buffer (using a syringe-needle). The gel plates were clamped to the electrophoresis unit and the upper and lower tanks were filled with 1X electrode buffer.
5. The proteins to be resolved were mixed with 1X sample buffer containing 5% v/v BME and 0.01% bromophenol blue, boiled for 3 min and loaded into the wells of the gel along with pre-stained protein ladder.
6. Electrophoresis was carried out at 22mA constant current till the dye reached the bottom of the gel. The gel was removed carefully and either stained with Coomassie blue to check equal loading of the proteins or processed for western blotting as described later.
7. For Coomassie blue staining, the gel was stained by immersing it in 0.5 % Coomassie Blue staining solution for 2 h. The gel was washed several times in destainer until a clear background was obtained and then transferred to 50 % methanol for 2-3 h. The gel was dried between gelatin papers (pre-soaked in 50 % methanol) at room temperature for 24 h.

3.24 Western Blot Analysis and Immuno-detection

The proteins separated by SDS-PAGE, were transferred to a PVDF membrane by western blotting technique.

Reagents:

1X transfer buffer: 25mM Tris, 192 mM Glycine, 20% Methanol. 3 g Tris and 14.4 g Glycine were dissolved in Milli-Q water and volume was made up to 800 ml with Milli-Q water. 200 ml Methanol was added to make 1 L. Buffer was chilled to 4°C before use. (1 L transfer buffer is sufficient for western blotting in Biorad's mini trans-blot electrophoretic transfer cell)

10X Tris-buffered saline (TBS): 0.1 M Tris, 1.5 M NaCl 12.1 g Tris and 87.6 g NaCl were dissolved in Milli-Q water, pH was adjusted to 8.0 with concentrated HCl and the final volume was made up to 1 L. Solution was autoclaved and stored at room temperature.

1X Tris-buffered saline with Tween-20 (TBST): 10X TBS was diluted to 1X with Milli-Q water (1 litre), 1 ml Tween-20 was added to the solution and kept on magnetic stirrer for 1 hr.

Ponceau-S staining solution: (0.2% Ponceau-S in 1% glacial acetic acid)

SuperSignal® West Pico chemiluminescent substrate

Antibodies: Catalogue No and companies mentioned in method.

Method:

1. The protein samples to be blotted were resolved by SDS-PAGE and the gel was kept in 1X transfer buffer for 15-20 min until the gel was free from the smell of β - mercapto ethanol (BME).
2. The Immobilon PVDF membrane, to be used for blotting, was cut to the size of the gel to be blotted. The membrane was pre-wet in methanol for about 30 seconds, kept in Milli-Q water for

10min. to wash off excess methanol and then placed in 1X transfer buffer for 20 min. Two pieces of a Whatmann 3MM filter paper little bigger than the size of the gel, were also cut.

3. The transfer assembly was prepared according to the manufacturer's instructions. The cassette was assembled in a tray containing 1X transfer buffer by arranging the components in the following sequence: First the cassette was placed, with the gray side down in a tray containing transfer buffer. A Scotch-Brite pad was placed over the grey portion of the cassette, and a piece of Whatman paper was placed over it. Then the transfer buffer equilibrated gel was carefully placed over the Whatman paper and the PVDF membrane was juxtaposed to the gel without trapping any air bubbles between the gel and the PVDF membrane. A small cut was given at one corner of the membrane and the gel for correct orientation. Another piece of Whatman paper and a Scotch-Brite pad were placed over the PVDF membrane. The cassette was closed firmly and locked with the white latch on top of the cassette, and slid into the grooves for holding the cassette in place with the grey portion (gel side) towards the cathode (negative electrode) and the transparent portion (membrane side) towards the anode (positive electrode). This whole assembly was placed inside the tank containing transfer buffer, and the electrodes were connected to the power supply. Transfer was carried out at 40mA constant current at 4°C for 16 hr.

4. After the transfer, the membrane was carefully removed from the cassette using a pair of forceps, rinsed once with Milli-Q water, and kept in destainer for 30 min (to aide in staining with Ponceau-S). Then the membrane was washed twice with TBST for 5 min each and stained with Ponceau-S till the protein bands were visible. The molecular weight marker positions were marked on the membrane with a soft lead pencil and then the Ponceau-S was completely

removed by washing the membrane with TBST. It was either probed immediately or stored at 4°C in TBST, for later use.

5. For probing, the membrane was first blocked with a 5% milk solution prepared in TBST. The membrane was kept in the milk solution for 1 h at room temperature on a rocker with gentle shaking.

6. The blocking solution was drained off and the membrane was washed 3 times for 5 min each with TBST, on the rocker with vigorous shaking.

7. TBST was drained off completely and the membrane was incubated with appropriately diluted antibody, with gentle shaking on the rocker. The working conditions of various antibodies used are given below in table 3.4

Table 3.4: Antibodies used for Western blotting.

Name of Antibody	Company/Catalogue No.	Type	Dilution	Duration
DDX3X (D19B4)	Cell signalling #8192	Rabbit Polyclonal	1:3000 in 2%BSA-TBST	O/N at 4°C
Beclin-1 (D40C5)	Cell signalling #3495	Rabbit Monoclonal	1:1000 in 2%BSA-TBST	O/N at 4°C
ATG5 (D5F5U)	Cell signalling #12994	Rabbit Monoclonal	1:1000 in 1%BSA-TBST	O/N at 4°C
LC3B	Cell signalling #2775	Rabbit Polyclonal	1:1000 in 1%BSA-TBST	O/N at 4°C
SQSTM1/p62	Cell signalling #5114	Rabbit Polyclonal	1:1000 in 5%BSA-TBST	O/N at 4°C
GAPDH	Santacruz Biotechnology	Mouse polyclonal	1:3000 in 2%BSA-TBST	O/N at 4°C
Γ-Tubulin	Sigma	Rabbit polyclonal	1:4000 in 1%BSA-TBST	O/N at 4°C
Goat Anti-mouse IgG	Thermos Scientific	Goat	1:4000 in 2% milk-TBST	1h at RT
Goat Anti-rabbit IgG	Thermos Scientific	Goat	1:4000 in 2% milk-TBST	1h at RT

The antibody solution was drained off and the membrane was washed six times for 5 min each with 1X TBST, on the rocker with vigorous shaking.

9. Then the membrane was incubated with appropriately diluted horseradish peroxidase (HRP) conjugated secondary antibody (anti-IgG) for 1 hr at RT on the rocker with gentle shaking. Anti-rabbit HRP-conjugated antibodies (Thermo-Scientific) were diluted 1:2000 in 1% milk-TBST. The antibody solution was drained off and the membrane was washed vigorously six times for 5 min each with 1X TBST and then three times with 1X TBS.

10. The excess buffer was drained off and the membrane was placed on a clean cling film and covered with commercial chemiluminescent substrate Super Signal West Pico for 5 min at room temperature.

11. Quickly, the detection solution was drained off; the membrane was wrapped in cling film, placed in an X-ray film cassette and exposed to X-ray film for 1-2 min. The signal was visualized after developing the X-ray film.

3.25 Bioinformatic methods

3.25.1 Quality analysis of fastq reads

FastQC (<http://www.bioinformatics.babraham.ac.uk/projects/fastqc/>) a quality control tool for high throughput sequence data was used for quality analysis of fastq reads. FastQC is a Graphical user interphase (GUI) based software. The fastq reads data was imported in to the software in .fastq or .bam format. Results were displayed after completion of the analysis by the software. The results were saved.

3.25.2 Alignment of fastq Reads to hg19 by BWA

The fastq files were aligned to the human reference genome hg19 with (BWA) Burrows-Wheeler Aligner version 0.6.2 (www.bio-bwa.sourceforge.net). Alignment of fastq reads to hg19 involves two steps i.e. first indexing of the reads followed by actual alignment which generates SAM file with read group. Following commands were used:

```
./bwa-0.6.2/bwa aln -f sample_read1.sai hg19_GATK sample_1.fq
./bwa-0.6.2/bwa aln -f sample_read2.sai hg19_GATK sample_2.fq
```

```
./bwa-0.6.2/bwa sampe -r '@RG\tID:HUMpxiXAAAAAAPEI-48\tPL:illumina\tPU:120418_I812_FCD0VLLACXX_L5_HUMpxiXAAAAAAPEI-48\tLB:HUMpxiXAAAAAAPEI-48\tSM:SAMPLE\tCN:BGI' -f sample.sam hg19_GATK.fa sample_read1.sai sample_read2.sai sample_1.fq sample_2.fq
```

3.25.3 Removal of duplicate reads

Duplicate reads were removed using the Picard Tools version 1.80 (<http://broadinstitute.github.io/picard>). It consists of two steps i.e. first conversion of SAM file to BAM file followed by marking PCR duplicates. Following commands were used:

- i. Conversion of SAM file format to BAM file format

```
java -Xmx4g -Djava.io.tmpdir=/home/Dell/tmp -jar SortSam.jar
SO=coordinate INPUT=sample.sam OUTPUT=sample_RG_picard.bam
VALIDATION_STRINGENCY=LENIENT CREATE_INDEX=true
```

- ii. Marking PCR duplicates

```
java -Xmx4g -Djava.io.tmpdir=/home/Dell/tmp -jar MarkDuplicates.jar
INPUT=sample_RG_picard.bam OUTPUT=sample_RG_picard_marked.bam
METRICS_FILE=metrics VALIDATION_STRINGENCY=LENIENT CREATE_INDEX=true
```

3.25.4 Refinement of Alignment by Genome Analysis Toolkit

The alignment files were refined by local realignment of the reads and base quality recalibration by the Genome Analysis Toolkit (GATK) version 2.1.3 (<https://www.broadinstitute.org/gatk>).

Following commands were used.

- i. For Listing out intervals that require realignment

```
java -Xmx4g -jar /GenomeAnalysisTK-2.1.3/GenomeAnalysisTK.jar -T
RealignerTargetCreator -R hg19_GATK.fa -o sample_RG_marked.bam.list -
I sample_RG_picard_marked.bam
```

- ii. Local realignment around those intervals

```
java -Xmx4g -Djava.io.tmpdir=/tmp -jar /GenomeAnalysisTK-
2.1.3/GenomeAnalysisTK.jar -T IndelRealigner -R hg19_GATK.fa -I
sample_RG_picard_marked.bam -targetIntervals
sample_RG_marked.bam.list -o actrec-1_RG_marked_realigned.bam
```

- iii. Fixing the mate information

```
java -Xmx4g -Djava.io.tmpdir=/tmp -jar /picard-tools-
1.80/FixMateInformation.jar INPUT=sample_RG_marked_realigned.bam
OUTPUT=sample_RG_marked_realigned_fixed.bam SO=coordinate
VALIDATION_STRINGENCY=LENIENT CREATE_INDEX=true
```

- iv. Quality Score Recalibration using GATK

```
java -Xmx4g -Djava.io.tmpdir=/tmp -jar /GenomeAnalysisTK.jar -l INFO
-R hg19_GATK.fa -knownSites:dbsnp,VCF hg19_dbsnp_132_sorted.vcf -I
sample_RG_marked_realigned_fixed.bam -T CountCovariates -cov
ReadGroupCovariate -cov QualityScoreCovariate -cov CycleCovariate -
cov DinucCovariate -recalFile sample_reacl_data.csv
```

```
java -Xmx4g -Djava.io.tmpdir=/tmp -jar /GenomeAnalysisTK.jar -l INFO
-R hg19_GATK.fa -I sample_RG_marked_realigned_fixed.bam -T
TableRecalibration --out sample.marked.realigned.fixed.recal.bam -
recalFile sample_reacl_data.csv
```

3.25.5 Creating Pileup of aligned reads

The VarScan somatic command accepts both a normal and a tumor file in SAMtools pileup format from sequence alignments in binary alignment/map (BAM) format. Therefore, realigned and recalibrated BAM files obtained from GATK were subjected to pileup command using Samtools and then pileup files were used for somatic variant calling using VarScan tool. Read pileup file was created using following command. Samtools (samtools.sourceforge.net/)version samtools-0.1.18 was used.

```
/samtools-0.1.18/samtools mpileup -f /hg19_GATK.fa
sample.marked.realigned.fixed.recal.bam >
sample.marked.realigned.fixed.recal.mpileup
```

3.25.6 Identification of Somatic Variants

Simple nucleotide variants (SNVs) and insertions and deletions (InDels) were identified using the VarScan variant detection tool version 2.3.5 (<http://varscan.sourceforge.net>). VarScan requires both Tumour and paired blood sample for calling variants hence for tumour samples having paired blood and for tumour samples not having paired blood analysis was done as described below:

- A. **For Paired Tumour Samples:** For Tumour samples having paired blood their corresponding paired blood sample was used as normal control.
- B. **For Unpaired Tumour Samples:** For Tumour samples not having paired blood, one of the blood sample from available paired blood sample was used as normal control.

VarScan analysis steps were as follows:

- i. Reads pileup files were input to VarScan to detect somatic single nucleotide variations with parameters described in the table below. The VarScan somatic outputs two files, one listing snps and other listing indels.

Filter	Description
min-coverage	Minimum coverage in normal and tumor to call variant (8)
min-coverage-normal	Minimum coverage in normal to call somatic (8)
min-coverage-tumor	Minimum coverage in tumor to call somatic (8)
tumor-purity	Estimated purity (tumor content) of tumor sample (0.8)

Command used was:

```
java -jar /Varscan2.3.9/VarScan.v2.3.9.jar somatic
sampleB.marked.realigned.fixed.recal.mpileup
sampleT.marked.realigned.fixed.recal.mpileup
sample.marked.realigned.fixed.recal_somatic_strn --min-coverage 8 --
min-coverage-normal 8 --min-coverage-tumor 8 --tumor-purity 0.80 --
output-vcf 1
```

- ii. The variant calls in the somatic output file were separated by somatic status (Germline, Somatic, LOH) and were classified as high-confidence (.hc) or low-confidence (.lc) using command processSomatic. Command used was:

For SNPs

```
java -jar /VarScan.v2.3.9.jar processSomatic
sample.marked.realigned.fixed.recal_somatic_strn.snp.vcf --min-tumor
.20 --max-normal-freq .05
```

For InDels

```
java -jar /VarScan.v2.3.9.jar processSomatic
sample.marked.realigned.fixed.recal_somatic_strn.indel.vcf --min-
tumor .20 --max-normal-freq .05
```

- iii. To further refine the somatic mutation list to identify true positive mutation calls somaticFilter Command was used with default minimum read depth of 4, minimum supporting 2 reads for a variant and atleast one read at each strand. Command used was:

For SNPs

```
java -jar /VarScan.v2.3.9.jar somaticFilter
sample.realigned.fixed.recal_somatic_strn.snp.Somatic.hc.vcf --
output-file
sample.marked.realigned.fixed.recal_somatic_strn.snp.Somatic.hc.vcf.f
ilterMinCov4MinReads2-2 --min-coverage 4 --min-reads2 2 --min-
strands2 1
```

For InDels

```
java -jar /VarScan.v2.3.9.jar somaticFilter
sample.realigned.fixed.recal_somatic_strn.indel.Somatic.hc.vcf --
output-file
sample.marked.realigned.fixed.recal_somatic_strn.indel.Somatic.hc.vcf
.filterMinCov4MinReads2-2 --min-coverage 4 --min-reads2 2 --min-
strands2 1
```

3.25.7 Annotation of Somatic Variants

Annotation of the somatic variants identified in the analysis of Exome data was done using the ANNOVAR software (www.openbioinformatics.org/annovar) (Wang et al., 2010).

- i. The vcf4 file output generated by VarScan software was converted into the annovar input format using following command.

For SNPs

```
/annovar/convert2annovar.pl -format vcf4 -includeinfo  
sample.marked.realigned.fixed.recal_somatic_strn.snp.Somatic.hc.vcf.f  
ilterMinCov4MinReads2-2 > sample_hc_snp.avinput
```

For InDels

```
/annovar/convert2annovar.pl -format vcf4 -includeinfo  
sample.marked.realigned.fixed.recal_somatic_strn.indel.Somatic.hc.vcf  
.filterMinCov4MinReads2-2 > sample_hc_indel.avinput
```

- ii. Variant annotation was carried out using summarize annovar script

For SNPs

```
/annovar/summarize_annovar.pl -buildver hg19 sample_hc_snp.avinput  
/home/Dell/annovar/hg19db/--remove --verdb SNP 137 --ver1000g  
1000g2012apr --veresp 6500si -genetype refgene --checkfile --  
alltranscript
```

For InDels

```
/annovar/summarize_annovar.pl -buildver hg19 sample_hc_indel.avinput  
/home/Dell/annovar/hg19db/--remove --verdb SNP 137 --ver1000g  
1000g2012apr --veresp 6500si -genetype refgene --checkfile --  
alltranscript
```

- iii. **(A) For tumours having paired blood samples:** From the ANNOVAR-annotated list variants located in segmental duplications were excluded. The remaining variants were manually verified in IGV (www.broadinstitute.org/igv).
- (B) For tumours not having paired blood samples:** From the ANNOVAR-annotated list variants located in segmental duplications were excluded. The remaining variants were compared with the 60000 exome sequence database (ExAC Broad Institute) and

shortlisted based on their absence database followed by manual verification in IGV (www.broadinstitute.org/igv).

3.26 Copy number variation analysis using CopywriteR

CopywriteR uses .bam files as an input. These files are processed in several steps to allow copy number detection from offtarget reads. These steps include:

1. Removing of low-quality and anomalous reads
2. Peak calling (in reference when available, otherwise in sample itself)
3. Discarding of reads in peak regions
4. Counting reads on bins of pre-defined size (20 kb for exome data)
5. Compensating for the difference in effective bin size upon discarding peaks in peak regions
6. Correcting for GC-content and mappability; applying a blacklist filter for CNV regions

The full analysis of copy number data with CopywriteR includes three sequential steps, using the preCopywriteR, CopywriteR and plotCNA functions respectively.

A. preCopywriteR

CopywriteR uses binned read count data as a basis for copy number detection. The preCopywriteR function allows to create the necessary helper files. The helper files are required to run CopywriteR command in next step.

The command used is:

```
>library(CopywriteR)
>data.folder <- tools::file_path_as_absolute(file.path(getwd()))
> preCopywriteR(output.folder = file.path(data.folder),
+ bin.size = 20000,
+ ref.genome = "hg19")
```

B. CopywriteR

The CopywriteR function allows to calculate binned read count data based on the helper files created by preCopywriteR. CopywriteR uses a peak calling algorithm to remove 'on-target' reads. And does all the six steps described earlier.

Command used is:

```
> path <- SCLCBam::getPathBamFolder()
> samples <- list.files(path = path, pattern = ".bam$", full.names = TRUE)
> controls <- samples
> sample.control <- data.frame(samples, controls)
> CopywriteR(sample.control = sample.control,
+ destination.folder = file.path(data.folder),
+ reference.folder = file.path(data.folder, "hg19_20kb"),
+ bp.param = bp.param)
```

CopywriteR will create a new folder named CNAProfiles in the directory specified by destination.folder. It generates the following files:

1. CopywriteR.log: contains log information of the R commands that have been used to perform the various functions
2. input.Rdata: contains a number of variables that are required to run the last function of the CopywriteR package plotCNA

3. `log2_read_counts.igv`: contains log2-transformed, normalized (ratios of) read counts. These data can be used for further downstream analysis, and are required for `plotCNA` to allow plotting of the copy number profiles
4. `qc`: contains contains quality control plots
5. `read_counts.txt`: Contains both uncompensated and compensated read counts for every sample

C. `plotCNA`

The `plotCNA` function allows segmentation of the copy number data using `DNACopy`, and subsequent plotting.

Command used is:

```
plotCNA(destination.folder = file.path(data.folder))
```

It creates two additional files:

1. `segmentR.data`: Containing the segmentation values
2. `plots`: Contains the copy number plots

Chapter 4

RESULTS

Results

Expression profiling segregates medulloblastomas into four distinct molecular subgroups viz. WNT, SHH, Group 3 and Group 4. WNT and SHH subgroup tumors are characterized by overexpression of WNT and SHH signalling pathway genes respectively [4]. An expression profiling study of protein-coding genes and microRNAs on a small cohort of medulloblastomas has been reported from our lab [13]. Based on the differential gene expression and microRNA expression in the four subgroups a real time RT-PCR assay was developed to molecularly classify medulloblastomas into the four subgroups [48]. Eleven fresh frozen medulloblastoma tumor tissues belonging to WNT subgroup were available for exome sequencing. Six of these 11 tumors were identified by genome wide expression profiling using Affimetrix gene 1.0 ST array whereas five of 11 were identified using real time RT-PCR analysis assay based on 12 protein coding gene and 9 miRNAs. Further, sequencing of exon 3 of the *CTNNB1* gene encoding beta-catenin showed specific known oncogenic mutation in each of these 11 tumor tissues. Mutation in beta-catenin encoding gene alone has been reported to bring about hyperproliferation but not malignant transformation in developing mouse brain [8]. Therefore, in order to delineate molecular mechanism underlying pathogenesis of the WNT subgroup medulloblastomas, it is necessary to identify complete repertoire of genetic alterations in the tumors that has become feasible due to the advent of Next Gen sequencing. Sequencing of the whole exome (44 Mb) of the 11 WNT subgroup medulloblastoma was therefore carried out to identify genetic alterations characteristic of the WNT subgroup tumors.

4.1 Identification of somatic mutations in WNT subgroup medulloblastoma by exome sequencing of tumour and paired blood DNAs

Before proceeding for DNA extraction, tumour content of atleast 90% was ensured by Hematoxylin and Eosin (H & E) staining of cryosections of the tumour tissues. As described before Sanger sequencing of exon 3 region of the *CTNNB1* gene from the eleven WNT subgroup tissues was done to confirm the mutation in β -catenin, a known characteristic of ~ 90% WNT subgroup medulloblastoma [39]. A single missense point mutation was confirmed in all the eleven WNT subgroup medulloblastoma and peak heights of mutated nucleotide confirmed that the tumour content was more than 90% in each sample (Table 4.1 and Appendix I-*CTNNB1* Mutations). Genomic DNA from the eleven tumours and six paired blood samples was extracted using QIAamp DNA mini kit as per manufacturer's protocol. Genomic DNA quantity was determined using Qubit fluorimeter 2.0 and quality was checked by agarose gel electrophoresis. Exome capture of 11 WNT subgroup tumor tissues and 6 paired blood sample DNA was done using Agilent SureSelect Human all exon 44 Mb kit and exome sequencing was done using Illumina HiSeq 2000 platform with an average coverage of 50X.

4.1.1 Exome sequence data Quality

Quality of the raw sequence data was analyzed using FastQC (<https://www.bioinformatics.babraham.ac.uk/projects/fastqc/>). Mean and median base Phred quality score for almost all bases was above 30. All exomes were sequenced at > 50 X average depth of coverage. Average read length of the data was 88-90 bp. Total coverage of the exome was more than 97 % in each case with more than 70% exome covered at atleast 20 X coverage and more than 82 % exome covered at atleast 10 X coverage. The detailed statistics of the total number of reads obtained, coverage of the targeted exomes is given in Table 4.2

Table 4.1: Point mutations and corresponding amino acid change in exon 3 of *CTNNB1* gene in the 11 WNT subgroup medulloblastomas as determined by Sanger sequencing.

Sample	Point Mutation	Amino Acid Change
MED 1	TCT-->CCT	S37P
MED 2	CCT-->TCT	S33P
MED 3	TCT-->TTT	S33F
MED 4	TCT-->TGT	S33C
MED 5	ATC-->AGC	I35S
MED 7	CCT-->TCT	S33P
MED 8	GAC-->CAC	D32H
MED 9	GAC-->AAC	S33C
MED 10	TCT-->TTT	S37F
MED 11	TCT-->TAT	S33Y
MED 13	TCT--TGT	S33C

4.1.2 Identification of single nucleotide variants in the WNT medulloblastoma tumour tissues

Reads obtained for each tumor and paired blood DNA exomes were aligned to human reference genome hg19 using BWA aligner [115]. Somatic single nucleotide variants (SNVs) and insertions and deletions (InDels) were identified using the VarScan [116] variant detection tool version 2.3.5 (<http://varscan.sourceforge.net>) using the filtering criteria of at least 4 reads in

tumour and paired blood with mapping quality of more than 60 and base quality more than 30. Functional annotation of the somatic variant list was done using the ANNOVAR software (www.openbioinformatics.org/annovar) [117]. From the ANNOVAR-annotated list, variants located in segmental duplications were excluded. The remaining variants were manually verified in IGV (www.broadinstitute.org/igv) [118].

Table 4.2: Exome sequencing data statistics of the 11 WNT subgroup medulloblastoma tumours.

Exome Sample	Total No. of Reads	Average Read Length	% of reads Uniquely mapped to genome	Coverage of Target region 1X	Coverage of Target Region 10X	Coverage of Target Region 20X
MED 1	48894304	88.88	91.90%	97.40%	83.70%	71.50%
MED 2	46136811	88.7	91.12%	98.20%	87.20%	76.50%
MED 3	40255669	88.97	90.52%	98.20%	84.00%	69.40%
MED 4	47954451	88.6	93.03%	98.20%	87.00%	75.80%
MED 5	46856756	88.89	91.26%	98.30%	87.30%	76.80%
MED 7	47211097	86.04	90.92%	97.30%	82.80%	70.10%
MED 8	47524618	88.94	91.92%	98.00%	85.90%	74.20%
MED 9	47954451	88.89	91.56%	97.50%	84.60%	73.10%
MED 10	48557900	88.83	91.88%	97.80%	85.50%	74.20%
MED 11	34381129	88.82	92.65%	96.00%	70.70%	49.10%
MED 13	51822795	88.84	91.29%	97.50%	85.00%	66.80%

In the case of 6 tumor tissues having paired blood sample, the number of novel somatic variants were found to range from 10 to 30. In the case of 5 tumors not having paired blood sample available, the variants were shortlisted based on their absence in the 60000 exome sequence database (ExAC Broad Institute) [119]. 30-50 novel non-synonymous SNPs/Indels were identified in each of the the unpaired medulloblastoma tissues. Total list of 243 single nucleotide variants shortlisted for 5 tumour samples not having paired blood samples is listed in Appendix

II after comparing it with 60000 exome sequence database. A total of 104 novel somatic variants (Non-synonymous - 78, synonymous – 11, splice site – 2, frame shift InDels – 4 and non-frameshift InDels – 9) have been identified in case of 6 tumour tissues having paired blood samples (Table 4.3) and 57 of these non-synonymous somatic variants were further confirmed by Sanger sequencing. Total list of 104 novel somatic variants is shown in Appendix III.

Table 4.3: Total number of variants in the of 11 WNT subgroup medulloblastoma exomes.

Sample	Somatic SNVs			InDels		Total	Validated by Sanger sequencing	Age	Gender	
	Nonsynonymous		Synonymous	splice site	Frameshift					Non frameshift
	Missense	stopgain								
Paired sample										
MED 1	20	2	4	2	3	2	33	19	26	F
MED 2	10	3	1	0	1	1	16	9	15	F
MED 10	16	3	1	0	0	1	21	12	19	F
MED 3	8	0	2	0	0	1	11	6	9	M
MED 4	8	2	2	0	0	1	13	7	10	M
MED 13	5	1	1	0	0	3	10	4	9	M
Unpaired sample										
MED 5	33	0	0	1	3	1	38	2	5	M
MED 7	51	0	0	1	2	3	57	0	45	M
MED 8	43	0	0	3	3	3	52	0	10	F
MED 9	41	1	0	3	3	1	49	2	12	F
MED 11	39	2	0	2	0	4	47	1	26	M

Mutation in exon 3 of *CTNNB1* gene in all eleven samples was confirmed in exome sequencing data. After *CTNNB1* mutation, the second most frequently mutated gene was found to be *DDX3X* gene which encodes a RNA helicase protein. Mutation in *DDX3X* gene was found in 3/11 tumours of which 2 are missense (Q265H and A367T) and one mutation (G242fs deletion) is a frameshift deletion (Fig. 4.1). AT-rich interactive domain-containing protein 1B (*ARID1B*), which is a member of SWI/SNF (SWItch/Sucrose Non-Fermentable) chromatin remodeling

complex was found to be mutated in 2/11 samples of which one is a frameshift insertion (P1027fs insertion) and the other is a nonsense mutation (C878X) (Fig. 4.2).

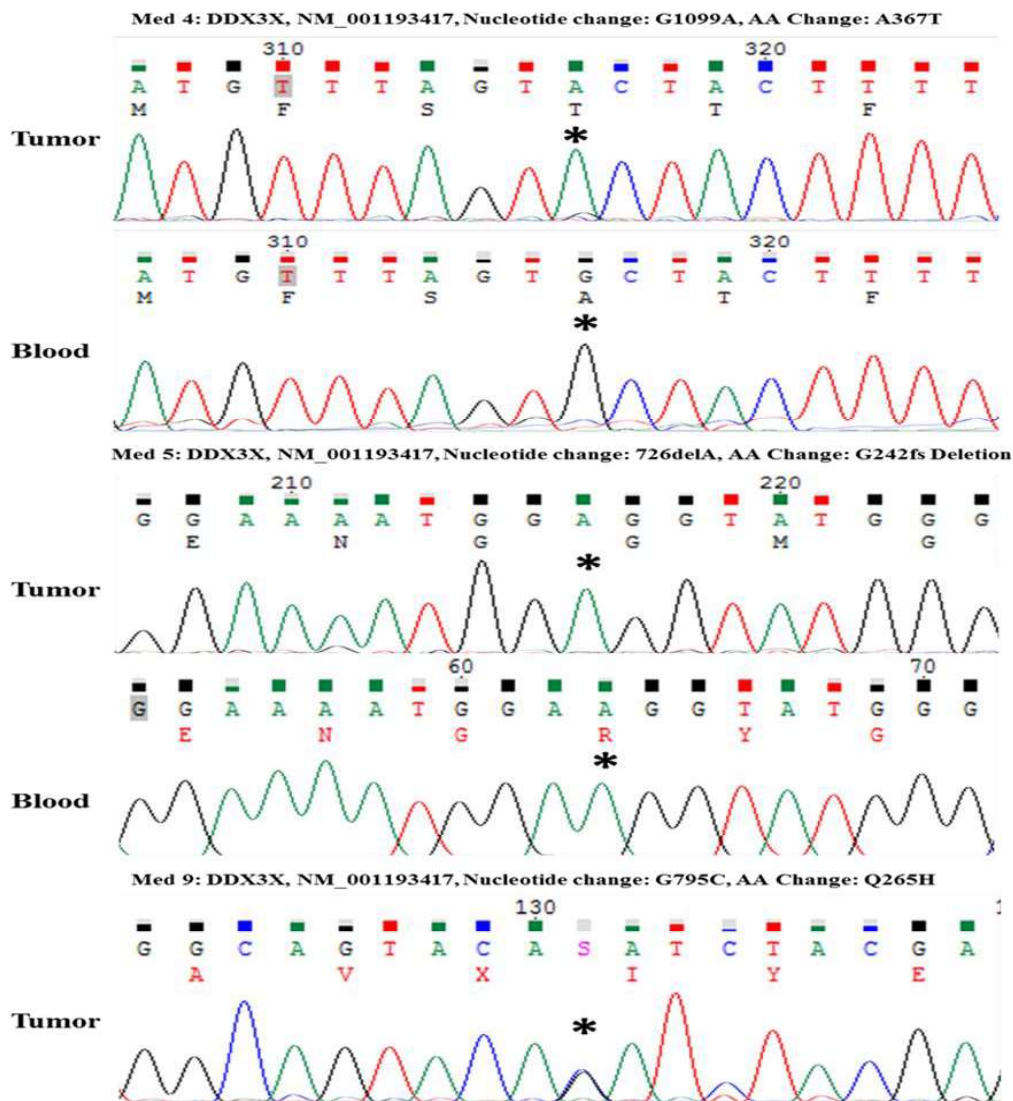


Figure 4.1: Mutations in the *DDX3X* gene identified in the WNT subgroup medulloblastomas

DDX3X gene mutations in three WNT subgroup medulloblastoma validated by Sanger Sequencing. The top panel shows the electropherograms for tumour DNA and bottom panel for its corresponding paired blood DNA, for Med 6 sample paired blood was not available. Altered nucleotide is indicated with ‘*’

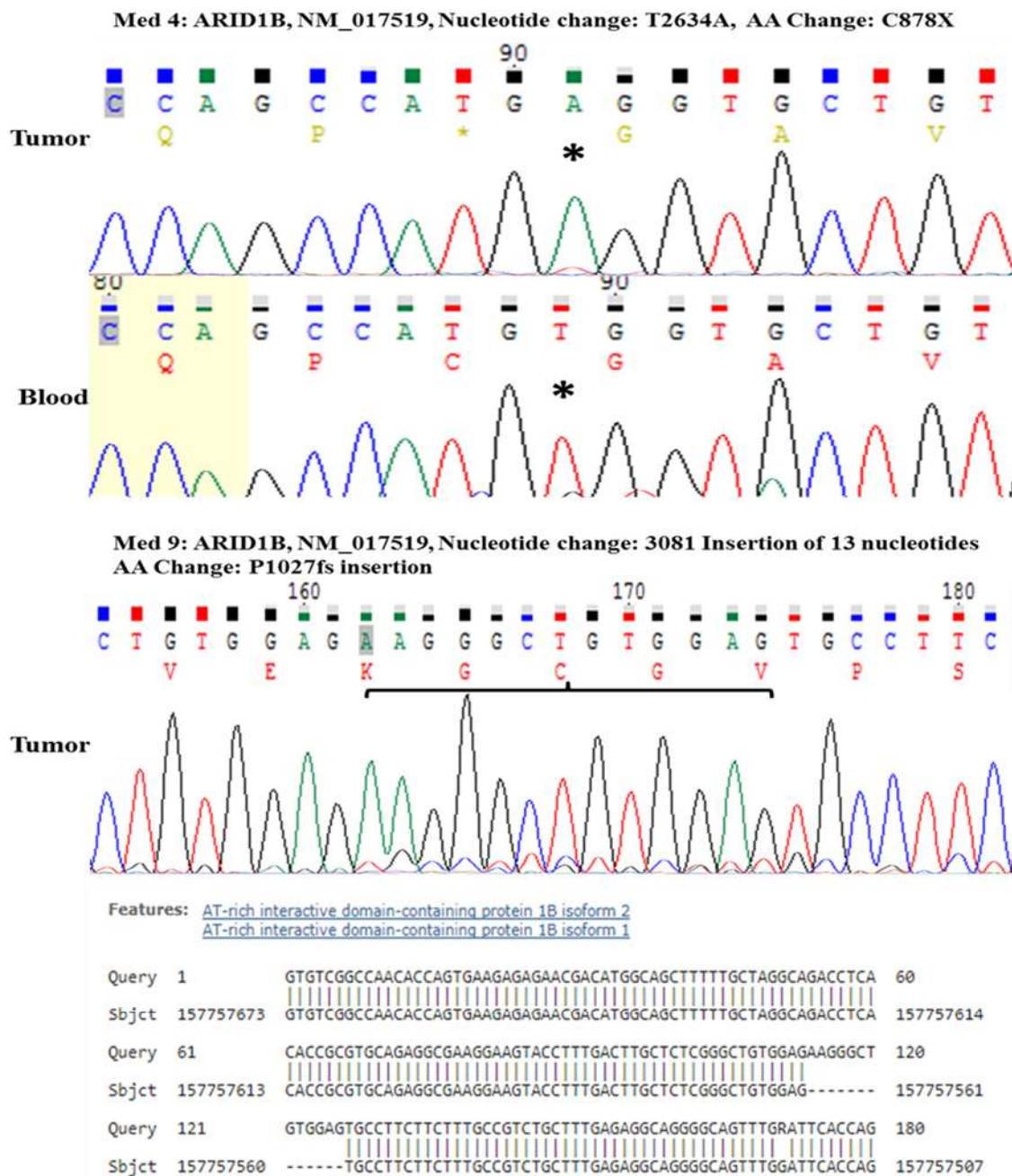


Figure 4.2: Mutations in SWI/SNF complex member ARID1B in the WNT subgroup medulloblastomas. Electropherograms showing altered nucleotide position in the genes ARID1B. Position of the altered nucleotide is indicated with '*'. The 13 nucleotides insertion in Med 9 is shown in a bracket.

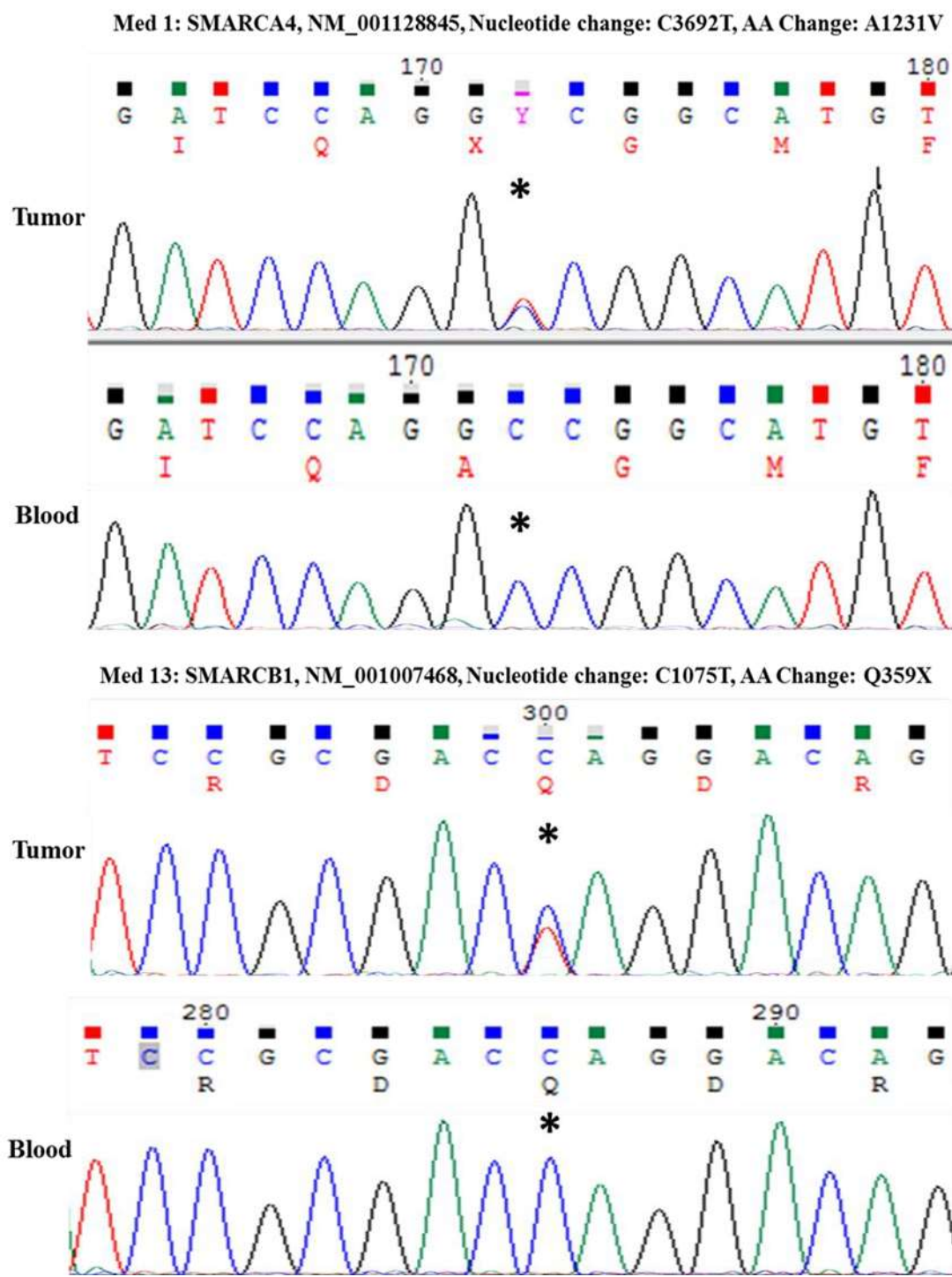


Figure 4.3: Mutations in SWI/SNF complex member SMARCA4 and SMARCB1 in the WNT subgroup medulloblastomas. Electropherograms showing altered nucleotide position in the genes SMARCA4 and SMARCB1. Position of the altered nucleotide is indicated with ‘*’.

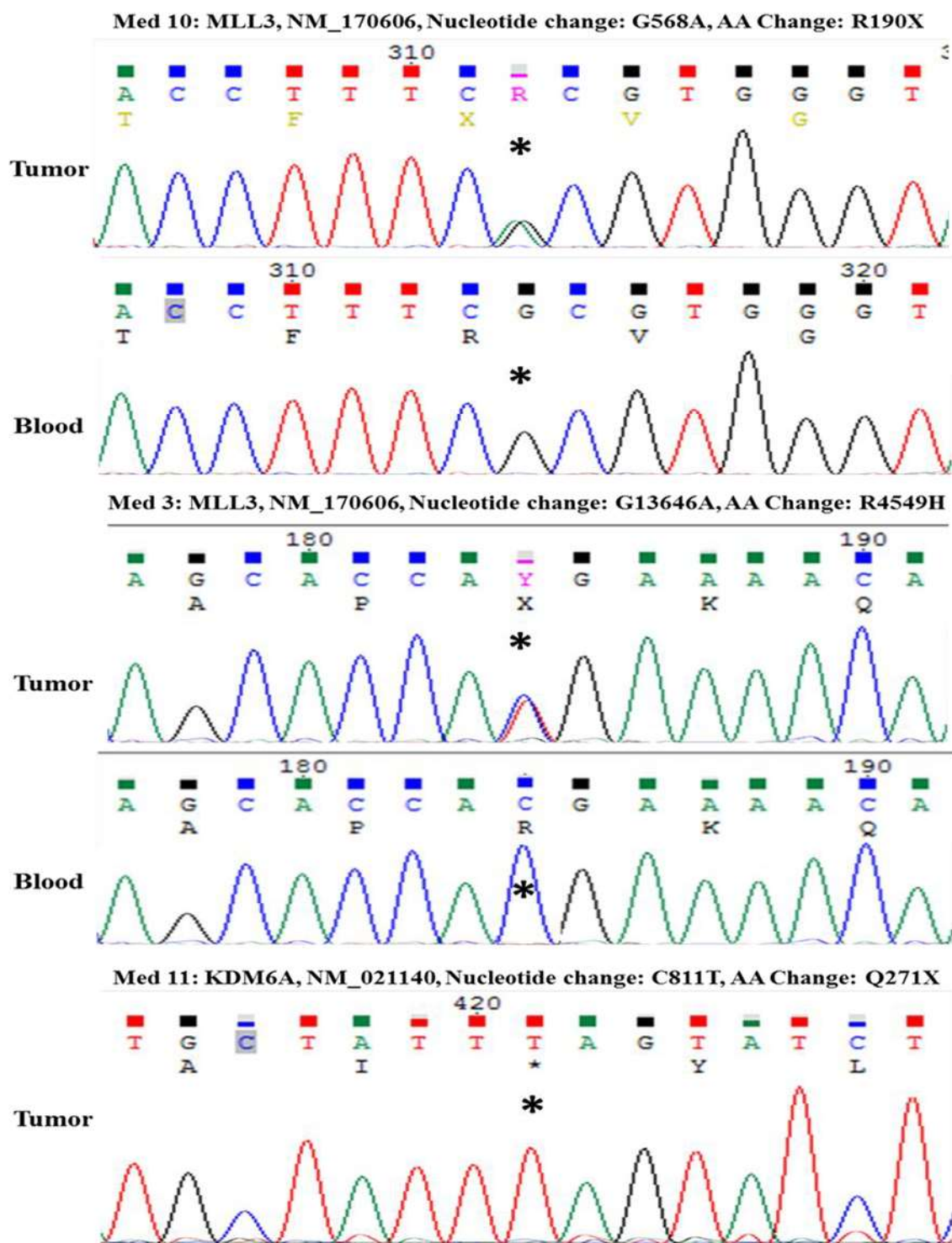


Figure 4.4: Mutations in the genes belonging to the ASCOM complex members MLL3 and KDM6A in the WNT subgroup medulloblastomas validated by Sanger sequencing. Position of the altered nucleotide is indicated by ‘*’

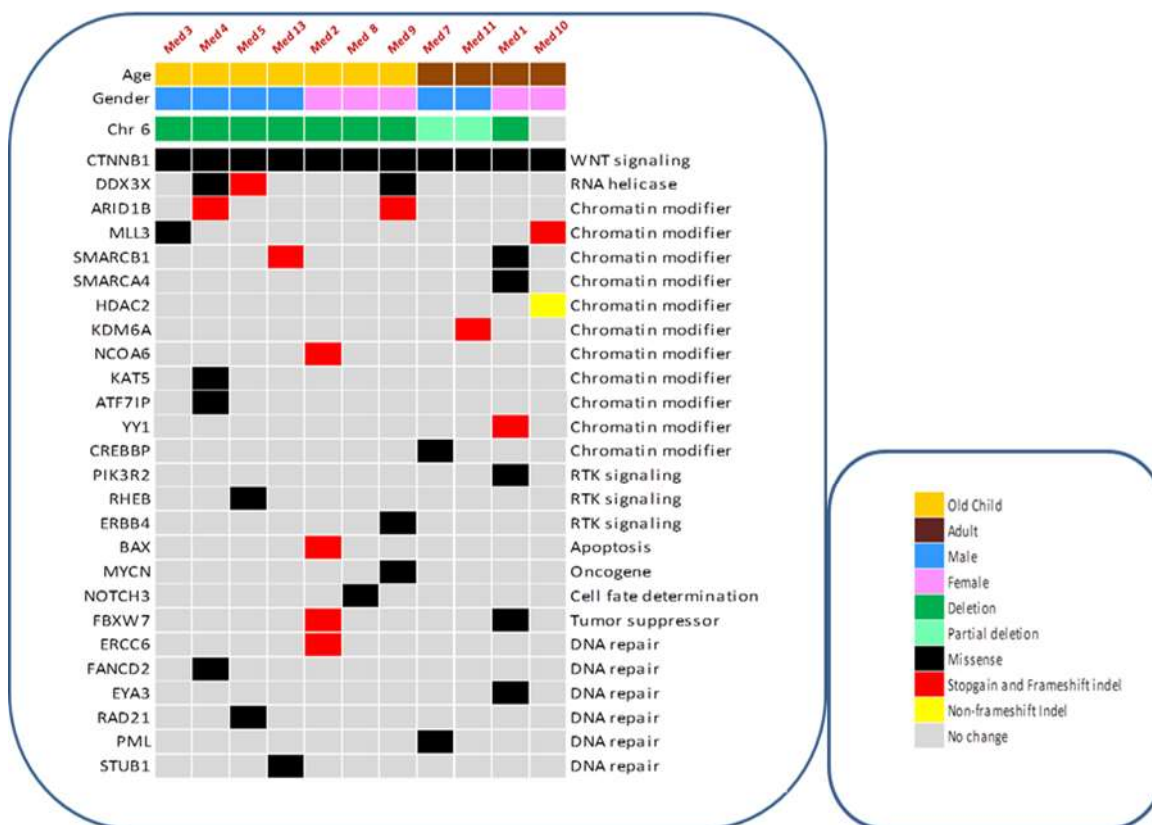


Figure 4.5: Recurrently altered genes and pathways in WNT subgroup medulloblastoma

The figure shows the different chromatin remodeling, cell signaling and DNA repair genes that are mutated in WNT subgroup medulloblastoma. It also shows the status of chromosome 6, gender distribution of WNT subgroup medulloblastoma.

SMARCB1 and *SMARCA4* that encode members of the SWI/SNF complex were also found to be mutated in 2 and one WNT tumor respectively (Fig. 4.3). The two mutations in *SMARCB1* are nonsense (Q359X) and missense (R357H) whereas the mutation in *SMARCA4* is of missense type (A1231V). Activating signal cointegrator-2 (ASC-2 or NCOA6) containing complexes (ASCOM) possesses histone methylation activity and are involved in transcriptional activation. Genes encoding Mixed lineage leukemia 3 (MLL3) and Nuclear receptor coactivator 6 (NCOA6), components of this ASCOM complex were **found** to be mutated in 2/11 and 1/11

tumors respectively. The two mutations in MLL3 are nonsense (R4549H) and missense (R190X) whereas the mutation in NCOA6 is a (E1514X) nonsense mutation. A Nonsense mutation (Q271X) in KDM6A also known as UTX gene, which has demethylase activity and demethylates tri or dimethylated but not mono-methylated H3K27 leading to de-repression of transcription, was identified in one tumor sample (Fig. 4.4). KAT5, a histone acetyl transferase which acetylates histones that also plays important role in chromatin remodeling, was found to be mutated (V348M) in one tumor tissue. Apart from mutations in DDX3X, and in the genes involved in chromatin remodeling and histone modification, mutations were identified in the genes involved in growth factor signaling (*ERBB4*, *PIK3R2* and *RHEB*) and DNA repair (*ERCC6*, *FANCD2*, *EYA3*, *RAD21*, *PML* and *STUB1*) (Fig. 4.5).

4.1.3 Copy number variations in the WNT subgroup Medulloblastoma

The copy number variation analysis for 11 WNT subgroup medulloblastoma was done using CopywriteR software (<https://github.com/PeeperLab/CopywriteR>) that identifies copy number variation using the exome sequence data [120]. CopywriteR uses the off-target reads to analyse the copy number variation data, thus each sample data can be analysed independent of other samples. Of the 11 tumor tissues studied, 8 tumors showed monosomy of chromosome 6 whereas 2 tumours showed partial loss of chromosome 6 and 1 tumour sample did not show loss of chromosome 6 as analysed by CopywriteR programme (Fig 4.6).

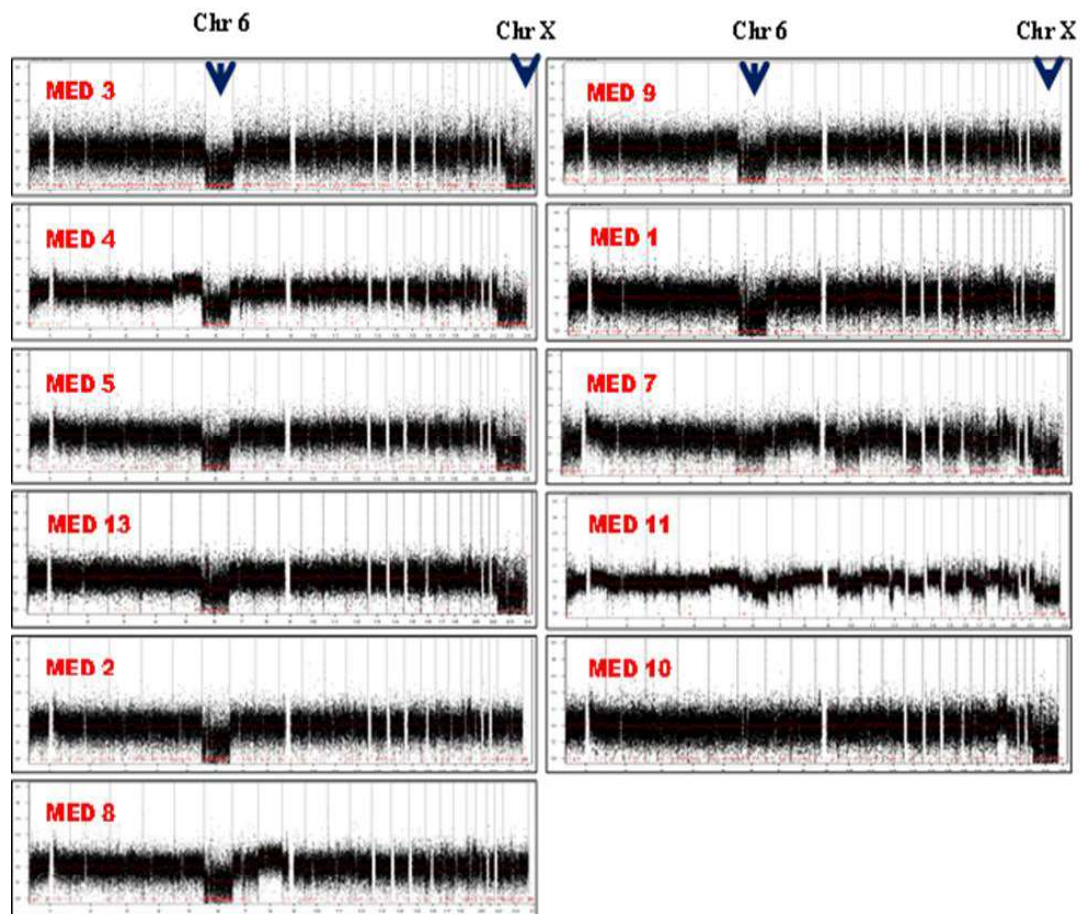


Figure 4.6: Copy number variation in the WNT subgroup medulloblastomas as analyzed by CopywriteR software. The positions of Chromosome 6 and Chromosome X are shown by arrowhead.

In exome sequencing analysis of the WNT subgroup medulloblastoma, *DDX3X* is found to be mutated in 3/11 WNT subgroup tumors. Recurrent truncating mutations in the *DDX3X* gene have been reported in Chronic Lymphocytic Leukemia while homozygous deletions have been reported in the gingivo-buccal oral squamous cell carcinomas from the Indian tobacco chewers and in HPV positive head & Neck carcinomas. Downregulation of *DDX3X* expression has been reported in the HBV positive hepatocellular carcinoma [80, 81, 83]. The presence of truncating

mutations, homozygous deletions and down-regulation of expression of the *DDX3X* gene suggest *DDX3X* to function as a tumor suppressor gene. On the other hand, *DDX3X* has also been shown to act as an oncogene by upregulating Snail transcription factor and repressing E-cadherin expression to bring about epithelial mesenchymal transition of MCF7 breast cancer cells [84]. *DDX3X* protein and mRNA levels positively correlate with tumorigenicity of breast cancer cell lines *i.e.* aggressive breast cancer cell line has higher levels of *DDX3X* protein [67]. Thus *DDX3X* has been reported to function as tumor suppressor or oncogene in different cancers. Next gen sequencing studies recently done in medulloblastoma also identified *DDX3X* as second most frequently mutated gene in medulloblastoma but its role in medulloblastoma pathogenesis is not yet understood hence it was decided to investigate its functional role in medulloblastoma pathogenesis.

4.2 Understanding the functional relevance of the identified genetic alterations in *DDX3X*, a DEAD box family RNA helicase

DDX3X is located on X-chromosome at p11.3-11.23 and encodes a 662 amino acid long protein. It is a member of DEAD-box family of RNA helicases. *DDX3X* has ATPase and ATPase dependent RNA helicase activity. *DDX3X* contains conserved ‘helicase motifs’ that reside on adjacent Rec-A like domains D1 and D2 connected by a linker. The name of DEAD-box is derived from the conserved amino acid sequence D-E-A-D (Asp-Glu-Ala-Asp) located in motif II of its 12 motifs. These 12 motifs play role in: ATP binding, RNA binding and linking ATP and RNA binding. . These motifs are located in D1 and D2 domain [61]. Three mutations were identified in the *DDX3X* gene in the WNT medulloblastoma tumors Two of them (Q265H and A367T) are located adjacent to the motif Ia and II respectively whereas the third mutation (G242fs deletion) leads to the truncation of the protein after motif I leading to the loss of major

part of D1 and entire D2 domain of DDX3X. Motif Ia and II are thought to be involved in interaction of DDX3X with RNA substrate. So the mutations identified in this study might be disrupting or altering RNA binding and/or disrupting helicase activity of DDX3X. Hence it was decided to study the effect of these mutations on DDX3X helicase activity by purifying the recombinant DDX3X protein.

4.2.1 Cloning of DDX3X in a bacterial expression vector pET-28a

DDX3X cDNA (a kind gift from Dr. Laura Madrigal-Estebas, Trinity College, Dublin) was cloned in pET28a vector (Novagen, Merck Millipore, USA) between BamHI and EcoRI site and confirmed by Sanger sequencing (Fig. 4.7). For cloning DDX3X cDNA a forward primer was designed that contained the first 21 nucleotides starting with initiation codon ATG and a TEV protease cleavage site upstream the ATG codon so as to enable release of DDX3X without the Histidine tag. This vector contains T7lac promoter that enables expression of gene of interest in an Isopropyl β -D-1-thiogalactopyranoside (IPTG) inducible manner and adds N-terminal 6X-HIS tag to the protein of interest, which enables its purification using Ni-NTA affinity columns.

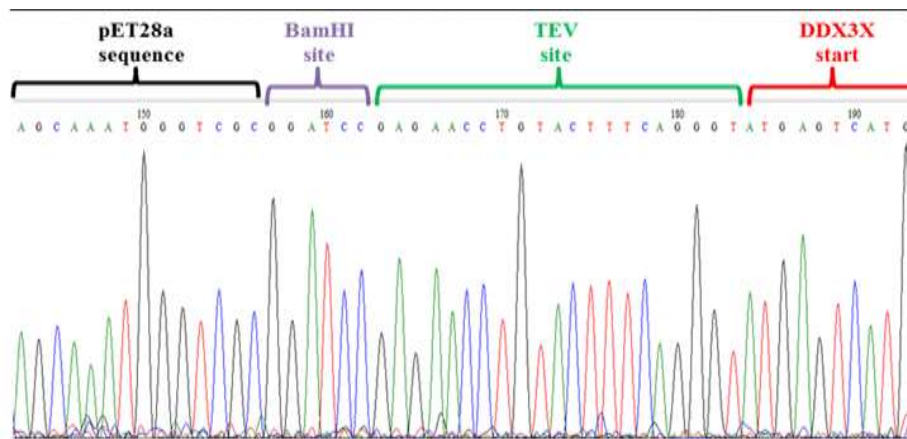


Figure 4.7: Validation of DDX3X cDNA clone in pET-28a vector using Sanger sequencing. Sequences of pET28a vector, cloning site BamHI, TEV protease site and DDX3X start site are seen after sequencing the pET28a-DDX3X construct with T7 promoter primer.

4.2.2 Expression of DDX3X cloned in a bacterial expression vector pET-28a as 6X-His fusion protein in *E. coli* BL21 cells

E. coli BL21 cells were transformed with pET-28a-DDX3X construct and grown till O.D.₆₀₀ reached 0.5 and then induced with different concentrations of IPTG ranging from 0.1 mM to 0.4 mM at two different temperatures of 18°C and 37°C. Abundant DDX3X expression was seen in pET-28a-DDX3X transformed *E. coli* BL21 cells induced at 37°C as well as at lower temperature of 18°C at the concentrations of IPTG ranging from 0.1 mM to 0.4 mM. However, DDX3X was found to be expressed only in the insoluble fraction. Explain soluble vs insoluble fraction (Fig. 4.8 A and B).

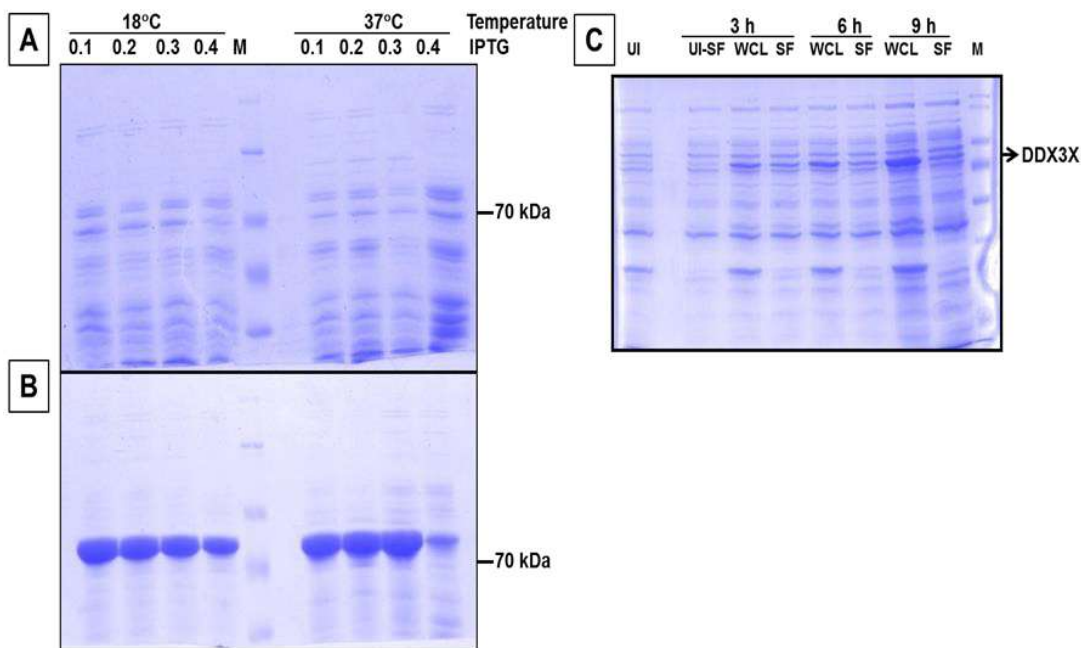


Figure 4.8: Expression of His-tagged DDX3X in *E. coli* BL21 cells.

SDS-PAGE analysis of soluble (A) and insoluble pellet (B) fractions of *E. coli* BL21 cells grown at 37 °C expressing pET28a-DDX3X construct and induced at the indicated concentration ranging from 0.1 to 0.4 mM of IPTG at 18°C or 37 °C. (C) SDS-PAGE analysis of uninduced soluble (UI-SF) and induced

soluble (SF) fractions as well whole cell lysates (WCL) of *E. coli. BL21* cells carrying the pET28a-DDX3X construct. The cells were grown at 18°C and induced at 18°C with 0.3 mM IPTG for the indicated time intervals. M indicates molecular weight markers ranging from 10-180 kDa.

Since the expression levels of DDX3X did not change appreciably even upon incubation at lower temperature or at low IPTG concentration, the *E. coli BL21* cells expressing pET28a-DDX3X construct were grown at 18°C until the O.D.₆₀₀ of the culture reached 0.5 and then IPTG induction was done at 0.3 mM concentration for increasing time intervals (3 h, 6 h and 9 h). Detectable DDX3X expression was obtained upon IPTG induction for 3 h that increased gradually with increasing incubation time of 6 h and 9 h in the whole cell lysates. However, significant DDX3X expression was not obtained at any of these time intervals in soluble fraction (Fig. 4.8 C). Thus, even after controlling DDX3X expression to a minimum detectable level by controlling temperature and time of induction, DDX3X expression was still obtained only in the insoluble fraction.

4.2.3 Solubilisation of recombinant 6X-His tagged DDX3X expressed in *E. coli BL21* cells using different non-ionic, ionic detergents and other additives

Detergents are known to increase the solubility of proteins hence increasing concentrations of different detergents *viz.* Triton X-100, NP-40 and Sarkosyl were used in lysis buffer for increasing solubility of DDX3X. *E. coli BL21* cells expressing pET-28a-DDX3X were grown at 37°C till O.D.₆₀₀ reached 0.5 and then induced with 0.3 mM IPTG concentration at 18°C for 16 h. The bacterial pellets were lysed in lysis buffers containing different detergents and solubilizing agents. The soluble and insoluble fractions were analysed by SDS-PAGE analysis. DDX3X was obtained in soluble fraction only in the presence of 0.3% to 1% Sarkosyl (Fig. 4.9 A and B).

Even 0.1% Sarkosyl was not found to be sufficient to solubilize DDX3X protein. The presence of sarkosyl does not allow efficient binding of the His-tagged protein to the Nickel column. Therefore, other additives like sucrose, glycol, mannitol, mannose, and sorbitol were also added to the extraction buffer to increase solubility of the protein. However, none of these additives could get DDX3X recombinant protein in the soluble fraction (Fig. 4.10).

4.2.4 Expression of DDX3X cloned in a bacterial expression vector pET-28a as 6X-His fusion protein in *E. coli Rosetta-gami 2 (DE3) pLysS* cells

E. coli Rosetta-gami 2(DE3) pLysS strain expresses T7 lysozyme that suppresses basal expression of T7 RNA polymerase thus completely eliminating expression of recombinant protein before induction with IPTG. The strain also promotes disulfide bond formation of eukaryotic proteins so that the proper protein folding takes place. *E. coli Rosetta-gami 2(DE3) pLysS* cells were transformed with pET-28a-DDX3X construct and grown at 37°C till O.D.₆₀₀ reached 0.5 and then induced with 0.3 mM IPTG concentration at 18°C and 24°C for different times intervals (5 h, 16 h and 24 h) followed by lysis of the bacterial pellets in lysis buffer and analysis of whole cell lysate (WCL) and soluble fractions (SF) on SDS-PAGE. In case of induction at 18°C DDX3X expression was observed at 16 h and 24 h in the whole cell lysates but not in the soluble fractions. In the case of induction at 24°C DDX3X expression was obtained at all three time intervals but not in the soluble fraction. So even after tightly controlling DDX3X expression by expressing in the *E. coli Rosetta-gami 2(DE3) pLysS* cells DDX3X expression was not found in the soluble fraction (Fig. 4.11)

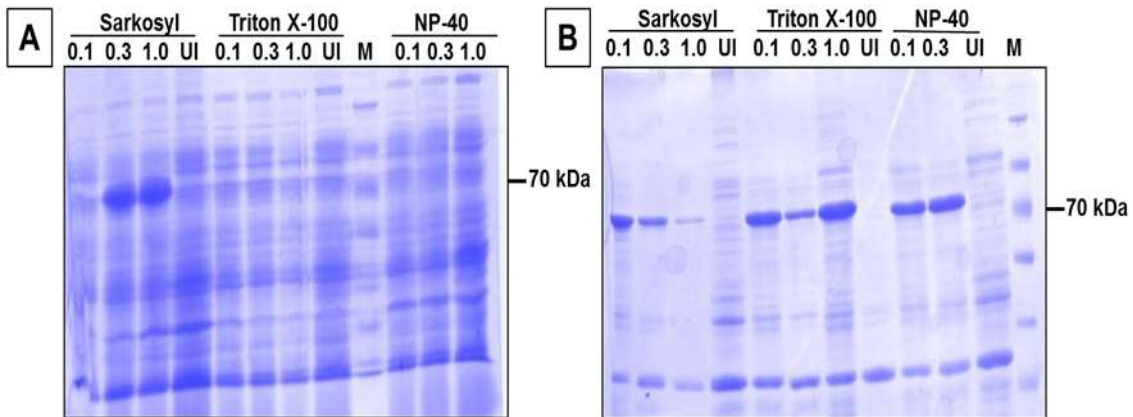


Figure 4.9: Expression of 6X His- tagged DDX3X in *E. coli* BL21 with lysis buffer containing different detergents

Expression of the recombinant DDX3X protein in fraction solubilized (A) with the indicated detergent at 0.1%, 0.3% and 1.0% concentration and the corresponding insoluble fraction (B). UI indicated un-induced lysate in 1% concentration of the indicated detergent. M indicates molecular weight marker.

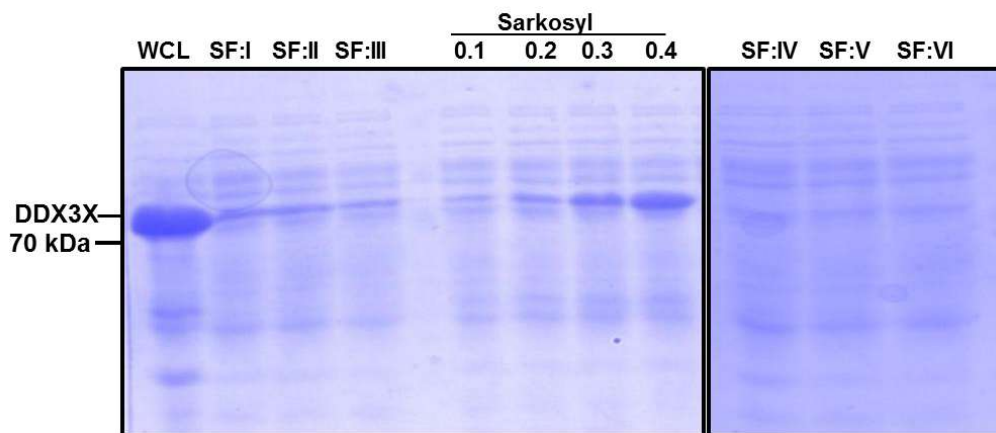


Figure 4.10: Expression of 6X His- tagged DDX3X in *E. coli* BL21 with lysis buffer containing different sugar additives. SDS-PAGE analysis of the expression of recombinant DDX3X protein in WCL: whole cell lysate; SF: Soluble Fractions in buffers (I, II, III, IV, V, VI) with various additives and those solubilized in the presence of 0.1% to 0.4% Sarkosyl. SF:I 10% Glycerol + 2% Glycol + 100 mM Sucrose; SF:II 10% Glycerol + 2% Glycol + 100 mM Mannose; SF:III 10% Glycerol + 2% Glycol + 100

mM Mannitol; SF:IV 100 mM Sucrose + 100 mM Sorbitol + 100 mM Mannitol; SF:V 100 mM Sucrose + 100 mM Sorbitol + 2% PEG 6000; SF: VI 100 mM Sucrose + 100 mM Sorbitol + 100 mM Mannose

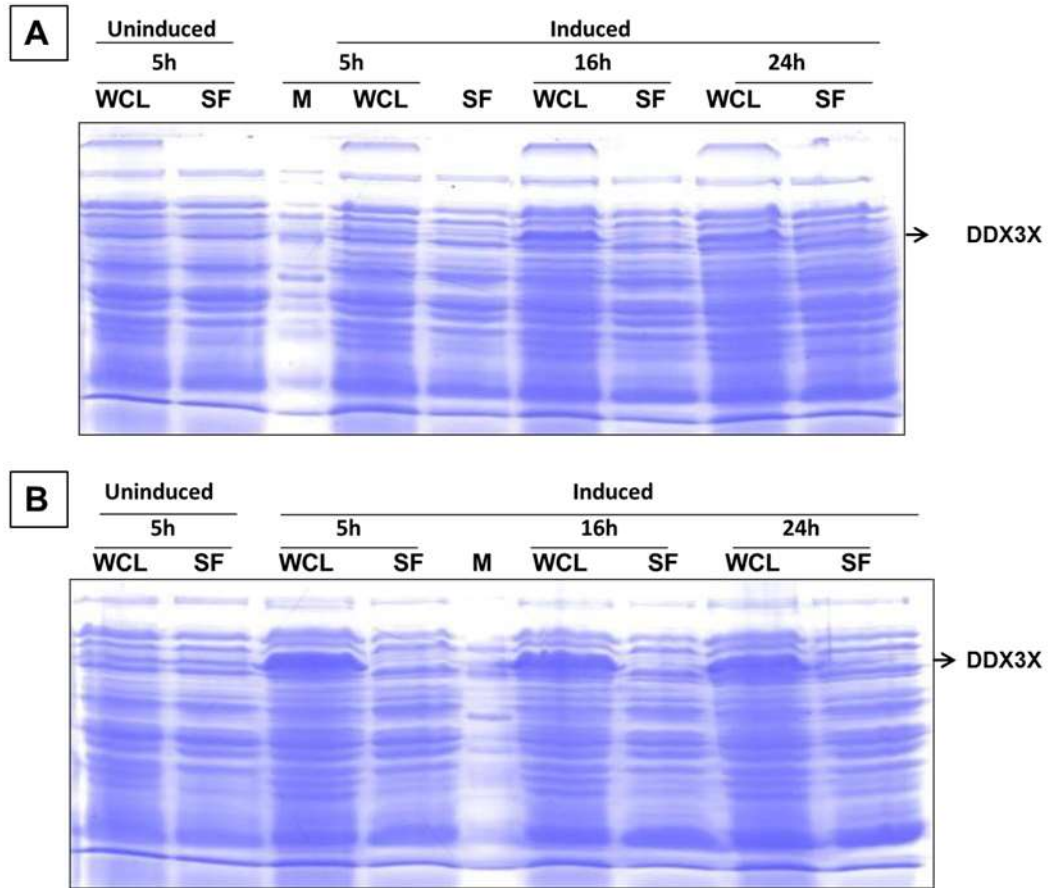


Figure 4.11: Expression of 6X His- tagged DDX3X in *E. coli Rosetta-gami 2(DE3) pLysS* strain.

SDS-PAGE analysis of pET28a-DDX3X expressed in *E. coli Rosetta-gami 2(DE3) pLysS* strain. The cells were induced with 0.3 mM IPTG for 5 h, 16 h and 24 h at 18°C (A) or 24°C and the whole cell lysate (WCL) and soluble fractions (SF) were analysed by SDS-PAGE.

4.2.5 Cloning and expression of DDX3X in a bacterial expression vector pMAL-c5E as MBP fusion protein

The pMAL-c5E vector expresses the gene of interest as a fusion downstream *maltE* gene encoding Maltose binding protein (MBP). The fusion protein can be purified by amylose affinity chromatography and the protein of interest can be cleaved of MBP using specific protease enterokinase. The MBP is known to enhance solubility of eukaryotic proteins it is fused to and the vector used expresses fusion protein in cytoplasm. Since all attempts to obtain expression of recombinant His-tagged DDX3X protein in soluble fraction failed, human DDX3X cDNA was then cloned in pMAL-c5E vector between BamHI and EcoRI site with forward primer having TEV site. *E. coli Rosetta DE3* cells were transformed with pMAL-c5E-DDX3X construct and grown till O.D.₆₀₀ reached 0.5 and then induced with 0.3 mM IPTG at different temperatures of 18⁰C, 24⁰C and 37⁰C. The MBP-DDX3X fusion protein (MW = 120 kDa) was found to be expressed at all the three temperatures 18⁰C, 24⁰C and 37⁰C tested in soluble fraction (Fig. 4.12).

MBP-DDX3X fusion protein was purified by binding of induced soluble fraction to amylose resin for an hour followed by 3 washes with wash buffer and then elution with elution buffer containing 10 mM maltose. All the purification steps like binding, washing and elution were done at 4⁰C. Eluted fractions from the amylose affinity column showed presence of more than 90% pure 120 kDa MBP-DDX3X fusion protein (Fig. 4.13). Purified MBP-DDX3X fusion protein was digested with TEV protease for 3 h at 4⁰C to release it from the fused MBP. However, after digestion with TEV, DDX3X precipitated.

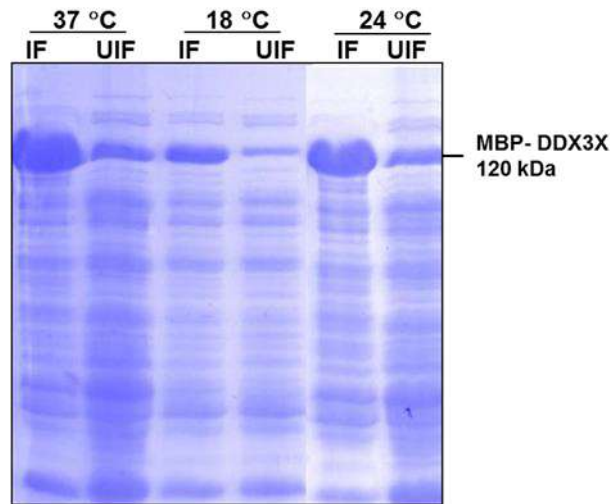


Figure 4.12: Expression of MBP tagged DDX3X in *E. coli Rosetta- DE3* strain.

SDS-PAGE analysis of the recombinant MBP-DDX3X fusion protein expressed in *E. coli. Rosetta DE3* grown at the indicated temperature and induced with 0.3 mM IPTG; UIF indicates uninduced fraction and IF indicates induced fraction.

Hence, MBP fused full length DDX3X protein was used for assessing the RNA helicase activity of DDX3X.

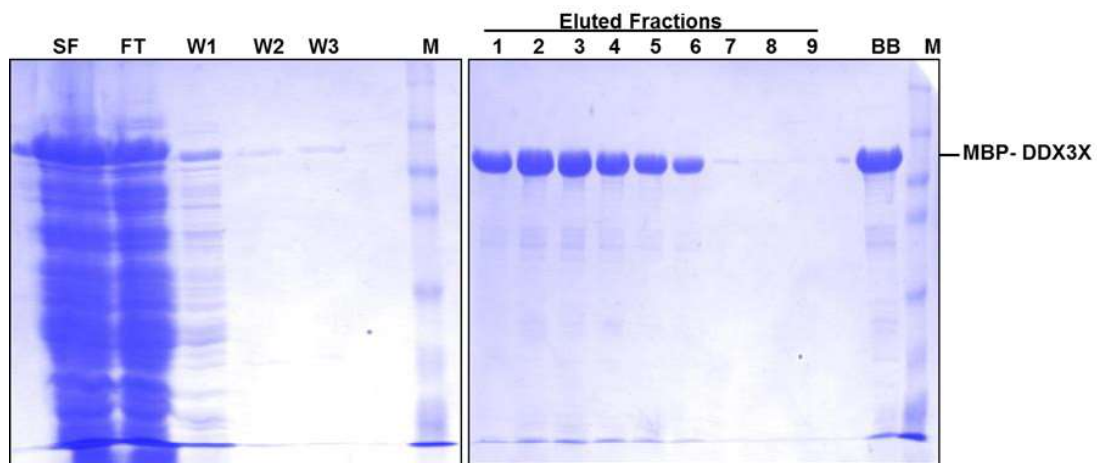


Figure 4.13: Purification of MBP tagged DDX3X in *E.coli Rosetta DE3* cells.

SDS-PAGE analysis of total soluble fraction (SF) of *E. coli. Rosetta DE3* Protein extract expressing recombinant MBP-DDX3X fusion protein and that separated on amylose affinity column. FT: Flow through fraction from the column; W1, W2, W3: 1st, 2nd and 3rd wash given to the column and eluted fractions 1 to 9 and BB: Column beads bound fraction; M: Molecular weight marker lane.

4.2.6 RNA helicase assay with MBP-DDX3X fusion protein

Before using for helicase assay, the maltose bound to the purified MBP-DDX3X protein was removed by using Amicon ultra centrifugal filter (cut off 50 kDA) in the dialysis buffer (20 mM Tris-HCl pH 7.5, 50 mM NaCl, 2 mM DTT and 10% Glycerol) and then used for RNA helicase assay. Amylose resin bound MBP-DDX3X protein was also resuspended in the dialysis buffer and used for helicase assay. Helicase activity of MBP-DDX3X fusion protein was assessed by incubating the protein with 20 nM of an 18 mer RNA oligonucleotide annealed to a complementary 36 mer RNA oligonucleotide resulting in a 18 mer duplex with 18 nucleotide overhang. Different concentrations (0.2 μ M to 0.8 μ M) of the fusion DDX3X protein was incubated with the annealed RNA oligos in a hybridization buffer supplemented with RNase inhibitor at 37⁰C for 40 min. After the incubation reaction was stopped by adding 5 X RNA loading dye containing (100 mM Tris-HCl [pH 7.5], 20 mM EDTA, 0.5% SDS, 0.1% Bromophenol Blue, 50% Glycerol) and then separated on a 8% native acrylamide gel by electrophoresis in the presence of 0.1% SDS to inhibit secondary structure formation. The 18 mer oligonucleotide was labeled using fluorescent dye 6-FAM so that its separation from the 18 mer/36 mer hybrid RNA can be traced using UV transilluminator. Incubation of the hybrid with the bead bound MBP-DDX3X protein but not with eluted MBP-DDX3X protein shows migration of the hybrid at intermediate position between that of hybrid and free 18 mer oligonucleotide indicating partial helicase activity of the fusion DDX3X protein (Fig. 4.14).

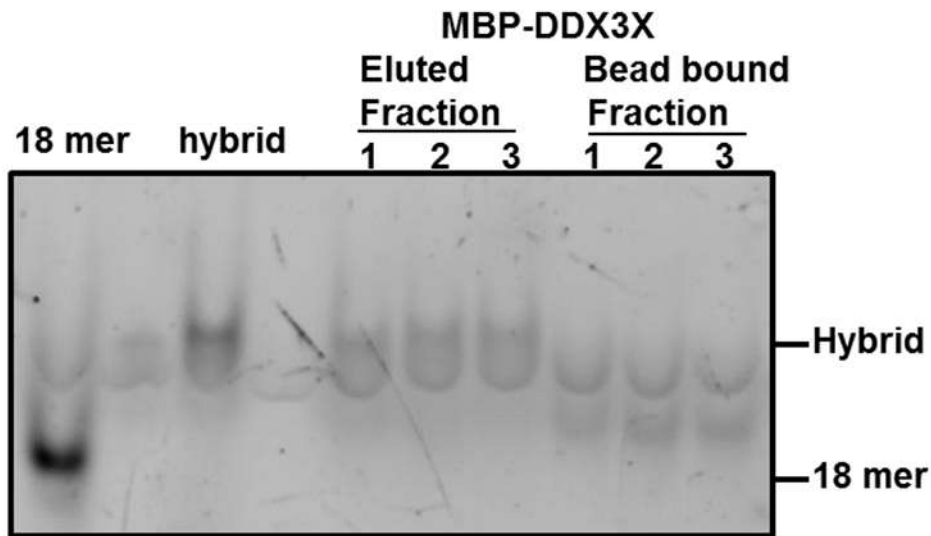


Figure 4.14: Helicase assay for recombinant MBP-DDX3X fusion protein. Helicase assay reaction products separated by native PAGE electrophoresis. The 18 mer / 36mer RNA hybrid Incubated with bead bound MBP-DDX3X fusion protein at increasing concentrations (0.2, 0.4 and 0.8 μ M) from 1 to 3 shows product at position intermediate between that of the hybrid and the 18 mer RNA oligonucleotide.

Since even the MBP fused DDX3X protein showed only partial helicase activity, effect of mutations on DDX3X helicase activity was studied. A recent Study by *LB Epling et al. 2015* has shown that some of the DDX3X mutants identified in pediatric medulloblastoma have defective RNA stimulated ATPase activity [62]. Even in this study, helicase activity of the recombinant DDX3X protein could not be studied due to lack of helicase activity of the recombinant DDX3X protein. In the present study, one WNT tumor was found to have truncating mutation in DDX3X that would not retain helicase activity of the protein. Thus the evidence so far indicates mutations in DDX3X result in loss of helicase activity.

4.2.7 Effect of DDX3X mutations on transcriptional regulatory activity of DDX3X

DDX3X, a RNA helicase has both ATPase and ATP dependent RNA helicase activity. DDX3X has been implicated to play multiple roles in RNA biology including splicing, mRNA export, transcription and translation. DDX3X is a multifunctional protein with its N-terminal domain reported to be required and sufficient for some of its transcriptional regulator activity that is independent of its ATPase and helicase activity. N-terminal domain (1-408 AA) of DDX3X has been reported to be sufficient for the induction of the IFN- β promoter [65]. Upregulation of the CDK inhibitor p21 by DDX3X has been reported to be dependent on the ATPase activity but independent of helicase activity of DDX3X [66]. The substrate specificity and regulation of enzyme activity of the DEAD box proteins is known to be influenced by protein cofactors *in vivo*. Therefore, the effect of DDX3X's role in transcriptional and translational regulation and effect of identified mutations on these activities of DDX3X needs to be investigated.

4.2.7.1 Effect of DDX3X expression on transcriptional activity of beta catenin

Cho *et al.*, (*Nature* 2012) in their study have shown that mutant DDX3X enhances the ability of mutant β -catenin to transactivate a TCF4-luciferase reporter by (TOP-flash) by 1.5-2.0 folds [121]. Therefore to check the effect of identified genetic alterations on ability of DDX3X on transcriptional activity of β -catenin, luciferase reporter assay was performed. For luciferase assay, mutant β -catenin construct, luciferase construct containing 3 TCF4 binding sites and DDX3X construct was prepared by cloning DDX3X in pcDNA3 vector using BamHI and EcoRI restriction sites. Mutants of DDX3X identified in this study (G242fs deletion, Q265H and A367T) and two other mutants (R534H and P568L) reported in medulloblastomas were

generated by Site directed mutagenesis PCR. For performing luciferase reporter assay, a luciferase construct TOP Flash cotransfected with mutant β -catenin, pcDNA3-GFP and wild type DDX3X or mutant DDX3X in 293FT cells, where GFP was used for normalization of transfection efficiency. Increase in TOP-FLASH reporter luciferase activity was obtained upon transfection with mutant β -catenin. But no further increase in the luciferase activity was observed upon cotransfection with the wild type or activating mutants (R534H and P568L) of DDX3X compared to that obtained with mutant β -catenin alone (Fig. 4.15).

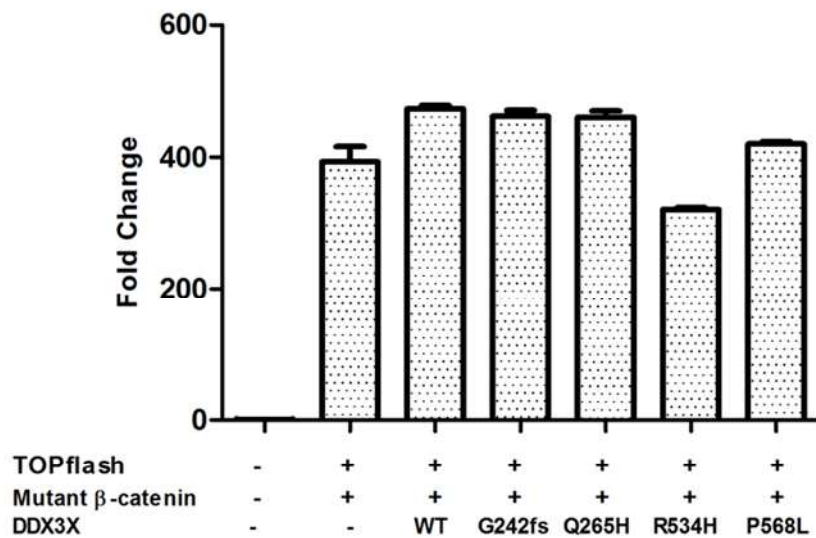


Figure 4.15: Luciferase reporter assay to check the effect of identified DDX3X mutants on trans-activation activity of mutant β -catenin. The luciferase reporter activity was studied upon transfection of the indicated constructs TOP-FLASH, mutant beta-catenin and DDX3X (wt: wild type or indicated mutant). Y-axis represent the fold change of relative luciferase activity obtained on transfection of the indicated constructs as compared to that obtained upon transfection of control vector alone.

4.2.7.2 Effect of DDX3X expression on IFN beta promoter activity

DDX3X has been reported to be a part of innate immune signaling pathways and contribute to the induction of anti-viral mediators such as type-I interferon (IFN- β). DDX3X has been shown to interact with and is phosphorylated by TBK-1 and IKK- ϵ . N-terminal domain (1-408 AA) of DDX3X was found to be sufficient for the induction of the IFN-beta promoter [65]. Different studies have reported that DDX3X enhances 3-4 fold TBK-1 mediated, 4-5 fold IKK- ϵ mediated and 2-4 fold IPS-1 mediated IFN- β promoter activity [122, 123] Therefore, to check the effect of identified genetic alteration in DDX3X on its ability to regulate IFN- β promoter, luciferase reporter assay was performed. Luciferase assay was performed by cotransfecting IFN- β promoter luciferase construct (obtained from addgene), pcDNA3-GFP, DDX3X wild type and TBK-1/IKK- ϵ /IPS-1 (obtained from addgene) in HEK 293FT cells, where GFP was used for normalization. The IFN- β promoter activity was found to increase about \sim 15 fold with TBK1, \sim 15 fold with IKK ϵ and about \sim 20 fold increase with IPS-1. However, DDX3X did not show any further induction of IFN-beta promoter activity (Fig. 4.16 A, B and C). Since HEK 293FT cells express considerable amount of endogenous DDX3X, it was decided to reduce the endogenous DDX3X levels by knockdown DDX3X by using the shRNA targeting DDX3X in inducible pLKO-Tet vector or knock-out DDX3X in HEK293FT cells using CRISPR-CAS9 technology.

In all the subsequent experiments two CRISPR mediated DDX3X knock-out clones *viz.* clone 10 and clone 11 of HEK 293FT cells (prepared by Ms Shalaka Masurkar) and shRNA (targeting 3' UTR and Open Reading Frame (ORF), refer to the Methods section for description) mediated DDX3X knock-down clones in HEK 293FT and Daoy cells were used to study DDX3X's functional role. For this purpose wild type DDX3X and mutant clones were generated in CRISPR and shRNA resistant DDX3X background by site directed mutagenesis. For generating

CRISPR resistant DDX3X construct the PAM site near the Guide RNA was mutated and for generating shRNA resistant DDX3X construct the shRNA binding sites in DDX3X was mutated by site directed mutagenesis.

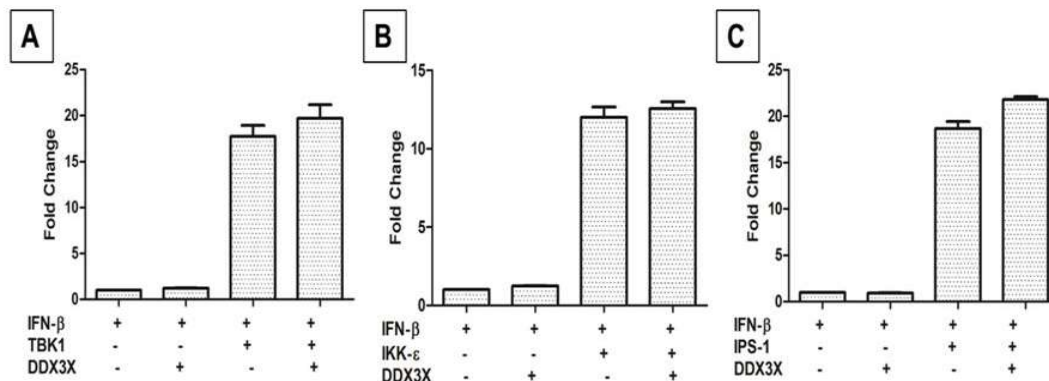


Figure 4.16: Luciferase reporter assay to check the effect of identified DDX3X mutants on IFN-β promoter activity. Y-axis represent the fold change of relative luciferase activity obtained on transfection of the indicated constructs as compared to that obtained upon transfection of control vector alone.

4.2.8 Downregulation of DDX3X expression in Daoy and HEK 293FT cells using shRNA cloned in pLKO-Tet vector

Daoy cell line belongs to SHH group of medulloblastoma and mutations in DDX3X have been reported in approximately 11% of child medulloblastoma and approximately 50% adult SHH medulloblastoma. Hence studying the effect of DDX3X mutations in Daoy cells would provide insight into the role of DDX3X in biology of medulloblastoma. Therefore, two shRNAs (one

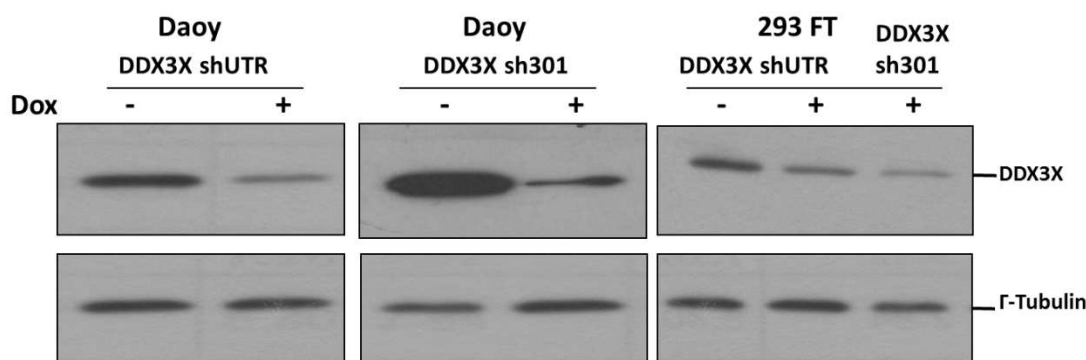


Figure 4.17: Western blot analysis of DDX3X expression in Daoy and 293 FT cells transduced with shRNAs against DDX3X and induced with doxycycline. Daoy and HEK 293 FT cells were transduced with two shRNAs targeting DDX3X in 5'UTR and ORF region. Stable polyclonal populations were selected for each shRNA and induced with doxycycline. Dox indicates doxycycline induction.

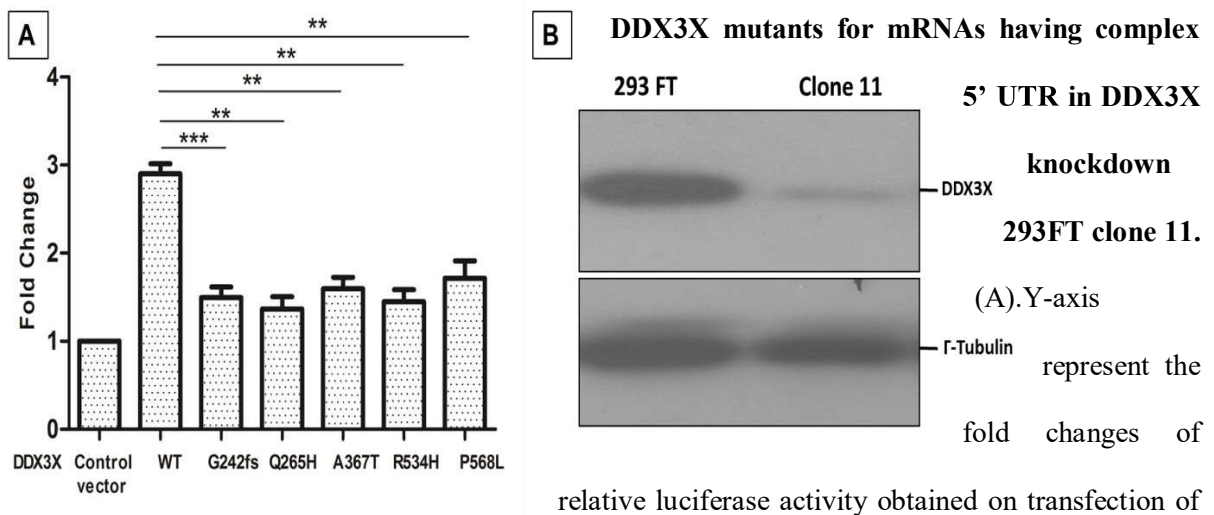
targeting 3'UTR region and other targeting ORF region nucleotide 301-320) were designed and cloned in a doxycycline inducible pLKO-Tet vector. Daoy and HEK 293FT cells were transduced with lentiviral particles of these shRNAs and polyclonal population was selected using puromycin selection. Almost 90% downregulation of DDX3X was observed in Daoy cells using shRNAs against UTR (Daoy shUTR) and ORF (Daoy sh301) induced by doxycycline. In the case of HEK 293FT cells 20-30% downregulation of DDX3X was observed with UTR shRNA whereas shRNA against ORF region showed more than 50% downregulation (Fig. 4.17).

4.2.9 Effect of identified genetic alterations in DDX3X on its translational control

DDX3X has been reported to facilitate translation initiation of mRNAs with long and complex 5'UTRs like Cyclin E1 through its helicase activity [76]. Therefore, to identify the effect of identified mutations on translation control activity of DDX3X luciferase reporter construct was generated by cloning complex 5' UTR of cyclin E1 in pGL3 control vector upstream of

luciferase gene and luciferase reporter assay was performed in DDX3X knock-out HEK 293FT clone 11. Luciferase reporter assay was performed by cotransfecting cyclin E1 5'UTR luciferase construct, pcDNA3-GFP and wild type or mutant DDX3X (G242Fs/Q265H/A367T/R534H/P568L) in 293FT clone 11. In clone 11 relative luciferase activity was found to be increased by approximately 3 fold ($p \leq 0.0001$) in the case of the cells transfected with CRISPR resistant pcDNA3-DDX3X as compared to the control cells transfected with pcDNA3 indicating that DDX3X enhances the expression of genes having complex 5'UTR, whereas all the mutant of DDX3X (G242Fs/Q265H/A367T/R534H/P568L) failed to increase luciferase activity indicating loss of function nature of these mutations (Fig. 4.18).

Figure 4.18: Luciferase reporter assay to check translational regulation function of identified



the indicated constructs as compared to that obtained upon transfection of control vector alone. ** indicates $p \leq 0.001$. (B) Western blot representing knockdown of DDX3X in 293FT clone 11 using CRISPR-CAS9 system. Γ -Tubulin is used as loading control.

4.2.10 Effect of DDX3X downregulation on proliferation of Daoy cells

The effect of DDX3X downregulation on proliferation of Daoy cells was studied by MTT reduction assay over a period of 10 days. Vector control populations of Daoy cells showed no significant difference in proliferation upon Doxycycline treatment compared to their untreated populations. Daoy stable polyclonal population expressing DDX3X shRNA sh301 cells showed approximately 75% ($p \leq 0.0001$) decrease in cell proliferation after doxycycline treatment on day 10. Whereas in the case of Daoy stable polyclonal population expressing DDX3X shRNA targeting 3'-UTR, 50% ($p \leq 0.0001$) reduction in proliferation was observed after doxycycline treatment compared to their uninduced counterparts (Fig. 4.19).

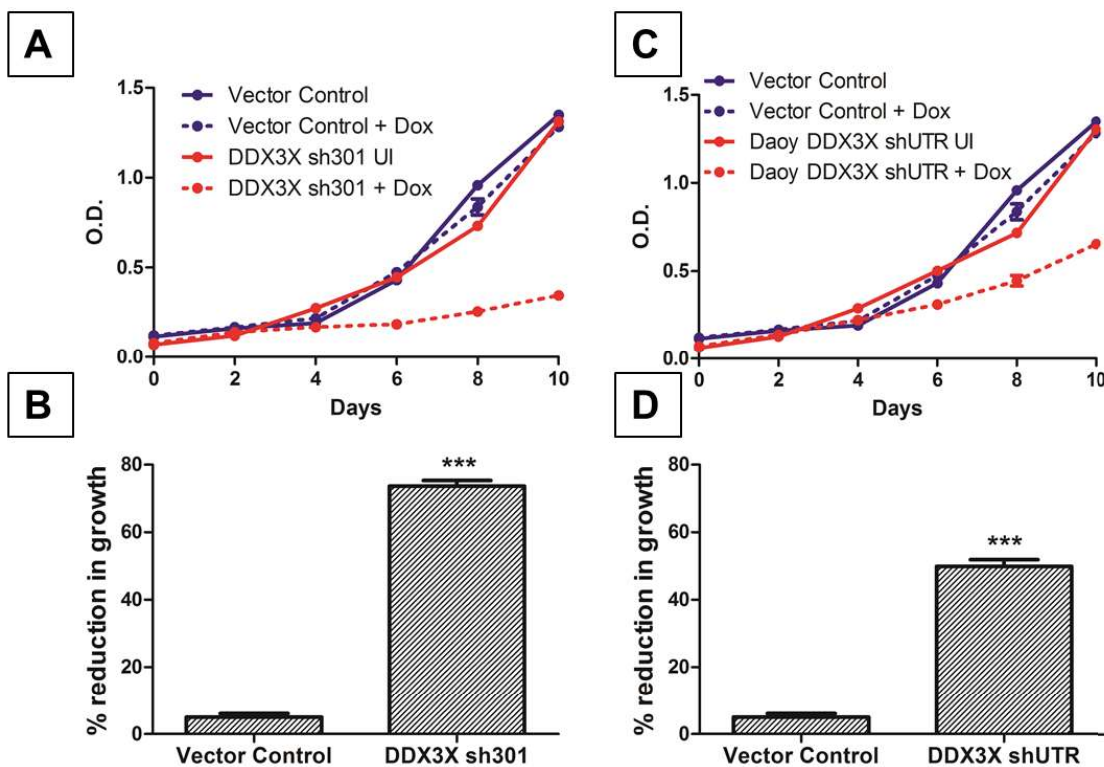


Figure 4.19: Effect of DDX3X downregulation on growth of Daoy medulloblastoma cell line.

Representative experiments showing growth curves of Daoy medulloblastoma cell line polyclonal populations (A) transduced with shRNA targeting DDX3X in ORF region (DDX3X sh301) and that (C)

transduced with shRNA targeting DDX3X in 5'UTR region or control vector with (+Dox) or without doxycycline induction (UI) as studied by MTT reduction assay over a period of 10 days. B, D: Y-axis denotes the percentage reduction in growth upon doxycycline treatment of the indicated population compared to un-treated population as studied by the MTT reduction assay. *** indicates $p \leq 0.0001$.

4.2.11 Effect of DDX3X downregulation on clonogenic potential of Daoy cells

The clonogenic potential of DDX3X downregulated Daoy cells was studied by clonogenic assay. Daoy cells formed 250-300 well separated, microscopically visible colonies 10 days post seeding of 1000 cells / 55 mm petridish. There was no significant difference in the number of colonies formed by the doxycycline induced vector control cells compared to their uninduced counterparts, whereas DDX3X knockdown Daoy sh301 cells showed ~90% ($p \leq 0.0001$) reduction in the number of colonies compared to their uninduced counterparts (Fig. 4.20 A and B), In the case of Daoy shUTR cells it was clonogenic potential was found to be reduced by ~50% ($p \leq 0.001$) compared to their uninduced counterparts (Fig. 4.20 C and D).

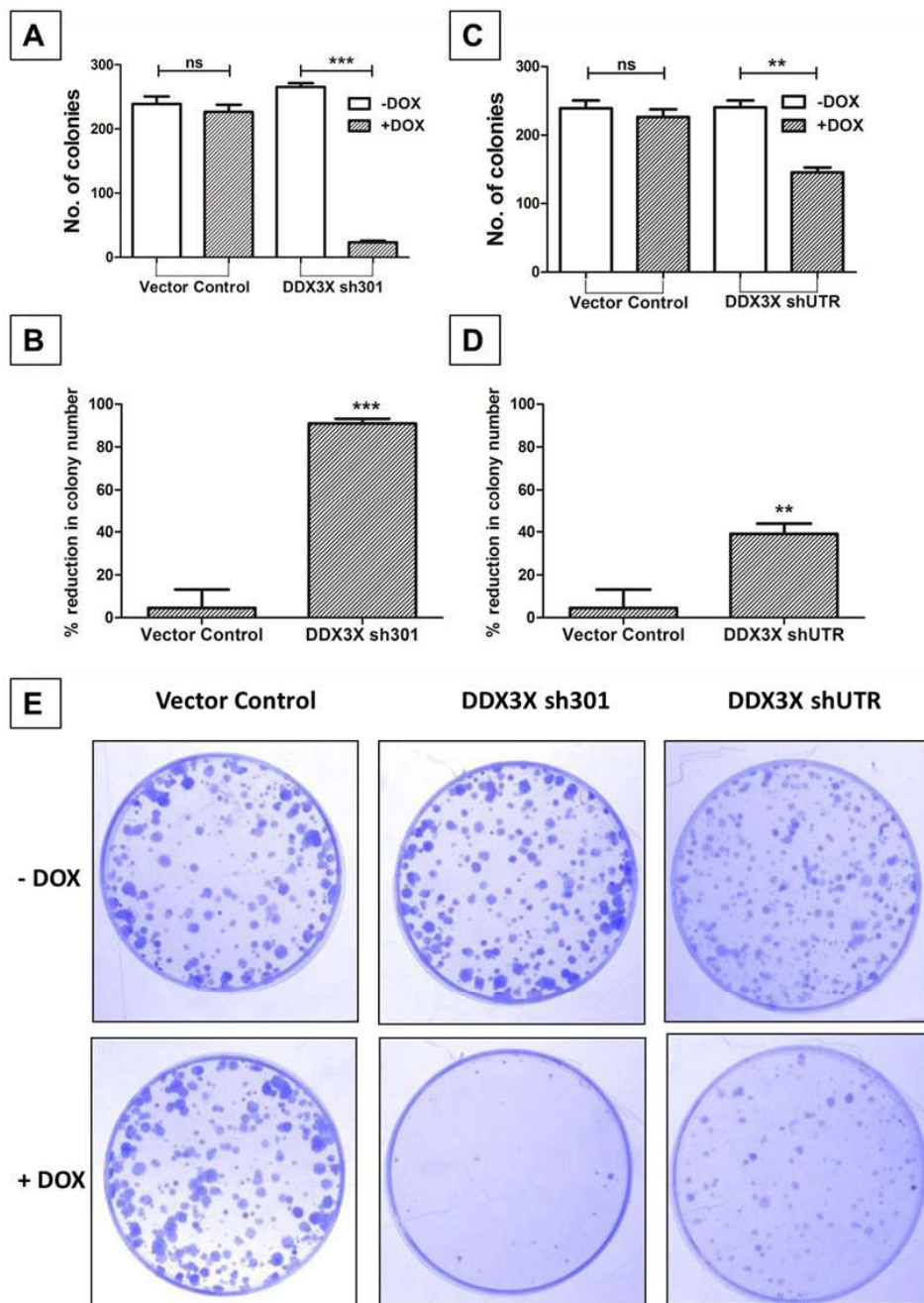


Figure 4.20: Effect of DDX3X downregulation on clonogenic potential of Daoy medulloblastoma cell line. Representative experiments showing the number of colonies formed by Daoy medulloblastoma cell line polyclonal population (A) transduced with shRNA targeting DDX3X in ORF region (DDX3X sh301) and that (C) transduced with shRNA targeting DDX3X in 5'UTR region or control vector with

(+Dox) or without (-Dox) doxycycline induction as studied by clonogenic assay. B, D: Y-axis denotes the percentage reduction in colony formation upon doxycycline treatment of the indicated population as compared to the un-treated population. 'ns' indicates non-significant, ** indicates $p \leq 0.001$ and *** indicates $p \leq 0.0001$. E: Representative images of the above mentioned experiments.

4.3 Delineate the role of has-miR-30a in medulloblastoma cell behavior

Genome wide expression profiling of medulloblastomas for protein coding genes and microRNAs, done in parallel using Affymetrix gene 1.0 ST arrays and Taqman Low Density Arrays respectively had shown differential microRNA expression in the four molecular subgroups of medulloblastomas [13]. MiR-30a, a microRNA located on chromosome 6 was found to be downregulated in all medulloblastomas as compared to its expression in normal cerebellum. In WNT subgroup of medulloblastomas one copy of chromosome 6 is lost in more than 75% cases [124]. MiR-30a expression has been reported to be down regulated in multiple cancers including breast cancer, lung cancers and colorectal cancers [125]. Hence it was decided to investigate the role of miR-30a in pathogenesis of medulloblastomas.

4.3.1 MiR-30a expression levels in medulloblastoma subgroups and normal brain tissues

MiRNA profiling of 19 medulloblastomas along with two developing and two adult normal cerebellums was done using Taqman Low Density array as described [13]. Expression of seven microRNAs belonging to the miR-30 family microRNAs (miR-30a-5p, miR-30a-3p, miR-30b, miR-30c, miR-30d, miR-30e-5p, miR-30e-3p) was found to be significantly ($p < .00001$) downregulated in medulloblastomas belonging to all the four subgroups as compared to normal cerebellar tissues (Fig. 4.21) . Cerebellum, the site of medulloblastoma, develops in the first year

after birth. MiR-30a levels in developing cerebellum from less than 1 year old infants were found to be lower (RQ = 5-10) as compared to that (RQ =10-50) in adult cerebellar tissues. MiR-30a-3p level was found to be 10 -50 fold (RQ 0.3-1.7), MiR-30a-5p 5-10 fold (RQ 4.8-20), miR-30b level 5-15 fold (RQ 5-40), miR-30c level 5-10 fold (RQ 13-80), miR-30d level 2-10 fold (RQ 3-25), miR-30e-3p level 4-10 fold and miR-30e-5p level (RQ 0.5-5) fold downregulated compared to normal developed cerebellum. Thus expression of miR-30a family microRNAs was found to be downregulated all four medulloblastoma subgroups (Fig. 4.21).

4.3.2 Evaluation of miR-30a expression in mouse medulloblastoma tumor tissues from the *Smo*^{+/+} transgenic mice and the *Ptch1*^{+/-} knock-out mice and normal cerebellum by SYBR green real time RT-PCR

The expression of murine homologue of human miR-30a was evaluated using SYBR green real time RT-PCR chemistry, in the normal developing cerebellum of *C57BL6* mice at post natal day 5, 14 and 21 and in medulloblastomas from the *Smo*^{+/+} transgenic mice and *Ptch*^{+/-} knock-out mice [50, 126]. These mouse models serve as models for SHH subgroup medulloblastomas. MiR-30a expression was found to be downregulated by ~10 fold (RQ = 0.013-0.055) in the *Smo*^{+/+} transgenic mice and by ~20 (RQ = 0.006-0.082) fold in the *Ptch*^{+/-} knock-out mice compared to their normal cerebellar counterparts (RQ = 0.4-2.9) (Fig. 4.22). Thus, miR-30a expression was found to be downregulated in medulloblastoma cell lines as well as in the tumors from SHH signaling driven medulloblastoma mouse models.

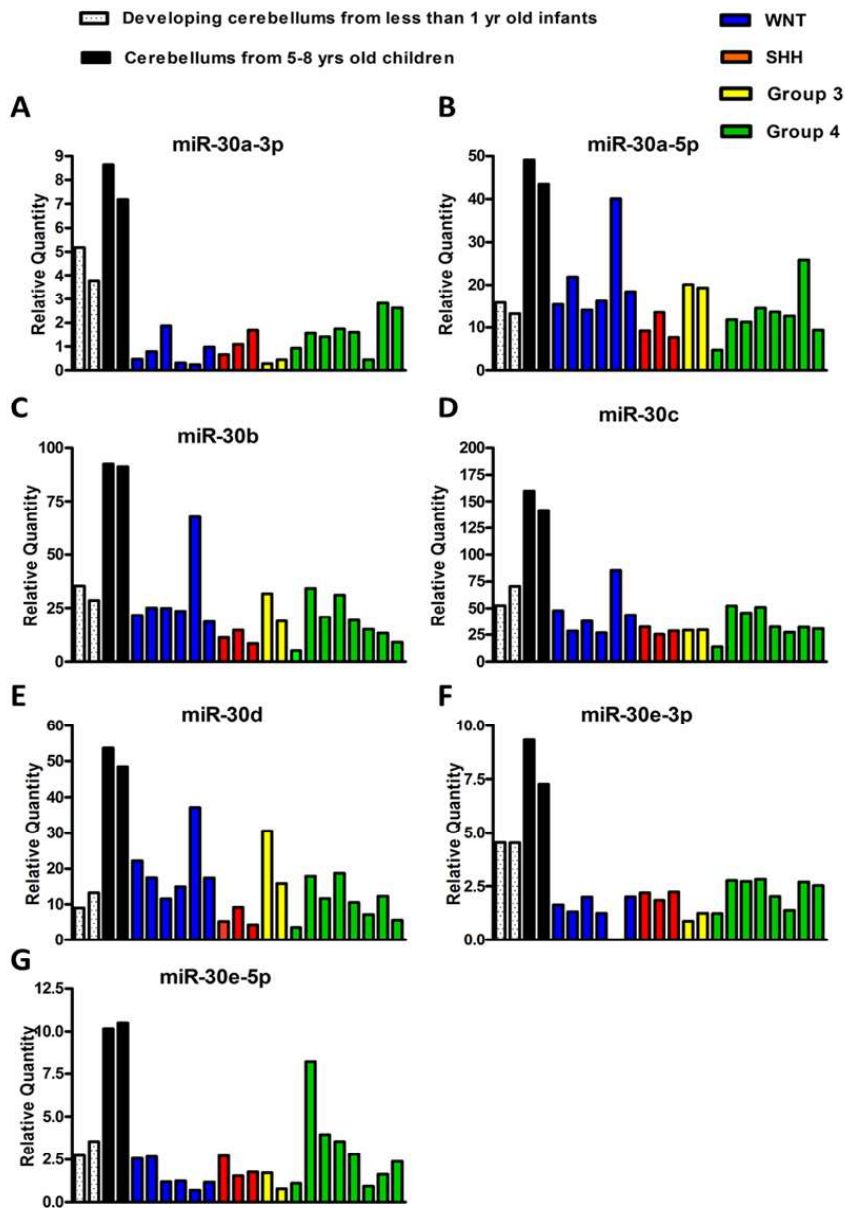


Figure 4.21: Expression levels of 7 miR-30 family miRNA in human normal cerebellar tissues and human medulloblastoma tumor tissues analysed by Taqman Low Density array. Y axis denotes Relative Quantity of the indicated microRNA as compared to that of housekeeping small RNA RNU48.

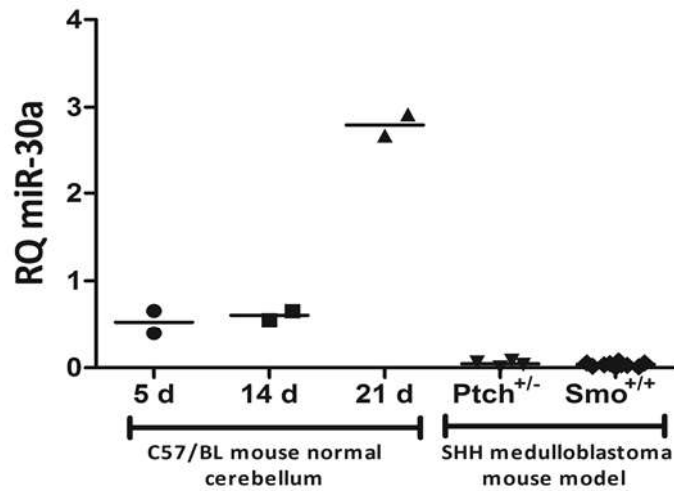


Figure 4.22: Expression level of miR-30a in the normal cerebellum and in medulloblastoma tissues from *Smo*^{+/+} and *Ptch1*^{+/-} medulloblastoma mouse models. Y axis denotes Relative Quantity of the indicated microRNA as compared to that of housekeeping small RNA *Sno202*.

4.3.3 Construction of an inducible lentiviral vector for the expression of miR-30a

The genomic region encoding miR-30a along with about 250 nucleotides long 5' and 3' flanking region ([Chr6: 71403372 - 71403916](#)) was cloned in the pTRIPZ lentiviral vector (Open biosystems, Lafayette, USA) between the HpaI and EcoRI restriction enzyme sites. The miRNA is expressed under the control of a doxycycline inducible promoter. The pTRIPZ vector consists of the tetracycline response element (TRE) and the reverse tetracycline transactivator 3 (rtTA3) which enable inducible expression of the miRNA. The TRE consists of a string of Tet operators fused to the minimal CMV promoter. The pTRIPZ transactivator, known as the reverse tetracycline transactivator 3 (rtTA3), binds to and activates expression from TRE promoters in the presence of doxycycline. The TRE also drives the expression of a TurboRFP reporter in addition to the miRNA. This enables monitoring of expression from the TRE promoter. This

vector construct was used for the stable, inducible expression of miR-30 in medulloblastoma cell lines (Fig.4.23).

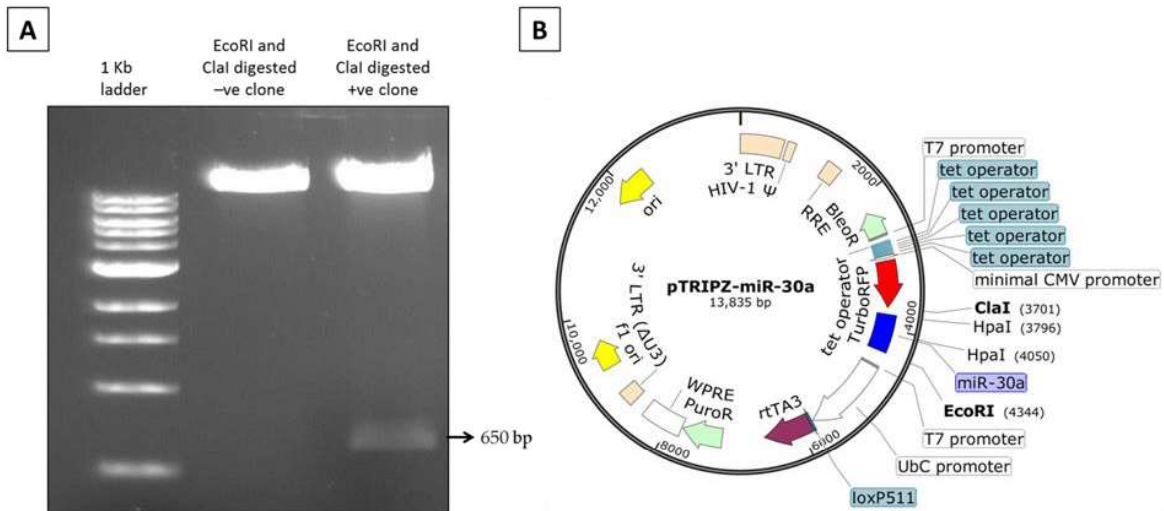


Figure 4.23: pTRIPZ-miR-30a vector construct (A) Ptripz-miR-30a vector construct map indicating cloning sites HpaI and EcoRI and location of other features of the vector backbone. (B) Agarose gel electrophoresis image of confirmation of the pTRIPZ-miR-30a construct.

4.3.4 Effect of miR-30a Expression on growth characteristics of established medulloblastoma cell lines

4.3.4.1 Generation of stable polyclonal populations expressing miR-30a on doxycycline induction

Expression of miR-30a was evaluated in three medulloblastoma cell lines Daoy, D283 and D425 and compared with its expression in developing and developed normal human cerebellum tissues using Taqman real time RT-PCR. Mir-30a expression was found to be approximately 5-100 fold downregulated in Daoy (RQ 1.4-1.8), D283 (RQ 0.17-0.37) and D425 (RQ 0.056-0.065), the three established medulloblastoma cell lines studied when compared with the developed normal human cerebellum (RQ 4.5-8.5) (Fig. 4.24 A). Daoy and D425 / D283 medulloblastoma cell

lines belong to SHH, and Group 3 molecular subgroup respectively based on their cytogenetic profiles. Daoy, D425 and D283 medulloblastoma cell lines were transduced with lentiviral particles of pTRIPZ-miR-30a construct that expressed miR-30a in a doxycycline inducible manner. Stable polyclonal populations of each of the three cell lines expressing miR-30a were selected in the presence of puromycin following transduction. MiR-30a expression in these stable populations was found to be in the range of RQ 9-38 (Fig. 4.24 B). The cells transduced with the viral particles of the empty pTRIPZ vector of the respective cell lines were used as vector controls. These cells along with their respective vector control population were used to study the effect of miR-30a expression on proliferation, clonogenic growth potential and anchorage independent growth potential of medulloblastoma cells.

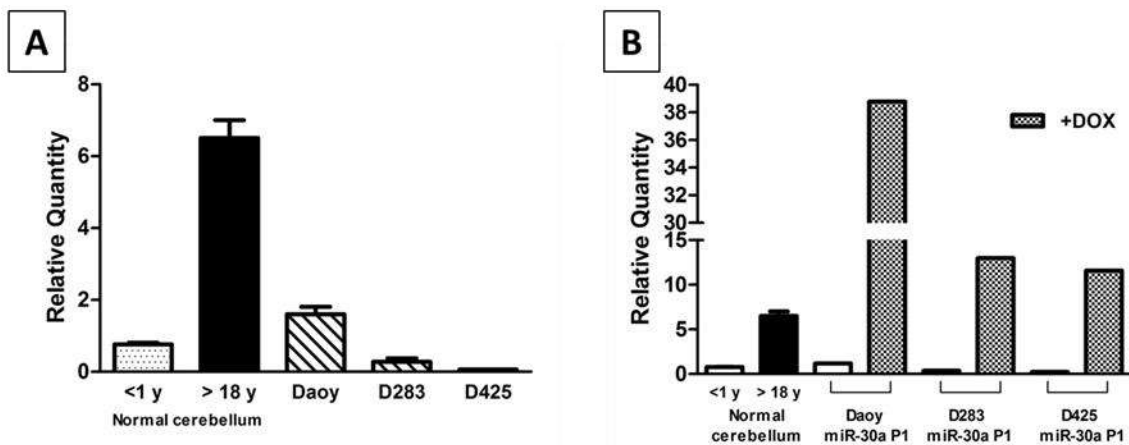


Figure 4.24: MiR-30a expression in the normal brain, medulloblastoma cell lines, and in the stable polyclonal populations expressing miR-30a. (A) MiR-30a expression in normal developing cerebellum (less than 1yr old infants), adult cerebellum, and in established medulloblastoma cell lines. (B) MiR-30a expression in normal developing cerebellum (less than 1yr old infants), adult cerebellum and in stable polyclonal populations of medulloblastoma cell lines expressing miR-30a established medulloblastoma cell lines. Y axis denotes Relative Quantity of the indicated microRNA as compared to that of housekeeping small RNA RNU48.

4.3.4.2 Effect of miR-30a expression on the proliferation of the medulloblastoma cell lines

The effect of miR-30a expression on the proliferation of medulloblastoma cell lines was studied using MTT reduction assay over a period of 10 days. Vector control populations of Daoy, D283 and D425 cells showed no significant difference in proliferation upon Doxycycline treatment compared to their untreated populations. MiR-30a expression upon doxycycline induction inhibited ($p < .0001$) growth of Daoy, D283 and D425 cells by 54.39 % (± 3.6), 60.73% (± 4.11) and 79.35% (± 2.01) respectively (Fig. 4.25). Thus miR-30a expression was found to inhibit the proliferation of all the three medulloblastoma cell lines studied.

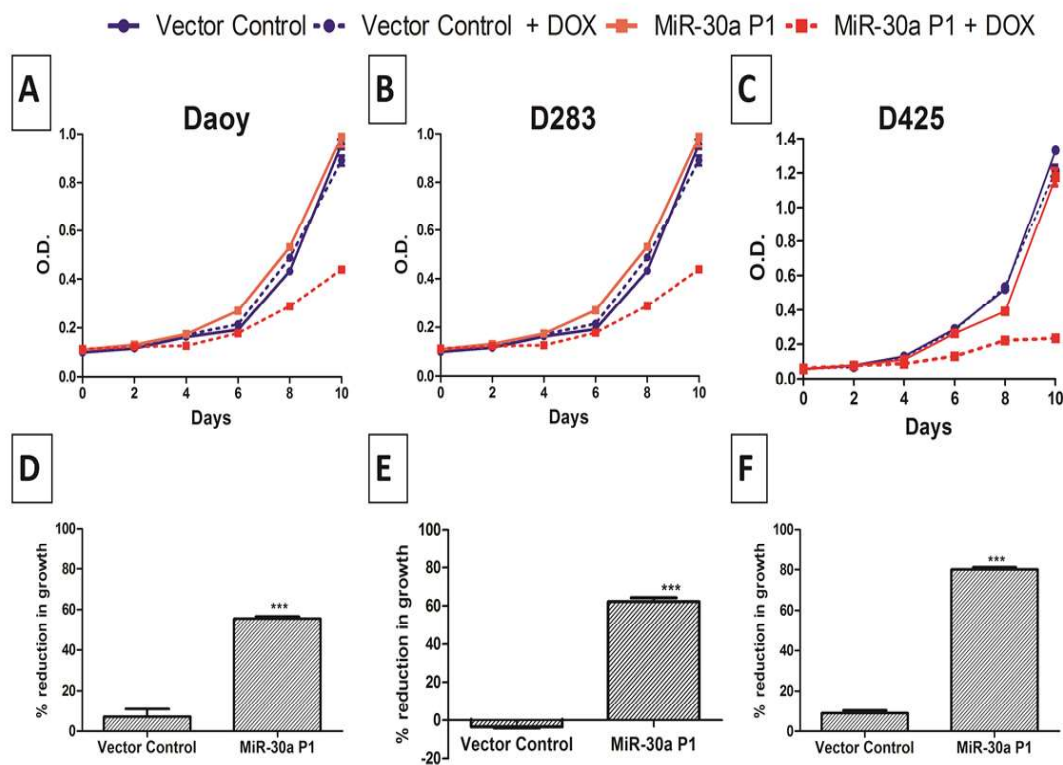


Figure 4.25: Effect of miR-30a expression on the growth of medulloblastoma cell lines.

(A, B and C) Representative experiments showing growth curves of the indicated medulloblastoma cell line polyclonal populations transduced with pTRIPZ vector control or pTRIPZ-miR-30a construct 'P1' with (+ DOX) or without doxycycline treatment as studied by the MTT reduction assay; (D, E and F) Y

axis denotes the percentage reduction in the growth upon doxycycline treatment of the indicated polyclonal populations compared to the un-treated population as studied by the MTT assay. ‘****’ indicates $p \leq 0.0001$

4.3.4.3 Effect of miR-30a expression on the clonogenic potential of Daoy medulloblastoma cells

The effect of miR-30a expression on the clonogenic potential of Daoy cells was studied by using clonogenic assay. Vector control and Daoy miR-30a P1 cells were treated with doxycycline for 72 h and then 1000 cells of untreated and doxycycline treated vector control and Daoy miR-30a P1 population were seeded in 60 mm plates and allowed to form microscopically visible colonies over a period of 10 days with replenishment of fresh medium every three days. After 10 days colonies were stained with crystal violet and counted. Daoy cells formed 300-350 well separated, microscopically visible colonies 10 days post seeding. There was no significant difference in number of colonies formed by doxycycline induced vector control cells compared to their uninduced counterparts, whereas miR-30a expressing Daoy cells showed 56.77% (± 1.65) ($p \leq 0.0001$) reduction in number of colonies compared to their uninduced counterparts (Fig. 4.26).

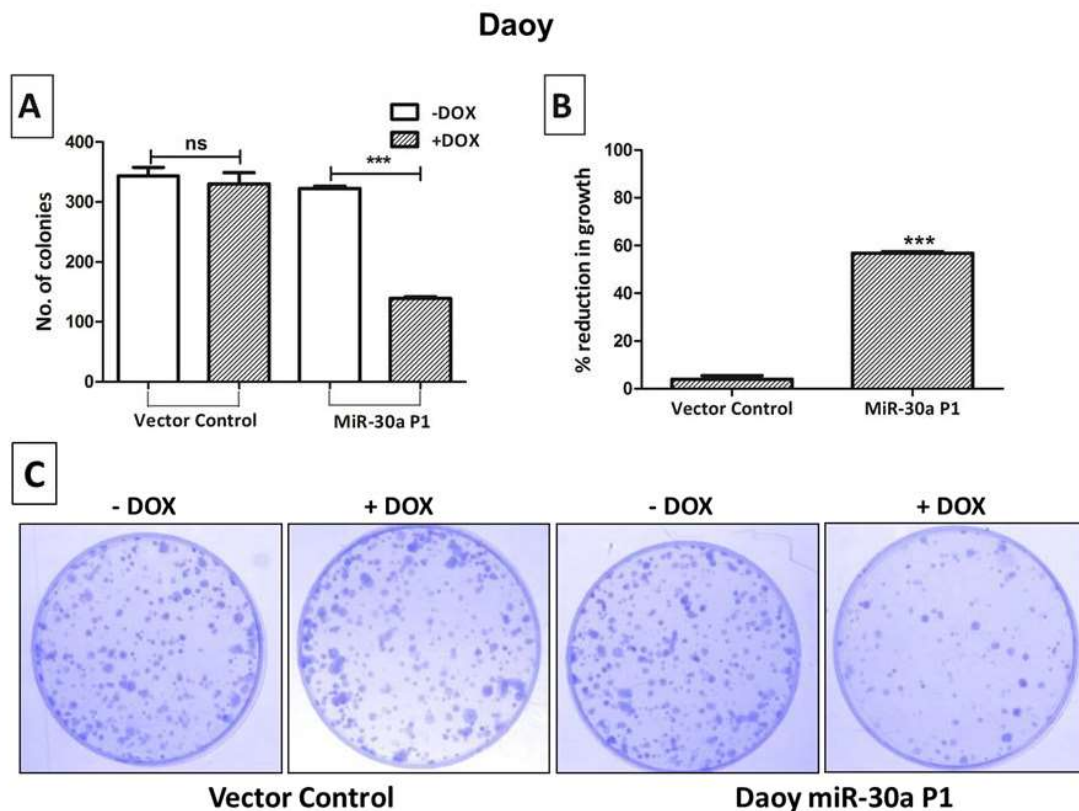


Figure 4.26: Effect of miR-30a expression on the clonogenic potential of Daoy medulloblastoma cell lines. (A) Representative experiments showing the number of colonies formed by Daoy medulloblastoma cell line polyclonal populations transduced with control pTRIPZ vector control or pTRIPZ-miR-30a construct ‘P1’ with (+ DOX) or without doxycycline treatment as studied by the clonogenic assay; (B) Y axis denotes the percentage reduction in colony formation upon doxycycline treatment of Daoy polyclonal populations compared to the un-treated population as studied by clonogenic assay. ‘****’ indicates $p \leq 0.0001$; (C) Representative images of above mentioned experiments.

4.3.4.4 Effect of miR-30a expression on the anchorage independent growth of medulloblastoma cells

The effect of miR-30a expression on the anchorage independent growth of Daoy, D283 and D425 was studied by using soft agar colony formation assay. For soft agar assay, 7500 cells of 72 h doxycycline treated and untreated Daoy vector control and Daoy miR-30a P1 populations

were seeded in a 35 mm culture dish and allowed to form microscopically visible colonies over the period of 2 weeks with fresh medium replenishment every third day. For D283 and D425 the numbers of cells plated were 1000 per 35 mm culture dish. The vector control Daoy, D283 and D425 cells formed ~600, ~300 and ~650 well separated colonies in 2 weeks post seeding respectively. There was no significant difference in the number of soft agar colonies formed by doxycycline induced vector control cells compared to their uninduced counterparts, whereas miR-30a expression in Daoy, D283 and D425 cells inhibited ($p \leq 0.0001$) soft agar colony formation by 54.14% (± 3.25), 51.04% (± 4.98) and 54.74% (± 0.87) respectively compared to their uninduced counterparts (Fig.4.27). Both D283 and D425 cell lines grow mostly as suspension and at best in semi-adherent manner. Therefore, inhibition of soft agar colony formation upon miR-30a expression indicates effect upon clonogenic potential rather than that upon anchorage-independent growth.

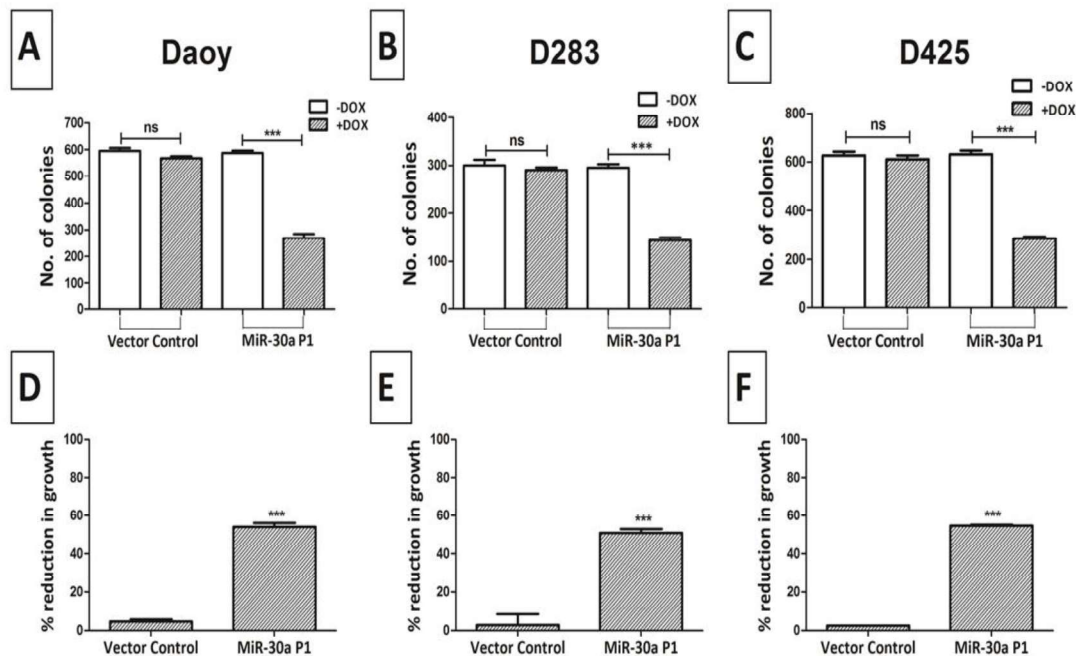


Figure 4.27: Effect of miR-30a expression on the anchorage independent growth of medulloblastoma cell lines. (A, B and C) Representative experiments showing the number of colonies formed by the indicated medulloblastoma cell line polyclonal populations transduced with pTRIPZ vector control or pTRIPZ-miR-30a construct 'P1' with (+ DOX) or without doxycycline treatment as studied by the soft agar assay; (B) Y axis denotes the percentage reduction in colony formation upon doxycycline treatment of the indicated polyclonal populations compared to the un-treated population as studied by soft agar assay. '***' indicates $p \leq 0.0001$

4.3.5 Effect of miR-30a expression on *in-vivo* tumorigenicity of D283 cell lines

D283 cell line as well as its polyclonal population stably transduced with pTRIPZ-miR-30a construct was engineered to express firefly luciferase. The D283 control vector cells and pTRIPZ- miR-30a population of D283 cells were induced with doxycycline for 72 h and then 2×10^5 cells were injected into the cerebellum of BALB/c Nude mice through 0.5 mm burr hole in the midline, 2 mm posterior to lambda at 2 mm depth, using small animal stereotaxic frame (Harvard Apparatus, MA, USA). The growth of the tumors was monitored using bioluminescence imaging. The normalized luminescence represented as average radiance reflects the tumor growth. Bioluminescence imaging showed almost 400 fold increase in average radiance of the tumors formed within 3 weeks in mice injected with the parental D283 cells. On the other hand, average luminescence of the tumors formed in D283 cells expressing miR-30a increased only about 10 fold within the same time period. Thus, upon miR-30a expression tumor growth was found to be reduced by more than 100 fold ($p < 0.0001$) (Fig. 4.28). Therefore, miR-30a expression was found to bring about substantial decrease in tumorigenicity of the D283 medulloblastoma cells.

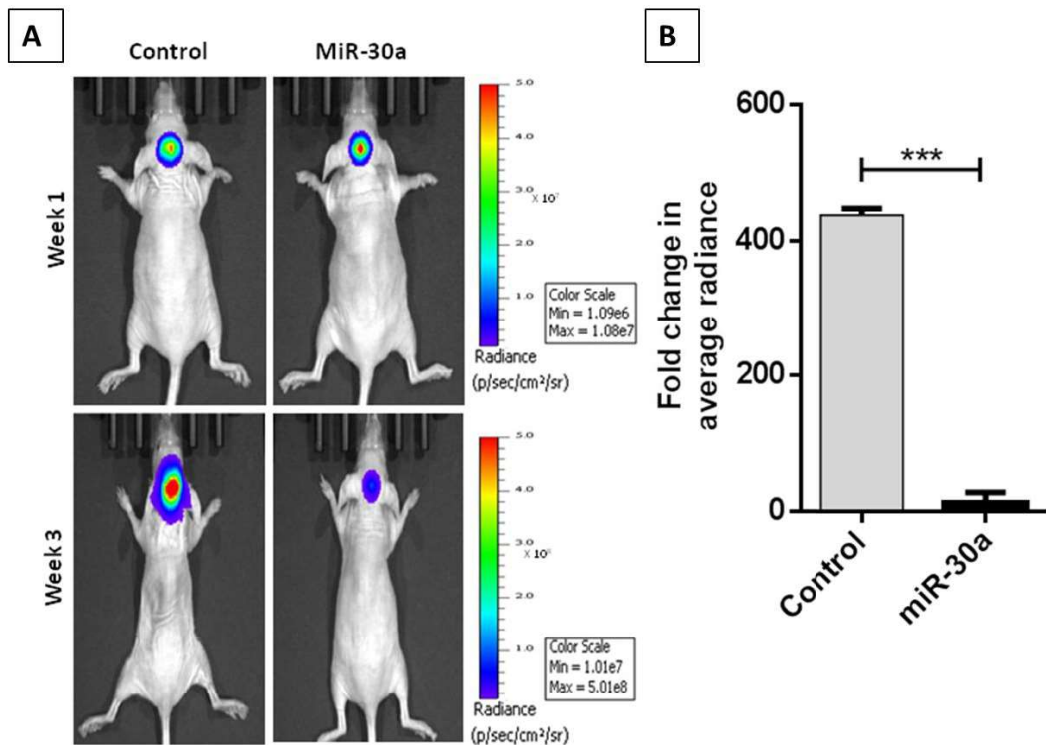


Figure 4.28: Effect of miR-30a expression on tumorigenicity of medulloblastoma cell line.

(A) Bioluminescence images of nude mice orthotopically injected with D283 stable polyclonal populations expressing firefly luciferase and either control pTRIPZ vector or miR-30a upon doxycycline (DOX) induction. (B) Y axis shows relative fold increase in the average radiance on 3rd week as compared to that on 1st week after injection in the indicated cells. *** indicates $p \leq 0.001$.

4.3.6 Molecular mechanism underlying growth inhibitory effect of miR-30a expression on medulloblastoma cells

MiR-30a has been reported to inhibit autophagy by downregulating expression of Beclin1 and ATG5 [127]. In order to identify molecular mechanism by which miR-30a expression affects growth and clonogenic potential of the medulloblastoma cells, levels of Beclin1 and ATG5 were studied by western blotting in miR-30a expressing medulloblastoma cells. Significant reduction

in Beclin1 as well as in ATG5 expression was observed upon miR-30a expression in D283 medulloblastoma cells (Fig. 4.29A). In order to check if miR-30a expression inhibited autophagy in medulloblastoma cells, change in the levels of LC3B, upon miR-30a expression was investigated by western blotting. Upon autophagy induction, total levels of LC3B decrease and/or LC3BI to LC3BII conversion decreases following LC3BI conjugation of phosphatidylethanolamine. LC3B II levels however, also decrease as a result of their degradation by lysosomal enzymes upon fusion of autophagosomes with lysosomes. Therefore, LC3BI and LC3BII levels were monitored both in the absence and presence of chloroquine, an inhibitor lysosomal pathway of protein degradation. Doxycycline induction of miR-30a expression resulted in downregulation of total LC3B levels (LC3BI and LC3BII) both in the presence and absence of lysosomal inhibitor indicating autophagy inhibition (Fig. 4.29B). Furthermore, even upon starvation induced autophagy induction, total levels of LC3B were found to be lower upon miR-30a expression, indicating inhibition of starvation induced autophagy by miR-30a expression (Fig. 4.29B). Accumulation of autophagic substrate SQSTM1/p62 is also used as a marker for autophagy. All the three medulloblastoma cell lines showed increased expression of SQST/p62 upon miR-30a expression indicating autophagy inhibition (Fig. 4.29C). Thus, miR-30a expression was found to inhibit autophagy in all the three medulloblastoma cell lines studied.

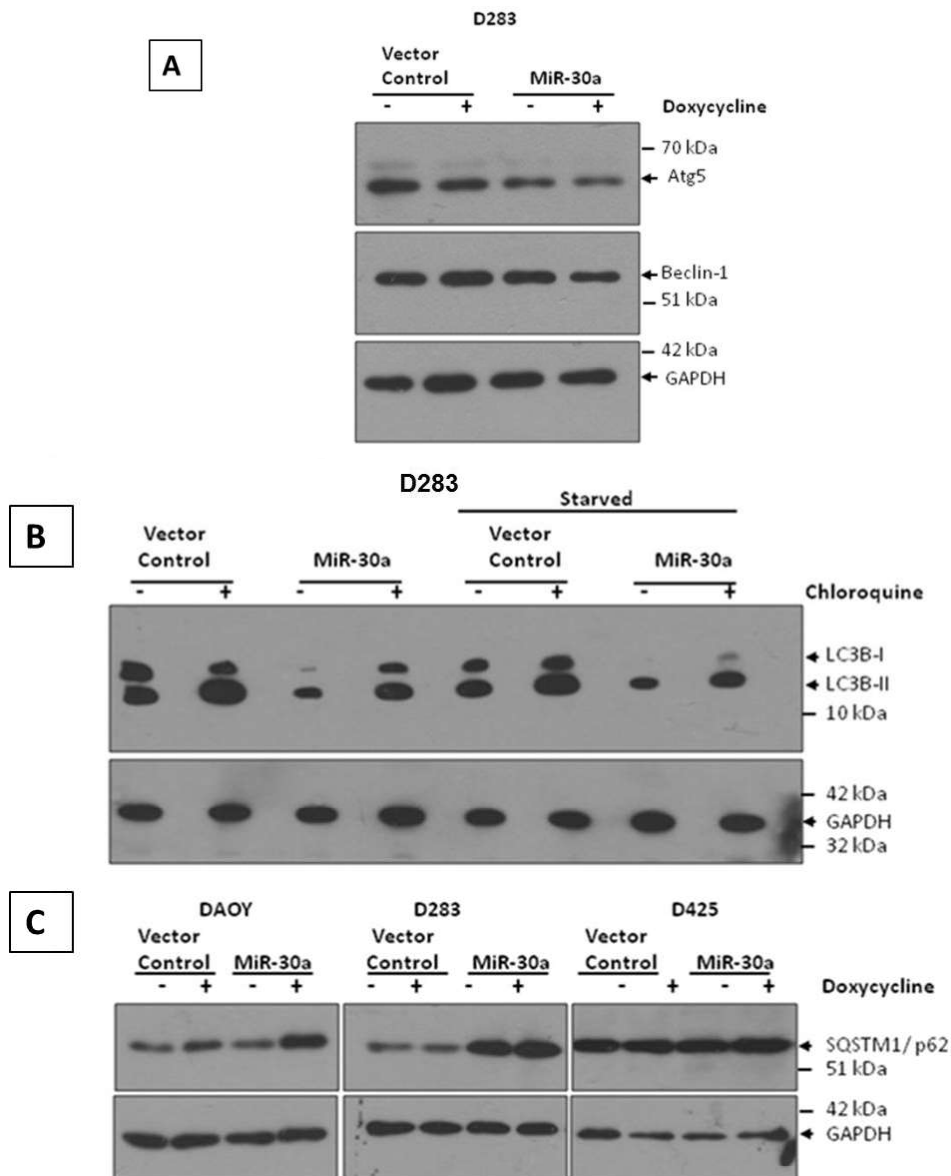


Figure 4.29: effect of miR-30a expression on autophagy in medulloblastoma cell lines.

(A) Beclin1, ATG5 and (B) LC3B levels were analysed by western blotting in D283 cells stably transduced with vector control or miR-30a constructs before and after doxycycline induction. LC3B levels were also analyzed with or without treatment with chloroquine as well as from the cells starved by incubation for 1 h in PBS. (C) Levels of SQSTM1/p62 analyzed in the indicated medulloblastoma cell line transduced with empty pTRIPZ vector or pTRIPZ-miR-30a construct before or after doxycycline induction. Housekeeping gene GAPDH was used as a loading control.

Chapter 4

RESULTS

Results

Expression profiling segregates medulloblastomas into four distinct molecular subgroups viz. WNT, SHH, Group 3 and Group 4. WNT and SHH subgroup tumors are characterized by overexpression of WNT and SHH signalling pathway genes respectively [4]. An expression profiling study of protein-coding genes and microRNAs on a small cohort of medulloblastomas has been reported from our lab [13]. Based on the differential gene expression and microRNA expression in the four subgroups a real time RT-PCR assay was developed to molecularly classify medulloblastomas into the four subgroups [48]. Eleven fresh frozen medulloblastoma tumor tissues belonging to WNT subgroup were available for exome sequencing. Six of these 11 tumors were identified by genome wide expression profiling using Affimetrix gene 1.0 ST array whereas five of 11 were identified using real time RT-PCR analysis assay based on 12 protein coding gene and 9 miRNAs. Further, sequencing of exon 3 of the *CTNNB1* gene encoding beta-catenin showed specific known oncogenic mutation in each of these 11 tumor tissues. Mutation in beta-catenin encoding gene alone has been reported to bring about hyperproliferation but not malignant transformation in developing mouse brain [8]. Therefore, in order to delineate molecular mechanism underlying pathogenesis of the WNT subgroup medulloblastomas, it is necessary to identify complete repertoire of genetic alterations in the tumors that has become feasible due to the advent of Next Gen sequencing. Sequencing of the whole exome (44 Mb) of the 11 WNT subgroup medulloblastoma was therefore carried out to identify genetic alterations characteristic of the WNT subgroup tumors.

4.1 Identification of somatic mutations in WNT subgroup medulloblastoma by exome sequencing of tumour and paired blood DNAs

Before proceeding for DNA extraction, tumour content of atleast 90% was ensured by Hematoxylin and Eosin (H & E) staining of cryosections of the tumour tissues. As described before Sanger sequencing of exon 3 region of the *CTNNB1* gene from the eleven WNT subgroup tissues was done to confirm the mutation in β -catenin, a known characteristic of ~ 90% WNT subgroup medulloblastoma [39]. A single missense point mutation was confirmed in all the eleven WNT subgroup medulloblastoma and peak heights of mutated nucleotide confirmed that the tumour content was more than 90% in each sample (Table 4.1 and Appendix I-*CTNNB1* Mutations). Genomic DNA from the eleven tumours and six paired blood samples was extracted using QIAamp DNA mini kit as per manufacturer's protocol. Genomic DNA quantity was determined using Qubit fluorimeter 2.0 and quality was checked by agarose gel electrophoresis. Exome capture of 11 WNT subgroup tumor tissues and 6 paired blood sample DNA was done using Agilent SureSelect Human all exon 44 Mb kit and exome sequencing was done using Illumina HiSeq 2000 platform with an average coverage of 50X.

4.1.1 Exome sequence data Quality

Quality of the raw sequence data was analyzed using FastQC (<https://www.bioinformatics.babraham.ac.uk/projects/fastqc/>). Mean and median base Phred quality score for almost all bases was above 30. All exomes were sequenced at > 50 X average depth of coverage. Average read length of the data was 88-90 bp. Total coverage of the exome was more than 97 % in each case with more than 70% exome covered at atleast 20 X coverage and more than 82 % exome covered at atleast 10 X coverage. The detailed statistics of the total number of reads obtained, coverage of the targeted exomes is given in Table 4.2

Table 4.1: Point mutations and corresponding amino acid change in exon 3 of *CTNNB1* gene in the 11 WNT subgroup medulloblastomas as determined by Sanger sequencing.

Sample	Point Mutation	Amino Acid Change
MED 1	TCT-->CCT	S37P
MED 2	CCT-->TCT	S33P
MED 3	TCT-->TTT	S33F
MED 4	TCT-->TGT	S33C
MED 5	ATC-->AGC	I35S
MED 7	CCT-->TCT	S33P
MED 8	GAC-->CAC	D32H
MED 9	GAC-->AAC	S33C
MED 10	TCT-->TTT	S37F
MED 11	TCT-->TAT	S33Y
MED 13	TCT--TGT	S33C

4.1.2 Identification of single nucleotide variants in the WNT medulloblastoma tumour tissues

Reads obtained for each tumor and paired blood DNA exomes were aligned to human reference genome hg19 using BWA aligner [115]. Somatic single nucleotide variants (SNVs) and insertions and deletions (InDels) were identified using the VarScan [116] variant detection tool version 2.3.5 (<http://varscan.sourceforge.net>) using the filtering criteria of at least 4 reads in

tumour and paired blood with mapping quality of more than 60 and base quality more than 30. Functional annotation of the somatic variant list was done using the ANNOVAR software (www.openbioinformatics.org/annovar) [117]. From the ANNOVAR-annotated list, variants located in segmental duplications were excluded. The remaining variants were manually verified in IGV (www.broadinstitute.org/igv) [118].

Table 4.2: Exome sequencing data statistics of the 11 WNT subgroup medulloblastoma tumours.

Exome Sample	Total No. of Reads	Average Read Length	% of reads Uniquely mapped to genome	Coverage of Target region 1X	Coverage of Target Region 10X	Coverage of Target Region 20X
MED 1	48894304	88.88	91.90%	97.40%	83.70%	71.50%
MED 2	46136811	88.7	91.12%	98.20%	87.20%	76.50%
MED 3	40255669	88.97	90.52%	98.20%	84.00%	69.40%
MED 4	47954451	88.6	93.03%	98.20%	87.00%	75.80%
MED 5	46856756	88.89	91.26%	98.30%	87.30%	76.80%
MED 7	47211097	86.04	90.92%	97.30%	82.80%	70.10%
MED 8	47524618	88.94	91.92%	98.00%	85.90%	74.20%
MED 9	47954451	88.89	91.56%	97.50%	84.60%	73.10%
MED 10	48557900	88.83	91.88%	97.80%	85.50%	74.20%
MED 11	34381129	88.82	92.65%	96.00%	70.70%	49.10%
MED 13	51822795	88.84	91.29%	97.50%	85.00%	66.80%

In the case of 6 tumor tissues having paired blood sample, the number of novel somatic variants were found to range from 10 to 30. In the case of 5 tumors not having paired blood sample available, the variants were shortlisted based on their absence in the 60000 exome sequence database (ExAC Broad Institute) [119]. 30-50 novel non-synonymous SNPs/Indels were identified in each of the the unpaired medulloblastoma tissues. Total list of 243 single nucleotide variants shortlisted for 5 tumour samples not having paired blood samples is listed in Appendix

II after comparing it with 60000 exome sequence database. A total of 104 novel somatic variants (Non-synonymous - 78, synonymous – 11, splice site – 2, frame shift InDels – 4 and non-frameshift InDels – 9) have been identified in case of 6 tumour tissues having paired blood samples (Table 4.3) and 57 of these non-synonymous somatic variants were further confirmed by Sanger sequencing. Total list of 104 novel somatic variants is shown in Appendix III.

Table 4.3: Total number of variants in the of 11 WNT subgroup medulloblastoma exomes.

Sample	Somatic SNVs			InDels		Total	Validated by Sanger sequencing	Age	Gender	
	Nonsynonymous		Synonymous	splice site	Frameshift					Non frameshift
	Missense	stopgain								
Paired sample										
MED 1	20	2	4	2	3	2	33	19	26	F
MED 2	10	3	1	0	1	1	16	9	15	F
MED 10	16	3	1	0	0	1	21	12	19	F
MED 3	8	0	2	0	0	1	11	6	9	M
MED 4	8	2	2	0	0	1	13	7	10	M
MED 13	5	1	1	0	0	3	10	4	9	M
Unpaired sample										
MED 5	33	0	0	1	3	1	38	2	5	M
MED 7	51	0	0	1	2	3	57	0	45	M
MED 8	43	0	0	3	3	3	52	0	10	F
MED 9	41	1	0	3	3	1	49	2	12	F
MED 11	39	2	0	2	0	4	47	1	26	M

Mutation in exon 3 of *CTNNB1* gene in all eleven samples was confirmed in exome sequencing data. After *CTNNB1* mutation, the second most frequently mutated gene was found to be *DDX3X* gene which encodes a RNA helicase protein. Mutation in *DDX3X* gene was found in 3/11 tumours of which 2 are missense (Q265H and A367T) and one mutation (G242fs deletion) is a frameshift deletion (Fig. 4.1). AT-rich interactive domain-containing protein 1B (*ARID1B*), which is a member of SWI/SNF (SWItch/Sucrose Non-Fermentable) chromatin remodeling

complex was found to be mutated in 2/11 samples of which one is a frameshift insertion (P1027fs insertion) and the other is a nonsense mutation (C878X) (Fig. 4.2).

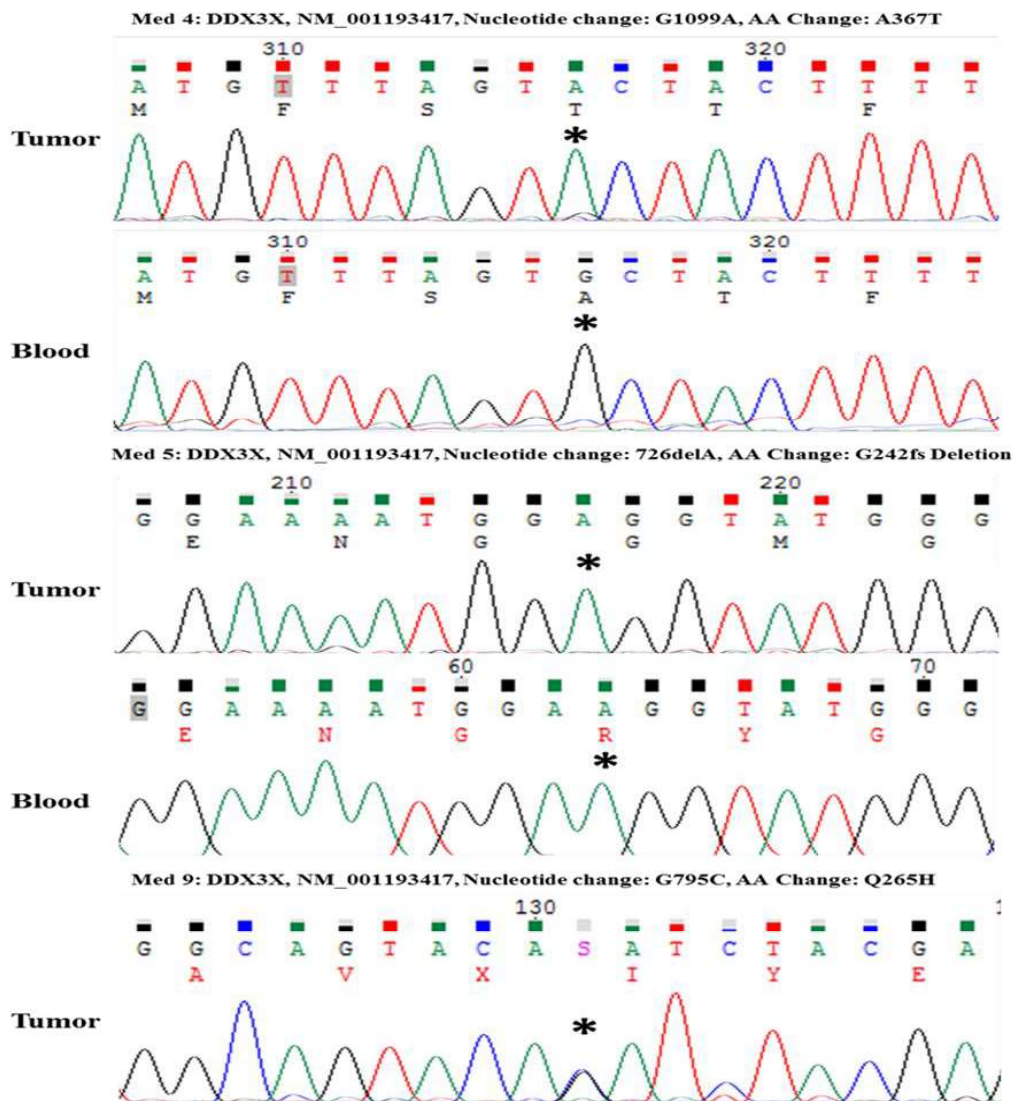


Figure 4.1: Mutations in the *DDX3X* gene identified in the WNT subgroup medulloblastomas

DDX3X gene mutations in three WNT subgroup medulloblastoma validated by Sanger Sequencing. The top panel shows the electropherograms for tumour DNA and bottom panel for its corresponding paired blood DNA, for Med 6 sample paired blood was not available. Altered nucleotide is indicated with ‘*’

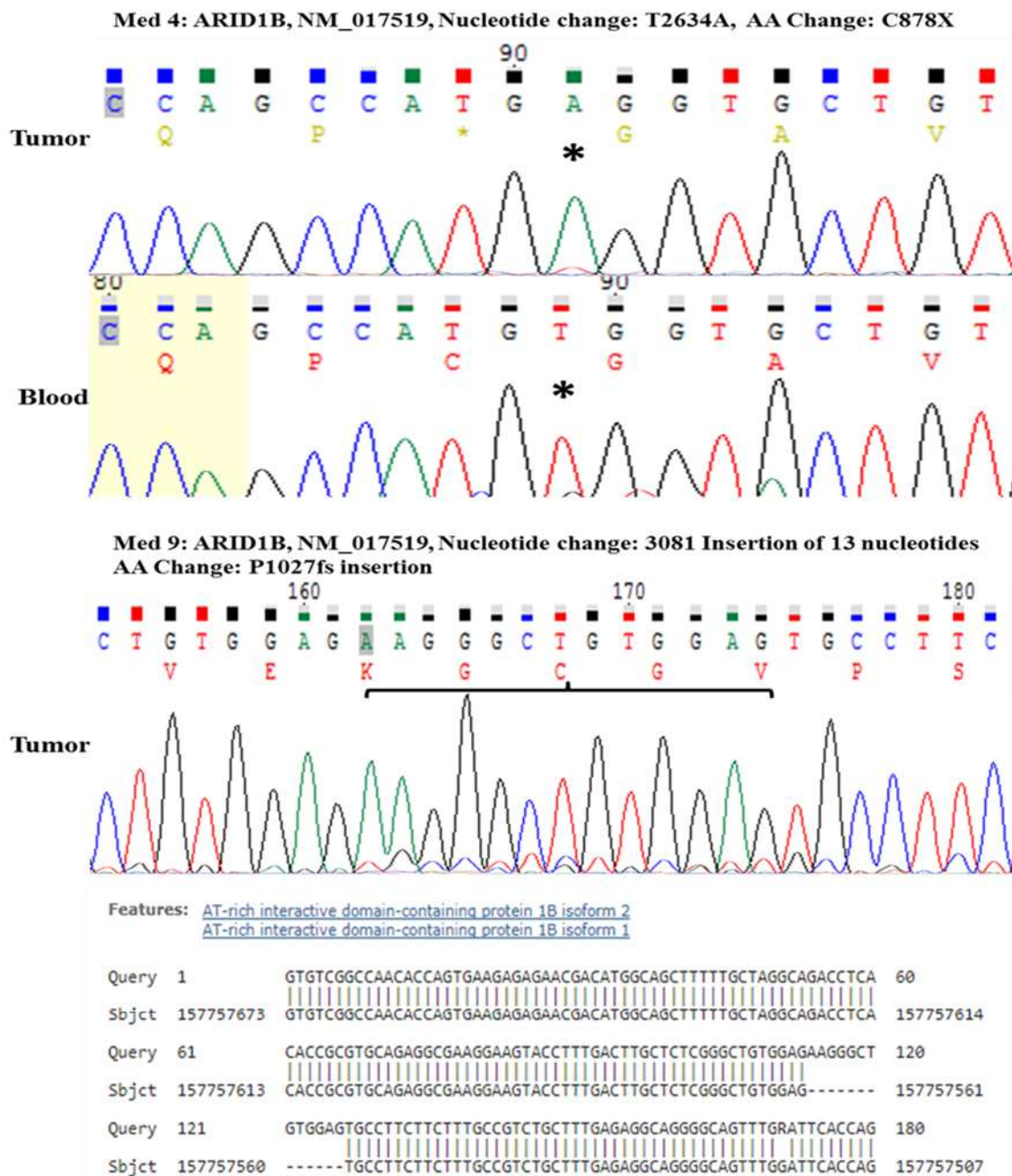


Figure 4.2: Mutations in SWI/SNF complex member ARID1B in the WNT subgroup medulloblastomas. Electropherograms showing altered nucleotide position in the genes ARID1B. Position of the altered nucleotide is indicated with '*'. The 13 nucleotides insertion in Med 9 is shown in a bracket.

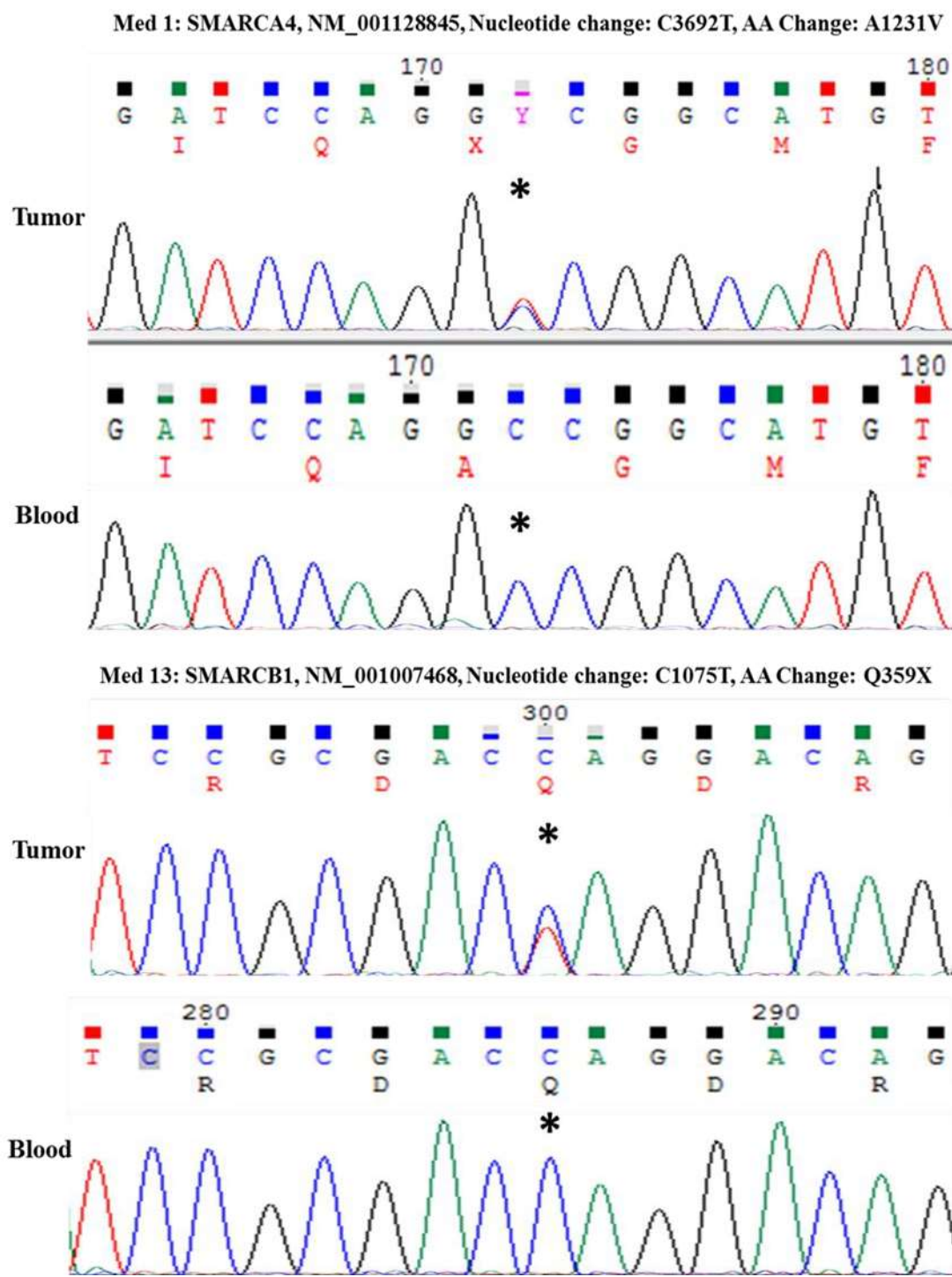


Figure 4.3: Mutations in SWI/SNF complex member SMARCA4 and SMARCB1 in the WNT subgroup medulloblastomas. Electropherograms showing altered nucleotide position in the genes SMARCA4 and SMARCB1. Position of the altered nucleotide is indicated with ‘*’.

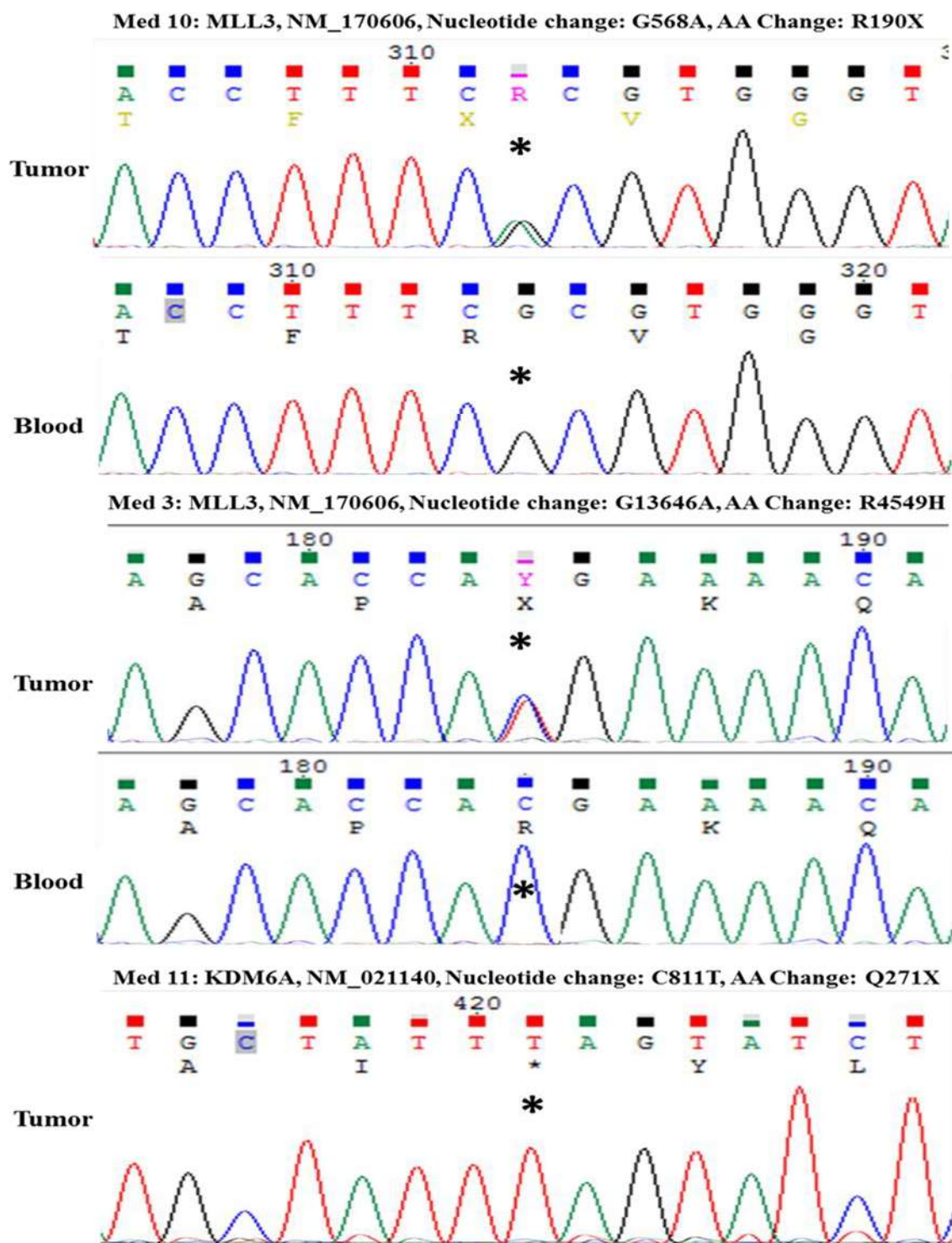


Figure 4.4: Mutations in the genes belonging to the ASCOM complex members MLL3 and KDM6A in the WNT subgroup medulloblastomas validated by Sanger sequencing. Position of the altered nucleotide is indicated by ‘*’

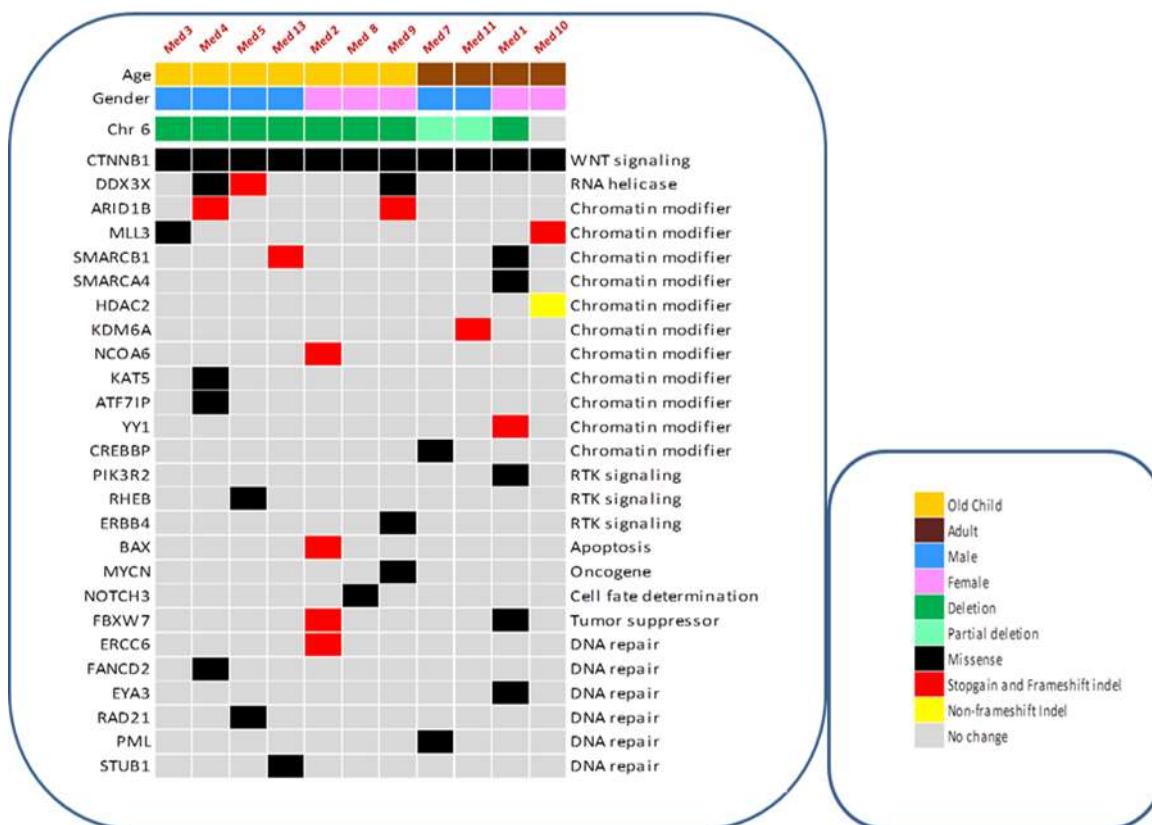


Figure 4.5: Recurrently altered genes and pathways in WNT subgroup medulloblastoma

The figure shows the different chromatin remodeling, cell signaling and DNA repair genes that are mutated in WNT subgroup medulloblastoma. It also shows the status of chromosome 6, gender distribution of WNT subgroup medulloblastoma.

SMARCB1 and *SMARCA4* that encode members of the SWI/SNF complex were also found to be mutated in 2 and one WNT tumor respectively (Fig. 4.3). The two mutations in *SMARCB1* are nonsense (Q359X) and missense (R357H) whereas the mutation in *SMARCA4* is of missense type (A1231V). Activating signal cointegrator-2 (ASC-2 or NCOA6) containing complexes (ASCOM) possesses histone methylation activity and are involved in transcriptional activation. Genes encoding Mixed lineage leukemia 3 (MLL3) and Nuclear receptor coactivator 6 (NCOA6), components of this ASCOM complex were **found** to be mutated in 2/11 and 1/11

tumors respectively. The two mutations in MLL3 are nonsense (R4549H) and missense (R190X) whereas the mutation in NCOA6 is a (E1514X) nonsense mutation. A Nonsense mutation (Q271X) in KDM6A also known as UTX gene, which has demethylase activity and demethylates tri or dimethylated but not mono-methylated H3K27 leading to de-repression of transcription, was identified in one tumor sample (Fig. 4.4). KAT5, a histone acetyl transferase which acetylates histones that also plays important role in chromatin remodeling, was found to be mutated (V348M) in one tumor tissue. Apart from mutations in DDX3X, and in the genes involved in chromatin remodeling and histone modification, mutations were identified in the genes involved in growth factor signaling (*ERBB4*, *PIK3R2* and *RHEB*) and DNA repair (*ERCC6*, *FANCD2*, *EYA3*, *RAD21*, *PML* and *STUB1*) (Fig. 4.5).

4.1.3 Copy number variations in the WNT subgroup Medulloblastoma

The copy number variation analysis for 11 WNT subgroup medulloblastoma was done using CopywriteR software (<https://github.com/PeeperLab/CopywriteR>) that identifies copy number variation using the exome sequence data [120]. CopywriteR uses the off-target reads to analyse the copy number variation data, thus each sample data can be analysed independent of other samples. Of the 11 tumor tissues studied, 8 tumors showed monosomy of chromosome 6 whereas 2 tumours showed partial loss of chromosome 6 and 1 tumour sample did not show loss of chromosome 6 as analysed by CopywriteR programme (Fig 4.6).

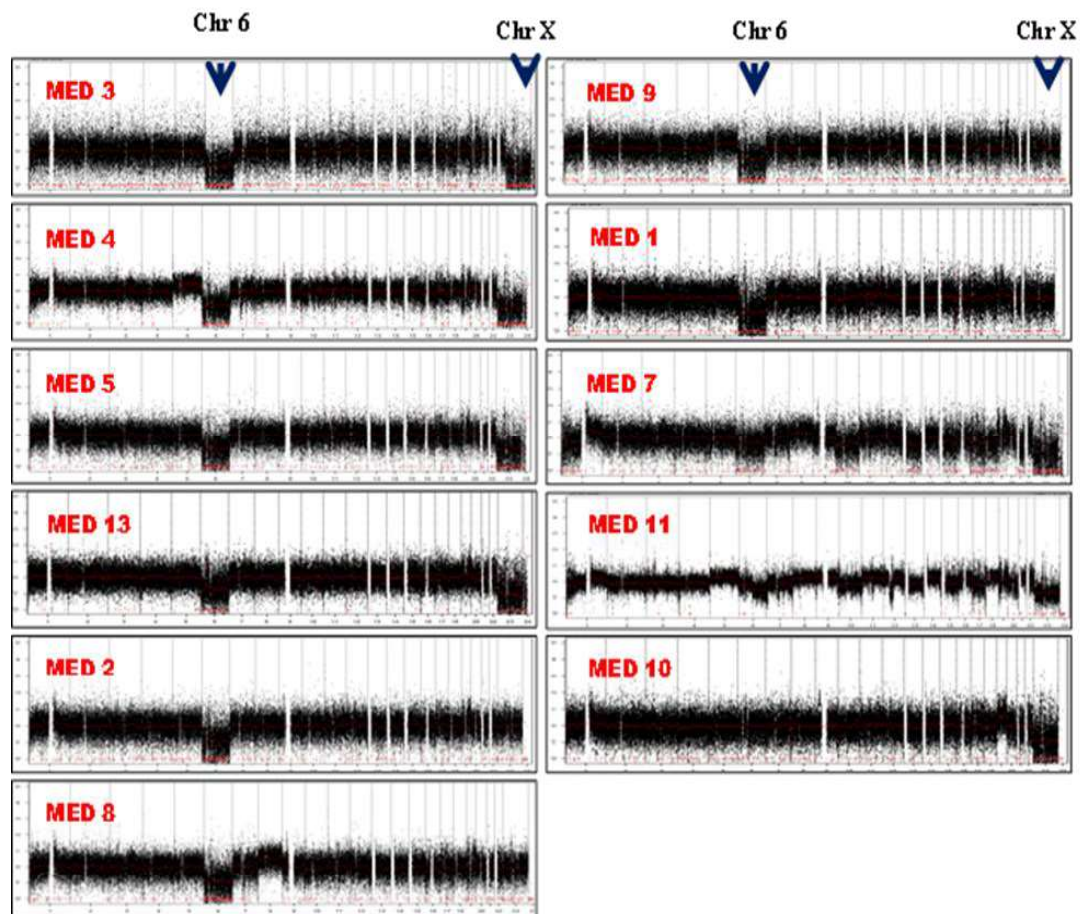


Figure 4.6: Copy number variation in the WNT subgroup medulloblastomas as analyzed by CopywriteR software. The positions of Chromosome 6 and Chromosome X are shown by arrowhead.

In exome sequencing analysis of the WNT subgroup medulloblastoma, *DDX3X* is found to be mutated in 3/11 WNT subgroup tumors. Recurrent truncating mutations in the *DDX3X* gene have been reported in Chronic Lymphocytic Leukemia while homozygous deletions have been reported in the gingivo-buccal oral squamous cell carcinomas from the Indian tobacco chewers and in HPV positive head & Neck carcinomas. Downregulation of *DDX3X* expression has been reported in the HBV positive hepatocellular carcinoma [80, 81, 83]. The presence of truncating

mutations, homozygous deletions and down-regulation of expression of the *DDX3X* gene suggest *DDX3X* to function as a tumor suppressor gene. On the other hand, *DDX3X* has also been shown to act as an oncogene by upregulating Snail transcription factor and repressing E-cadherin expression to bring about epithelial mesenchymal transition of MCF7 breast cancer cells [84]. *DDX3X* protein and mRNA levels positively correlate with tumorigenicity of breast cancer cell lines *i.e.* aggressive breast cancer cell line has higher levels of *DDX3X* protein [67]. Thus *DDX3X* has been reported to function as tumor suppressor or oncogene in different cancers. Next gen sequencing studies recently done in medulloblastoma also identified *DDX3X* as second most frequently mutated gene in medulloblastoma but its role in medulloblastoma pathogenesis is not yet understood hence it was decided to investigate its functional role in medulloblastoma pathogenesis.

4.2 Understanding the functional relevance of the identified genetic alterations in *DDX3X*, a DEAD box family RNA helicase

DDX3X is located on X-chromosome at p11.3-11.23 and encodes a 662 amino acid long protein. It is a member of DEAD-box family of RNA helicases. *DDX3X* has ATPase and ATPase dependent RNA helicase activity. *DDX3X* contains conserved ‘helicase motifs’ that reside on adjacent Rec-A like domains D1 and D2 connected by a linker. The name of DEAD-box is derived from the conserved amino acid sequence D-E-A-D (Asp-Glu-Ala-Asp) located in motif II of its 12 motifs. These 12 motifs play role in: ATP binding, RNA binding and linking ATP and RNA binding. . These motifs are located in D1 and D2 domain [61]. Three mutations were identified in the *DDX3X* gene in the WNT medulloblastoma tumors Two of them (Q265H and A367T) are located adjacent to the motif Ia and II respectively whereas the third mutation (G242fs deletion) leads to the truncation of the protein after motif I leading to the loss of major

part of D1 and entire D2 domain of DDX3X. Motif Ia and II are thought to be involved in interaction of DDX3X with RNA substrate. So the mutations identified in this study might be disrupting or altering RNA binding and/or disrupting helicase activity of DDX3X. Hence it was decided to study the effect of these mutations on DDX3X helicase activity by purifying the recombinant DDX3X protein.

4.2.1 Cloning of DDX3X in a bacterial expression vector pET-28a

DDX3X cDNA (a kind gift from Dr. Laura Madrigal-Estebas, Trinity College, Dublin) was cloned in pET28a vector (Novagen, Merck Millipore, USA) between BamHI and EcoRI site and confirmed by Sanger sequencing (Fig. 4.7). For cloning DDX3X cDNA a forward primer was designed that contained the first 21 nucleotides starting with initiation codon ATG and a TEV protease cleavage site upstream the ATG codon so as to enable release of DDX3X without the Histidine tag. This vector contains T7lac promoter that enables expression of gene of interest in an Isopropyl β -D-1-thiogalactopyranoside (IPTG) inducible manner and adds N-terminal 6X-HIS tag to the protein of interest, which enables its purification using Ni-NTA affinity columns.

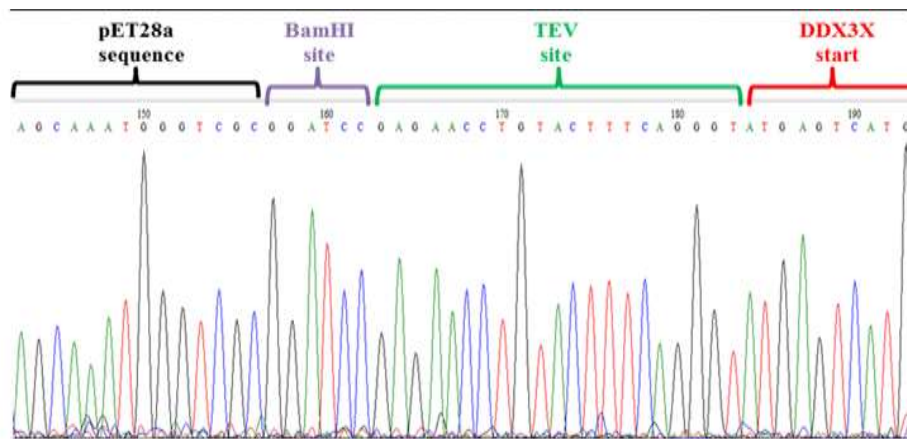


Figure 4.7: Validation of DDX3X cDNA clone in pET-28a vector using Sanger sequencing. Sequences of pET28a vector, cloning site BamHI, TEV protease site and DDX3X start site are seen after sequencing the pET28a-DDX3X construct with T7 promoter primer.

4.2.2 Expression of DDX3X cloned in a bacterial expression vector pET-28a as 6X-His fusion protein in *E. coli* BL21 cells

E. coli BL21 cells were transformed with pET-28a-DDX3X construct and grown till O.D.₆₀₀ reached 0.5 and then induced with different concentrations of IPTG ranging from 0.1 mM to 0.4 mM at two different temperatures of 18°C and 37°C. Abundant DDX3X expression was seen in pET-28a-DDX3X transformed *E. coli* BL21 cells induced at 37°C as well as at lower temperature of 18°C at the concentrations of IPTG ranging from 0.1 mM to 0.4 mM. However, DDX3X was found to be expressed only in the insoluble fraction. Explain soluble vs insoluble fraction (Fig. 4.8 A and B).

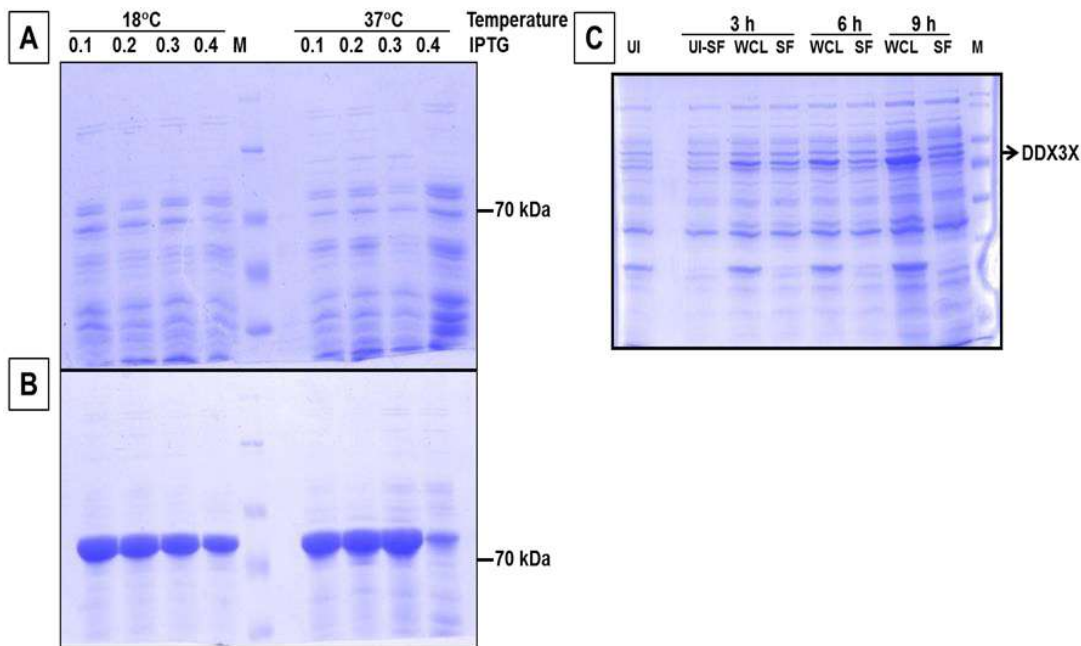


Figure 4.8: Expression of His-tagged DDX3X in *E. coli* BL21 cells.

SDS-PAGE analysis of soluble (A) and insoluble pellet (B) fractions of *E. coli* BL21 cells grown at 37 °C expressing pET28a-DDX3X construct and induced at the indicated concentration ranging from 0.1 to 0.4 mM of IPTG at 18°C or 37 °C. (C) SDS-PAGE analysis of uninduced soluble (UI-SF) and induced

soluble (SF) fractions as well whole cell lysates (WCL) of *E. coli. BL21* cells carrying the pET28a-DDX3X construct. The cells were grown at 18°C and induced at 18°C with 0.3 mM IPTG for the indicated time intervals. M indicates molecular weight markers ranging from 10-180 kDa.

Since the expression levels of DDX3X did not change appreciably even upon incubation at lower temperature or at low IPTG concentration, the *E. coli BL21* cells expressing pET28a-DDX3X construct were grown at 18°C until the O.D.₆₀₀ of the culture reached 0.5 and then IPTG induction was done at 0.3 mM concentration for increasing time intervals (3 h, 6 h and 9 h). Detectable DDX3X expression was obtained upon IPTG induction for 3 h that increased gradually with increasing incubation time of 6 h and 9 h in the whole cell lysates. However, significant DDX3X expression was not obtained at any of these time intervals in soluble fraction (Fig. 4.8 C). Thus, even after controlling DDX3X expression to a minimum detectable level by controlling temperature and time of induction, DDX3X expression was still obtained only in the insoluble fraction.

4.2.3 Solubilisation of recombinant 6X-His tagged DDX3X expressed in *E. coli BL21* cells using different non-ionic, ionic detergents and other additives

Detergents are known to increase the solubility of proteins hence increasing concentrations of different detergents *viz.* Triton X-100, NP-40 and Sarkosyl were used in lysis buffer for increasing solubility of DDX3X. *E. coli BL21* cells expressing pET-28a-DDX3X were grown at 37°C till O.D.₆₀₀ reached 0.5 and then induced with 0.3 mM IPTG concentration at 18°C for 16 h. The bacterial pellets were lysed in lysis buffers containing different detergents and solubilizing agents. The soluble and insoluble fractions were analysed by SDS-PAGE analysis. DDX3X was obtained in soluble fraction only in the presence of 0.3% to 1% Sarkosyl (Fig. 4.9 A and B).

Even 0.1% Sarkosyl was not found to be sufficient to solubilize DDX3X protein. The presence of sarkosyl does not allow efficient binding of the His-tagged protein to the Nickel column. Therefore, other additives like sucrose, glycol, mannitol, mannose, and sorbitol were also added to the extraction buffer to increase solubility of the protein. However, none of these additives could get DDX3X recombinant protein in the soluble fraction (Fig. 4.10).

4.2.4 Expression of DDX3X cloned in a bacterial expression vector pET-28a as 6X-His fusion protein in *E. coli Rosetta-gami 2 (DE3) pLysS* cells

E. coli Rosetta-gami 2(DE3) pLysS strain expresses T7 lysozyme that suppresses basal expression of T7 RNA polymerase thus completely eliminating expression of recombinant protein before induction with IPTG. The strain also promotes disulfide bond formation of eukaryotic proteins so that the proper protein folding takes place. *E. coli Rosetta-gami 2(DE3) pLysS* cells were transformed with pET-28a-DDX3X construct and grown at 37°C till O.D.₆₀₀ reached 0.5 and then induced with 0.3 mM IPTG concentration at 18°C and 24°C for different times intervals (5 h, 16 h and 24 h) followed by lysis of the bacterial pellets in lysis buffer and analysis of whole cell lysate (WCL) and soluble fractions (SF) on SDS-PAGE. In case of induction at 18°C DDX3X expression was observed at 16 h and 24 h in the whole cell lysates but not in the soluble fractions. In the case of induction at 24°C DDX3X expression was obtained at all three time intervals but not in the soluble fraction. So even after tightly controlling DDX3X expression by expressing in the *E. coli Rosetta-gami 2(DE3) pLysS* cells DDX3X expression was not found in the soluble fraction (Fig. 4.11)

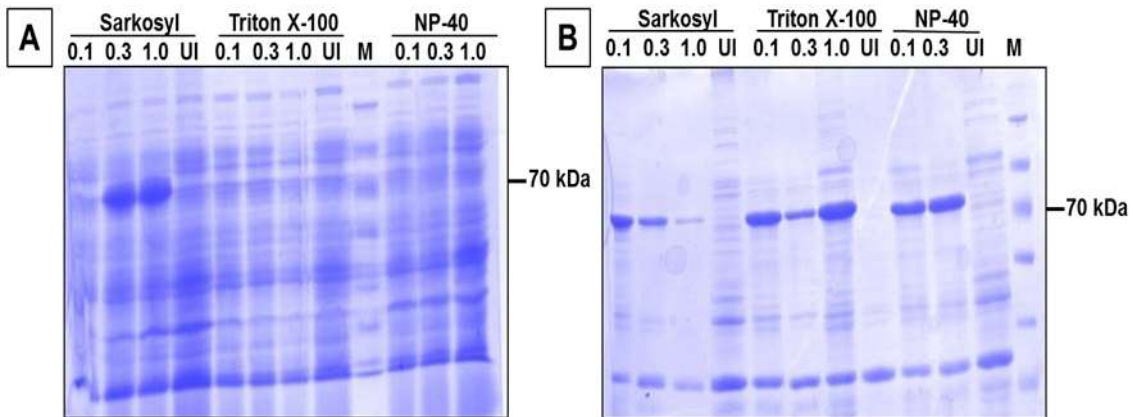


Figure 4.9: Expression of 6X His- tagged DDX3X in *E. coli* BL21 with lysis buffer containing different detergents

Expression of the recombinant DDX3X protein in fraction solubilized (A) with the indicated detergent at 0.1%, 0.3% and 1.0% concentration and the corresponding insoluble fraction (B). UI indicated un-induced lysate in 1% concentration of the indicated detergent. M indicates molecular weight marker.

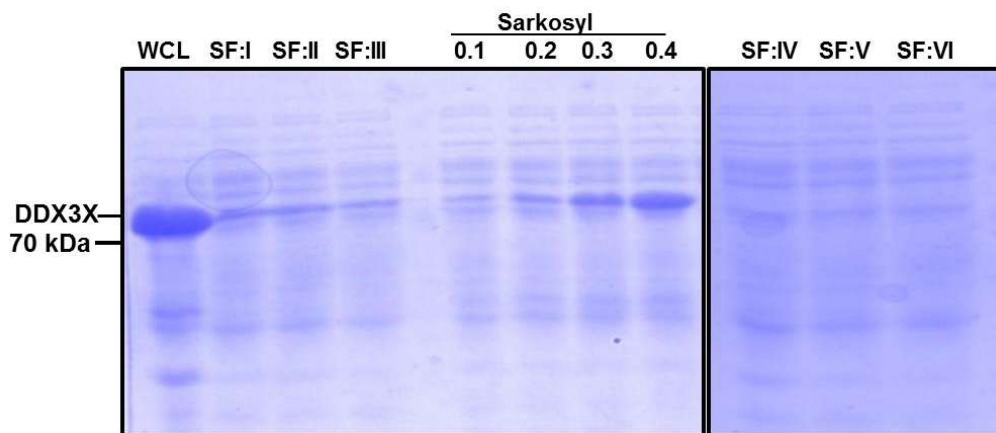


Figure 4.10: Expression of 6X His- tagged DDX3X in *E. coli* BL21 with lysis buffer containing different sugar additives. SDS-PAGE analysis of the expression of recombinant DDX3X protein in

WCL: whole cell lysate; SF: Soluble Fractions in buffers (I, II, III, IV, V, VI) with various additives and those solubilized in the presence of 0.1% to 0.4% Sarkosyl. SF:I 10% Glycerol + 2% Glycol + 100 mM Sucrose; SF:II 10% Glycerol + 2% Glycol + 100 mM Mannose; SF:III 10% Glycerol + 2% Glycol + 100

mM Mannitol; SF:IV 100 mM Sucrose + 100 mM Sorbitol + 100 mM Mannitol; SF:V 100 mM Sucrose + 100 mM Sorbitol + 2% PEG 6000; SF: VI 100 mM Sucrose + 100 mM Sorbitol + 100 mM Mannose

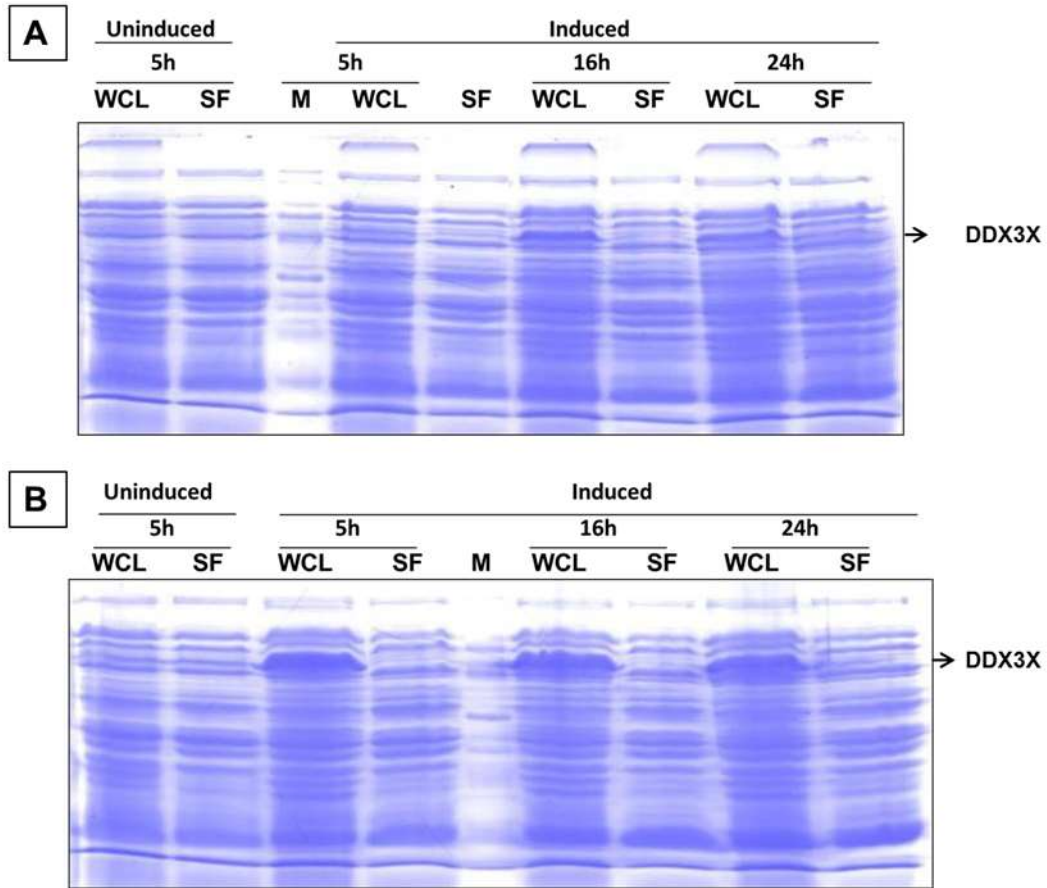


Figure 4.11: Expression of 6X His- tagged DDX3X in *E. coli Rosetta-gami 2(DE3) pLysS* strain.

SDS-PAGE analysis of pET28a-DDX3X expressed in *E. coli Rosetta-gami 2(DE3) pLysS* strain. The cells were induced with 0.3 mM IPTG for 5 h, 16 h and 24 h at 18°C (A) or 24°C and the whole cell lysate (WCL) and soluble fractions (SF) were analysed by SDS-PAGE.

4.2.5 Cloning and expression of DDX3X in a bacterial expression vector pMAL-c5E as MBP fusion protein

The pMAL-c5E vector expresses the gene of interest as a fusion downstream *maltE* gene encoding Maltose binding protein (MBP). The fusion protein can be purified by amylose affinity chromatography and the protein of interest can be cleaved of MBP using specific protease enterokinase. The MBP is known to enhance solubility of eukaryotic proteins it is fused to and the vector used expresses fusion protein in cytoplasm. Since all attempts to obtain expression of recombinant His-tagged DDX3X protein in soluble fraction failed, human DDX3X cDNA was then cloned in pMAL-c5E vector between BamHI and EcoRI site with forward primer having TEV site. *E. coli Rosetta DE3* cells were transformed with pMAL-c5E-DDX3X construct and grown till O.D.₆₀₀ reached 0.5 and then induced with 0.3 mM IPTG at different temperatures of 18⁰C, 24⁰C and 37⁰C. The MBP-DDX3X fusion protein (MW = 120 kDa) was found to be expressed at all the three temperatures 18⁰C, 24⁰C and 37⁰C tested in soluble fraction (Fig. 4.12).

MBP-DDX3X fusion protein was purified by binding of induced soluble fraction to amylose resin for an hour followed by 3 washes with wash buffer and then elution with elution buffer containing 10 mM maltose. All the purification steps like binding, washing and elution were done at 4⁰C. Eluted fractions from the amylose affinity column showed presence of more than 90% pure 120 kDa MBP-DDX3X fusion protein (Fig. 4.13). Purified MBP-DDX3X fusion protein was digested with TEV protease for 3 h at 4⁰C to release it from the fused MBP. However, after digestion with TEV, DDX3X precipitated.

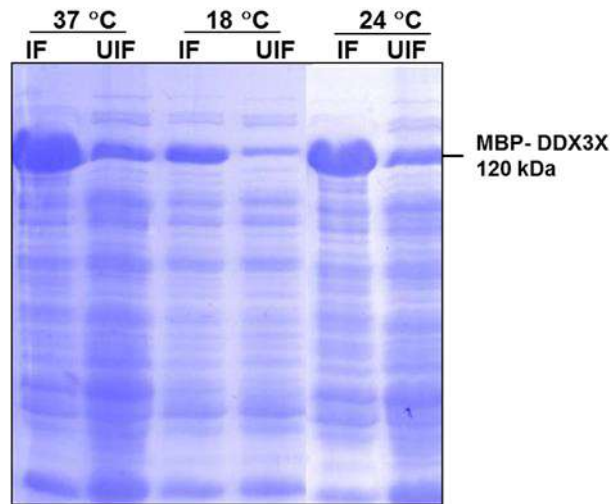


Figure 4.12: Expression of MBP tagged DDX3X in *E. coli Rosetta- DE3* strain.

SDS-PAGE analysis of the recombinant MBP-DDX3X fusion protein expressed in *E. coli. Rosetta DE3* grown at the indicated temperature and induced with 0.3 mM IPTG; UIF indicates uninduced fraction and IF indicates induced fraction.

Hence, MBP fused full length DDX3X protein was used for assessing the RNA helicase activity of DDX3X.

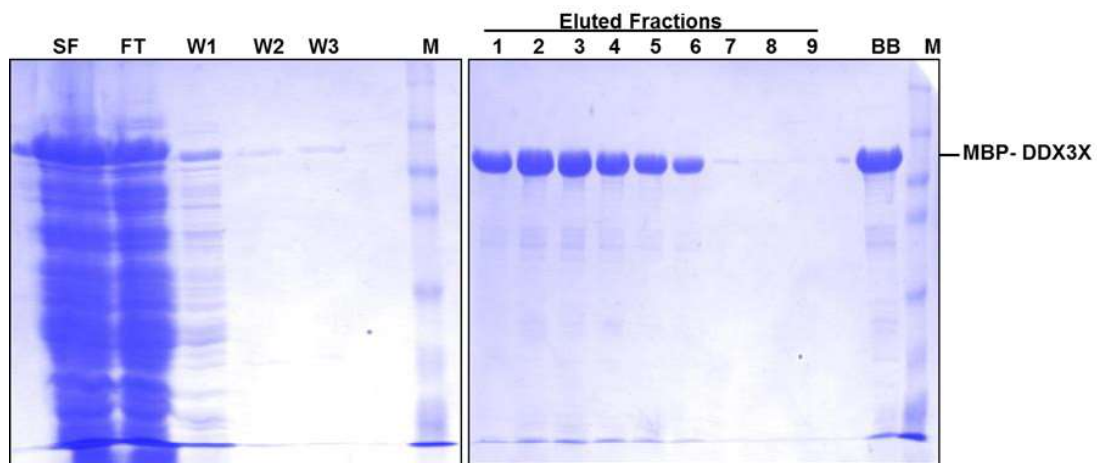


Figure 4.13: Purification of MBP tagged DDX3X in *E.coli Rosetta DE3* cells.

SDS-PAGE analysis of total soluble fraction (SF) of *E. coli. Rosetta DE3* Protein extract expressing recombinant MBP-DDX3X fusion protein and that separated on amylose affinity column. FT: Flow through fraction from the column; W1, W2, W3: 1st, 2nd and 3rd wash given to the column and eluted fractions 1 to 9 and BB: Column beads bound fraction; M: Molecular weight marker lane.

4.2.6 RNA helicase assay with MBP-DDX3X fusion protein

Before using for helicase assay, the maltose bound to the purified MBP-DDX3X protein was removed by using Amicon ultra centrifugal filter (cut off 50 kDA) in the dialysis buffer (20 mM Tris-HCl pH 7.5, 50 mM NaCl, 2 mM DTT and 10% Glycerol) and then used for RNA helicase assay. Amylose resin bound MBP-DDX3X protein was also resuspended in the dialysis buffer and used for helicase assay. Helicase activity of MBP-DDX3X fusion protein was assessed by incubating the protein with 20 nM of an 18 mer RNA oligonucleotide annealed to a complementary 36 mer RNA oligonucleotide resulting in a 18 mer duplex with 18 nucleotide overhang. Different concentrations (0.2 μ M to 0.8 μ M) of the fusion DDX3X protein was incubated with the annealed RNA oligos in a hybridization buffer supplemented with RNase inhibitor at 37⁰C for 40 min. After the incubation reaction was stopped by adding 5 X RNA loading dye containing (100 mM Tris-HCl [pH 7.5], 20 mM EDTA, 0.5% SDS, 0.1% Bromophenol Blue, 50% Glycerol) and then separated on a 8% native acrylamide gel by electrophoresis in the presence of 0.1% SDS to inhibit secondary structure formation. The 18 mer oligonucleotide was labeled using fluorescent dye 6-FAM so that its separation from the 18 mer/36 mer hybrid RNA can be traced using UV transilluminator. Incubation of the hybrid with the bead bound MBP-DDX3X protein but not with eluted MBP-DDX3X protein shows migration of the hybrid at intermediate position between that of hybrid and free 18 mer oligonucleotide indicating partial helicase activity of the fusion DDX3X protein (Fig. 4.14).

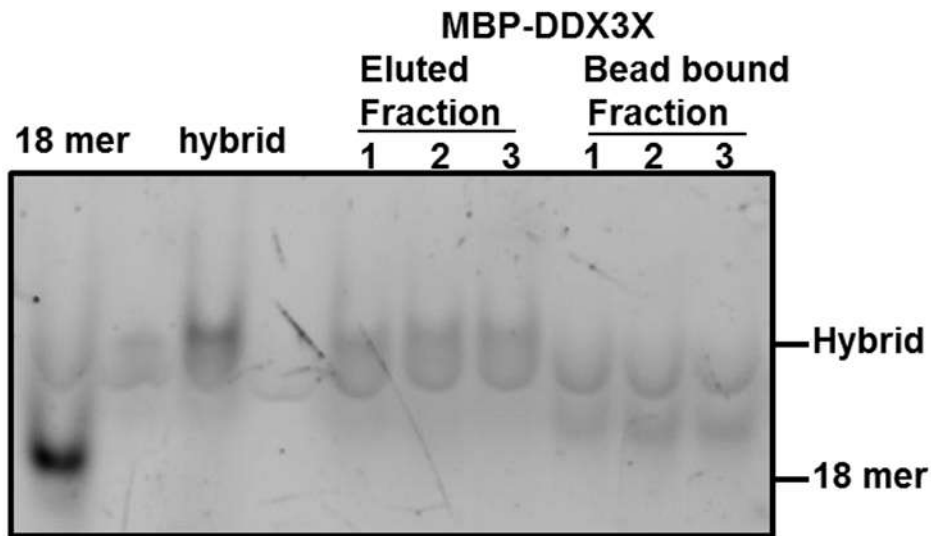


Figure 4.14: Helicase assay for recombinant MBP-DDX3X fusion protein. Helicase assay reaction products separated by native PAGE electrophoresis. The 18 mer / 36mer RNA hybrid Incubated with bead bound MBP-DDX3X fusion protein at increasing concentrations (0.2, 0.4 and 0.8 μ M) from 1 to 3 shows product at position intermediate between that of the hybrid and the 18 mer RNA oligonucleotide.

Since even the MBP fused DDX3X protein showed only partial helicase activity, effect of mutations on DDX3X helicase activity was studied. A recent Study by *LB Epling et al. 2015* has shown that some of the DDX3X mutants identified in pediatric medulloblastoma have defective RNA stimulated ATPase activity [62]. Even in this study, helicase activity of the recombinant DDX3X protein could not be studied due to lack of helicase activity of the recombinant DDX3X protein. In the present study, one WNT tumor was found to have truncating mutation in DDX3X that would not retain helicase activity of the protein. Thus the evidence so far indicates mutations in DDX3X result in loss of helicase activity.

4.2.7 Effect of DDX3X mutations on transcriptional regulatory activity of DDX3X

DDX3X, a RNA helicase has both ATPase and ATP dependent RNA helicase activity. DDX3X has been implicated to play multiple roles in RNA biology including splicing, mRNA export, transcription and translation. DDX3X is a multifunctional protein with its N-terminal domain reported to be required and sufficient for some of its transcriptional regulator activity that is independent of its ATPase and helicase activity. N-terminal domain (1-408 AA) of DDX3X has been reported to be sufficient for the induction of the IFN- β promoter [65] . Upregulation of the CDK inhibitor p21 by DDX3X has been reported to be dependent on the ATPase activity but independent of helicase activity of DDX3X [66]. The substrate specificity and regulation of enzyme activity of the DEAD box proteins is known to be influenced by protein cofactors *in vivo*. Therefore, the effect of DDX3X's role in transcriptional and translational regulation and effect of identified mutations on these activities of DDX3X needs to be investigated.

4.2.7.1 Effect of DDX3X expression on transcriptional activity of beta catenin

Cho *et al.*, (*Nature* 2012) in their study have shown that mutant DDX3X enhances the ability of mutant β -catenin to transactivate a TCF4-luciferase reporter by (TOP-flash) by 1.5-2.0 folds [121]. Therefore to check the effect of identified genetic alterations on ability of DDX3X on transcriptional activity of β -catenin, luciferase reporter assay was performed. For luciferase assay, mutant β -catenin construct, luciferase construct containing 3 TCF4 binding sites and DDX3X construct was prepared by cloning DDX3X in pcDNA3 vector using BamHI and EcoRI restriction sites. Mutants of DDX3X identified in this study (G242fs deletion, Q265H and A367T) and two other mutants (R534H and P568L) reported in medulloblastomas were

generated by Site directed mutagenesis PCR. For performing luciferase reporter assay, a luciferase construct TOP Flash cotransfected with mutant β -catenin, pcDNA3-GFP and wild type DDX3X or mutant DDX3X in 293FT cells, where GFP was used for normalization of transfection efficiency. Increase in TOP-FLASH reporter luciferase activity was obtained upon transfection with mutant β -catenin. But no further increase in the luciferase activity was observed upon cotransfection with the wild type or activating mutants (R534H and P568L) of DDX3X compared to that obtained with mutant β -catenin alone (Fig. 4.15).

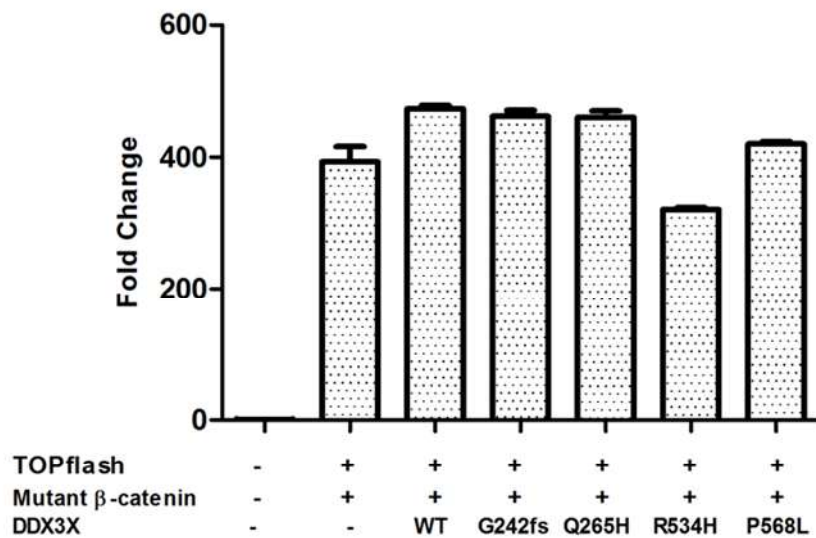


Figure 4.15: Luciferase reporter assay to check the effect of identified DDX3X mutants on trans-activation activity of mutant β -catenin. The luciferase reporter activity was studied upon transfection of the indicated constructs TOP-FLASH, mutant beta-catenin and DDX3X (wt: wild type or indicated mutant). Y-axis represent the fold change of relative luciferase activity obtained on transfection of the indicated constructs as compared to that obtained upon transfection of control vector alone.

4.2.7.2 Effect of DDX3X expression on IFN beta promoter activity

DDX3X has been reported to be a part of innate immune signaling pathways and contribute to the induction of anti-viral mediators such as type-I interferon (IFN- β). DDX3X has been shown to interact with and is phosphorylated by TBK-1 and IKK- ϵ . N-terminal domain (1-408 AA) of DDX3X was found to be sufficient for the induction of the IFN-beta promoter [65]. Different studies have reported that DDX3X enhances 3-4 fold TBK-1 mediated, 4-5 fold IKK- ϵ mediated and 2-4 fold IPS-1 mediated IFN- β promoter activity [122, 123] Therefore, to check the effect of identified genetic alteration in DDX3X on its ability to regulate IFN- β promoter, luciferase reporter assay was performed. Luciferase assay was performed by cotransfecting IFN- β promoter luciferase construct (obtained from addgene), pcDNA3-GFP, DDX3X wild type and TBK-1/IKK- ϵ /IPS-1 (obtained from addgene) in HEK 293FT cells, where GFP was used for normalization. The IFN- β promoter activity was found to increase about \sim 15 fold with TBK1, \sim 15 fold with IKK ϵ and about \sim 20 fold increase with IPS-1. However, DDX3X did not show any further induction of IFN-beta promoter activity (Fig. 4.16 A, B and C). Since HEK 293FT cells express considerable amount of endogenous DDX3X, it was decided to reduce the endogenous DDX3X levels by knockdown DDX3X by using the shRNA targeting DDX3X in inducible pLKO-Tet vector or knock-out DDX3X in HEK293FT cells using CRISPR-CAS9 technology.

In all the subsequent experiments two CRISPR mediated DDX3X knock-out clones *viz.* clone 10 and clone 11 of HEK 293FT cells (prepared by Ms Shalaka Masurkar) and shRNA (targeting 3' UTR and Open Reading Frame (ORF), refer to the Methods section for description) mediated DDX3X knock-down clones in HEK 293FT and Daoy cells were used to study DDX3X's functional role. For this purpose wild type DDX3X and mutant clones were generated in CRISPR and shRNA resistant DDX3X background by site directed mutagenesis. For generating

CRISPR resistant DDX3X construct the PAM site near the Guide RNA was mutated and for generating shRNA resistant DDX3X construct the shRNA binding sites in DDX3X was mutated by site directed mutagenesis.

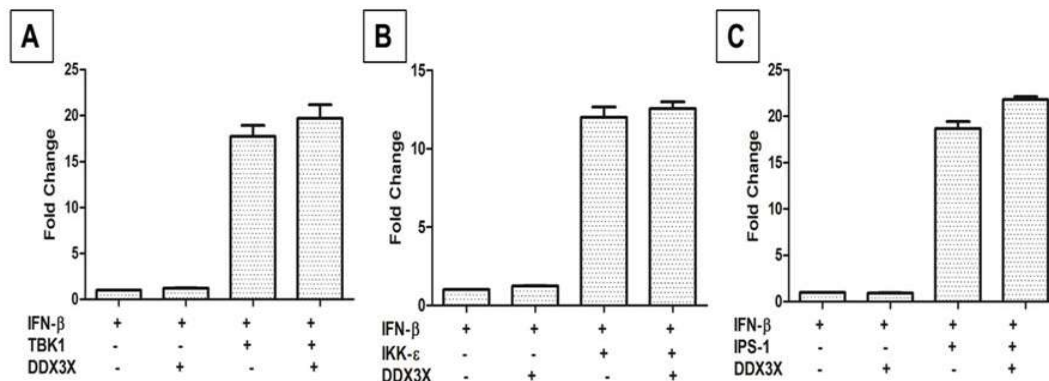


Figure 4.16: Luciferase reporter assay to check the effect of identified DDX3X mutants on IFN- β promoter activity. Y-axis represent the fold change of relative luciferase activity obtained on transfection of the indicated constructs as compared to that obtained upon transfection of control vector alone.

4.2.8 Downregulation of DDX3X expression in Daoy and HEK 293FT cells using shRNA cloned in pLKO-Tet vector

Daoy cell line belongs to SHH group of medulloblastoma and mutations in DDX3X have been reported in approximately 11% of child medulloblastoma and approximately 50% adult SHH medulloblastoma. Hence studying the effect of DDX3X mutations in Daoy cells would provide insight into the role of DDX3X in biology of medulloblastoma. Therefore, two shRNAs (one

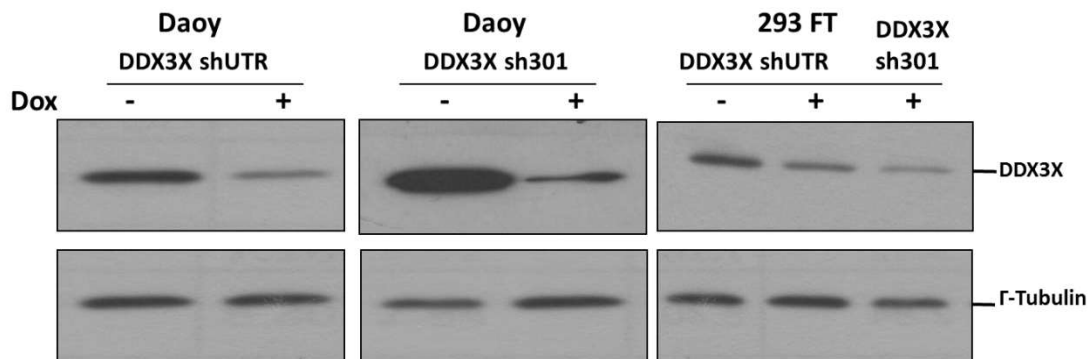


Figure 4.17: Western blot analysis of DDX3X expression in Daoy and 293 FT cells transduced with shRNAs against DDX3X and induced with doxycycline. Daoy and HEK 293 FT cells were transduced with two shRNAs targeting DDX3X in 5'UTR and ORF region. Stable polyclonal populations were selected for each shRNA and induced with doxycycline. Dox indicates doxycycline induction.

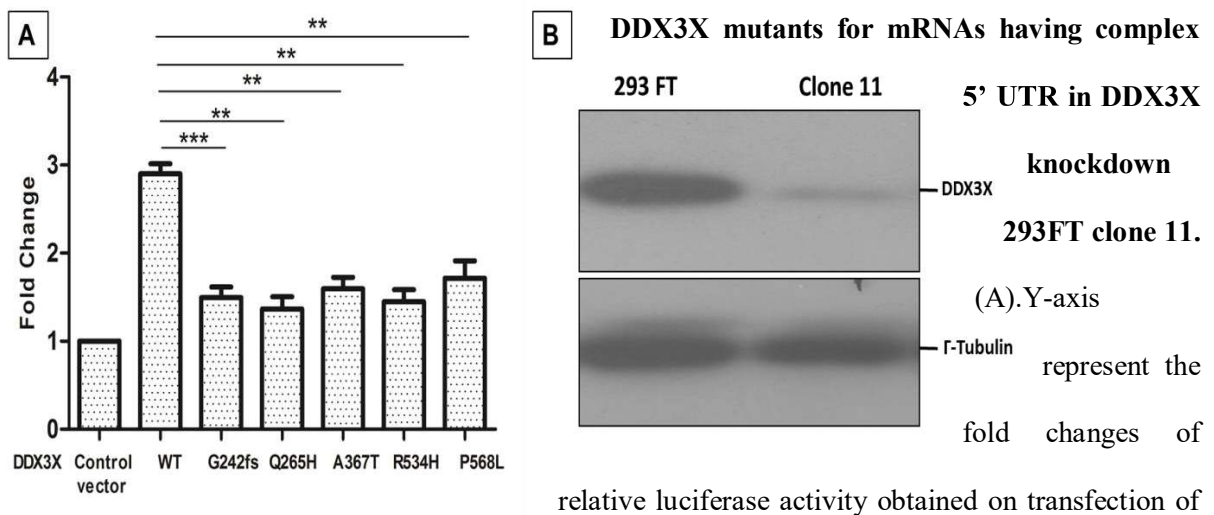
targeting 3'UTR region and other targeting ORF region nucleotide 301-320) were designed and cloned in a doxycycline inducible pLKO-Tet vector. Daoy and HEK 293FT cells were transduced with lentiviral particles of these shRNAs and polyclonal population was selected using puromycin selection. Almost 90% downregulation of DDX3X was observed in Daoy cells using shRNAs against UTR (Daoy shUTR) and ORF (Daoy sh301) induced by doxycycline. In the case of HEK 293FT cells 20-30% downregulation of DDX3X was observed with UTR shRNA whereas shRNA against ORF region showed more than 50% downregulation (Fig. 4.17).

4.2.9 Effect of identified genetic alterations in DDX3X on its translational control

DDX3X has been reported to facilitate translation initiation of mRNAs with long and complex 5'UTRs like Cyclin E1 through its helicase activity [76]. Therefore, to identify the effect of identified mutations on translation control activity of DDX3X luciferase reporter construct was generated by cloning complex 5' UTR of cyclin E1 in pGL3 control vector upstream of

luciferase gene and luciferase reporter assay was performed in DDX3X knock-out HEK 293FT clone 11. Luciferase reporter assay was performed by cotransfecting cyclin E1 5'UTR luciferase construct, pcDNA3-GFP and wild type or mutant DDX3X (G242Fs/Q265H/A367T/R534H/P568L) in 293FT clone 11. In clone 11 relative luciferase activity was found to be increased by approximately 3 fold ($p \leq 0.0001$) in the case of the cells transfected with CRISPR resistant pcDNA3-DDX3X as compared to the control cells transfected with pcDNA3 indicating that DDX3X enhances the expression of genes having complex 5'UTR, whereas all the mutant of DDX3X (G242Fs/Q265H/A367T/R534H/P568L) failed to increase luciferase activity indicating loss of function nature of these mutations (Fig. 4.18).

Figure 4.18: Luciferase reporter assay to check translational regulation function of identified



the indicated constructs as compared to that obtained upon transfection of control vector alone. ** indicates $p \leq 0.001$. (B) Western blot representing knockdown of DDX3X in 293FT clone 11 using CRISPR-CAS9 system. Γ -Tubulin is used as loading control.

4.2.10 Effect of DDX3X downregulation on proliferation of Daoy cells

The effect of DDX3X downregulation on proliferation of Daoy cells was studied by MTT reduction assay over a period of 10 days. Vector control populations of Daoy cells showed no significant difference in proliferation upon Doxycycline treatment compared to their untreated populations. Daoy stable polyclonal population expressing DDX3X shRNA sh301 cells showed approximately 75% ($p \leq 0.0001$) decrease in cell proliferation after doxycycline treatment on day 10. Whereas in the case of Daoy stable polyclonal population expressing DDX3X shRNA targeting 3'-UTR, 50% ($p \leq 0.0001$) reduction in proliferation was observed after doxycycline treatment compared to their uninduced counterparts (Fig. 4.19).

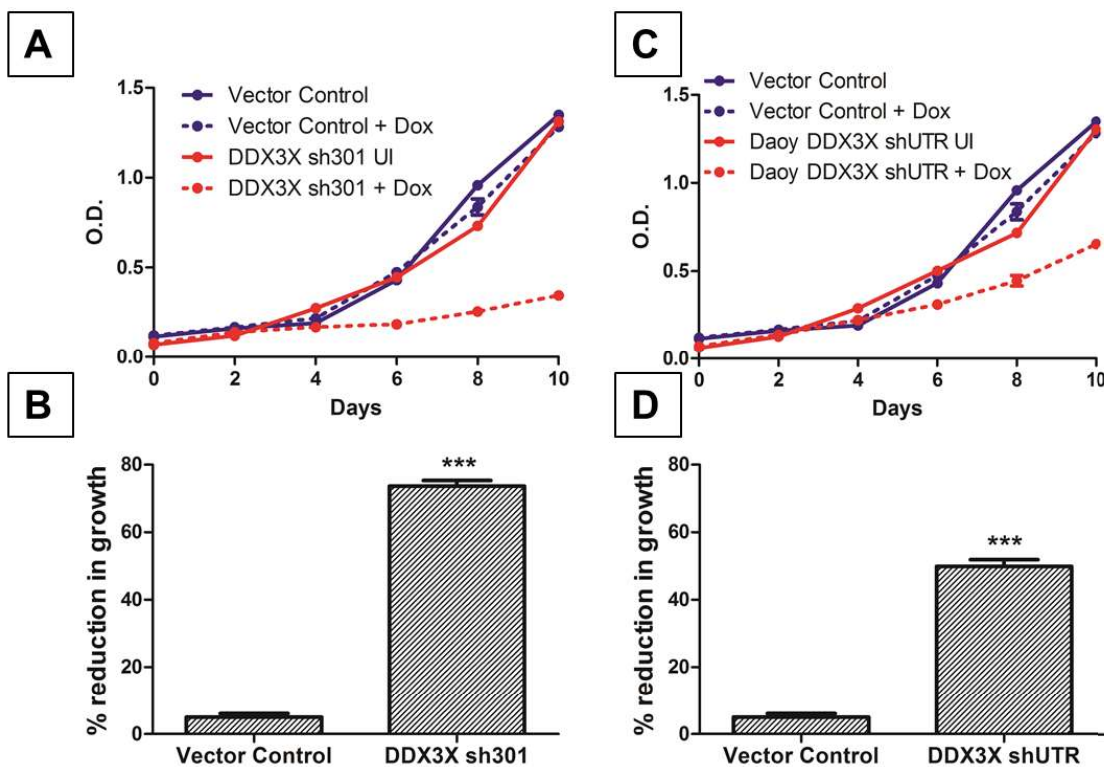


Figure 4.19: Effect of DDX3X downregulation on growth of Daoy medulloblastoma cell line.

Representative experiments showing growth curves of Daoy medulloblastoma cell line polyclonal populations (A) transduced with shRNA targeting DDX3X in ORF region (DDX3X sh301) and that (C)

transduced with shRNA targeting DDX3X in 5'UTR region or control vector with (+Dox) or without doxycycline induction (UI) as studied by MTT reduction assay over a period of 10 days. B, D: Y-axis denotes the percentage reduction in growth upon doxycycline treatment of the indicated population compared to un-treated population as studied by the MTT reduction assay. *** indicates $p \leq 0.0001$.

4.2.11 Effect of DDX3X downregulation on clonogenic potential of Daoy cells

The clonogenic potential of DDX3X downregulated Daoy cells was studied by clonogenic assay. Daoy cells formed 250-300 well separated, microscopically visible colonies 10 days post seeding of 1000 cells / 55 mm petridish. There was no significant difference in the number of colonies formed by the doxycycline induced vector control cells compared to their uninduced counterparts, whereas DDX3X knockdown Daoy sh301 cells showed ~90% ($p \leq 0.0001$) reduction in the number of colonies compared to their uninduced counterparts (Fig. 4.20 A and B), In the case of Daoy shUTR cells it was clonogenic potential was found to be reduced by ~50% ($p \leq 0.001$) compared to their uninduced counterparts (Fig. 4.20 C and D).

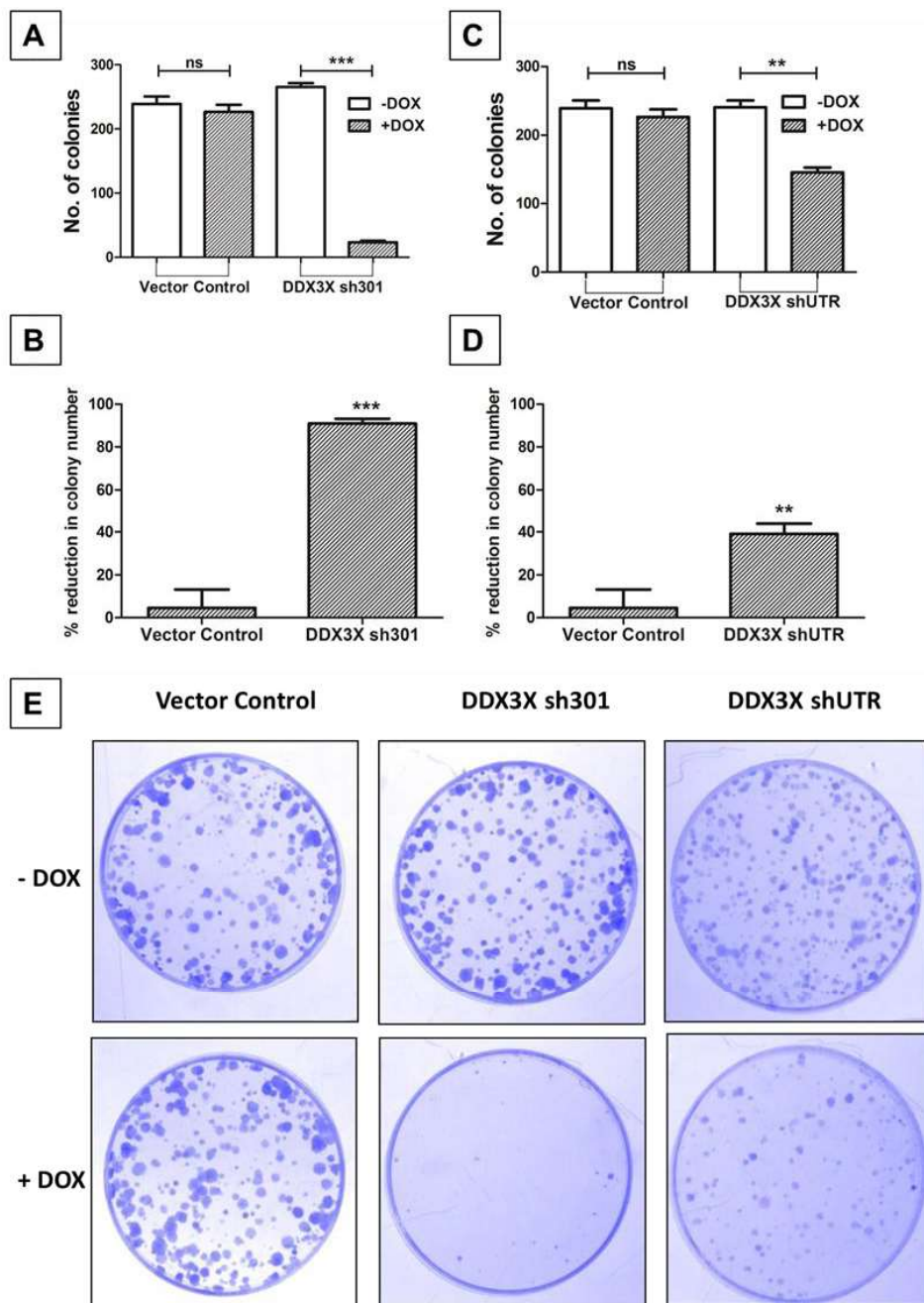


Figure 4.20: Effect of DDX3X downregulation on clonogenic potential of Daoy medulloblastoma cell line. Representative experiments showing the number of colonies formed by Daoy medulloblastoma cell line polyclonal population (A) transduced with shRNA targeting DDX3X in ORF region (DDX3X sh301) and that (C) transduced with shRNA targeting DDX3X in 5'UTR region or control vector with

(+Dox) or without (-Dox) doxycycline induction as studied by clonogenic assay. B, D: Y-axis denotes the percentage reduction in colony formation upon doxycycline treatment of the indicated population as compared to the un-treated population. 'ns' indicates non-significant, ** indicates $p \leq 0.001$ and *** indicates $p \leq 0.0001$. E: Representative images of the above mentioned experiments.

4.3 Delineate the role of has-miR-30a in medulloblastoma cell behavior

Genome wide expression profiling of medulloblastomas for protein coding genes and microRNAs, done in parallel using Affymetrix gene 1.0 ST arrays and Taqman Low Density Arrays respectively had shown differential microRNA expression in the four molecular subgroups of medulloblastomas [13]. MiR-30a, a microRNA located on chromosome 6 was found to be downregulated in all medulloblastomas as compared to its expression in normal cerebellum. In WNT subgroup of medulloblastomas one copy of chromosome 6 is lost in more than 75% cases [124]. MiR-30a expression has been reported to be down regulated in multiple cancers including breast cancer, lung cancers and colorectal cancers [125]. Hence it was decided to investigate the role of miR-30a in pathogenesis of medulloblastomas.

4.3.1 MiR-30a expression levels in medulloblastoma subgroups and normal brain tissues

MiRNA profiling of 19 medulloblastomas along with two developing and two adult normal cerebellums was done using Taqman Low Density array as described [13]. Expression of seven microRNAs belonging to the miR-30 family microRNAs (miR-30a-5p, miR-30a-3p, miR-30b, miR-30c, miR-30d, miR-30e-5p, miR-30e-3p) was found to be significantly ($p < .00001$) downregulated in medulloblastomas belonging to all the four subgroups as compared to normal cerebellar tissues (Fig. 4.21) . Cerebellum, the site of medulloblastoma, develops in the first year

after birth. MiR-30a levels in developing cerebellum from less than 1 year old infants were found to be lower (RQ = 5-10) as compared to that (RQ =10-50) in adult cerebellar tissues. MiR-30a-3p level was found to be 10 -50 fold (RQ 0.3-1.7), MiR-30a-5p 5-10 fold (RQ 4.8-20), miR-30b level 5-15 fold (RQ 5-40), miR-30c level 5-10 fold (RQ 13-80), miR-30d level 2-10 fold (RQ 3-25), miR-30e-3p level 4-10 fold and miR-30e-5p level (RQ 0.5-5) fold downregulated compared to normal developed cerebellum. Thus expression of miR-30a family microRNAs was found to be downregulated all four medulloblastoma subgroups (Fig. 4.21).

4.3.2 Evaluation of miR-30a expression in mouse medulloblastoma tumor tissues from the *Smo*^{+/+} transgenic mice and the *Ptch1*^{+/-} knock-out mice and normal cerebellum by SYBR green real time RT-PCR

The expression of murine homologue of human miR-30a was evaluated using SYBR green real time RT-PCR chemistry, in the normal developing cerebellum of *C57BL6* mice at post natal day 5, 14 and 21 and in medulloblastomas from the *Smo*^{+/+} transgenic mice and *Ptch*^{+/-} knock-out mice [50, 126]. These mouse models serve as models for SHH subgroup medulloblastomas. MiR-30a expression was found to be downregulated by ~10 fold (RQ = 0.013-0.055) in the *Smo*^{+/+} transgenic mice and by ~20 (RQ = 0.006-0.082) fold in the *Ptch*^{+/-} knock-out mice compared to their normal cerebellar counterparts (RQ = 0.4-2.9) (Fig. 4.22). Thus, miR-30a expression was found to be downregulated in medulloblastoma cell lines as well as in the tumors from SHH signaling driven medulloblastoma mouse models.

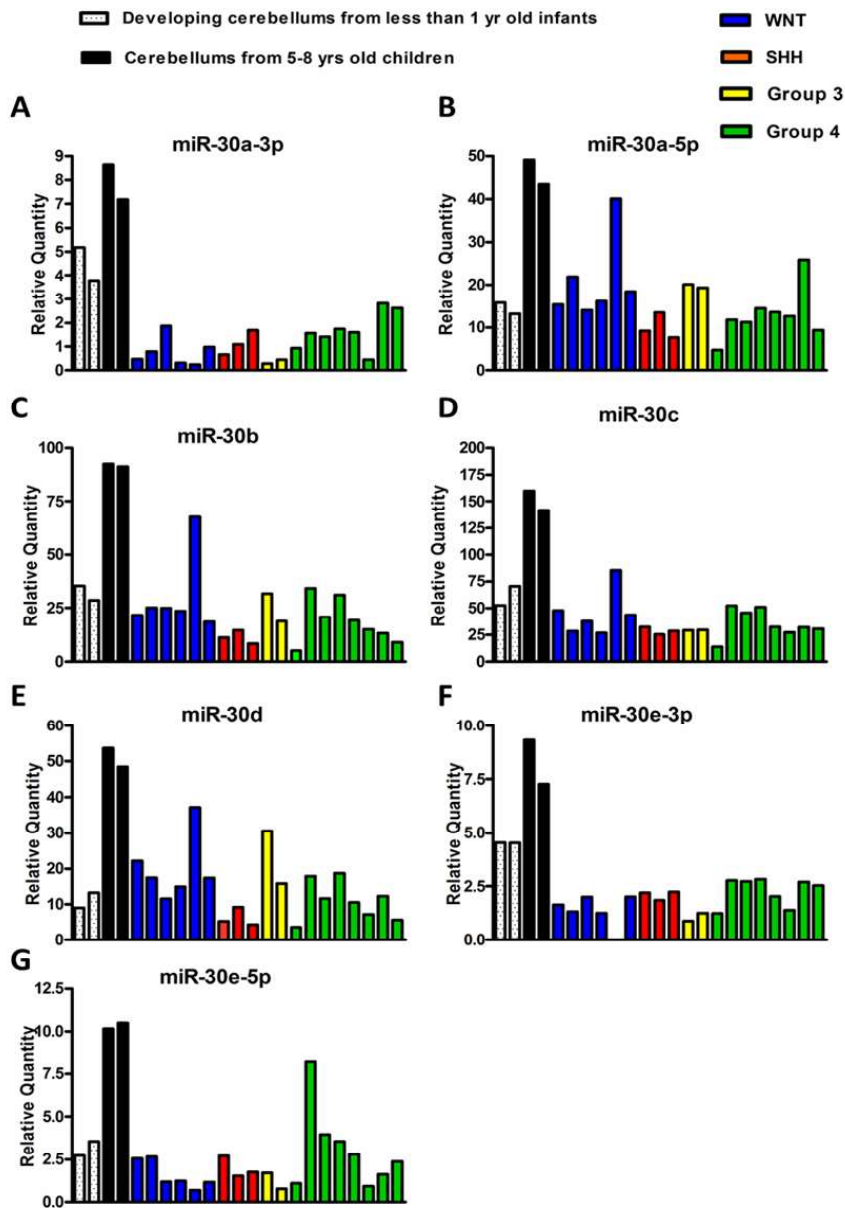


Figure 4.21: Expression levels of 7 miR-30 family miRNA in human normal cerebellar tissues and human medulloblastoma tumor tissues analysed by Taqman Low Density array. Y axis denotes Relative Quantity of the indicated microRNA as compared to that of housekeeping small RNA RNU48.

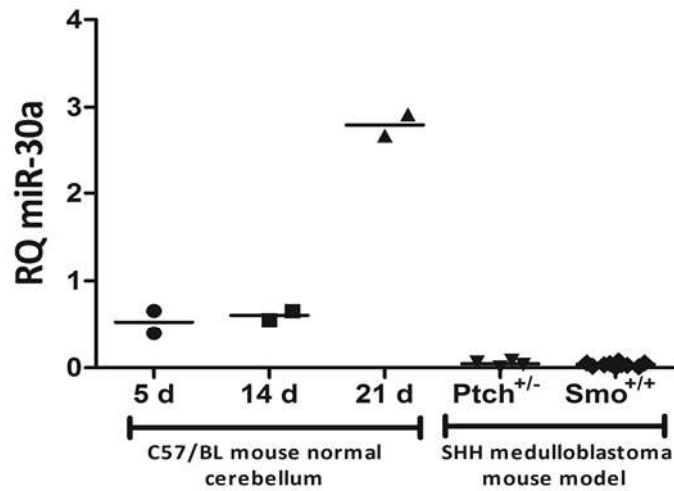


Figure 4.22: Expression level of miR-30a in the normal cerebellum and in medulloblastoma tissues from *Smo*^{+/+} and *Ptch1*^{+/-} medulloblastoma mouse models. Y axis denotes Relative Quantity of the indicated microRNA as compared to that of housekeeping small RNA *Sno202*.

4.3.3 Construction of an inducible lentiviral vector for the expression of miR-30a

The genomic region encoding miR-30a along with about 250 nucleotides long 5' and 3' flanking region ([Chr6: 71403372 - 71403916](#)) was cloned in the pTRIPZ lentiviral vector (Open biosystems, Lafayette, USA) between the HpaI and EcoRI restriction enzyme sites. The miRNA is expressed under the control of a doxycycline inducible promoter. The pTRIPZ vector consists of the tetracycline response element (TRE) and the reverse tetracycline transactivator 3 (rtTA3) which enable inducible expression of the miRNA. The TRE consists of a string of Tet operators fused to the minimal CMV promoter. The pTRIPZ transactivator, known as the reverse tetracycline transactivator 3 (rtTA3), binds to and activates expression from TRE promoters in the presence of doxycycline. The TRE also drives the expression of a TurboRFP reporter in addition to the miRNA. This enables monitoring of expression from the TRE promoter. This

vector construct was used for the stable, inducible expression of miR-30 in medulloblastoma cell lines (Fig.4.23).

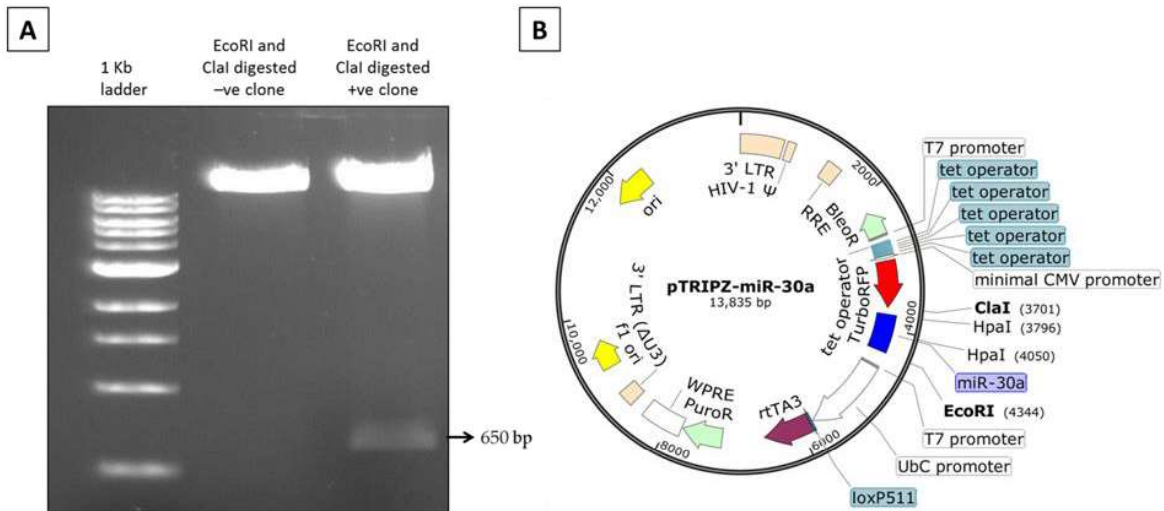


Figure 4.23: pTRIPZ-miR-30a vector construct (A) Ptripz-miR-30a vector construct map indicating cloning sites HpaI and EcoRI and location of other features of the vector backbone. (B) Agarose gel electrophoresis image of confirmation of the pTRIPZ-miR-30a construct.

4.3.4 Effect of miR-30a Expression on growth characteristics of established medulloblastoma cell lines

4.3.4.1 Generation of stable polyclonal populations expressing miR-30a on doxycycline induction

Expression of miR-30a was evaluated in three medulloblastoma cell lines Daoy, D283 and D425 and compared with its expression in developing and developed normal human cerebellum tissues using Taqman real time RT-PCR. Mir-30a expression was found to be approximately 5-100 fold downregulated in Daoy (RQ 1.4-1.8), D283 (RQ 0.17-0.37) and D425 (RQ 0.056-0.065), the three established medulloblastoma cell lines studied when compared with the developed normal human cerebellum (RQ 4.5-8.5) (Fig. 4.24 A). Daoy and D425 / D283 medulloblastoma cell

lines belong to SHH, and Group 3 molecular subgroup respectively based on their cytogenetic profiles. Daoy, D425 and D283 medulloblastoma cell lines were transduced with lentiviral particles of pTRIPZ-miR-30a construct that expressed miR-30a in a doxycycline inducible manner. Stable polyclonal populations of each of the three cell lines expressing miR-30a were selected in the presence of puromycin following transduction. MiR-30a expression in these stable populations was found to be in the range of RQ 9-38 (Fig. 4.24 B). The cells transduced with the viral particles of the empty pTRIPZ vector of the respective cell lines were used as vector controls. These cells along with their respective vector control population were used to study the effect of miR-30a expression on proliferation, clonogenic growth potential and anchorage independent growth potential of medulloblastoma cells.

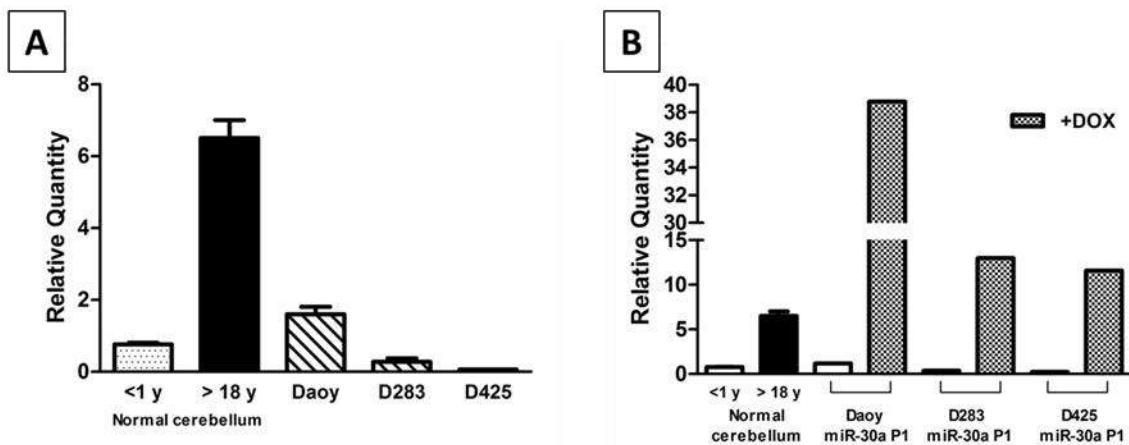


Figure 4.24: MiR-30a expression in the normal brain, medulloblastoma cell lines, and in the stable polyclonal populations expressing miR-30a. (A) MiR-30a expression in normal developing cerebellum (less than 1yr old infants), adult cerebellum, and in established medulloblastoma cell lines. (B) MiR-30a expression in normal developing cerebellum (less than 1yr old infants), adult cerebellum and in stable polyclonal populations of medulloblastoma cell lines expressing miR-30a established medulloblastoma cell lines. Y axis denotes Relative Quantity of the indicated microRNA as compared to that of housekeeping small RNA RNU48.

4.3.4.2 Effect of miR-30a expression on the proliferation of the medulloblastoma cell lines

The effect of miR-30a expression on the proliferation of medulloblastoma cell lines was studied using MTT reduction assay over a period of 10 days. Vector control populations of Daoy, D283 and D425 cells showed no significant difference in proliferation upon Doxycycline treatment compared to their untreated populations. MiR-30a expression upon doxycycline induction inhibited ($p < .0001$) growth of Daoy, D283 and D425 cells by 54.39 % (± 3.6), 60.73% (± 4.11) and 79.35% (± 2.01) respectively (Fig. 4.25). Thus miR-30a expression was found to inhibit the proliferation of all the three medulloblastoma cell lines studied.

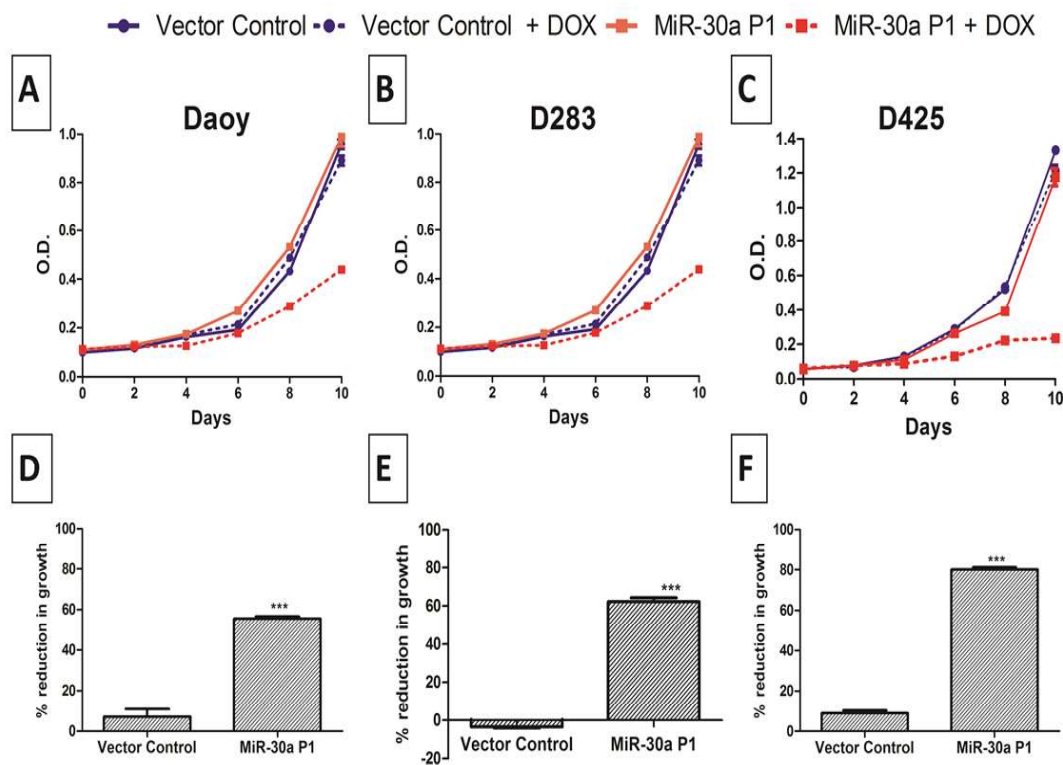


Figure 4.25: Effect of miR-30a expression on the growth of medulloblastoma cell lines.

(A, B and C) Representative experiments showing growth curves of the indicated medulloblastoma cell line polyclonal populations transduced with pTRIPZ vector control or pTRIPZ-miR-30a construct 'P1' with (+ DOX) or without doxycycline treatment as studied by the MTT reduction assay; (D, E and F) Y

axis denotes the percentage reduction in the growth upon doxycycline treatment of the indicated polyclonal populations compared to the un-treated population as studied by the MTT assay. ‘****’ indicates $p \leq 0.0001$

4.3.4.3 Effect of miR-30a expression on the clonogenic potential of Daoy medulloblastoma cells

The effect of miR-30a expression on the clonogenic potential of Daoy cells was studied by using clonogenic assay. Vector control and Daoy miR-30a P1 cells were treated with doxycycline for 72 h and then 1000 cells of untreated and doxycycline treated vector control and Daoy miR-30a P1 population were seeded in 60 mm plates and allowed to form microscopically visible colonies over a period of 10 days with replenishment of fresh medium every three days. After 10 days colonies were stained with crystal violet and counted. Daoy cells formed 300-350 well separated, microscopically visible colonies 10 days post seeding. There was no significant difference in number of colonies formed by doxycycline induced vector control cells compared to their uninduced counterparts, whereas miR-30a expressing Daoy cells showed 56.77% (± 1.65) ($p \leq 0.0001$) reduction in number of colonies compared to their uninduced counterparts (Fig. 4.26).

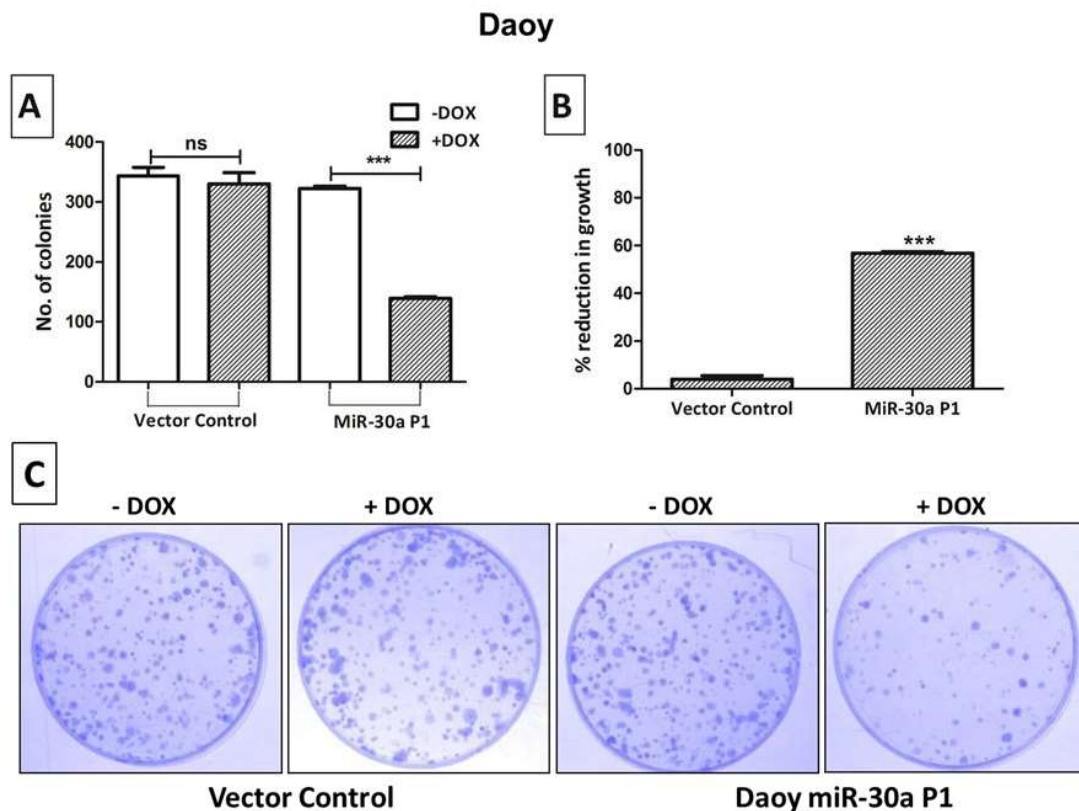


Figure 4.26: Effect of miR-30a expression on the clonogenic potential of Daoy medulloblastoma cell lines. (A) Representative experiments showing the number of colonies formed by Daoy medulloblastoma cell line polyclonal populations transduced with control pTRIPZ vector control or pTRIPZ-miR-30a construct ‘P1’ with (+ DOX) or without doxycycline treatment as studied by the clonogenic assay; (B) Y axis denotes the percentage reduction in colony formation upon doxycycline treatment of Daoy polyclonal populations compared to the un-treated population as studied by clonogenic assay. ‘****’ indicates $p \leq 0.0001$; (C) Representative images of above mentioned experiments.

4.3.4.4 Effect of miR-30a expression on the anchorage independent growth of medulloblastoma cells

The effect of miR-30a expression on the anchorage independent growth of Daoy, D283 and D425 was studied by using soft agar colony formation assay. For soft agar assay, 7500 cells of 72 h doxycycline treated and untreated Daoy vector control and Daoy miR-30a P1 populations

were seeded in a 35 mm culture dish and allowed to form microscopically visible colonies over the period of 2 weeks with fresh medium replenishment every third day. For D283 and D425 the numbers of cells plated were 1000 per 35 mm culture dish. The vector control Daoy, D283 and D425 cells formed ~600, ~300 and ~650 well separated colonies in 2 weeks post seeding respectively. There was no significant difference in the number of soft agar colonies formed by doxycycline induced vector control cells compared to their uninduced counterparts, whereas miR-30a expression in Daoy, D283 and D425 cells inhibited ($p \leq 0.0001$) soft agar colony formation by 54.14% (± 3.25), 51.04% (± 4.98) and 54.74% (± 0.87) respectively compared to their uninduced counterparts (Fig.4.27). Both D283 and D425 cell lines grow mostly as suspension and at best in semi-adherent manner. Therefore, inhibition of soft agar colony formation upon miR-30a expression indicates effect upon clonogenic potential rather than that upon anchorage-independent growth.

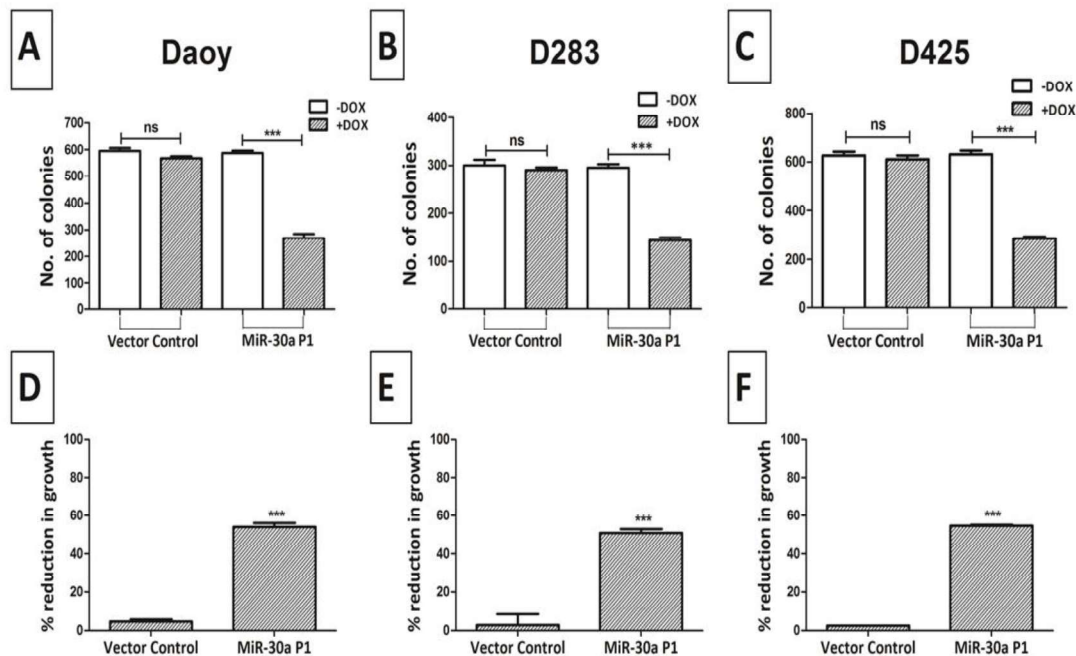


Figure 4.27: Effect of miR-30a expression on the anchorage independent growth of medulloblastoma cell lines. (A, B and C) Representative experiments showing the number of colonies formed by the indicated medulloblastoma cell line polyclonal populations transduced with pTRIPZ vector control or pTRIPZ-miR-30a construct 'P1' with (+ DOX) or without doxycycline treatment as studied by the soft agar assay; (B) Y axis denotes the percentage reduction in colony formation upon doxycycline treatment of the indicated polyclonal populations compared to the un-treated population as studied by soft agar assay. '***' indicates $p \leq 0.0001$

4.3.5 Effect of miR-30a expression on *in-vivo* tumorigenicity of D283 cell lines

D283 cell line as well as its polyclonal population stably transduced with pTRIPZ-miR-30a construct was engineered to express firefly luciferase. The D283 control vector cells and pTRIPZ- miR-30a population of D283 cells were induced with doxycycline for 72 h and then 2×10^5 cells were injected into the cerebellum of BALB/c Nude mice through 0.5 mm burr hole in the midline, 2 mm posterior to lambda at 2 mm depth, using small animal stereotaxic frame (Harvard Apparatus, MA, USA). The growth of the tumors was monitored using bioluminescence imaging. The normalized luminescence represented as average radiance reflects the tumor growth. Bioluminescence imaging showed almost 400 fold increase in average radiance of the tumors formed within 3 weeks in mice injected with the parental D283 cells. On the other hand, average luminescence of the tumors formed in D283 cells expressing miR-30a increased only about 10 fold within the same time period. Thus, upon miR-30a expression tumor growth was found to be reduced by more than 100 fold ($p < 0.0001$) (Fig. 4.28). Therefore, miR-30a expression was found to bring about substantial decrease in tumorigenicity of the D283 medulloblastoma cells.

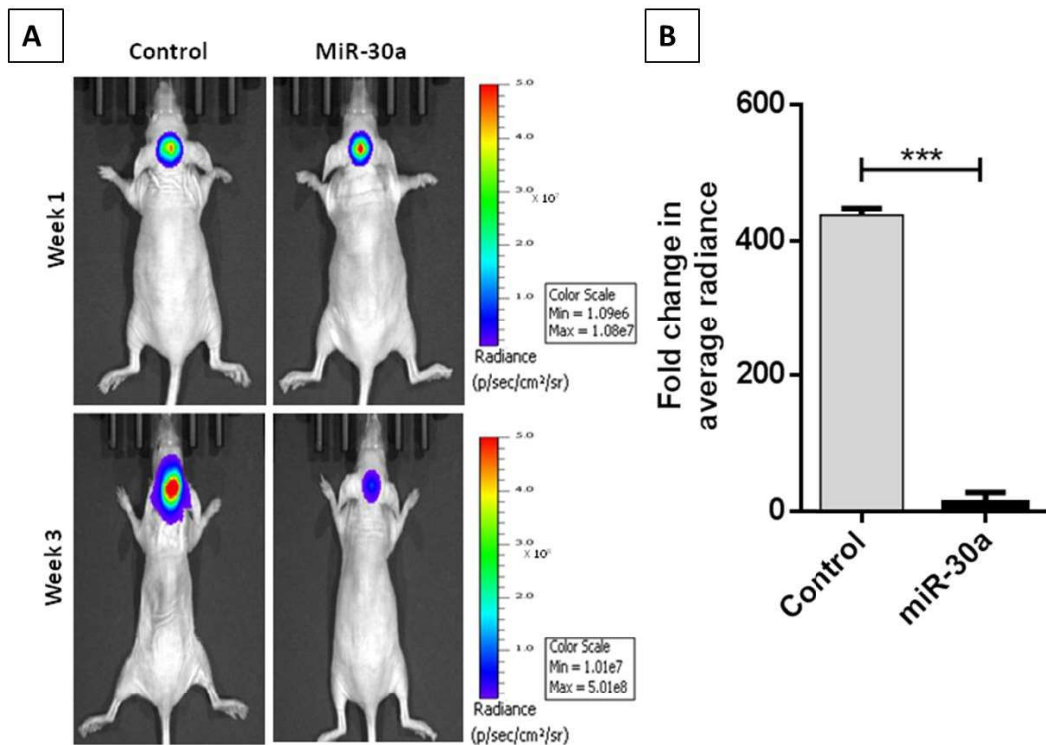


Figure 4.28: Effect of miR-30a expression on tumorigenicity of medulloblastoma cell line.

(A) Bioluminescence images of nude mice orthotopically injected with D283 stable polyclonal populations expressing firefly luciferase and either control pTRIPZ vector or miR-30a upon doxycycline (DOX) induction. (B) Y axis shows relative fold increase in the average radiance on 3rd week as compared to that on 1st week after injection in the indicated cells. *** indicates $p \leq 0.001$.

4.3.6 Molecular mechanism underlying growth inhibitory effect of miR-30a expression on medulloblastoma cells

MiR-30a has been reported to inhibit autophagy by downregulating expression of Beclin1 and ATG5 [127]. In order to identify molecular mechanism by which miR-30a expression affects growth and clonogenic potential of the medulloblastoma cells, levels of Beclin1 and ATG5 were studied by western blotting in miR-30a expressing medulloblastoma cells. Significant reduction

in Beclin1 as well as in ATG5 expression was observed upon miR-30a expression in D283 medulloblastoma cells (Fig. 4.29A). In order to check if miR-30a expression inhibited autophagy in medulloblastoma cells, change in the levels of LC3B, upon miR-30a expression was investigated by western blotting. Upon autophagy induction, total levels of LC3B decrease and/or LC3BI to LC3BII conversion decreases following LC3BI conjugation of phosphatidylethanolamine. LC3B II levels however, also decrease as a result of their degradation by lysosomal enzymes upon fusion of autophagosomes with lysosomes. Therefore, LC3BI and LC3BII levels were monitored both in the absence and presence of chloroquine, an inhibitor lysosomal pathway of protein degradation. Doxycycline induction of miR-30a expression resulted in downregulation of total LC3B levels (LC3BI and LC3BII) both in the presence and absence of lysosomal inhibitor indicating autophagy inhibition (Fig. 4.29B). Furthermore, even upon starvation induced autophagy induction, total levels of LC3B were found to be lower upon miR- 30a expression, indicating inhibition of starvation induced autophagy by miR-30a expression (Fig. 4.29B). Accumulation of autophagic substrate SQSTM1/p62 is also used as a marker for autophagy. All the three medulloblastoma cell lines showed increased expression of SQST/p62 upon miR-30a expression indicating autophagy inhibition (Fig. 4.29C). Thus, miR-30a expression was found to inhibit autophagy in all the three medulloblastoma cell lines studied.

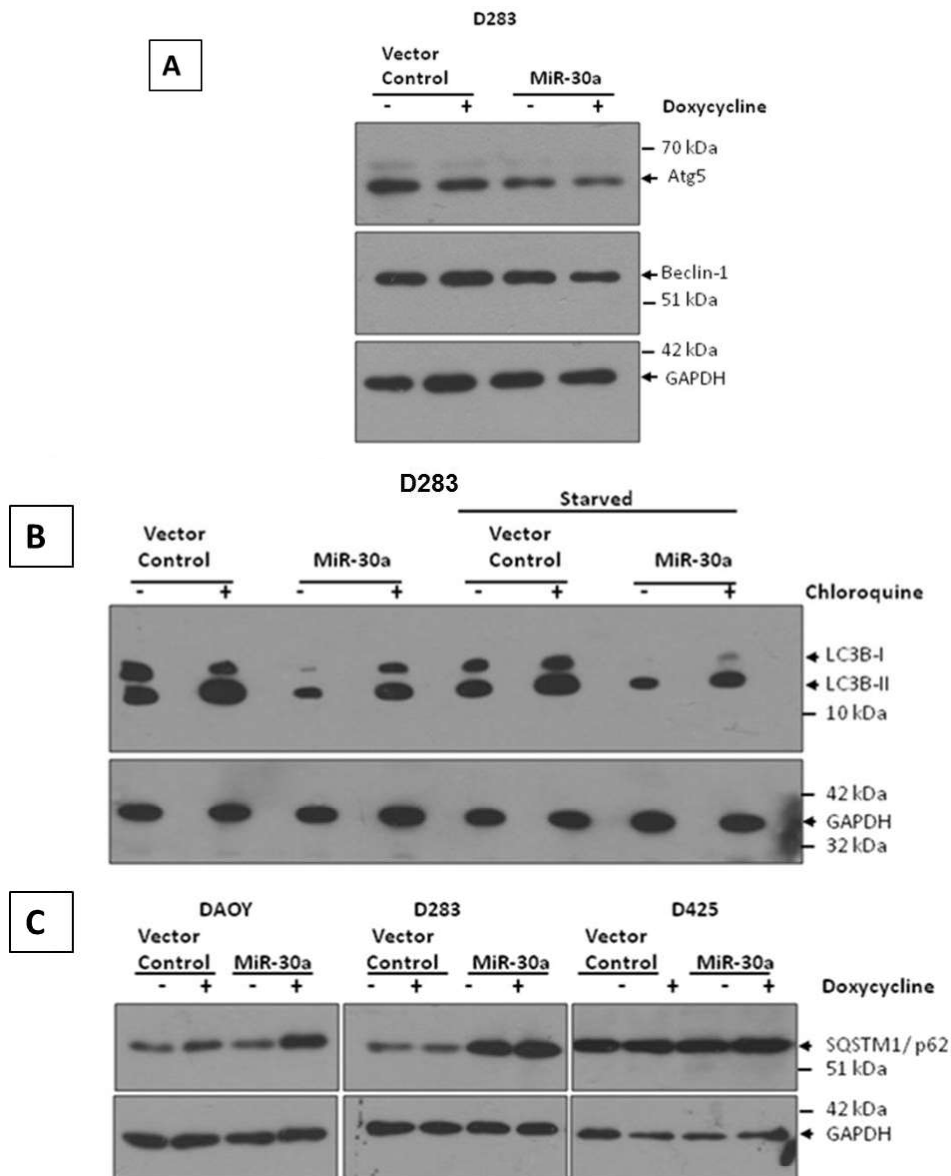


Figure 4.29: effect of miR-30a expression on autophagy in medulloblastoma cell lines.

(A) Beclin1, ATG5 and (B) LC3B levels were analysed by western blotting in D283 cells stably transduced with vector control or miR-30a constructs before and after doxycycline induction. LC3B levels were also analyzed with or without treatment with chloroquine as well as from the cells starved by incubation for 1 h in PBS. (C) Levels of SQSTM1/p62 analyzed in the indicated medulloblastoma cell line transduced with empty pTRIPZ vector or pTRIPZ-miR-30a construct before or after doxycycline induction. Housekeeping gene GAPDH was used as a loading control.

Chapter 5

DISCUSSION

Discussion

Medulloblastoma is the most common and highly malignant brain tumor in children. Expression profiling studies from our lab and other groups have shown that it consists of four molecular subgroups *viz.* WNT, SHH, Group 3 and Group 4 [4, 13]. WNT and SHH subgroups tumors are characterized by overexpression of the WNT and SHH signaling genes respectively, whereas for Group 3 and Group 4 no specific signaling or developmental pathways have been attributed. Based on the expression profiling studies in the lab, 11 fresh medulloblastoma tumor tissues were identified to belong to the WNT subgroup medulloblastoma [13]. This classification into the WNT subgroup was further validated by sequencing of exon 3 of *CTNNB1* gene that identified known oncogenic mutations in the gene in each of these tumors. Mutation in beta-catenin encoding gene *CTNNB1* is known to bring about hyperproliferation but not malignant transformation in developing mouse brain [8]. Therefore, in order to identify other genetic alterations that act as second hit for the development of WNT tumors pathogenesis and delineate the mechanism underlying pathogenesis of the WNT subgroup tumors, it is necessary to identify the entire spectrum of genetic alterations in WNT subgroup tumors. For this purpose, whole exome sequencing of 11 WNT subgroup tumors was carried out and data was analysed to identify the genetic alterations.

5.1 The WNT subgroup medulloblastomas possess low number of genetic alterations

The number of somatic variants identified in the WNT subgroup medulloblastoma were in the range of 10-30 per tumor tissue. The loss of one copy of chromosome 6 was observed in 8 tumors and 2 tumors showed partial loss of chromosome 6 whereas in 1 tumor both the copies of chromosome were found to be intact. The rest of the genome of the WNT subgroup tumor was

found to be stable as reported in the previous studies [124]. This low number of somatic variants (0.52 per Mb) in medulloblastoma indicates that medulloblastomas have low number of somatic mutations and distinguishes it from other adult solid tumors (median 3.6 per Mb) which have comparatively high number of passenger mutations [128]. Higher load of somatic mutations is seen cancers like lung cancer, melanoma wherein external mutagen like tobacco smoke, UV rays are known to be involved [128]. Medulloblastoma being a pediatric tumor it is unlikely to have involvement of any external agent. Brain is protected by blood brain barrier that also minimizes role of external chemicals in pathogenesis. The number of passenger mutations in a tumor indicates the number of cell divisions required by that tumor to become clinically significant [129]. Low number of passenger mutations in medulloblastoma indicates that it required low number of cell divisions for it to become clinically significant that is consistent with its embryonal nature.

5.2 Mutations in the genes involved in the chromatin remodeling SWI/SNF complex and histone modifying ASCOM complex appear to play role in pathogenesis of the WNT subgroup medulloblastomas

Mutations in the genes *ARID1B*, *SMARCA4* and *SMARCB1* encoding components of the SWI/SNF complex were identified in the WNT subgroup medulloblastoma. *ARID1B* mutations were identified in two tumor tissues whereas *SMARCA4* and *SMARCB1* mutations were found in two and one tumor respectively. Both the mutations identified in *ARIB1B* (C878X and P1027fs insertion) were loss of function mutations. *ARID1B* is located on chromosome 6 and approximately 75% of WNT subgroup tumors show the loss of one copy of chromosome 6

leading to loss of one copy of *ARID1B* in these 75% cases [124]. So the loss of function mutation in the second copy of *ARID1B* indicates tumor suppressive role for this gene in medulloblastoma tumorigenesis. *SMARCB1* was found to be mutated in two (Q359X and R357H) tumors and *SMARCA4* in one (A1231V) tumor tissue. Next gene sequencing studies done on medulloblastoma have identified mutations in *SMARCA4* gene in approximately 26% of WNT subgroup and 10% of Group 3 tumors [10]. Mutations in the genes encoding different components of the SWI/SNF complex (*ARID1A*, *ARID1B*, *SMARCA4* and *SMARCB1*) have been reported in several cancers including rhabdoid tumors of brain, diffuse large B-cell lymphomas, head and neck cancers, ovarian cancers, gastric and pancreatic cancers [130].

The SWI/SNF (**SWI**tch/**S**ucrose **N**on-**F**ermentable) complexes are large (> 1 MDa) ATP-dependent chromatin remodeling complexes that are composed of 10–15 biochemically-distinct subunits [131, 132]. *SMARCA2* (*BRM*) and *SMARCA4* (*BRG*) are the ATPase enzymatic subunits of the SWI/SNF complexes and are mutually exclusive. These complexes also contain either of the three mutually exclusive subunits *ARID1A* (*BAF250A*), *ARID1B* (*BAF250B*), or *PBRM1* (*BAF180*), which confer functional specificity to these complexes. *ARID1A* and *ARID1B* are found associated with “BAF” complexes (*BRG1*- or *hBRM*-associated factors), which contain either *SMARCA2* or *SMARCA4* enzymatic subunit. *SMARCB1* is also known as *INI1* or *SNF5* is one of the core units of the SWI/SNF complexes. These complexes have essential roles during lineage specification and in the maintenance of stem cell pluripotency [133]. They regulate the transcription of target genes by chromatin remodeling. The SWI/SNF complexes, by themselves have very less DNA binding specificity hence it is likely that *in vivo* recruitment of the SWI/SNF complexes is dependent on the presence of sequence specific transcription factors. It has been shown that the carboxyl terminus of beta catenin interacts with

SMARCA4 and recruits it to TCF responsive elements to facilitate the expression of target genes [134]. However, recent reports also show that ARID1B acts downstream of the destruction complex, that mediates β -catenin degradation, to down regulate Wnt/ β -catenin signaling [135]. Distinct SWI/SNF complexes and their interaction with combination of transcription factors may determine their functional specificity regarding either activation or repression of a particular signaling pathway associated with them. It has also been reported that loss of SMARCB1 (SNF5) upregulates the Wnt/ β -catenin signaling [136]. Thus it is possible that loss of function mutations in different SWI/SNF complex components in the WNT subgroup tumors may assist mutant beta-catenin in transcriptional regulation of its target genes or may regulate genes other than in the canonical WNT signaling pathway that cooperate with the activated WNT signaling in pathogenesis of medulloblastoma.

ASC-2 (activating signal cointegrator 2) also known as NCOA6 complex (ASCOM complex) are transcriptional coactivators that along with nuclear hormone receptors facilitate transcription of target genes by their histone modification activity [137, 138]. ASCOM complex consists of histone methyl transferases (like MLL proteins) which bring about H3K4 methylation and histone demethylase KDM6A that erases H3K27 methylation mark. Mutations in the *KMT2C* also known as *MLL3* (mixed lineage leukemia protein 3) and *KDM6A* (lysine specific demethylase 6A) also known as *UTX* gene were identified in two (R190X and R4549H) and one (Q271X) WNT subgroup tumor respectively. Mutations identified in *MLL3* and *KDM6A* are of loss of function in nature. *NCOA6* (nuclear receptor coactivators 6) was also found to be mutated (E1514X) in one tumor tissue. *MLL3* mutations have been reported to occur in ~ 5% of the Group 4 tumors whereas *MLL2* mutations are reported in ~ 12% of WNT subgroup and 5% of Group 4 tumors. Mutations in the *KDM6A* gene are reported in ~13% of Group 4 tumors [139,

140]. *MLL3* and *KDM6A* are part of ASCOM complex. Loss of function mutations were identified in different components of the ASCOM complex, indicating that ASCOM complex might be non-functional in these WNT tumors. *MLL3* functions as a histone lysine N-methyl transferase that brings about H3K4 mono, di or trimethylation [137]. *KDM6A* functions as a histone lysine demethylase and is associated with de-methylation H3K27me3. The H3K27 trimethyl mark (H3K27me3) is repressive histone code and it represses lineage-specific genes in stem cells whereas H3K4me3 is transcription activation code. H3K27me3 is written by the polycomb repressive complex 2 (PRC2) that includes the methylase (EZH2/1) and is erased during differentiation by the demethylase *KDM6A*. During the development stem cells differentiation is modulated by *KDM6A*. It demethylates the repressive H3K27me3 mark which is followed by recruitment of chromatin remodellers to activating H3K4me3 mark to allow expression of differentiation related genes to promote differentiation. These processes are tightly controlled during development and inactivating mutations in these methylases and demethylases might lead to deregulation of normal development and abnormal proliferation of precursor cells ultimately resulting in cancers. Next gen sequencing studies done on medulloblastoma have reported *TP53* mutation in approximately 12.5% of WNT subgroup patients whereas in none of the 11 WNT tumors showed mutation in the *TP53* gene [121, 140]. Mutations in chromatin remodeling and histone modifying enzymes have been reported to be subgroup specific with *MLL3* and *KDM6A* mutations restricted to Group 4 tumors while in the present study, mutations were identified in the *MLL3* and *KDM6A* gene in the WNT subgroup medulloblastoma. None of the 11 WNT tumors were found to carry mutation in *MLL2* gene that is reported to be mutated in the WNT subgroup medulloblastoma. Thus, although the present cohort also showed mutations in the chromatin modifier genes that have been reported to be mutated in medulloblastomas, the

present cohort did not conform to the subgroup specificity of reported. Whether ethnic difference contributes to these differences identified in the Indian cohort remains to be determined. Despite these differences it is evident that mutations in epigenetic modifiers are central to medulloblastoma pathogenesis and these mutations might be acting as second hit in addition to mutant beta catenin in pathogenesis of WNT subgroup medulloblastoma. Role of these mutations need to be further functionally validated in appropriate experimental systems to elucidate their role in medulloblastoma pathogenesis. Evolution of DNA sequencing technologies in the last decade made it possible to rapidly sequence large number of samples in multiple cancers and these studies have shown that mutations in epigenetic modifiers as frequently mutated genes in several cancers. Shain *et al.* analysed the mutation spectrum of 20 SWI/SNF subunits genes across 18 different cancers from 24 different whole exome sequencing studies representing 669 patients and showed that the average the frequency of SWI/SNF complex mutations (18%) in these cancers was reaching to that of *TP53* (26%), the single most mutated tumor suppressor gene [130]. The frequency SWI/SNF complex mutation was found to be higher in ovarian clear cell cancer, renal cell cancer, hepatocellular cancer, gastric cancer and melanoma. Thus, mutations in these epigenetic regulators are not just central to medulloblastoma but they appear to play key role in tumorigenesis of many cancers. The epigenetic alterations are reversible, unlike the DNA mutations hence these can be targeted for therapeutic intervention in many cancers [141, 142].

5.3 DEAD-box helicase (*DDX3X*) is the second most frequently mutated gene in medulloblastoma after *CTNNB1* gene

The present study identified the DEAD-box helicase *DDX3X* as the second most mutated gene after *CTNNB1* gene in the WNT subgroup medulloblastomas. Mutations in the *DDX3X* gene

were identified in 3/11 WNT subgroup medulloblastomas, of which two were missense mutations (Q265H and A367T) located in the D1 subdomain of the helicase domain and the third was frameshift deletion mutation at the amino acid residue G242 leading to truncation of the DDX3X protein and loss of its almost entire central helicase core domain. *DDX3X* has been reported as the second most frequently mutated gene in the WNT subgroup medulloblastoma after *CTNNB1* by other studies as well [121, 140]. *DDX3X* has been reported to be mutated in approximately 50% of WNT subgroup tumors and approximately 11% of SHH subgroup tumors. In case of adult SHH cases the *DDX3X* mutation has been reported in approximately 50% tumors. These mutations are restricted to the D1 and D2 domain of the central helicase core structure, indicating their functional relevance.

5.4 Mutations result in loss of enzymatic activity of DDX3X

DDX3X is a RNA helicase which has ATPase dependent RNA helicase activity [59]. Robinson *et al.* have shown that the DDX3X mutations identified in the WNT subgroup of medulloblastoma potentiate proliferation of lower rhombic lip (LRP) progenitor cells leading to increase in tumor incidence in the WNT subgroup mouse model suggesting these mutations to be activating mutations [140]. Another study also reported the activating nature of DDX3X mutants by showing that DDX3X mutants but not wild type, increases the transactivation function of mutant beta catenin in HEK 293 cells [121]. However, in the present study, a truncating mutation was identified in one WNT subgroup tumor, which would lead to loss of its enzymatic activities. Nonetheless, such a protein truncating mutation is rare with all the mutations reported to be missense mutations in the helicase and ATPase domain of DDX3X. Therefore to check if the missense mutations also lead to loss of enzymatic activity experiments were undertaken to purify recombinant wild type and mutant DDX3X proteins in bacterial system and study their helicase

activity. However, recombinant DDX3X protein in bacterial system was found to be insoluble. MBP fusion DDX3X protein although expressed in soluble fraction was found to have partial helicase activity. Recently another study showed that some of the DDX3X mutations reported in medulloblastomas are defective in RNA stimulated ATPase activity supporting the loss enzymatic activity nature of the mutations [62]. As full length DDX3X was not expressed as soluble protein, this group was also unable to perform *in vitro* RNA helicase assay. DDX3X is known to regulate the translation of mRNAs containing complex 5'-UTR by using its ATPase dependent RNA helicase activity to resolve the complex RNA secondary structure near the translation start site [76]. Therefore effect of the mutations in DDX3X on this translation regulatory activity was investigated Three DDX3X mutants identified in this study (Q265H, A367T and G242 frames-shift deletion) along with two transcriptional activating mutations reported (R534H and P568L) in medulloblastoma were found to be defective in translational activation of the mRNAs containing complex 5'-UTR structure as judged by the luciferase assay in HEK 293FT cells using a luciferase vector containing complex 5'-UTR structure of Cyclin E1 before luciferase gene. Thus, DDX3X mutations identified in the WNT subgroup medulloblastomas appear to lead to loss of its ATPase dependent RNA helicase activity *i.e.* loss of function nature of the mutations, which is characteristic of a tumor suppressor gene.

5.5 DDX3X: Tumor Suppressor or Oncogene?

DDX3X has been suggested to function as a tumor suppressor in some cancers like Chronic Lymphocytic Leukemia, gingivo-buccal oral squamous cell carcinomas from the Indian tobacco chewers based on the presence of truncating mutations, deletion/s of the DDX3X gene identified

in these cancers as well as down regulation of its expression in the HPV positive head & Neck carcinomas [81, 143, 144]. DDX3X down regulation in NIH3T3 cells lead to premature entry into S-phase accompanied with increased proliferation, lower levels of cell cycle inhibitor p21/CDKN1A and increased level of CyclinD1 in NIH3T3 cells also supports it's tumor suppressor role [66]. On the other hand, in the case of breast cancer it has been reported to function as an oncogene by promoting Epithelial Mesenchymal Transition (EMT) of MCF7 cells and by increasing anchorage independent growth, motility and invasion of MCF10A cells [67]. Therefore to elucidate the role of DDX3X mutations in medulloblastoma pathogenesis, DDX3X expression was downregulated using an inducible DDX3X shRNA in Daoy medulloblastoma cell line. Since no WNT subgroup medulloblastoma cell line has been established so far and mutations in DDX3X are also reported in SHH subgroup medulloblastomas, Daoy cell line belonging to the SHH subgroup was chosen for the study. DDX3X down regulation in Daoy cell line resulted in almost 90% reduction in proliferation and clonogenic potential suggests that DDX3X gives proliferation advantage to Daoy cells. Thus, DDX3X appears to act as an oncogene in Daoy cells. N-terminal domain (amino acids 1 - 408) of DDX3X has been reported to be sufficient to regulate transcription of some genes like IFN β , independent of its enzymatic activities [65]. While the mutations in DDX3X appear to be loss of function in nature with respect to the ATPase/helicase activity, N-terminal domain of DDX3X may still be sufficient to regulate some genes at transcriptional level that could explain pro-proliferative/oncogenic role of the mutant DDX3X. Thus, the loss of DDX3X's enzymatic activity seems necessary while at the same time, N-terminal domain needs to be retained for its role in medulloblastoma tumorigenesis explaining rare occurrence of truncating mutations. The role of loss of DDX3X's enzymatic activity in pathogenesis of cancers including medulloblastoma remains to be understood. By

identifying genes regulated at the transcriptional and translational level by DDX3X in medulloblastoma cells, it would be possible to delineate role of DDX3X in medulloblastoma pathogenesis.

5.6 Expression of miR-30 family miRNAs is downregulated in medulloblastoma

Loss of a copy of chromosome 6 occurs in ~ 75% WNT subgroup medulloblastomas, indicating presence of a tumor suppressor gene/s on chromosome 6 [124]. As per the Knudson's hypothesis, the second copy of tumor suppressor gene/s on chromosome 6 would be expected to undergo mutational inactivation [145]. Alternatively, expression of the putative tumor suppressor gene/s may be down regulated at RNA or protein level. Exome sequencing identified mutations in only one gene *ARID1B* located on chromosome 6 in only 2 out of 11 WNT tumors. It is likely that other than *ARID1B*, additional genes located on chromosome 6 may also play role in pathogenesis. Expression of two microRNAs *viz.* miR-206 and miR-30a located on chromosome 6 was found to be down regulated not only in the WNT subgroup but all medulloblastoma subgroups. Earlier study from the lab has shown MiR-206 to act as a tumor suppressor gene by targeting *OTX2*, a known oncogene in medulloblastoma [146]. Not just miR-30a but expression of seven miRNAs belonging to the miR-30 family (miR-30a-5p, miR-30a-3p, miR-30b, miR-30c, miR-30d, miR-30e-5p, miR-30e-3p) was found to be down regulated in medulloblastomas belonging to all the four medulloblastoma subgroups compared to normal cerebellum. MiR-30a expression is down regulated by 10-100 fold in Daoy, D283 and D425 medulloblastoma cell lines belonging to three different medulloblastoma subgroups (SHH, Group 3, Group 4). MiR-30a expression was also found to be down regulated in medulloblastomas from two SHH

subgroup mouse models viz. *Smo*^{+/+} transgenic mice and *Ptch*^{+/-} knock-out mice [126]. Expression of miR-30 family microRNAs is reported to be downregulated in several other cancers like breast cancer, lung cancer, colorectal cancer, esophageal squamous cell carcinoma [147]. So our finding of miR-30 downregulation in medulloblastoma is in concordance with earlier reported studies related to miR-30 family miRNA expression in tumors.

5.7 MiR-30a inhibits proliferation, anchorage independent growth and *in vivo* tumorigenicity of medulloblastoma cells by inhibiting autophagy

Restoration of miR-30a expression resulted in inhibition of proliferation and clonogenic potential of Daoy, D283 and D425 medulloblastoma cell lines. MiR-30a has been reported to inhibit proliferation of breast cancer, colon cancer, lung cancer and prostate cancer cell by targeting *Eya2*, denticleless protein homolog (DTL), IGF1R and SOX4 gene respectively [125, 148, 149]. MiR-30a expression was also found to inhibit the tumorigenicity of medulloblastoma cell by almost 100 fold as seen by orthotopic injection of miR-30a expressing medulloblastoma cells in the cerebellum of nude mouse. MiR-30a has been shown to inhibit the tumorigenicity of breast cancer cells, colon cancer cells and clear cell renal cell carcinoma cell by targeting *metadherin*, *HP1 γ* and *HIF2 α* respectively [150-152]. Thus the tumor suppressive role miR-30a in medulloblastoma is consistent with its role in other cancers.

Beclin1, a key regulator of autophagy, is one of the known targets of miR-30a [127, 153]. Autophagy is an essential conserved physiological process that selectively degrades cellular components and balances energy sources to enable cells to survive under metabolic and environmental stress [154]. Autophagy involves formation of Phagophore (isolation membrane)

which requires ULK1 kinase complex (ULK1, ATG13 and ATG17) and class III Phosphatidylinositol kinase Vps34. Interaction between Vps34 and beclin1 is essential for phagophore formation [153, 155]. Phagophore formation is followed by multimerization of ATG5, ATG12 and ATG16 for elongation of phagophore to form autophagosome (growing isolation membrane around cellular components). During autophagosome formation cytosolic LC3-I is converted to membrane-bound lipidated form (LC3-II) by ATG5-ATG12-ATG16 complex. The conjugation of LC3II to phosphatidylethanolamine PE and its incorporation in autophagosome is catalyzed by ATG3 and ATG7 followed by cleavage of LC3 by ATG4. This is followed by the fusion of cellular debris engulfed mature autophagosome with lysosome where the engulfed cellular debris is degraded by lysosomal acid proteases. LC3 remains on the mature autophagosome until its fusion with lysosome and is used to monitor autophagy. P62/SQSTM1 is an adapter protein that associates polyubiquitinated proteins to LC3BII targeting them for autophagic degradation. Upon autophagy induction p62/SQSTM1 bound cargo is degraded while upon autophagy inhibition protein levels of p62/SQSTM1 increase as degradation is inhibited. SQSTM1 is also used as marker to detect autophagy inhibition [155]. MiR-30a expression in medulloblastoma cells showed reduction in Beclin1 and ATG5 protein levels suggesting inhibition of autophagy by miR-30a. LC3B levels were studied before and after miR-30a expression in medulloblastoma cells to monitor autophagy. Upon autophagy induction, total levels of LC3B decrease and/or LC3BI to LC3BII conversion decreases, following LC3B1 conjugation of phosphatidylethanolamine. LC3B II levels however, also decrease as a result of their degradation by lysosomal enzymes upon fusion of autophagosomes with lysosomes. Therefore, LC3BI and LC3BII levels were monitored both in the absence and presence of chloroquine, an inhibitor lysosomal pathway of protein degradation., Doxycycline induction of miR-30a expression

resulted in down regulation of total LC3B levels (LC3BI and LC3BII) both in the presence and absence of lysosomal inhibitor indicating autophagy inhibition. Furthermore, even upon starvation induced autophagy induction, total levels of LC3B were found to be lower upon miR-30a expression, indicating inhibition of starvation induced autophagy by miR-30a expression. Increased in p62/SQSTM1 protein levels in miR-30a expressing medulloblastoma further confirmed the inhibition of autophagy by miR-30a. Thus down regulation of miR-30a expression appears to play role in medulloblastoma pathogenesis by eliminating miR-30a mediated autophagy inhibition. To our knowledge, this is for the first time role of autophagy in medulloblastoma pathogenesis is reported.

Autophagy has been reported to play role in cancer by acting as a tumor suppressor as it removes the damaged organelles and proteins, thereby limits the cell damage and genomic instability [154]. Reports showing that, Beclin1^{+/-} mouse are tumor prone also supports the autophagy as tumor suppressive role. On the other hand, autophagy is also known to help tumor cells survive in cellular stress conditions like hypoxia by recirculating components of damaged organelles and proteins and maintain energy balance [156].

In vitro as well as pre-clinical animal models have shown autophagy inhibition leading to growth inhibition, cell death induction in response to radiation/chemotherapy in established tumor cells. Autophagy is one of the many mechanisms that tumor cells develop to overcome the cytotoxic effects of chemotherapeutic drugs. Autophagy has been shown to play role in development of chemo-resistance and recurrence of tumors post-chemotherapy [157]. In both animal and cell culture models, forced expression of miR-30a has been shown to sensitize tumor cells to platinum based drug treatment, which is used for treatment of many cancers [158]. In case of chronic myeloid leukemia cells it has been reported that miR-30a mediated autophagy

enhances the imatinib activity [159]. MiR-30a has potential to be a therapeutic agent in medulloblastoma treatment in combination with chemotherapy that would make treatment more effective in high-risk cases and may bring about reduction in the intensity of chemotherapy treatment thereby reduce long term side effects of chemotherapy in medulloblastoma survivors. In the treatment of medulloblastoma by systemic drugs the major obstacle is blood-brain barrier (BBB), but advancement in miRNA delivery systems like use of RVG SSPEI (short peptide of rabies virus glycoprotein linked by disulfide bond to polyethylenimine) to deliver neuron specific manner - can be explored for the use of miR-30a as a therapeutic agent in medulloblastoma [160].

Chapter 6

SUMMARY & CONCLUSIONS

Medulloblastoma is the most common and highly malignant brain tumor in children and consists of four molecular subgroups *viz.* WNT, SHH, Group 3 and Group 4. WNT subgroup tumors are characterized by overexpression of a number of genes involved in the WNT signaling pathway... Mutation in *CTNNB1* gene is reported in ~ 90% of the WNT subgroup tumors. WNT subgroup patients have excellent survival but suffer from long term sequelae of the conventional cytotoxic treatment. It is therefore necessary to delineate molecular mechanism underlying pathogenesis of the WNT subgroup tumors so that treatment aimed at specific targets could be both effective and minimize the side effects. Mutation in beta catenin encoding gene *CTNNB1* is known to bring about hyperproliferation but not malignant transformation in developing mouse brain. Loss of one copy of chromosome 6 is reported in ~75% of the WNT subgroup tumors. Expression of a microRNA located on chromosome 6 was found to be downregulated in medulloblastomas.. Therefore, the present study was undertaken:

1. To identify genetic alteration/s in the WNT subgroup medulloblastoma that act as additional hits in addition to the mutation in beta catenin encoding gene *CTNNB1* .
2. To delineate the role of miR-30a in pathogenesis of medulloblastoma.

Briefly, the salient findings of the present study are:

- Whole exome sequencing of WNT subgroup tumors identified 10-30 somatic variants in each WNT subgroup tumor along with the loss of one copy of chromosome 6 in 7 out of 11, partial loss of chromosome 6 in two and intact chromosome 6 in one WNT subgroup tumors indicating that WNT subgroup tumors have low number of passenger mutations and stable genome compared to other common adult cancers.

- Truncating mutations were identified in the chromatin modifying SWI/SNF complex components (ARID1B, SMARCB1 and SMARCA4) and ASCOM complex components (MLL3 and KDM6A) in the WNT subgroup medulloblastoma, indicating that epigenetic modifiers play role in medulloblastoma pathogenesis.
- DEAD-box helicase *DDX3X* mutations were identified in three WNT subgroup tumors, with two tumors having missense and one tumor having frameshift truncating mutation. This is for the first time truncating mutation in *DDX3X* is identified in medulloblastoma.
- *DDX3X* mutations identified in the WNT subgroup medulloblastomas appear to lead to loss of its ATPase dependent RNA helicase activity *i.e.* loss of function nature of the mutations, which is characteristic of a tumor suppressor gene as judged by loss of its translation up regulating activity of complex 5'-UTR of Cyclin E1.
- Downregulation of *DDX3X* in Daoy, medulloblastoma cells leads to almost 90% reduction in proliferation and clonogenic potential. Thus, *DDX3X* gives proliferation advantage to Daoy cells and appears to act as an oncogene in Daoy cells belonging to the SHH subgroup medulloblastoma.
- Expression of miR-30a along with six other miRNAs belonging to the miR-30 family (miR-30a-5p, miR-30a-3p, miR-30b, miR-30c, miR-30d, miR-30e-5p, miR-30e-3p) was found to be down regulated in medulloblastomas belonging to all the four medulloblastoma subgroups compared to normal cerebellum.
- MiR-30a expression is down regulated by 10-100 fold in Daoy, D283 and D425 medulloblastoma cell lines belonging to the three different medulloblastoma subgroups (SHH, Group 3, Group 4) along with its downregulation in tumors from two SHH subgroup mouse models viz. *Smo*^{+/+} transgenic mice and *Ptch*^{+/-} knock-out mice.

- MiR-30a expression was found to inhibit proliferation, clonogenic potential of Daoy, D283 and D425 medulloblastoma cell line. MiR-30a expression was also found to inhibit tumorigenicity of medulloblastoma cells by almost 100 fold as seen by orthotopic injection of miR-30a expressing D283 medulloblastoma cells in the cerebellum of nude mouse.
- MiR-30a expression after induction was found to inhibit the autophagy in medulloblastoma cells as seen by decrease in Beclin1, ATG5 and total LC3B protein expression levels and increase in SQSTM1/p62 protein expression level. This is for the first time the role of autophagy in medulloblastoma is reported.

In conclusion, the present study identifies truncating mutations in the epigenetic modifiers in the WNT subgroup medulloblastoma tumor tissues. In last decade, with the advancement in the DNA sequencing technologies, mutations in the epigenetic modifiers have been reported in several cancers, thus epigenetic modifiers appear to play role in pathogenesis of not only medulloblastoma but many other cancers as well. Mutations in the epigenetic modifiers are reversible using simple chemical agents, hence can be explored for the development of therapeutic interventions for many cancers. *DDX3X* was identified as the second most mutated in gene in the WNT subgroup medulloblastoma after mutations in the beta catenin encoding gene *CTNNB1*. *DDX3X* mutations identified in medulloblastoma appear to lead to loss of its enzymatic activities, a characteristic of tumor suppressor gene. On the other hand, *DDX3X* appears to have pro-proliferative/oncogenic role in Daoy medulloblastoma cell line. Thus exact role and mechanism of *DDX3X* in pathogenesis of medulloblastoma needs to be investigated. Expression of MiR-30a located on chromosome 6 was found to be downregulated all four subgroups of medulloblastoma compared to normal cerebellum. Its expression in

medulloblastoma leads to inhibition of proliferation, clonogenic potential and decrease in *in vivo* tumorigenesis of medulloblastoma cell lines Daoy, D283 and D425 by inhibiting autophagy. Autophagy is one of the mechanisms that tumor cells use to develop resistance to chemo-therapy and radiation therapy, hence miR-30a can be a potential therapeutic agent in combination with chemotherapy / radiation therapy that could improve survival of high-risk medulloblastoma cases and reduce intensity of .the cytotoxic therapy thereby minimizing long term side effects.